Seventeenth Edition

Photovoltaics International

THE TECHNOLOGY RESOURCE FOR PV PROFESSIONALS

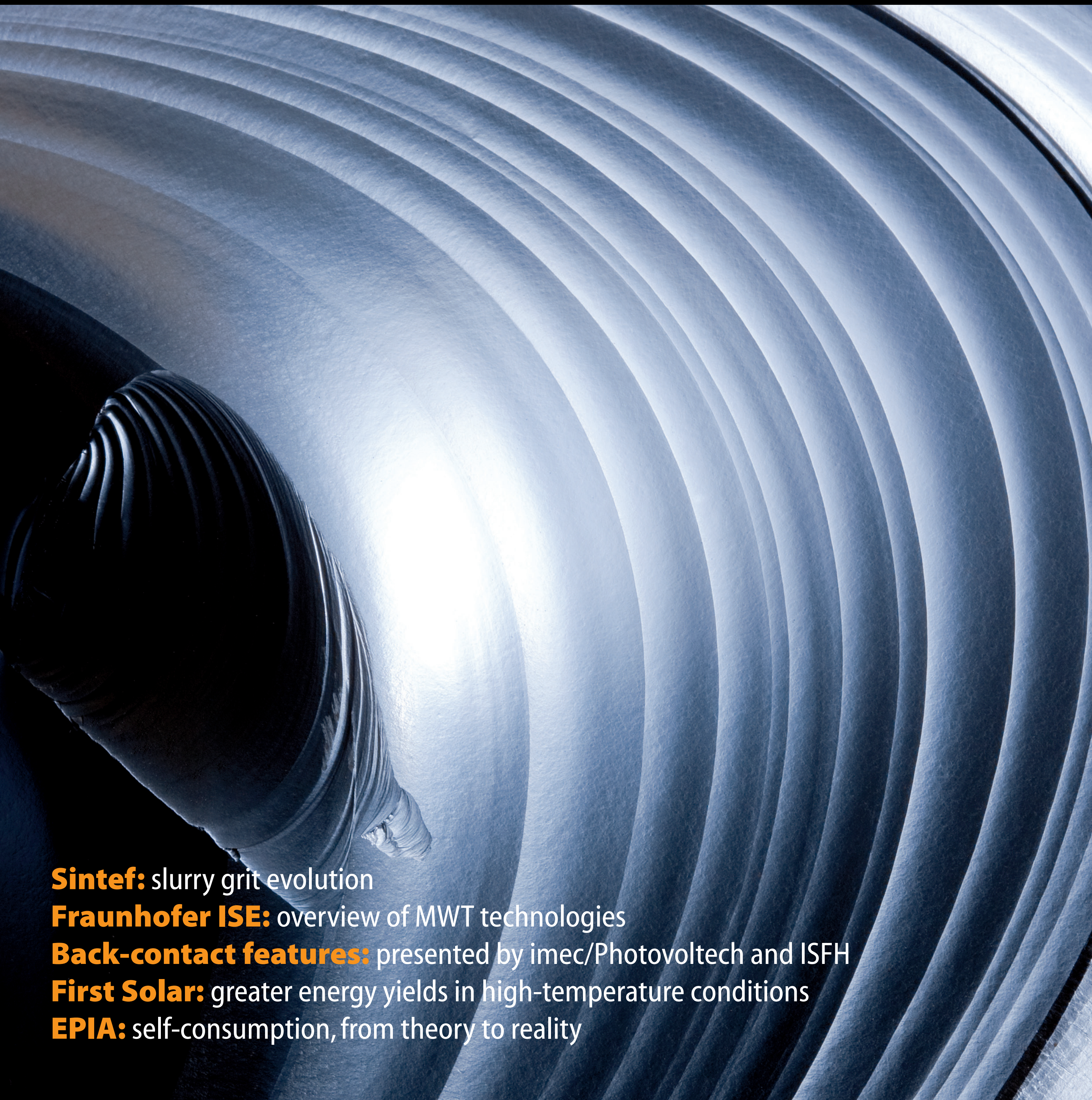

Sintef: slurry grit evolution
Fraunhofer ISE: overview of MWT technologies
Back-contact features: presented by imec/Photovoltech and ISFH
First Solar: greater energy yields in high-temperature conditions
EPIA: self-consumption, from theory to reality

Third Quarter, August 2012
www.pv-tech.org

Photovoltaics International

Published by:
Solar Media Ltd.,
Trans-World House, 100 City Road, London
EC1Y 2BP, UK
Tel: +44 (0) 207 871 0123
Fax: +44 (0) 207 871 0101
E-mail: info@pv-tech.org
Web: www.pv-tech.org

Publisher: David Owen

Commissioning Editor: Adam Morrison
Sub-Editor: Steve D. Brierley
Senior News Editor: Mark Osborne
Web & Publications Editor: Nilima Choudhury
News Editor: Syanne Olson
Editorial Consultant: Graham Anderson
Design & Production: Daniel H Brown
Production: Viki Hämmerle

Sales Director: David Evans
Account Managers: Adam Morrison, Graham Davie, Daniel Ryder, Gary Kakoullis, Nick Richardson, Ben Irving & Peter Gibson
Marketing & Operations Director: Joy-Fleur Brettschneider

Cover image shows REC Silicon's polysilicon, which is used in various solar processes and manufactured with ultra-pure Signature Silane (R) . Image courtesy of REC Silicon: www.recgroup.com.

Printed by Buxton Press
Photovoltaics International
Seventeenth Edition
Third Quarter 2012
Photovoltaics International is a quarterly journal published in February, May, August and November.

Distributed in the USA by Mail Right International, 1637 Stelton Road B4, Piscataway, NJ 08854.

ISSN: 1757-1197

USPS Information
USPS Periodical Code: 025 313

Periodicals Postage Paid at New Brunswick, NJ
Postmaster: Send changes to: Photovoltaics International, Solar Media Ltd., C/o 1637 Stelton Road, B-4, Piscataway, NJ 08854, USA

Foreword

Manufacturing solar modules is a difficult business at the moment, with many companies struggling to survive the so-called 'shakeout.' Manufacturers have seen average selling prices (ASPs) of PV modules in freefall for the past 12 months. So far, prices in 2012 have dropped by almost 41 per cent.

Go back two years and these same companies were accessing large sums of capital investment to fund aggressive capacity expansions on the promise of stable markets in Western Europe, the USA and China. These traditional PV markets have levelled off as generous subsidies are reined in by politicians dealing with an almost global recession.

New markets are emerging to plug the deployment gaps left by countries such as Spain, the Czech Republic and Italy. As a result, deployment should reach between 28 and 32GW in 2012. This creates a flat market or even a small increase year on year. So what is the problem?

Profitless prosperity is the way Mark Osborne, Senior News Editor at www.pv-tech.org, characterizes the PV manufacturing supply chain at the moment. Despite deployment levels remaining relatively steady, the influx of capital into the manufacturing supply chain two years ago has created a glut of PV modules. While manufacturers may have increased shipments, their profit margins are falling to the point where some are forced to sell a product below the cost of producing it.

It is clear that – with Brent crude once again rising to $115 per barrel, increasing awareness of global climate issues, and of course the advent of grid parity in many markets – the fundamentals underlying the solar energy industry are sound.

The winning manufacturers in the solar supply chain will be those best able to maintain a technological advantage in manufacturing, while at the same time establishing consistent volume sales channels worldwide.

Technology is helping to drive the cost of production down further. Solar Buzz analysts predict that leading manufacturers are looking at buying equipment and materials that will take advantage of new technology, over the coming six to nine months, They draw comparisons with the semiconductor industry, which goes through separate technology and expansion purchasing cycles. The next expansion cycle is unlikely to take place until 2013, after the supply chain has matured further.

Right now, everyone is talking about metal wrap through (MWT) technology for crystalline solar cell production as a way to reduce silver consumption. In this issue Fraunhofer ISE (page 61) presents an overview of MWT technologies and calls on manufacturers to "quickly bring these techniques to industrialisation." Additionally, back-contact cells and modules are featured extensively, with valuable contributions from imec/Photovoltech (page 116) and ISFH (page 50).

As a result of aggressive component pricing, the capex for solar installations has dropped to the point of near grid parity in many markets. Now the challenge is one of public perception and stimulating regional and local markets to create a robust sales channel for the PV sector's products.

The NYU Stern Business School and Yale University (page 160) look at the peer effects of cluster-based deployment of residential solar installations, while EPIA (page 166) gives us a valuable overview of net metering and self-consumption schemes so we can assess how they may drive deployment.

There is no question that the solar industry will thrive in the future. What remains to be seen is which companies will still be around to enjoy it.

David Owen
Publisher
Solar Media Ltd

Photovoltaics International

Photovoltaics International's primary focus is on assessing existing and new technologies for "real-world" supply chain solutions. The aim is to help engineers, managers and investors to understand the potential of equipment, materials, processes and services that can help the PV industry achieve grid parity. The Photovoltaics International advisory board has been selected to help guide the editorial direction of the technical journal so that it remains relevant to manufacturers and utility-grade installers of photovoltaic technology. The advisory board is made up of leading personnel currently working first-hand in the PV industry.

Editorial Advisory Board

Our editorial advisory board is made up of senior engineers from PV manufacturers worldwide. Meet some of our board members below:

Gary Yu, Senior Vice President, Operations

Mr. Yu served as Trina Solar's Vice President of Manufacturing since May 2007 and in July 2010 was promoted to the position of Senior Vice President of Operations. Mr. Yu has 17 years' manufacturing management experience in semiconductor-related industries. Before joining Trina Solar, he was Managing Director of Wuxi Lite-On Technology, an LED assembly company based in China. Prior to Wuxi Lite-On Technology, he served as a Director of Manufacturing for 1st Silicon Sdn. Bhd. in Malaysia, prior to which he worked at Macronix International, a semiconductor integrated device manufacturer in Taiwan. Mr. Yu has a master's degree in Industrial Engineering and Management from National Chiao Tung University in Taiwan and a bachelor's degree in Chemical Engineering from Tunghai University.

Takashi Tomita, Senior Executive Fellow, Sharp Solar

Takashi Tomita has been working at Sharp for 34 years and is widely recognised as a fore-father of the solar industry in Japan. He was responsible for setting up Sharp's solar cell manufacturing facilities in Nara and silicon production in Toyama. Takashi's passion for solar power has led him to hold numerous posts outside of his roles at Sharp, including: Vice Representative at the Japan Photovoltaic Industry Association; Committee Member of Renewable Energy Portfolio Standard of METI; Adviser Board Member of Advanced Technology of Nara; Visiting Professor of Tohoku University; Adviser of ASUKA DBJ Partners (JAPAN) and Adviser of Global Catalyst Partners (US).

Dr. Peng Heng Chang, CEO, Motech Industries, Inc.

Dr. P.H. Chang was elected CEO of Motech in March 2010. Dr. Chang has over 30 years of experience in management at multinational technology companies and in-depth knowledge in Materials Engineering. Prior to joining Motech, Dr. Chang was VP of Materials Management and Risk Management, VP of Human Resources and Senior Director of Materials Management at Taiwan Semiconductor Manufacturing Co. (TSMC); VP of Administration at Worldwide Semiconductor Manufacturing Co. and Professor of Materials Science and Engineering at National Chiao Tung University in Hsinchu, Taiwan. Dr. Chang also worked for Inland Steel Co. and Texas Instruments in the US prior to 1990. He received his Ph.D. degree in materials engineering from Purdue University in 1981.

Professor Eicke R. Weber, Director of the Fraunhofer Institute for Solar Energy Systems ISE in Freiburg

Professor Eicke R. Weber is the Director of the Fraunhofer Institute for Solar Energy Systems ISE in Freiburg. Weber has earned an international reputation as a materials researcher for defects in silicon and III-V semiconductors such as gallium arsenide and gallium nitride. He spent 23 years in the U.S. in research roles, most recently as Professor at the University of California in Berkeley. Weber is also the Chair of Applied Physics, Solar Energy, at the University of Freiburg, and during his career has been the recipient of several prestigious awards including the Alexander von Humboldt Prize in 1994, and the German Cross of Merit on ribbon in June 2006.

Dr. Zhengrong Shi, Executive Chairman and Chief Strategy Officer, Suntech

Dr. Zhengrong Shi is founder, CEO and Chairman of the board of directors of Suntech. Prior to founding Suntech in 2001, he was a Research Director and Executive Director of Pacific Solar Pty., Ltd., the next-generation thin-film technology company, before which he was a Senior Research Scientist and leader of the Thin Film Solar Cells Research Group in the Centre of Excellence for Photovoltaic Engineering at the University of New South Wales in Australia. Dr. Shi holds 11 patents in PV technologies and is a much-published author in the industry. His work has earned him such accolades as "Hero of the Environment" (TIME magazine 2007) and "Corporate Citizen of the Year" at the China Business Leaders Awards 2007. A member of the NYSE advisory board, Dr. Shi has a Bachelor's degree in optical science, a Master's degree in laser physics and a Ph.D. in electrical engineering.

Dr. Sam Hong, President and COO of Neo Solar Power

Dr. Hong has more than 30 years of experience working in the solar energy industry. He has served as the Research Division Director of Photovoltaic Solar Energy Division at Industry Technology Research Institute (ITRI), a research organization that serves to strengthen the technological competitiveness of Taiwan, and Vice President and Plant Director of Sinonar Amorphous Silicon Solar Cell Co., which is the first amorphous silicon manufacturer in Taiwan. In addition, Dr. Hong was responsible for Power Subsystem of ROCSAT 1 for the Taiwan National Space Program. Dr. Hong has published three books and 38 journal and international conference papers, and is a holder of seven patents. Dr. Hong was the recipient of Outstanding Achievement Award from the Ministry of Economic Affairs, Taiwan, and was recently elected as chairman of the Taiwan Photovoltaic Industry Association.

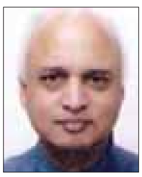

Dr. G. Rajeswaran, President and CTO of Moser Baer Photovoltaic Ltd

Raj served as President and CTO of Moser Baer Photovoltaic Ltd. from July 2007 until October 2008, since which time he has been Group CTO for all the Moser Baer business units and holder of the CEO function for launching new businesses. He spent 22 years with Eastman Kodak Company as the Vice President of Advanced Development & Strategic Initiatives, where he managed Kodak's Japan display operations including technology & business development in Japan, Taiwan, Korea and China. He has also served as Vice President and on the board of SK Display Corporation, and worked in technology development with Brookhaven National Laboratory. Raj has a Ph.D., an M.Tech. and a B.E. in electrical engineering. A much-published author, speaker and patent holder, Raj is a member of the Society for Information Display (SID) and has chaired several international conferences in the field of OLEDs.

NextSi™ Granular Polysilicon: Blend In to Stand Out

See us at Solar Power Int'l
Sept. 10-13, 2012
Booth 2218
Orlando, Florida

How do PV ingot manufacturers stand out? They blend NextSi™ Granular Polysilicon with Siemens chunk polysilicon. A 50/50 mix increases initial crucible load weight by 29%, while reducing load time 41%.

In a marketplace where cost is king, these density and operational performance advantages can add up quickly for crystalline cell producers.

REC Silicon NextSi™ is:

- Designed to mix with any grade of chunk polysilicon.
- Ready to use, pourable and more safely handled than chunk.
- Beneficial to any crucible charge regardless of blend ratio.

As the world's largest manufacturer of granular polysilicon and silane gas, REC Silicon continues to build a culture of innovation and industry-leading silicon material solutions to help meet your business goals.

➔ Take your solar strategy to the NextSi™ level. Learn the facts of silicon blending results in our "FBR Granular" white paper: **recgroup.com/nextsi**

*Data from REC Silicon "FBR Granular" white paper, March 2011.

REC Silicon

SOLAR & ELECTRONIC GRADE POLYSILICON | SILICON GASES

Contents

9

50

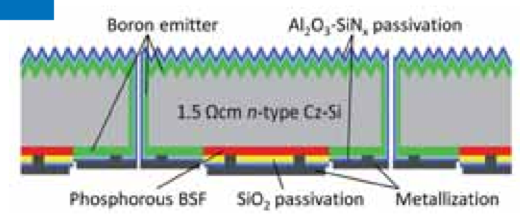

Contents

Fab & Facilities

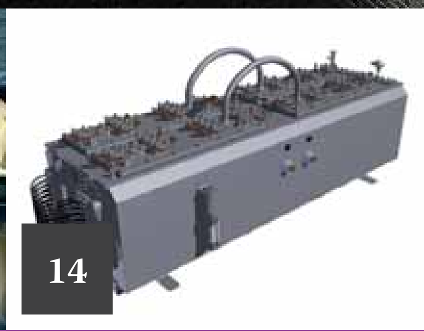

News

SolarWorld holds first supplier award event

Unlike the semiconductor industry, the recognition of suppliers from PV manufacturers is limited. However, SolarWorld has organized its first supplier award event to acknowledge the important role suppliers have in the success of its operations. In a statement, several categories were highlighted by the module manufacturer, which included awards to Kostal, 3M and Gigasolar.

Kostal Solar Electric was said to have won the 'technology award' for the joint development of a battery inverter that is marketed by SolarWorld under the brand name of SunPac K. 3M's Renewable Energy Division received the award for 'outstanding achievements in the field of sustainability and environmental compatibility.' The company produces module backsheet and other consumable materials used in module manufacturing. SolarWorld noted that it had given 'special recognition' to 3M for its sustainability report.

SolarWorld also highlighted its 'performance award' went to metallization paste supplier Gigasolar Materials Corporation for its logistics performance and product quality.

SolarWorld awards go to Kostal, 3M and Gigasolar.

Capacity News Focus

REC to wind up REC Wafer Norway via bankruptcy

To avoid further drains on its battered balance sheet, REC said it would start winding up REC Wafer Norway via bankruptcy proceedings. The solar wafer operations at two sites in Glomfjord and at Herøya have already been permanently closed down. The bankruptcy of REC Wafer Norway was said to not have had an effect on REC Solar and REC Silicon operations, which continue to operate as normal.

REC said that the carrying value of liabilities for REC Wafer Norway had exceeded the estimated value of assets by as much as NOK1.2 billion (US$204 million), which, if the company continued to support the winding-up of the operations, would be financially liable. However, REC said that it would still be liable for additional costs and losses related to certain guarantees, loans and indemnity agreements related to REC Wafer Norway, which the company said could be as much as NOK0.4 billion(US$68 million), but was subject to change.

Source: REC Solar

To avoid further drains on its battered balance sheet, REC said it would start winding up REC Wafer Norway via bankruptcy proceedings.

ET Solar subsidiary's factory receives inspection certificate from IMQ

The Italian Institute for the Quality Mark (IMQ) has awarded ET Solar's subsidiary, ET Solar Industry Limited, a factory inspection certificate. The organization offers factory inspection certificates and attestation services in the alternative energy sector.

Source: GEOLEC

ET Solar Industry Limited granted factory inspection certificate from IMQ.

ET Solar noted that prior to the IMQ certification, its factories had been evaluated by various third-party organizations and received certificates from agencies such as SGS, DNV, VDE and 3E.

Emcore to replace multiple legacy manufacturing systems with Camstar Enterprise platform

Emcore and Camstar Systems announced that Emcore will be replacing various legacy manufacturing systems with the Camstar Enterprise platform. The changes will be incorporated into different systems, including the manufacturing execution (MES), quality management and statistical process control (SPC). The solution aims to simplify the system complexities essential to running Emcore's wafer and cell processing and assembly, test and panel manufacturing.

SolarCity expands Maryland operations centre

SolarCity has now opened an expanded operations centre in Beltsville, USA. The company is ensuring new jobs in Maryland and aims to give the state's homeowners, businesses and non-profit organizations better energy options that can cost less than their utility bills. Attendees at the grand opening included US senator Ben Cardin, as well as state senator Jim Rosapepe and state delegate Joseline Peña-Melnyk.

Over the last eighteen months, SolarCity claims it has grown from 12 to over 100 Maryland employees, while providing solar energy services to more than 1,000 buildings across the state. SolarCity is currently offering Marylanders the ability to install solar energy for free and pay less for solar electricity than they pay for utility power.

BYD opens new R&D facility with focus on solar cell development

Claimed to be the first R&D facility in China focusing on solar cell technology development, Chinese conglomerate BYD has opened the BYD Ningbo PV R&D Centre in the Beilun Free Trade Zone. The new facility was said to be an important strategic initiative of the company and would also employ semiconductor production equipment to develop next-generation solar cells.

ReneSola continues polysilicon expansion plans

ReneSola reported that its in-house polysilicon production capacity expansion remained on schedule and that it continued to lower production costs. The company said that production had increased to approximately 1,119MW, up from 900MT in the first quarter.

Production costs were said to have been reduced significantly from US$33/kg in the first quarter of 2012 to US$25.8/kg at the end of the second quarter, though upgrades and maintenance on the power grid to its poly-plant in the previous quarter had impacted production and therefore costs.

Production costs were expected to decrease to approximately US$24/kg by the end of the third quarter and reach US$22/kg by year end, which was lower than previously guided but still higher than spot market prices.

However, after its Phase II polysilicon plant expansion is completed, which would boost polysilicon production to 10,000MT annually, Phase II polysilicon production costs were expected to be around US$18/kg, lowering its blended average costs near to larger rivals production cost levels.

Other News

SolarWorld celebrates fifth year anniversary in Hillsboro

It appears the waivered salary in 2011 by Frank Asbeck, CEO for SolarWorld, was not wasted. The company has invested a total of US$27million to upgrade and replace several factory systems at its Hillsboro, Oregon, USA, plant. This particular facility was considered to be one of the 'last plants standing' in September 2011 because production lines were shuttered in Germany and throughout the USA. The Hillsboro location also houses a demonstration park to debut technological advances, which SolarWorld hopes will boost the power output of its high-performance solar panels. The new initiatives push SolarWorld's total capital investment in Hillsboro to more than US$600 million.

Work to install new manufacturing systems from now, through the first quarter of 2013, will implement three technological advances fostered and tested by SolarWorld R&D specialists in Oregon and Europe, with the goal of increasing the power output of its PV cells.

Single PV technology roadmap to evolve as important catalyst to end profitless prosperity

Desperate times call for desperate measures, according to the latest PV industry analysis from NPD Solarbuzz. According to the market research firm, tier 1 PV manufacturers are set to align on one technology roadmap in 2013 and beyond to combat overcapacity and support aggressive cost reductions.

Talk of a single technology roadmap within the PV industry wasn't on the agenda when the industry was capacity constrained and ramping to multi-gigawatt levels. Fast forward a few years and massive overcapacity has spawned a period of profitless prosperity and debates over how the industry can survive. Within this landscape, several PV technology roadmaps have appeared to tackle cost reductions and improve conversion efficiencies. However, any meaningful roadmap has been driven by those with money to spend and those leading the technology race, though not necessarily either profitable or successful in gaining market share.

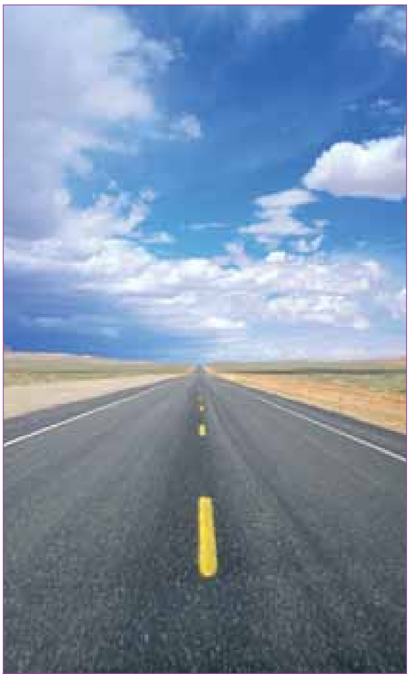

Source: Writers Café

According to NPD Solarbuzz, tier 1 PV manufacturers are set to align on one technology roadmap in 2013 and beyond to combat overcapacity and support aggressive cost reductions.

Heritage Global Partners and Schneider Industries partner for AEP auction

Heritage Global Partners and Schneider have entered a partnership for an asset auction, the companies have announced. The auction will include the entire production facility as well as equipment, technologies and rights to intellectual property. The auction will be sectioned into lots one through seven.

Trina Solar establishes Canadian subsidiary and partners with Silfab Ontario

Trina Solar has established a Canadian subsidiary, Trina Solar (Canada), with a sales and business development office in Ontario, Canada. Concurrently the company has formed an OEM partnership with Silfab Ontario, enabling Trina Solar to offer modules that are locally manufactured for the Canadian market and therefore take advantage of Ontario's domestic content feed-in tariff. Headquartered in Mississauga, Ontario, Silfab will be responsible for providing Trina with sufficient production capacity to support its venture into the Canadian market.

German flexible CIGS thin-film firm starts production

A next-generation roll-to-roll CIGS thin-film firm, Solarion AG, has started production at its first plant in a new industrial park in Zwenkau-Sued near Leipzig, Germany. Primarily planning to target the difficult BIPV and commercial rooftop markets, the company is claiming an initial 10% cell efficiency and a 20MW annual capacity.

Solarion said that it had invested approximately €60 million in the new facility, with €20 million provided by Saechsische Aufbaubank. The company said that the plant would eventually employ as many as 150 people. Initial products will actually be glass-glass CIGS modules, while its flexible modules are planned to be launched in 2013 after receiving IEC certification.

Solarion invested €60 million in the roll-to-roll plant.

3M completes manufacturing expansion of solar film at Missouri plant

3M advised that it had completed its manufacturing expansion on time for its Ultra Barrier Solar Film in Columbia, Missouri, allowing the company to help support the increasing demand for high-efficiency flexible PV modules. 3M's Ultra Barrier Solar Film acts as a replacement for glass and is said to provide high light transmission, excellent moisture barrier performance and weatherability.

Spanish Siliken workers protest against lay-offs

With two new offices having opened to support the Asian-Pacific region in July to help strengthen Siliken's position in the Asian market, workers from its centre in Rafelbunyol, Valencia, Spain, are protesting after the solar company presented an ERE (Expediente de Regulación de Empleo) — a Spanish administrative redundancy procedure which employers must comply with — to 100 employees, the CCOO Industry Federation has revealed.

The demonstration is the first of several planned protests. As part of the protest, workers began a march starting from San Agustín Square.

Source: INMA TORMOS SANCHOv

Workers from Siliken's Rafelbunyol centre in Spain are protesting against the firm's plans to cut 100 jobs.

A cheaper, faster and greener solar panel manufacturing process

George-Felix Leu, **Chris Egli** & **Edgar Hepp**, Oerlikon Solar, Trübbach, Switzerland, &
Bertrand Le Faou, **Jean-Charles Cigal** & **Greg Shuttleworth**, The Linde Group, Munich, Germany

ABSTRACT
The cleaning performance of three different fluorine-containing precursors – sulphur hexafluoride (SF_6), nitrogen trifluoride (NF_3) and molecular fluorine (F_2) – is compared from theoretical, experimental and commercial points of view. Experiments were performed using an Oerlikon Solar KAI Gen 5 (1300mm × 1100mm) R&D platform. For the experiments with F_2, an 'on-site/on-demand' generator from The Linde Group was installed at the Oerlikon Solar facility in Trübbach, Switzerland. The SF_6-based cleaning process was found to be up to 75% less efficient than the corresponding NF_3 or F_2 process. A comparison between NF_3 and F_2 indicates that a significantly larger process window is available for reactor cleaning when F_2 is used in place of NF_3. This leads to both time and gas mass savings, improving productivity and bringing down the cost of ownership of the reactor cleaning process. As a direct consequence, Oerlikon Solar has decided to transfer the process to their production KAI MT plasma-enhanced chemical vapour deposition (PECVD) platforms.

Introduction

The removal of deposited silicon in a plasma-enhanced chemical vapour deposition (PECVD) chamber is an essential step for thin-film Si PV production. In situ cleaning using gases containing fluorine (F) is a widely adopted process that offers many advantages over mechanical cleaning: the latter requires scheduled downtime of the equipment, resulting in higher operational costs and lower throughput. The established cleaning gases of choice for PECVD chamber cleaning are fluorine-containing gases, such as nitrogen trifluoride (NF_3) and sulphur hexafluoride (SF_6). From these gases, fluorine radicals are created; these then react with the unwanted silicon deposits, creating volatile SiF_4, which is subsequently pumped out.

> "The removal of deposited silicon in a PECVD chamber is an essential step for thin-film Si PV production."

As the chamber cleaning process represents a significant part of the gas cost for the PECVD process, manufacturers have been looking for more cost-effective and environmentally friendly alternatives, as both of these greenhouse gases have high global-warming potential. This paper presents the progress made in the implementation of molecular fluorine (F_2) as the cleaning gas on the Oerlikon Solar KAI platform.

Theoretical comparison of processes that use SF_6, NF_3 and F_2

Fluorine radicals are created either by in situ RF activation or by using a remote plasma source (RPS). The latter technique has been implemented during the development of NF_3 as a cleaning gas, in order to achieve full usage of the molecule at high flows of the precursor gas. As will be seen later, this is a requirement for an efficient NF_3-based cleaning process, but not essential when molecular fluorine is used.

The cleaning reactions will first be reviewed from a theoretical point of view, independently of activation technology or recipe development. Understanding the possible reaction pathways will allow the precursor to be identified for which cleaning is expected to be more efficient. Recipe development and a clean performance comparison on a KAI R&D platform will be discussed in the last part of this paper.

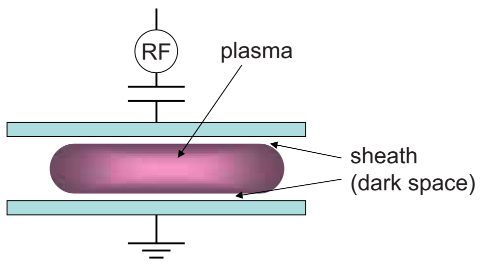

Figure 1. Plasma sheath.

1. The active radicals

The plasma created during the cleaning process of a PECVD reactor is a very complex medium. It contains neutral atoms and molecules, and different types of ions, electrons, photons, neutral molecular fragments, etc. It is believed that the PECVD cleaning processes used by Oerlikon Solar are mainly driven by neutrals (atoms, molecules and molecular fragments), and not by ions, for the following reasons:

- The KAI PECVD reactors are almost symmetrical, leading to very low DC bias values, so that the positive ions receive little acceleration in the plasma sheath.
- The cleaning processes occur at pressures above 0.3mbar, and, under some conditions, pressures higher than 1.0mbar are used. In such cases the energy of positive ions reaching the surface is very much reduced because of collisions with other molecules in the plasma sheath.
- Measurements show that the ion density in such plasmas can lie below $1E+10cm^{-3}$, but in order to achieve the observed etching rates of several tens of angstroms per second, a density of active radicals greater than $1E+14cm^{-3}$ is required. This is the same order of magnitude as the densities of neutral species and not of positive ions.

Since the number of negative ions is lower than that of positive ions, it can be concluded that the cleaning processes in the Oerlikon Solar chamber are driven by neutral species and not by ions.

The most important cleaning radical is atomic fluorine (F) [1]. The fluorine atoms reaching the surface react with the deposited silicon, forming SiF_4, which is volatile and is in turn pumped away:

$$4F + Si(wall) \rightarrow SiF_4(gas) \quad (1)$$

Although less important than atomic fluorine F, another neutral – molecular fluorine F_2 – also plays a role in the cleaning process [2], via reactions such as:

$$2F_2 + Si(wall) \rightarrow SiF_4(gas) \quad (2)$$

The reaction pathway for the creation of those neutrals from the different fluorine-containing gases that are used as the precursor will be discussed next.

2. Creation/destruction of active radicals

The main reaction pathway for the creation of atomic fluorine, in plasma, is via electron dissociative attachment [3,4]:

$$SF_6 + e \rightarrow SF_5 + F^- \quad (3)$$

$$NF_3 + e \rightarrow NF_2 + F^- \quad (4)$$

$$F_2 + e \rightarrow F + F^- \quad (5)$$

The activation energy for these reactions is very low (below 1eV), so the likelihood of them happening is very high. The corresponding neutral dissociation has a higher energy threshold (several eV) and is therefore of less importance.

The negative ions are further neutralized through ion–ion recombination:

$$F^- + I^+ \rightarrow F + I \quad (6)$$

where 'I' might be SF_5, NF_2 or F_2 (or one of the smaller radicals).

Another neutralization mechanism goes through detachment, for example:

$$F^- + J \rightarrow F + J + e \quad (7)$$

where 'J' might be SF_5, NF_2 or F_2 (or one of the smaller radicals).

It can be concluded that in all cases it is fairly easy to dissociate the first fluorine atom from the precursor molecule; this is the main reason why all of these precursors can be (and are) used.

In contrast with the creation of the first fluorine atom, the mechanisms for destruction of the cleaning radicals are very different for the said three precursors, and this fact leads to significant differences in cleaning performance.

SF_6 plasma

In the case of SF_6 there is a very strong recombination reaction channel of the form:

$$SF_x + F \rightarrow SF_{(x+1)} \quad (8)$$

where x = 0, 1, ... 5. This reaction is so rapid that the resulting density of atomic fluorine in SF_6 plasmas is quite low, despite the ease with which atomic fluorine is created. One way of reducing the impact of recombination on cleaning performance is the introduction of oxygen (O_2) into the discharge. The molecular oxygen is dissociated in the discharge, and then reacts with SF_x components, producing components such as SF_xO_y, which are fairly stable and do not recombine further with atomic fluorine. This method is used but has some disadvantages:

- The atomic oxygen will react not only with the SF_x radicals but also with the deposited Si, creating SiO_2, which is more difficult to clean than Si.

- The dissociation of oxygen requires energy, since one channel lies around 5.12eV, leading to the decrease of electron density and consequently slowing down all of the other reactions in plasmas.

The limitation induced by the recombination channel (Equation 8) is inherent in SF_6 plasmas. It can be reduced but not overcome by process measures, such as increasing the applied power or adding some more reactants.

NF_3 plasma

There are two cases that can be distinguished.

Case 1: If the applied power is high enough to completely dissociate the NF_3 molecule via a reaction of the type

$$NF_3 + e \rightarrow N + 3F + e \qquad (9)$$

(the reaction must be seen as the integral results of the reactions in Equations 4, 6 and 7) then a very fast recombination channel between N atoms appears:

$$N + N + \text{Wall} \rightarrow N_2 \qquad (10)$$

This channel prohibits the F recombination back to NF_x radicals, leaving only the following possibility for recombination of the F atoms:

$$F + F + \text{Wall} \rightarrow F_2 \qquad (11)$$

Case 2: If the NF_3 molecule is not completely dissociated, then the following scenarios might occur:

$$N + NF_x \rightarrow NF + NF_{(x-1)} \qquad (12)$$

$$F_2 + NF_{(x-1)} \rightarrow NF_x + F \qquad (13)$$

The reactions given in Equations 12 and 13 can be summarized as $N + F_2 \rightarrow NF + F$ with NF_x as the catalyzer, which is a destruction channel for atomic nitrogen as well as directly for cleaning radicals (out of a molecule of F_2 only one F atom remains as a cleaning radical – the cleaning activity of NF has not been demonstrated). In these circumstances, the reaction

$$F + NF_x \rightarrow NF_{(x+1)} \qquad (14)$$

becomes a relevant destruction channel for cleaning radicals.

A threshold applied power is therefore expected, above which should yield full conversion of NF_3 to cleaning radicals, with N_2 as a by-product. This observation led to the introduction of RPSs for NF_3 plasma, allowing high power to be used for dissociation outside the PECVD chamber. The high level of power coupling in an RPS allows a large dissociation rate of high flows of NF_3 so that recombination does not have a negative impact on the cleaning rate [5]. For low NF_3 flows, the in situ power coupling is sufficient to allow a large dissociation rate of NF_3 precursor.

F_2 plasma

Considering now the case of F_2 plasma, it is observed that all of the previously discussed plasmas are a combination of a F_2 plasma and something else:

$$F_2 + SF_x + O_y + SF_zO_t \qquad (15)$$

in the case of SF_6 plasmas, and

$$F_2 + N_2 + NF_x \qquad (16)$$

in the case of NF_3. The first advantage of using F_2 becomes apparent, namely that the energy usage is the most efficient in a pure F_2 plasma: all of the other molecules lead to energy loss, slowing down the cleaning reactions.

> "The biggest advantage of F_2 plasma is the absence of loss channels."

The biggest advantage of F_2 plasma is the absence of loss channels. The only recombination possible, shown in Equation 11, leads to F_2 formation, which still has some cleaning properties, even if lower than those of atomic fluorine (F) (see Leu et al. [2] for more details). In conclusion, for a given set of parameters (pressure, flow, power coupled to the plasma), the F_2 cleaning is expected to be more efficient than cleaning using any other precursor.

3. The impact of negative ions

All cleaning plasmas are electronegative, i.e. there are a significant number of negative ions in plasmas (see reactions in Equations 3, 4 and 5). Although a very interesting feature from a scientific viewpoint, it is however of less importance from a technological one. The main reason for this, as mentioned previously, is the fact that our processes are driven by neutrals and not by ions.

The presence of negative ions can nonetheless indirectly affect the cleaning processes in two ways, both of which are easy to overcome by technological means:

- The impedance of an electronegative plasma (as in the cleaning process) is very different from the impedance of an electropositive plasma (as in the deposition process). This means that the requirements for the RF matching box are different for deposition and cleaning. The challenge is then to use a suitable RF matching box that is able to match both deposition and cleaning plasmas. This challenge was met by designing a matching box that covers the whole required parameter window.
- The difference in plasma impedance might lead to some inhomogeneities in the case of cleaning plasmas in large area reactors if the reactor was primarily designed for deposition use. This challenge was met by careful design of the PECVD reactor.

If necessary, for very special cleaning processes, some electropositive gases (such as Ar or N_2) could be added to the cleaning recipes: these significantly reduce the electronegativity of the plasma and consequently improve the process homogeneity.

4. Comparison from cost and environmental points of view

The F_2 molecule consists (in terms of mass) of 100% fluorine, while the NF_3 molecule has only 80% fluorine, and SF_6 only 78%. By switching from NF_3 to F_2 and neglecting all of the previously mentioned process advantages of F_2, there is a reduction in mass consumption (in terms of mass/run) of 20%. Because gas is purchased on a per kilogram basis, this means that even if NF_3 and F_2 were purchased at the same price, it will be 20% cheaper to use F_2 while performing the same cleaning. As will be seen below, the unique performance of F_2 as a cleaning agent leads to an increase in mass saving that is well above this minimum theoretical value of 20%; when combined with a lower price per kilogram of F_2 than of NF_3, the effect of the total cost saving from on-site fluorine on annual gas consumption is considerable.

Molecular fluorine also has zero global-warming potential, whereas NF_3 (with a global-warming potential of 17,200) and SF_6 (22,600) are well-known greenhouse gases. Conversion to fluorine will therefore help dramatically reduce the CO_2-equivalent footprint of the solar panel manufacturing process.

On-site/on-demand generation of F_2: successful Linde concept

Given the chemical properties of molecular fluorine, the adoption of fluorine by the PV industry has raised some genuine concerns. The conservativeness of the PV industry, as well as its reluctance to introduce new materials in general, convinced both groups – Oerlikon and Linde – to develop a systematic approach in order to overcome all safety concerns and technology hurdles, and offer end users a proven solution for chamber cleaning. Working together with Linde – who have more than thirty similar systems installed worldwide, along with an excellent safety and reliability record – Oerlikon have addressed these concerns and installed an on-site fluorine generator at their solar facility in Trübbach. The generator, a Generation F 800 SC, is able

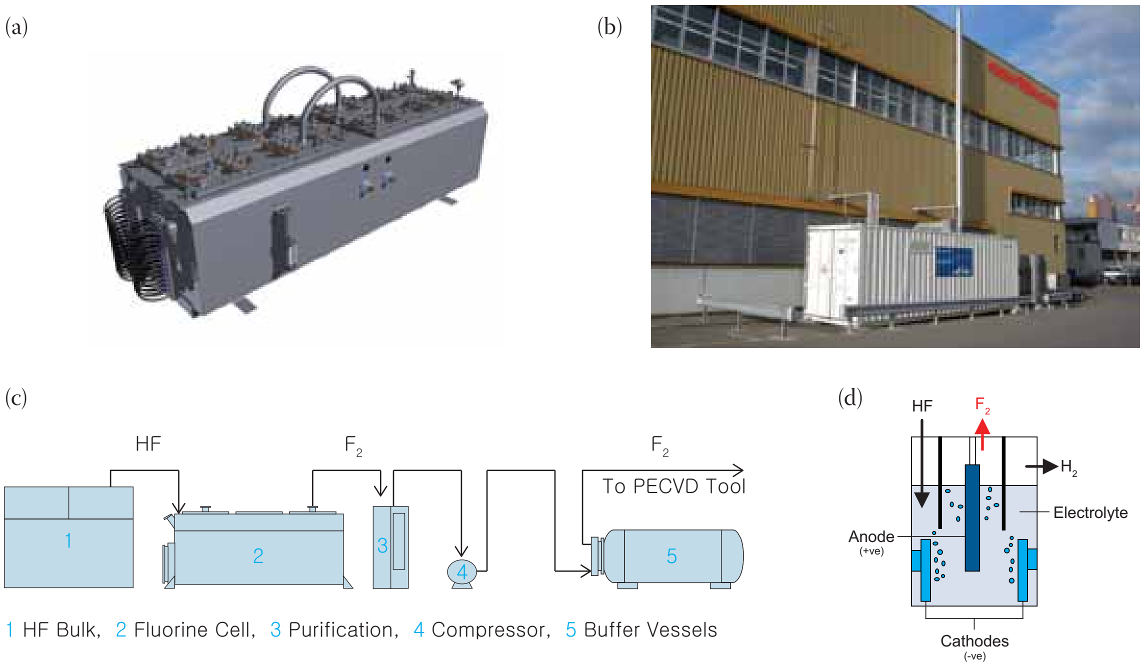

Figure 2. (a) Electrolysis cell; (b) containerized F_2 generator; (c) process flow chart; (d) principle of fluorine generation.

to produce 800 standard litres per hour (corresponding to a consumption of 32kg/day).

> "The only viable supply of molecular fluorine for production purposes is on-site generation."

Safety regulations severely limit the amount of fluorine that can be stored or transported in a high-pressure cylinder. Because of the large amount of cleaning gas to be considered for a PV production line, the only viable supply of molecular fluorine for production purposes is on-site generation. This concept has been successfully developed and implemented by Linde in the past few years, with the installation of hundreds of tons of on-site fluorine production capacity worldwide for semiconductor, flat-panel display and photovoltaic manufacturing.

In contrast with SF_6 or NF_3, fluorine is a highly reactive material, even in its molecular form, and therefore material compatibility of all wetted materials from the generator to the KAI process chamber must be ensured. Before using F_2 in the PECVD chamber, the piping from the buffer tank to the process chamber must be passivated. However, there are no particular concerns regarding the material used in the chamber and downwards to the abatement system, as the configuration has been proved for dissociated NF_3 or SF_6.

On-site and on-demand generation of fluorine offers many benefits, including a simplified supply chain (no fluorine transport is required), a low site inventory (as fluorine is produced on demand), and a safer delivery path (there is no F_2 cylinder exchange operation) compared to a cylinder supply because of the much lower pressures involved.

On-site fluorine generation is based on the electrolytic decomposition of anhydrous hydrofluoric acid (HF), first used by Moissan in his isolation of elemental fluorine in 1886. Anhydrous HF can be supplied in either gas or liquid phases to the working fluid, KF_2HF (which is a liquid only above 70°C), contained in a fluorine-resistant alloy vessel that also serves as the cathode. Current applied through the proprietary anodes determines the rate of fluorine production, and the evolved fluorine and hydrogen are physically separated to prevent recombination. The H_2 is diluted for direct disposal, or can be easily and completely abated in situ with proprietary passive catalytic oxidation.

Fluorine is filtered and purified to reduce residual vapour-phase HF to levels below 20ppm; it can then be used at its nominally atmospheric production pressure, or compressed and buffered to a safe working pressure of up to around 20psig. To supply processes that have been developed using diluted sources of fluorine, a near-zero pressure drop blender can supply on-demand blends of fluorine and inert gases, such as argon and nitrogen, in a dilution range of 0–100%. On-site fluorine generators are sized according to the total volume required, and all rely on the same simple low-pressure, low-temperature and low-inventory process design.

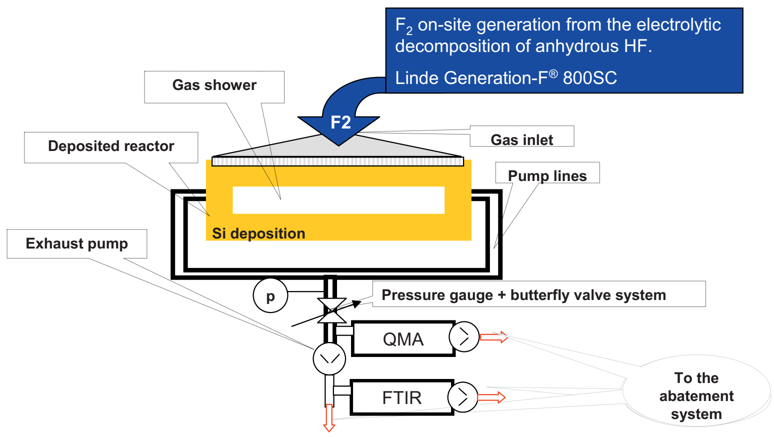

Figure 3. Experimental set-up.

KAI reactor and experimental set-up

Molecular fluorine was used to carry out a series of cleaning tests on a KAI R&D platform, a process chamber with a single Gen 5 (1300mm × 1100mm) reactor; the results were compared to those previously obtained using either NF_3 or SF_6. To monitor the cleaning performance of the different gases, different analytical tools were installed, including mass spectrometry (QMA) and infrared absorption spectroscopy (FTIR) (see Fig. 3).

A typical overview mass spectrum (QMA) for NF_3 cleaning is shown in Fig. 4, while a typical infrared spectrum (FTIR) is shown in Fig. 5. A detailed analysis of these two methods or of the taken spectra is beyond the scope of the present paper. In principle, in both cases one obtains spectra, from which two pieces of information can be inferred: the composition of the exhaust gas and the relative amount of every component. Ideally we want quantitative data from the chamber only – QMA gives us good information but it is difficult to interpret. FTIR, however, is easier to understand but the data is compromised by the measurement point being downstream of the pumps, so it is difficult to know if the data is the result of reactions in the process chamber or in the pumps downstream of the chamber.

By monitoring some of the QMA lines over a complete cleaning cycle, the curve shown in Fig. 6 can be generated. To compare different cleaning procedures, an arbitrary measure is used, specifically the 'cleaning rate 10%' (CR10%), defined as the thickness of the deposited layer divided by the time until the main cleaning signature (amu85 – SiF_3) decreases to 10% of its maximum. This is not the actual cleaning time but offers a good way of comparing different cleaning processes for a given deposition (see Leu et al. [5] for more details about this type of measurement applied to another type of cleaning).

The etching rate on a deposited glass was also measured by means of ellipsometry: the deposition thickness was measured before and after a short cleaning treatment performed with the glass inside the reactor. The results are expressed in terms of atomic fluorine flow so that a direct comparison of the efficiency of the cleaning can be made on the basis of the number of atoms of F supplied. For example, each molecule of NF_3 contains three F atoms, while a F_2 molecule contains two; thus, to supply the same number of F atoms, you need to supply 50% more F_2 molecules (flow) than NF_3 molecules.

F_2 etching uniformity

The first series of tests was the measurement of the a-Si etch rate on a deposited glass. The film thickness was measured immediately after the deposition process. The reactor was then cleaned, and the glass reintroduced into the clean reactor; the cleaning process was performed for a few tens of seconds, and the film thickness on the glass measured again. The deposition thickness before and after the short F_2 etching is shown in Fig. 7. The etching uniformity is remarkably good across the whole measured parameter window, confirming the results already obtained from another KAI R&D chamber, albeit with a different configuration [6].

Comparative evaluation of cleaning gases

A comparison was made between the best known method recipes for SF_6 and NF_3, and a series of NF_3 and F_2 cleaning

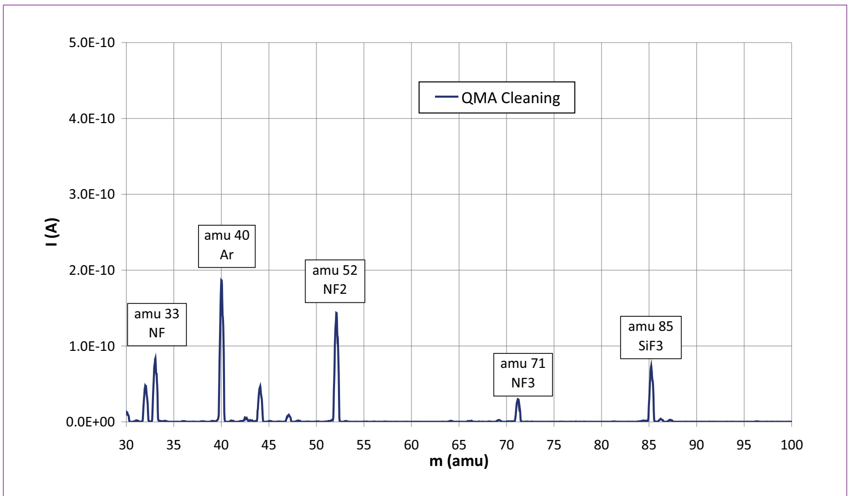

Figure 4. Typical overview of the QMA spectrum.

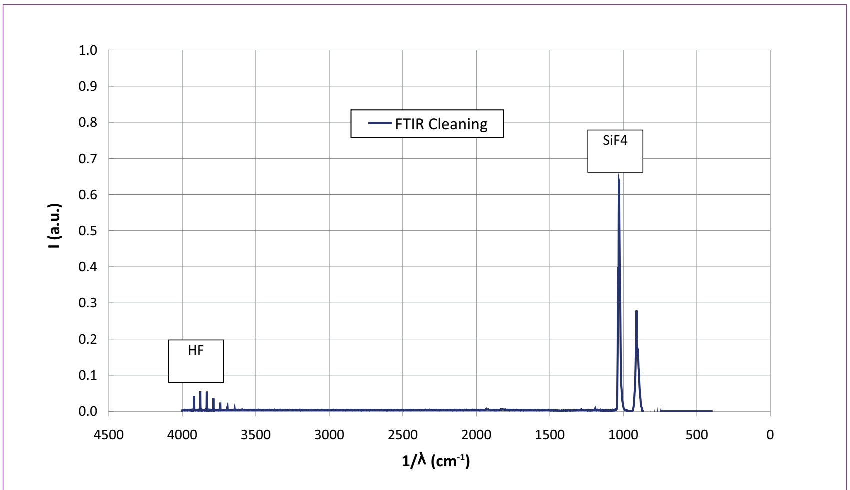

Figure 5. Typical overview of the FTIR spectrum.

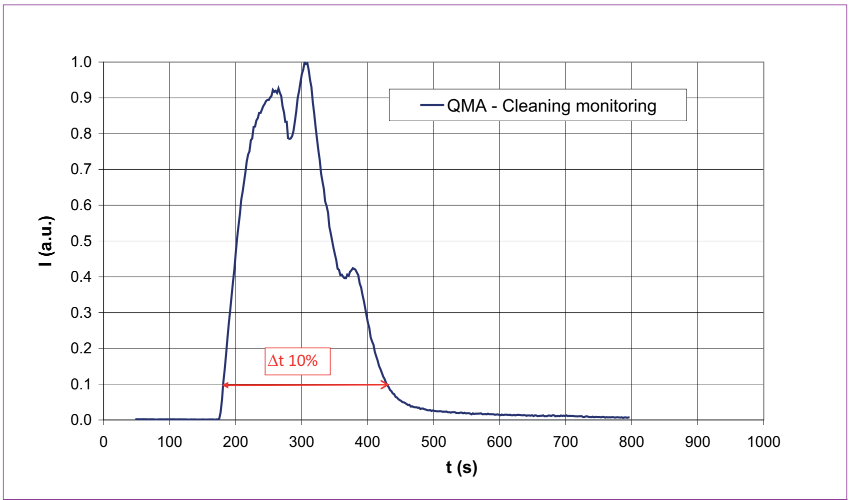

Figure 6. QMA cleaning monitoring.

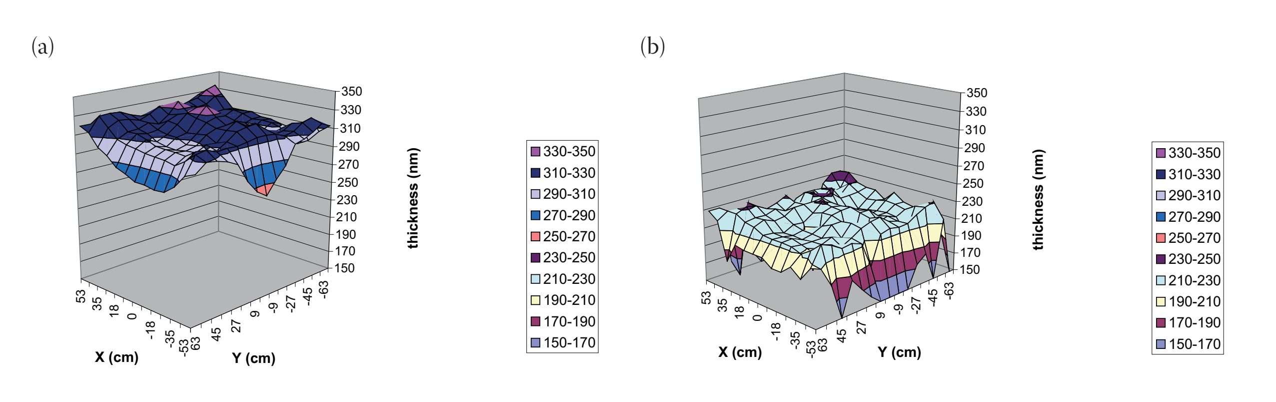

Figure 7. F_2 etching experiments:(a) before F_2 cleaning, and (b) after short F_2 cleaning.

development recipes (see Fig. 8). No direct comparison between SF_6 and NF_3 cleaning was possible, because SF_6 requires the addition of oxygen (see the discussion about the theoretical comparison between different cleaning precursors), and the presence of oxygen changes the power balance in the plasmas.

The SF_6 cleaning was found to be up to 75% less efficient than NF_3 and F_2. The comparison between the best known NF_3 method recipe and the corresponding (in terms of flow of atomic fluorine) F_2 recipe shows that the F_2 cleaning is about 10% faster. By increasing the F_2 flow at constant power, a linear increase in cleaning rate was measured. In comparison, an increase of NF_3 flow at constant power was shown to lead to insignificant increases in etching rate. An increase in RF-coupled power is necessary to obtain increased etching rates with increasing NF_3 flow; even using higher RF powers, the etch rate in the case of NF_3 tends to saturate. This behaviour confirms the hypothesis made above that SF_6 cannot reach the performance of NF_3, because of the rapidity of the volume recombination channel: $SF_{x-1} + F \rightarrow SF_x$. For low gas flows the NF_3 is dissociated into N and F atoms, the recombination channel $N + N + Wall \rightarrow N_2$ prohibits the recombination of F to NF_x radicals, and consequently the performances of NF_3 and those of F_2 are comparable. With increasing NF_3 flows, higher and higher power levels are required in order to achieve the dissociation of NF_3 molecules into atoms, making the NF_3 process less efficient than the F_2 one.

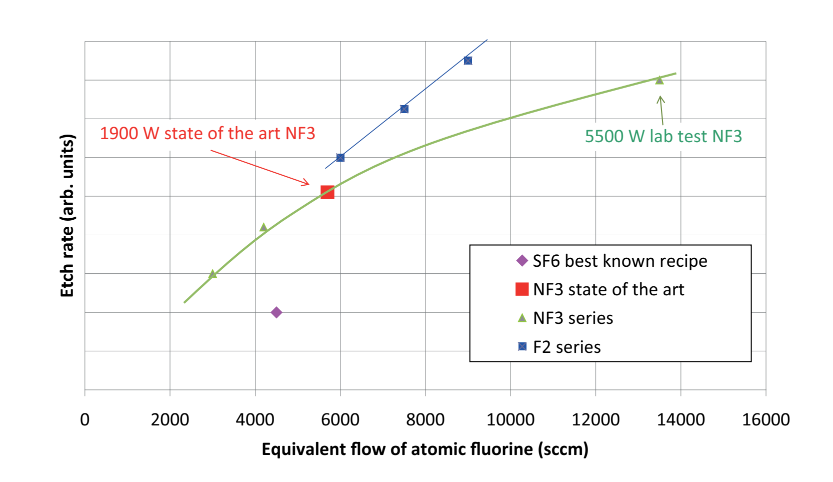

Figure 8. Etching experiments: comparison of SF_6, NF_3 and F_2.

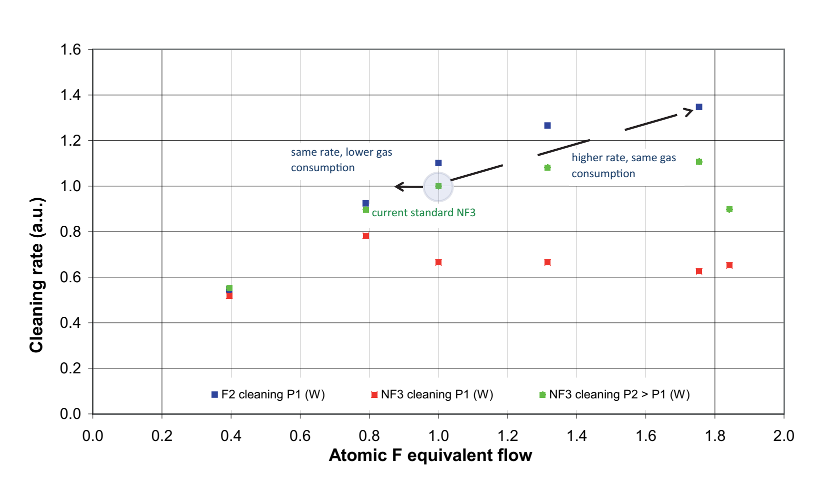

Figure 9. CR10%: comparison of NF_3 and F_2.

A second series of tests was carried out using a quadrupole mass analyzer (QMA) to monitor the signal of mass 85 (corresponding to SiF_3 and indicating the presence of SiF_4) until it reached 10% of its maximum value (see Fig. 9). The results also confirm the hypothesis made from the theoretical comparison between different cleaning precursors.

For low flows at a given RF power, the gas usage is almost 100% for both NF_3 and F_2, and the cleaning rate is much the same for similar flows of atomic fluorine. If the flow is increased at constant power, the cleaning rate will increase; however, a point will eventually be reached at which an increase in flow has no further effect on the cleaning rate, as the power available can only activate so many molecules, and non-activated molecules will just be pumped through the system without making any contribution to the cleaning. Thus, there is a maximum flow for optimum cleaning for a given coupled power.

This main advantage of F_2 over NF_3 is that the maximum flow for optimum cleaning is higher for F_2 than for NF_3: higher flows of F_2 can be used for the same coupled power while still having almost the full usage of precursors. As a consequence, depending on the target to be achieved – a higher cleaning rate or a lower gas consumption (see Fig. 10 for a comparison of the NF_3 and F_2 processes in terms of gas consumption) – there are two development strategies for F_2 cleaning:

Ontario Paid for by the Government of Ontario.

HERE'S YOUR NEXT BIG IDEA

Ontario's North is a dynamic environment, rich with new and exciting business opportunities and a rewarding lifestyle. Competitive business costs and one of the most generous R&D incentive programs in the world fuel possibility. You need to be where growth is happening. Make Ontario's North your next big idea.

YourNextBigIdea.ca

CENTRAL LOCATION IN NORTH AMERICA
Global access through efficient and reliable road, rail, marine and air transport networks

TALENTED WORKFORCE
A resourceful and skilled workforce in a broad range of industries including clean energy, biomass, aerospace and mining

WEALTH OF OPPORTUNITIES
From one of the largest chromite finds in the world to jet fuel from wood

- Using a higher F_2 flow can lead to a 35% decrease in cleaning time compared to NF_3 while keeping the cleaning gas mass consumption per module at the same level.
- Using a lower F_2 flow leads to the same effective cleaning time, whereas the F_2-mass consumption is reduced by up to 30% compared to NF_3.

> "A significantly larger process window is available for reactor cleaning when F_2 is used in place of NF_3 or SF_6."

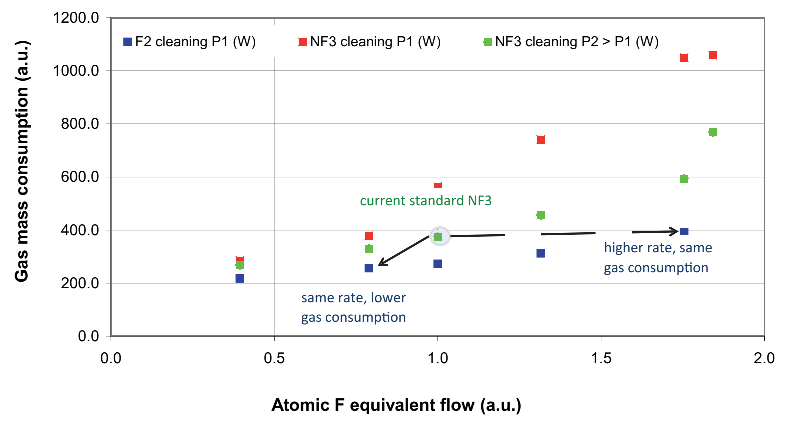

Figure 10. Gas mass consumption: comparison of NF_3 and F_2.

Conclusions

The results obtained show that a significantly larger process window is available for reactor cleaning when F_2 is used in place of NF_3 or SF_6. This leads to both time and gas mass saving, improving productivity and bringing down the cost of ownership of the reactor cleaning process.

The successful experiments on the KAI R&D platform with Gen5 glass size has allowed Oerlikon Solar to confidently transfer the process for use on KAI MT platforms, the PECVD production platforms commercialized by Oerlikon Solar.

The joint development work being carried out between two key companies in the thin-film solar industry is helping to reduce the cost of chamber cleaning, and establish molecular fluorine as the mainstream cleaning gas for thin-film silicon solar cell technology, to the benefit of both the customer and the environment.

Acknowledgement

The research leading to these results was funded by the European Union's Seventh Framework Programme FP7/2007-2013 under the 'PEPPER' project and the grant agreement no. 249782.

References

[1] Flamm, D.L. et al. 1981, "The reaction of fluorine atoms with silicon", *J. Appl. Phys.*, Vol. 52, pp. 3633–3639.

[2] Leu, G.F. et al. 2011, "Reaction coefficient of molecular fluorine at wall coated with amorphous silicon: Preliminary results", *Proc. 30th ICPIG*, Belfast, Northern Ireland, UK.

[3] Kokkoris, G. et al., 2009, "A global model for SF_6 plasmas coupling reaction kinetics in the gas phase and on the surface of the reactor walls", *J. Phys. D. Appl. Phys.*, Vol. 42, p. 055209.

[4] Kastenmeier, B.E.E. et al. 1998, "Remote plasma etching of silicon nitride and silicon dioxide using NF_3/O_2 gas mixtures", *J. Vac. Sci. Technol. A*, Vol. 16, No. 4, p. 2047.

[5] Leu, G.F. et al. 2011, "Remote plasma cleaning after mc-Si deposition", *Proc. 26th EU PVSEC*, Hamburg, Germany.

[6] Petri, S. et al. 2010, "Fluorine chamber cleaning for AKT and KAI PECVD tools", *Proc. 25th EU PVSEC*, Valencia, Spain.

About the Authors

George-Felix Leu is currently a reactor development engineer and project manager at Oerlikon Solar. He received a Physicist-Engineer Licence Diploma in optotechnics and technologies with plasmas and lasers from the University of Bucharest, Romania, and was later awarded a Ph.D. in electrical engineering by the University of Wuppertal, Germany. George's current work involves the development and qualification of the reactor for PECVD technology used in the PV industry, and also the development of fluorine-based dry cleaning.

Chris Egli received his diploma in 1995 from the University of Applied Sciences and Technology in Buchs, Switzerland; he was also awarded a diploma in engineering and business administration by the University of Liechtenstein in 2003. Chris joined Oerlikon Solar as a PECVD product manager in 2008 and managed the commercial aspects of the fluorine project from the outset. He has over 20 years' experience in various positions in the vacuum and thin-film industry.

Edgar Hepp is manager of the Product Lifecycle Management Team within the PECVD department at Oerlikon Solar. He received a diploma in engineering from the Technical University of Friedrichshafen and a Master of Business and Engineering degree from Steinbeis University in Berlin. Edgar joined Oerlikon Solar five years ago and is currently responsible for the definition of new products and new product features (e.g. cleaning gas), covering all marketing, commercial and technical aspects.

Bertrand Le Faou is currently commercial manager of the F_2 Division of Linde Electronics, with a focus on solar and semiconductor applications; he is also the Linde programme manager for fluorine qualification with Oerlikon Solar. Bertand graduated in industrial chemistry process engineering from the ENSTIMAC, France, and has extensive experience in the electronics industry, having worked in both Asia and Europe.

Jean-Charles Cigal is currently OEM programme manager with Linde Electronics. He received a master's degree in applied physics from the Université Pierre et Marie Curie, Paris, France, followed by a Ph.D. in applied physics from Eindhoven University of Technology in the Netherlands. In his current work, Jean-Charles helps equipment manufacturers to develop and implement new processes and technologies for the semiconductor, display and PV industries.

Greg Shuttleworth is currently product manager, equipment for Linde Electronics, helping develop and supply material delivery solutions for new processes and technologies within electronics manufacturing. He has a master's degree in metallurgy and science of materials from Oxford University and more than 20 years' experience in the electronics industry.

Enquiries

Dr. George-Felix Leu
Email: George-Felix.Leu@oerlikon.com

Bertrand LeFaou
Email: bertrand.le.faou@cn.linde-gas.com

Materials

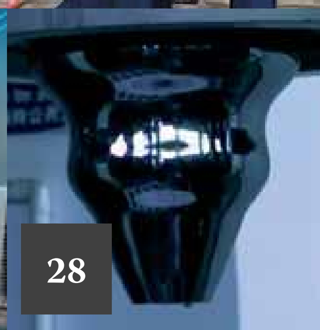

REC wins one of five grants from CERP program for clean energy development in Singapore

Renewable Energy Corporation (REC) advised that it was one of five solar energy research teams selected for a grant totalling €6.9 million under the Clean Energy Research Program (CERP). The CERP was created by the Energy Innovation Program Office (EIPO) in 2007 to accelerate the development of the clean energy industry in Singapore. This is the CERP's fifth and final grant and concentrates on two areas including the improvement of silicon wafer-based solar cell manufacturing processes and technologies, and thin-film solar cells based on the chalcopyrite materials system. REC received a grant for its proposal to develop and industrialize cost-effective and high-performing back-contact modules based on back-contacted cells using high-efficiency metal wrap through technology. REC plans to work closely with its partner ASM Technology Singapore for the project.

Source: REC Solar

REC selected for grant through CERP.

Business News Focus

Negative order intake clouds GT Advanced Technologies 2Q results

New orders for PV equipment suppliers recently reached a critical low point when SEMI posted a PV book-to-bill ratio of 0.40 for the first quarter of 2012. However, market conditions look to have worsened in the second quarter after leading equipment supplier GT Advanced Technologies (GTAT) reported a new order intake of only US$13.8 million, while a negative adjustment to its strong order backlog totalled US$31.9 million. Acute weakness in new orders from the PV and polysilicon segments underlines the current dire conditions at PV manufacturers who are forced to preserve cash and tackle structural overcapacity.

The new orders for the second quarter of 2012 included US$0.4 million of polysilicon orders, US$8.5 million of PV orders and US$4.9 million in sapphire orders. The company had US$31.9 million of negative adjustments of backlog. Revenue for the second quarter of 2012 was US$167.3 million, compared to US$353.9 million in the first quarter of 2012 and US$231.1 million in the second quarter of 2011. However, GTAT did beat guidance for the quarter, which had been set within the range of US$105 million and US$125 million.

GTAT continues to invest in new technologies to lower customer production costs.

Polysilicon headwinds unchanged at Hemlock

In reporting first-half year financial results, Dow Corning noted that "polysilicon prices remain depressed" because of overcapacity within the polycrystalline silicon markets, while "the economic and political uncertainty surrounding the solar industry" remained challenging. Dow Corning reported that overall sales were down 5% in the first six months of 2012, compared to the same period a year ago, while falling prices, especially for polysilicon, led to a 48% decline in net income. Sales overall reached US$3.09 billion and net income reached US$192 million. Hemlock and other major polysilicon producers outside of China are concerned about a trade war between the USA and China getting out of control, which could lead to punitive duties on imported polysilicon into China, despite many Tier 1 Chinese PV manufacturers depending on high-quality poly for higher performance modules, predominantly supplied by companies outside of China.

Wacker polysilicon sales down 22% as customers revise deliveries

After a rebound in polysilicon sales in the first quarter of 2012, Wacker's polysilicon sales declined 22% in the second quarter owing to customers delaying or reducing delivery quantities. Sales in the second quarter reached €286.8 million, down from €366.6 million in the prior quarter. However, the major reason for the sales decline was the substantial reduction in polysilicon prices, which will also result in lower sales being achieved this year than in 2011, according to the company.

Wacker's polysilicon division reported a second quarter EBITDA of €120.3 million, which contained €19.4 million in advance payments due to the termination of polysilicon supply agreements. However, margins remained high at 41.9%. Polysilicon plants were running close to full capacity during the quarter.

Sunways, Deutsche Solar settle on agreement for early termination of long-term supply contracts

Sunways' management board approved the conclusion of, and entered into, an agreement with Deutsche Solar in order to resolve the early termination of two long-term contracts, originally concluded in 2006 and 2007, that provide for the supply of PV wafers by Deutsche Solar. The agreement sees Sunways waiving its claim for repayment of down payments to the remaining amount of nearly €7.5 million. Furthermore, both companies agreed on an amendment of the previous terms of delivery, which provided for wafer deliveries until the end of 2017 and 2018, respectively. Sunways will decisively accept the delivery of wafers in a total volume of approximately 60MW in 2012 and 2013. The agreement has a term until December 31, 2013. Once Sunways' agreed purchase obligations have been completed the two long-term supply agreements will be considered amicably terminated.

Source: Deutsche Solar

Once Sunways' agreed purchase obligations have been completed the two long-term supply agreements will be considered amicably terminated.

Module sales at REC rebound in 2Q12

Renewable Energy Corporation (REC) reported a 13% increase in sales for the second quarter of 2012. Revenue reached NOK1,987 million (US$327 million) with an EBITDA of NOK267 million (US$44 million). Sales improved across polysilicon, silane and modules in the quarter but the company was impacted by impairment charges for the closure of its wafer operations in Norway. REC reported a quarterly loss of NOK4.1 billion (US$674 million), compared to a loss of

NOK0.2 billion in the previous quarter and generated net cash from total operating activities of NOK0.6 billion.

Management noted that the industry-wide overcapacity continued to negatively impact prices. Polysilicon and module prices declined 8% in the quarter, while silane prices fell 14%.

GCL-Poly posts loss after 60% price declines for polysilicon and wafers

GCL-Poly said that both polysilicon and wafer shipments increased in the first-half of 2012, but price declines of over 60% from the same period a year ago led to losses of HK$330 million (US$42.5 million approx), as compared with a net profit of HK$3,550 million (US$458 million approx.) for the same period of 2011.

GCL-Poly said wafer production costs were approximately US$0.26/W, a decrease of 48.1%.

GCL-Poly reported revenue of HK$11,782 million (US$1.58 billion), a decrease of 22.4% from HK$15,174 million for the prior year period. The Group's gross profit margin was 14.3%, compared with 38.6% in the prior year period. Gross profit margin for the solar business decreased from 44.2% in the first-half of 2011 to 15.5% for the first half of 2012. Gross profit was approximately HK$1.70 billion, a 71% decrease, compared with the same period in 2011.

The company reported polysilicon production continued to ramp, increasing 109.8% to 25,233MT, compared to 12,026MT for the prior year period. Wafer production also increased significantly in the first half of 2012, reaching 3,042MW, up 46.5% from 2,076MW for the six months of 2011. Polysilicon ASPs declined around 62%, while production costs only declined 14.5%, from US$22.1 per kilogram for the six months ended 30 June 2011 to approximately US$18.9 per kilogram for the same period of 2012.

Wafer production costs were approximately US$0.26/W, a decrease of 48.1%, compared with approximately US$0.51/W in the prior year period. Wafer processing cost was approximately US$0.13/W.

The company sold 9,012MT of polysilicon and 3.2GW of wafer respectively during the six-month period, representing an increase of 498% and 50%, respectively as compared with the same period last year.

Other News

Airtech's Solairtech frontsheet film receives TÜV Mark approval

Airtech International revealed that its Solairtech SA-2200 frontsheet film had received TÜV Mark approval under certificate number R 60077406001. The company's technology is used for flexible PV modules and has additionally been recognized under UL file number E33748.

Source: Renewable Energy Network

The Solairtech SA-2200 frontsheet film by Airtech International.

Airtech noted that both certifications provide flexible PV module makers with another option when looking for enhanced performance and frontsheet cost reductions in designing or building flexible, thin-film PV modules.

Heraeus hits back at DuPont's IP theft claims

Patent infringement and claims of IP theft by DuPont, on rival materials supplier Heraeus and customer SolarWorld, were put in question by the accused as the legal spat continued to be played out in public. Heraeus said in a strongly worded statement that DuPont was attempting to threaten customers over possible legal action, while Heraeus believes DuPont is attempting to discredit Heraeus' products with misleading information. The company also contested DuPont's most recent press release claims of IP theft, believing that it contradicted DuPont's posture in the current litigation and may violate the law. In its complaints - prepared under oath - relating to the '254 or '504 patents, DuPont does not allege wilfulness against Heraeus. Therefore, DuPont has effectively admitted that it has no support for any allegations of copying or 'theft' of its allegedly patented pastes, according to the Heraeus press statement.

Heraeus offers words of wisdom to EU, discouraging anti-dumping charges against China

Heraeus has joined the SolarWorld mêlée, offering words of wisdom to its peers. The Hanau, Germany-based precious metals and technology group believes the European Union should reject the recently filed complaint by SolarWorld that seeks the introduction of import duties on solar modules manufactured in China.

Dow Corning completes European Solar Energy Exploration and Development research centre

Dow Corning has completed its new European Solar Energy Exploration and Development research centre (SEED), the company has announced. SEED is part of a

Source: Heraeus

Heraeus has joined the SolarWorld mêlée, offering words of wisdom to its peers.

network of Dow Corning research facilities, with two other centres located in the USA and Korea. The European research centre includes the Solar Application Center and the Silicon Technology Center as well as a solar cell laboratory. Its aim is the development of new technologies and solar cells to increase energy efficiency, and the evaluation of materials. The cost for the construction of the facility is estimated at €9 million.

ReneSola develops Gen II Virtus wafer technology

In a conference call to discuss second quarter results, ReneSola management revealed for the first time efforts to develop a second-generation 'Virtus' wafer and cell processing technology that would be used for its expanding module business.

The company has developed a second-generation Virtus wafer, which uses a newly developed and proprietary in-house manufacturing process, the Virtus A++ process, which reduces wafers without the use of monocrystalline seeds. This new manufacturing process results in lower light-induced degradation and lower processing costs, which in turn results in a production of more distributed ingots with a greater percentage of high-efficiency products.

The CEO said that the Virtus A++ processing cost was close to US$0.12/W, far lower than its overall processing cost of US$0.17/W, though processing details were not disclosed.

However, he said that management had confidence in costs decreasing further to around US$0.11/W by the end of the year, partly due to expected cell efficiency improvements.

At present, ReneSola said that the Virtus A++ process produces wafers with average cell efficiency of 17.5% and that its next-gen

ReneSola's Virtus A++ process reduces wafer costs by not using monocrystalline seed.

Virtus II modules would have 250 watts to 260 watts of power based on a 60-cell layout. A 72-cell layout was being planned that would potentially generate as much as 300-310 watts of power.

However, modules based on its Virtus A++ wafers using the Virtus A++ manufacturing process were said to make up perhaps only a small percentage of production in the third and fourth quarters of 2012.

Product Reviews

CAMECA

CAMECA's IMS 7f-Auto key tool for optimizing Si-based PV device performance

Product Outline: CAMECA has introduced the IMS 7f-Auto Secondary Ion Mass Spectrometer, the latest version of its IMS 7f system. The new instrument is designed to deliver precision elemental and isotopic analyses, with increased ease of use and productivity for advanced materials research applications.

Problem: For solar PV installations, different material systems are being employed while combining two apparently contradictory challenges: increasing solar cell yield and reducing manufacturing costs. Silicon-based solar cell device manufacturing is based on PV Si feedstock of upgraded metallurgical-grade silicon with at least 6N purity. The quality control of the Si purification process is mandatory to ensure high-yield manufacturing.

Solution: CAMECA's new IMS 7f-Auto provides quantitative measurements of the trace element impurity concentration in PV Si feedstock, with detection limits from the ppm down to the ppb range, depending on the species to be analyzed. The analysis of light elements (H, C, O, N), main Si dopants (B, P, As), and metals (Al, Cr, Fe, Ni, Cu, et al) are particularly important capabilities. Opposite to time-of-flight SIMS tools, the detection limits of the IMS 7f-Auto are improved when increasing the profiling speed. PV Si can be analyzed in its original physical form, with fast and easy sample preparation.

Applications: R&D of novel PV cells, process control of Si-based PV devices.

Platform: The sophisticated magnetic sector Secondary Ion Mass Spectrometer integrates mature technologies from CAMECA's SIMS with additional developments, including a fully redesigned primary column, a motorized storage chamber and new advanced automation routines.

Availability: Currently available.

Bruker

Bruker's pcAFM performs OPV cell characterization in R&D environments

Product Outline: Bruker has launched its Photoconductive Atomic Force Microscopy (pcAFM) module for its Dimension Icon platform that enables sample illumination while performing nanoscale electrical characterization. In conjunction with Bruker's PeakForce TUNA technology, it is claimed to provide the highest resolution photoconductivity and correlated nanomechanical mapping for research on fragile OPV device samples.

Problem: Nanoscale structure and properties are at the core of key OPV performance parameters, which require the highest resolution data for research into OPV technologies. Special care is also required to prevent damage to fragile samples.

Solution: The Dimension Icon pcAFM accessory is a modular addition to the Dimension Icon platform designed to retain the system's top levels of performance while enabling photoconductivity measurements on OPVs and other photoelectric materials. It provides uniform back-side sample illumination and can be fibre coupled to industry-standard solar simulators. In combination with Bruker's exclusive PeakForce TUNA, it addresses the key challenge to avoid sample damage on fragile OPV samples, thus retaining high spatial resolution photoconductivity data.

Applications: Photoconductivity measurements on OLEDs, OPVs and other photoelectric materials and samples.

Platform: The pcAFM module is said to be compatible with Bruker's turnkey 1ppm glove box configuration, addressing the most stringent environmental control needs of organic photoelectric materials.

Availability: August 2012 onwards.

DuPont

DuPont Solamet PV51G offers 25% less material usage and improved adhesion

Product Outline: DuPont Microcircuit Materials has introduced its next-generation back-side silver material for high-efficiency solar cells. DuPont Solamet PV51G PV metallization is claimed to decrease dependence on silver metals by reducing overall material consumption in solar cells by up to 25%.

Problem: Reducing material costs to support aggressive reductions in overall PV module manufacturing costs continues to be key as ASP declines continue. The high price of silver continues to be a concern. Providing greater opportunities to reduce silver paste usage while helping higher conversion efficiencies is required.

Solution: Solamet PV51x series PV metallization paste products are tabbing conductors made with a breakthrough formulation that enables cell makers to use up to 25% less material and delivers comparable electrical performance versus the leading incumbent, according to the company. This helps reduce dependence on silver metals and offsets some of the impact of high silver prices. All the Solamet PV51x series products provide a wide printability window and the ability to co-fire with current Solamet front-side silver pastes, as well as an improved adhesion window. A reduced laydown and a reduced tab footprint are possible without lead or cadmium.

Applications: Back-side silver metallization.

Platform: Solamet PV51G Back-side paste is a highly conductive, solderable silver composition, developed to provide improved adhesion when used in conjunction with back-side aluminium compositions. The paste is applied in a standard screen-printing process. The pastes are part of a broad portfolio of products represented by DuPont Photovoltaic Solutions.

Availability: May 2012 onwards.

Slurry grit evolution

Halvor Dalaker & **Shawn Wilson**, SINTEF Materials and Chemistry, Trondheim, Norway

ABSTRACT

In slurry-based wafering of silicon bricks using multi-wire saws, the slurry is subject to significant evolution with time as the grits become worn and the silicon kerf accumulates. A good understanding of this evolution would allow wafer producers to make better-informed decisions on when and how to replenish slurry during wafering. This paper summarizes certain important slurry properties and presents some experimental results regarding their evolution. Sampling the slurry at the front and rear of silicon bricks during wafering has allowed the effect of a single pass through the sawing channel to be studied. The wear on the slurry grit is interpreted in terms of identifying what portion of the particle-size distribution plays the most critical role in wafering, and how this critical region changes as the slurry ages. It is found that in a relatively fresh slurry, the particles around the median size and slightly larger are the most active, while particles more than a few µm below the median play only a small part. As the slurry ages, the active region of the particle-size distribution becomes narrower, and shifts towards larger particles even though there are fewer such particles available. This leads to less slurry–brick interaction and poorer material removal properties.

Introduction

The overall goal of the photovoltaic industry is to lower the cost at which energy can be delivered to the end users. In particular, the aim is to reduce this cost to a level comparable to that of conventional energy sources, in order to achieve the long-sought grid parity. Excluding political intervention, this can be done by increasing the power output of the photovoltaic cells, and by decreasing the energy, labour and material costs of their production.

For cells based on silicon wafers, the process of cutting bricks into wafers affects the end energy price mainly through its contribution to production costs (although poor wafering practices may lead to reductions in efficiency). This is connected to the silicon material lost as kerf, the energy necessary to run the wafering process, the waste of wafers and half-completed cells as a result of inferior mechanical strength, the consumables of the wafering process and so on.

In the present economic climate, rapidly changing prices of materials and products make it difficult to gauge the exact cost contribution of the wafering step, but it has previously been estimated to be 22% of the cell cost [1]. However, that the cost is significant cannot be debated, and the nature of the global market situation makes even minuscule cost reductions worthy of pursuit.

Amid the evolution of fixed abrasive wafering and exotic kerf-free wafering techniques, the industry workhorse remains slurry wafering with multi-wire saws. In this process, a single wire is passed in many hundreds of windings around a set of guide rolls to create a wire web. The wire moves continuously in a single direction at speeds of around 15m/s, necessitating wire lengths of several hundred kilometres. The bricks are forced down onto the moving wire web while an abrasive slurry of polyethylene glycol (PEG) and silicon carbide (SiC) particles is being homogeneously applied to the web in front of the brick. The wire and the carrier fluid transports the abrasive particles to the brick, where the forces from the wire lead to a three-body abrasion process between the particles, the wire and the silicon brick.

Naturally, the properties of the abrasive slurry will influence the wafering process and the resulting wafers. While the exact microscopic details of the wafering, and thus the role of the slurry grit parameters, are not fully understood, the choice of slurry parameters, in the experience of academic and industrial players, is frequently a matter of compromise between optimizing different outputs, for example productivity versus wafer surface quality.

> “A better understanding of slurry grit evolution would allow industry players to make better-informed choices on how and when best to replace the slurry in their operations.”

As the slurry grit passes through the sawing channel, the forces acting upon it lead to the breakage of particles, and thus changes in both size distribution and shape. As a constant volume of slurry is being circulated in the machine throughout the cut, these changes accumulate. In addition, the silicon kerf and steel particles from the wire build up, changing the composition of the dry matter. The slurry is thus subject to significant evolution, and the lifetime of a batch of slurry is limited. Industrial practices vary, but after a given exposure, all or part of the slurry is dumped and replaced with freshly mixed materials.

A better understanding of slurry grit evolution would allow industry players to make better-informed choices on how and when best to replace the slurry in their operations.

As the wafer quality is determined by a combination of slurry and machine settings, a perfect understanding of slurry evolution would allow operators to change the machine parameters to match a non-static optimum point; this is the ultimate goal of slurry evolution studies. Whereas slurry evolution also involves changes in the carrier fluid (such as pH and water absorption), this discussion will focus on the SiC particles.

Slurry grit parameters

The influence of some key slurry properties has already been summarized by Anspach & Lawerenz in 2010 [2], and only a brief description of the most important parameters – particle size and shape – will be given here.

The particle-size distributions of grits available on the market conform to specifications set out in FEPA, ANSI or JIS standards. As these standards are not uniformly defined, but rather give ranges of permitted values for certain size parameters, powders following the same standard definition may still have slightly different particle-size distributions.

Coarse particles unsurprisingly have a greater abrasive effect than finer ones, and are therefore desirable from a productivity point of view. However, they also lead to more surface damage and roughness, greater kerf loss and larger thickness variation across the wafer.

The particle shape can be described by a number of different parameters, such as aspect ratio or, most commonly, circularity. The circularity of a particle is defined as the ratio between the circumference of a circle and the perimeter P of the particle, Materials

where the area of the circle is equal to the maximum area projected by the particle in 2D (A): circularity = $(4A\pi)^{1/2}/P$. Although circularity is not a perfect parameter for describing the sharpness of particles, a low value correlates to a high sharpness, and is frequently used for this purpose. A certain level of sharp particles is desired in powders for silicon wafering, so while shape parameters are not part of any of the common standards, grit manufacturers often provide information about circularity.

Particles of low circularity, in other words high sharpness, in general have better material-removal properties than blocky and near-spherical particles of high circularity, and are thus preferable from a productivity point of view. However, such particles also give rise to a higher surface roughness and may lead to greater sub-surface damage.

It should also be noted that in a powder sample the particles with the very lowest circularities are often long, thin, needle-like particles. These have a large influence on the average circularity measurement of the sample, but are not believed by the present authors to play an important role in wafering.

Experimental work

At SINTEF Materials and Chemistry a Meyer Burger 265/4 wafer saw was used for studying slurry grit evolution and other wafering-related topics. The saw had been modified to provide access to the wire web during operation, allowing slurry samples to be extracted immediately at the front and rear of the silicon brick. This set-up was used with F800 slurry grit to perform three consecutive cuts. The slurry was not replenished during this period, and samples were taken throughout the process.

Slurry size and shape was analyzed using a Sysmex FPIA 3000 sheath flow particle imaging instrument. After the analyses, the FPIA software was used to extract more detailed information, in particular by looking at certain fractions defined by limits in size and/or circularity. The samples were chemically treated to completely dissolve iron and silicon fines prior to analysis.

> "There is a clear trend towards a reduction in particle size with slurry age."

Fig. 1 shows the circle equivalent (CE) diameter of the analyzed powders as a function of cutting time. There is a clear trend towards a reduction in particle size with slurry age, explained by the wear of the wafering process on the particles. There is also a clear difference between the slurry sampled at the front and at the rear of the

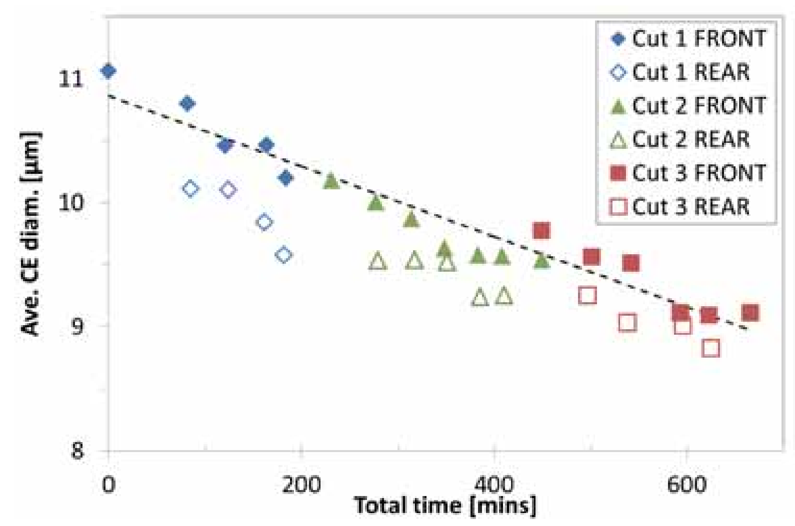

Figure 1. Average circle equivalent (CE) diameter of the analyzed powders when only particles between d50 and d3 are taken into account.

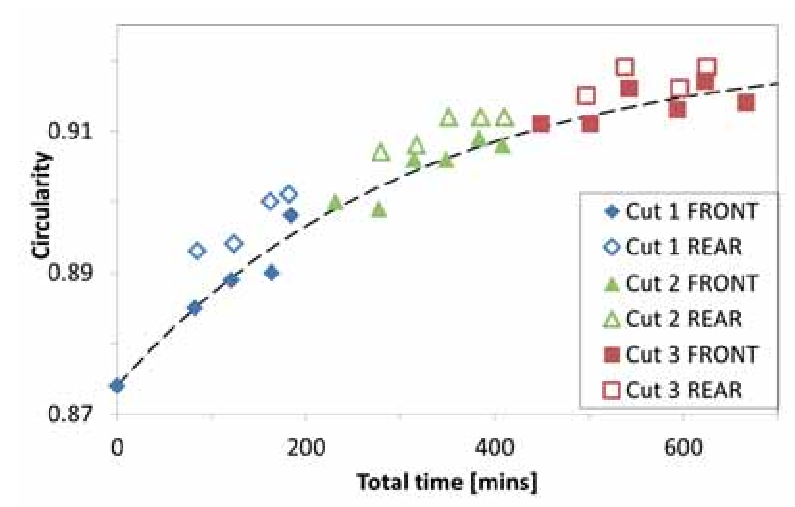

Figure 2. Circularity of the analyzed powders when only particles between d50 and d3 are taken into account.

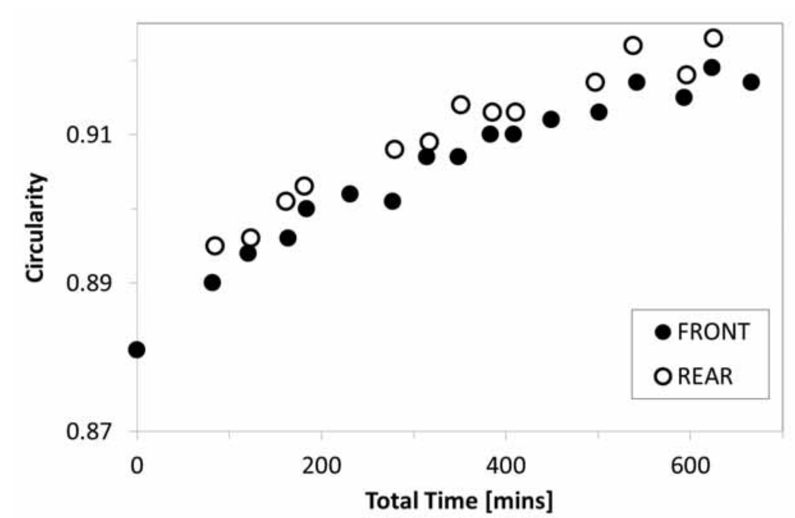

Figure 3. Circularity of particles with CE diameter between 9 and 10µm, extracted at the front and rear of the brick throughout three cuts.

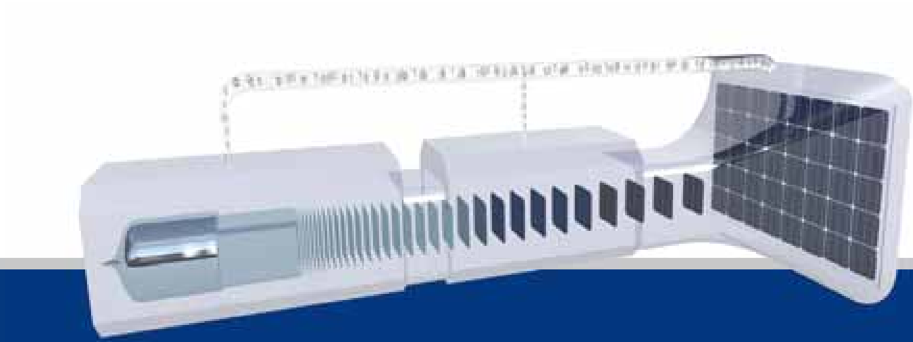

brick: the powder at the rear of the brick contains much smaller particles on average.

Fig. 2 shows the circularity of the analyzed powders. Again, two observations can be made: there is a trend of increasing circularity over the course of three cuts, and the particles extracted at the rear of the brick are typically more rounded than particles extracted from the front of the brick at a similar point in the sawing process.

The intuitive explanation is that the silicon carbide is being worn down to smaller and more spherical particles by the sawing action: the changes seen between the front and rear represent the wear on a small sample of slurry during one pass through the sawing channel, and the cumulative effect of multiple passes results in the long-term trend. However, as reported in the literature [3], it is a known theory that the larger particles are more frequently expelled from the sawing channel than the finer grit; thus the size difference seen between two samples extracted at the front and the rear is not necessarily only due to the wearing down of particles. In addition, since the shape of particles varies with size, the same issue applies to the apparent changes in circularity.

To determine if the changes seen between the front and the rear of the brick are due to the wear in the sawing channel, the circularity of the powders was analyzed and compared in fixed intervals: 9–10µm, 10–11µm and 11–12µm. The results for the first of these intervals are shown in Fig. 3: it is evident that there is a visible and significant circularity change taking place in a single pass through the brick.

In an attempt to illustrate the slurry evolution in greater detail, a more thorough examination of four powder samples will now be presented. These powder samples are all from the same batch of slurry, used to perform three consecutive cuts. The samples represent two pairs of samples, each pair having one sample from the front of the brick and one from the rear, which are taken more or less simultaneously. The first pair of samples was extracted midway through the first cut (fresh slurry), and the second pair from midway through the third cut (worn slurry), with no replacement or replenishing of the slurry. The shape analysis was performed with the Sysmex FPIA 3000 as before.

The shape analysis data for each powder was grouped in 1µm-wide size intervals (plus a >15µm bin). Figs. 4 and 5 show the particle-size distribution at the front and rear of the brick for the fresh and worn slurry respectively. As expected, in both cases there is a change in the size distribution between the front and rear of the brick. The number of large particles is seen to decrease between the front and the rear in both cases, while

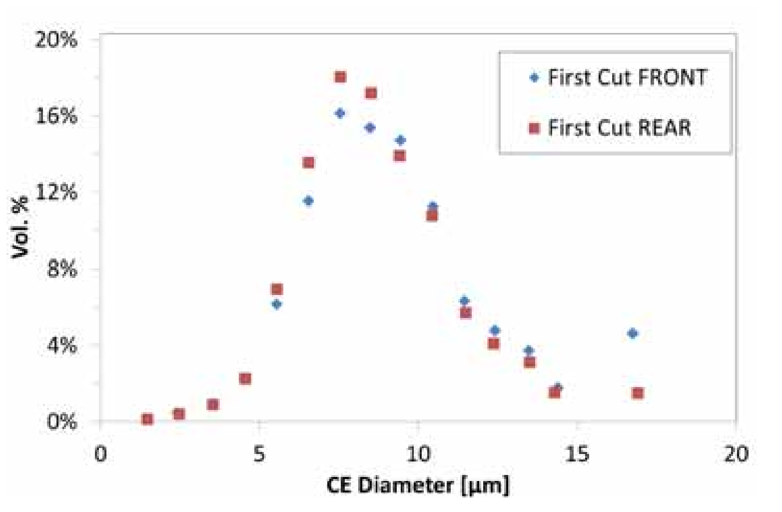

Figure 4. Particle-size distribution of samples extracted from the front and rear of the brick midway through the first cut.

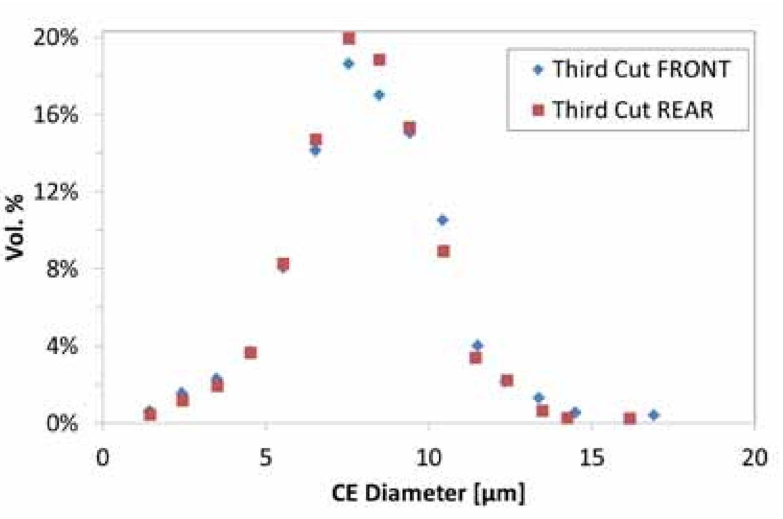

Figure 5. Particle-size distribution of samples extracted from the front and rear of the brick midway through the third cut.

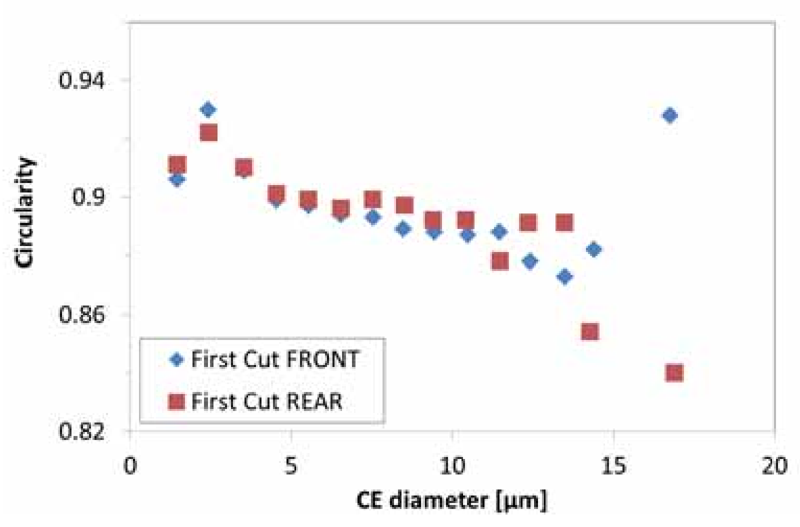

Figure 6. Circularity as a function of circle equivalent diameter: samples extracted at the front and rear of the brick midway through the first of three cuts.

there is an increase in particles around the d50 and immediately below. Moreover, the particle-size distribution for the worn slurry, in addition to being shifted to the left as expected, is somewhat narrower when compared to the fresher slurry.

> "There are more fines in the samples extracted at the front than in those taken from the rear."

A curious fact is that for both slurries there are more fines in the samples extracted at the front than in those taken from the rear. This is the opposite of what would perhaps be intuitively expected, as the fines obviously originate from the sawing channel. However, comparing worn with fresh slurry, there is no doubt that the number of fines increases with time.

The average circularity of each 1μm-size bin is plotted versus the average CE diameter of those bins and shown in Figs. 6 and 7. For the largest particles, there is significant scatter in the data, mainly caused by a low number of particles in this range. The focus can therefore be put on the particles between approximately 7 and 11μm, where in Fig. 6 it is clear that there is significant rounding of particles at the rear compared to the front. For the worn slurry in Fig. 7, the difference is much slighter.

It should be noted that Figs. 6 and 7 do not in themselves justify the conclusion that the particles from 7 to 11μm are the most important for the cutting process. It must be remembered that these two figures give only the average circularity and the change in this measurement. The number of particles represented by each point in the graphs is not taken into account.

In an attempt to visualize the combined change in particle shape and size, a 'cutting potential' is defined for each size bin. This quantity takes into account the fact that rounder particles are less able to remove material, and also that a particle bin with a larger volume fraction of the total number of particles has a greater potential to affect the sawing process. A first attempt at defining such a cutting potential is then: potential = (1 – circularity) × vol%.

The cutting potentials at the front and rear for the fresh and worn slurry are shown in Fig. 8. The areas where there is a large change in this potential are the parts of the particle-size distribution which are the most changed in terms of vol% and/or shape. It can perhaps be assumed that these areas are therefore also the areas that have the greatest effect on the sawing process (and thus wafer quality).

Looking first at the change between the front and rear for the fresh slurry, one can see that there is a large decrease in cutting potential of large particles. This is hardly surprising, as these large particles are being ground down and, in the same process, rounded. It must also be remembered that this is an area of large uncertainty because of the low number of particles present. There is also an area between

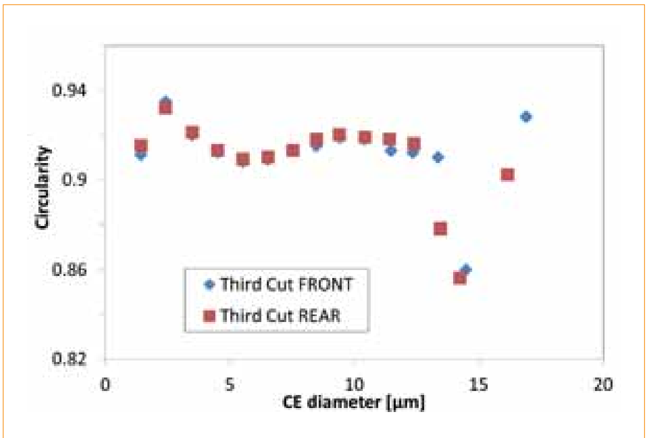

Figure 7. Circularity as a function of circle equivalent diameter: samples extracted at the front and rear of the brick midway through the last of three cuts.

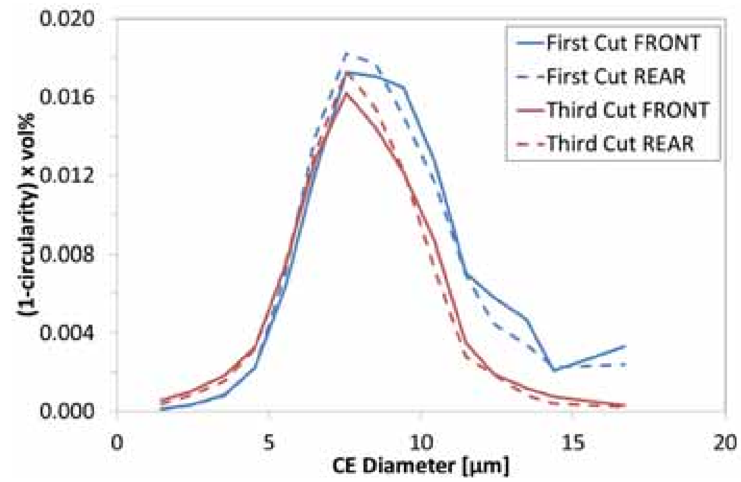

Figure 8. 'Cutting potential,' defined as the product of (1 – circularity) and vol%, plotted as a function of circle equivalent diameter. The curves show the situation at the front and rear of the brick, halfway through the first of three cuts and halfway through the last.

~5 and 8µm where there is a considerable increase in the cutting potential, meaning that the number and sharpness of particles in this range increase. This could perhaps be caused by the larger particles being broken down, leading to an increase in the number of particles, and perhaps these particles are also sharper than the 'original' particles in this size range. These two last suppositions agree with Figs. 4 and 6.

It would be natural, then, to assign the 'active region' of the cutting potential to the region that sees the largest decrease in cutting potential. For the fresh slurry, this is the region from the 9–10µm bin to the 13–14µm bin.

For the older slurry, the first observation is that the cutting potential has a narrower and lower peak, indicating a decline in material-removal properties. The cutting potential is all but gone for large particles, while there is a significant build-up of fines on the right side. There is a significant shift of the rightmost edge of the main 'bell curve' towards smaller particles, while the leftmost edge is much less affected. Particles in the 9–10µm range in the worn slurry do not, on average, have their cutting potential much changed between the front and the rear. For the fresh slurry, this had been the particle bin with the greatest reduction in cutting potential. Below this, as for the fresh slurry, there is a region down to about 5µm where the cutting potential is increased. The 'active region' has moved towards larger particles, with its lower bound now limited by the 10–11µm bin. This would mean that the cutting is now due to slightly larger particles than to the fresh slurry. As such particles are far less plentiful than in the fresh slurry, one would expect a significant reduction in material-removal properties. This is reflected in the fact that the total change in cutting potential in the active region has dropped to around half of what was observed for the fresh slurry, which – if slurry wear correlates to silicon wear – would also suggest that the action of the slurry upon the silicon block is less powerful.

"Particles around d50, and a few µm larger, are the ones most influenced by the sawing process, while particles below d50 are not affected so much."

Summary

The effect of the sawing process upon slurry grits is significant enough to be observable after one pass through the sawing channel. Accumulated over time, this leads to significant evolution of the slurry grit properties, and in how the grits interact with the silicon brick.

For a relatively fresh slurry, the large particles still play a role, while these are almost insignificant for an older slurry. Particles around d50, and a few µm larger, are the ones most influenced by the sawing process, while particles below d50 are not affected so much.

As the slurry ages and the particles are reduced in size and sharpness, the interaction with the silicon brick also changes. The region of greatest change narrows with slurry age, but the region of greatest decrease in cutting potential actually shifts towards larger particles, even though there are fewer such particles available. However, the total change of the powder is much less in an old slurry, indicating less interaction and poorer material-removal properties, as expected.

Acknowledgements

The authors gratefully acknowledge their colleagues at SINTEF Materials and Chemistry, particularly S. Armada.

References

[1] Kreutzmann, A. & Schmela, M. 2008, "Emancipation from subsidy programs", *Photon International*, Vol. 12, pp. 84–92.

[2] Anspach, O. & Lawerenz, A. 2010, "Understanding the role of abrasives used in the multi-wire sawing process", *Photovoltaics International*, 6th Edn, pp. 36–43.

[3] Kaminski, S. et al. 2010, "The role of the slurry transport in multi-wire sawing of solar silicon wafers", *Proc. 25th EU PVSEC*, Valencia, Spain, pp. 1312–1317.

About the Authors

Halvor Dalaker is a research scientist with the PV-Silicon group at SINTEF Materials and Chemistry. He holds an M.Sc. in physics and a Ph.D. in materials science from the Norwegian University of Science and Technology. Halvor has worked within the field of PV silicon for seven years, and since 2009 has been leading the activities on slurry-based silicon wafering at SINTEF.

Shawn Wilson is a senior engineer in the metallurgy department of SINTEF Materials and Chemistry. He holds a B.Sc. in Chemical Engineering from the University of Alberta, and has extensive experience in mechanical work after seven years as a journeyman mechanic with Sherritt International. His fields of expertise include the running of the multi-wire saw. Shawn is currently working on his M.Sc. thesis in materials science.

Enquiries

SINTEF Materials and Chemistry
Richard Birkelands vei 2 B
7034 Trondheim
Norway
Email: Halvor.dalaker@sintef.no
Shawn.Wilson@sintef.no
Website: www.sintef.no

Cell Processing

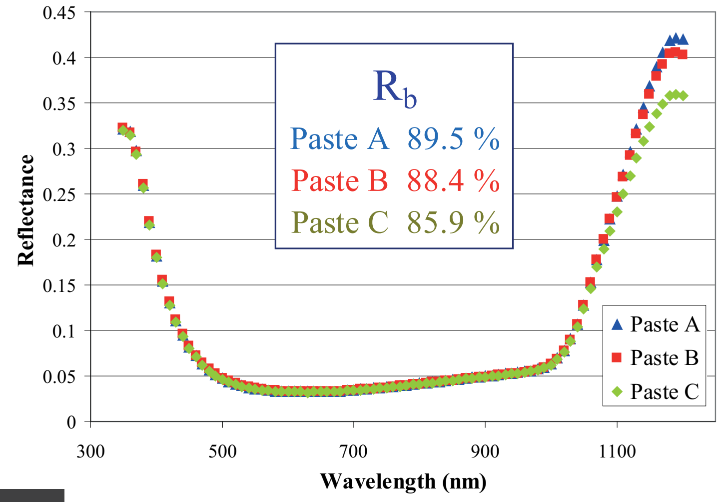

80

42

50

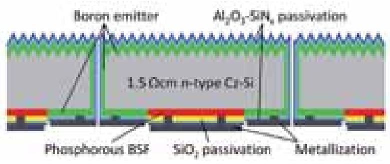

Chemtura | Organometallics

Tailor made Organometallic Specialties for high efficiency photovoltaics

AXION®

AXION® EZ 2201 HP
Diethylzinc (DEZ) Solar Grade

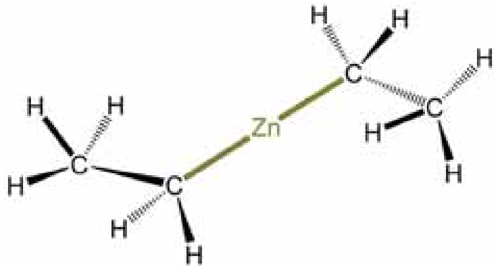

AXION® EA 1301
Trimethylaluminum (TMA) Solar Grade

AXION® EA 1303 HP
Trimethylaluminum (TMA) Solar Grade HP

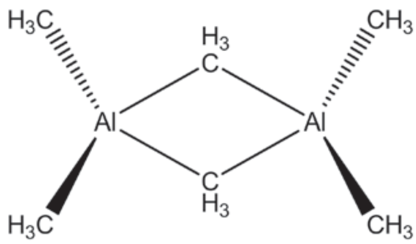

Chemtura Organometallic Specialties
Certified Quality and Environmental Management System
in accordance with DIN EN ISO 9001:2000/14001
Reg.-Nr.: 000251 QM/UM

Email: Joachim.Brueggenwerth@chemtura.com
Tel: +49 2307 661 2567
www.chemtura-organometallics.com

News

News

SunPower's next capex spending cycle not until 2014: touts cell cost reductions

Despite improving business conditions for its US residential and utility-scale businesses that have led to capacity utilization rates topping 90%, SunPower's management ruled out the need for a capital spending increase. Debottlenecking and new process migrations for all lines at Fab 2 and Fab 3 would negate the need for a new capital equipment spending cycle until some time in the first-half of 2014, which would then require the construction of Fab 4.

Production 'step-reduction' cost initiatives target a cost per watt of approximately US$1.10 by year-end, a significant improvement over the previous target of US$1.25/W and 25% lower than the 2011 cost of US$1.45/W.

SunPower highlighted both thinner wafers and supply-chain savings as two key cost reduction catalysts going forward and expects module costs of approximately US$1.0/W to US$0.75/W on an efficiency-adjusted basis, a full year ahead of previous targets.

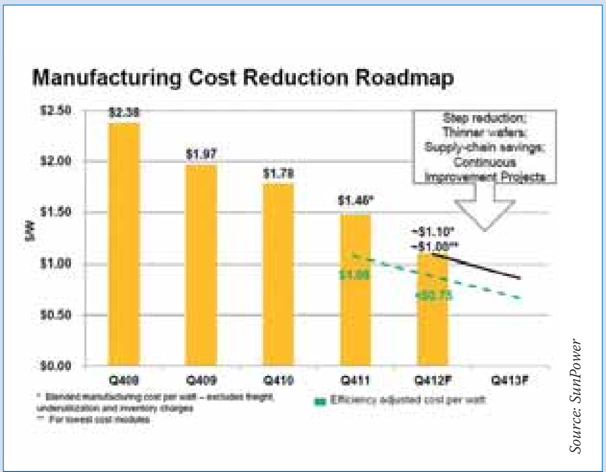

SunPower targets cost per watt of around US$1.10 by year-end.

R&D News Focus

Natcore to use cheaper nanoparticles for 'Black Silicon' solar cells

Even before 'Black Silicon' technology, based on IP developed by the National Renewable Energy Laboratory (NREL) and licensed to Natcore Technology, had reached commercialization, the technology will undergo a major material shift to reduce costs.

Reflecting the challenges of bringing new technology to the PV market during a phase of steep material price declines, NREL has expanded its licence agreement with the start-up to use copper nanoparticles in the etching process instead of nanoparticles of gold or silver.

Black silicon refers to the apparent colour of the surface of a silicon wafer after it has been etched with nanoscale pores; the black colour results from the virtual absence of reflected light from the porous wafer surface. NREL and Natcore scientists claimed a reflectance in the visible and near-infrared region of the solar spectrum of 0.3%, boosting conversion efficiencies.

SERIS purchases ALD tool from SoLayTec

The Solar Energy Research Institute of Singapore (SERIS) has ordered an ALD process tool from SoLayTec that will see the former utilize the process at several global research institutes. SERIS has also entered into a three-year research agreement with SoLayTec and metalorganics material supplier AkzoNobel to study the viability of the integration of Al_2O_3 into new cell concepts. The contract also extends SoLayTec's reach into Asian markets.

Kaneka, imec's 6" heterojunction silicon solar cell reaches 22.68% conversion efficiency

Fraunhofer ISE recently confirmed that Kaneka and imec's six-inch, semi-square, heterojunction silicon solar cell has a certified power conversion efficiency of 22.68%. The solar cell has an electroplated copper contact grid on top of a transparent oxide layer, which essentially replaces the traditional silver screen printing and is said to lead to higher efficiencies with lower manufacturing costs.

The silicon solar cell was developed at Kaneka's Osaka lab using its copper electroplating technology, which is based on imec's copper electroplating background.

The results were said to prove the capabilities of copper metallization for next-generation solar cells and that in the future copper would play an important role in high-efficiency and sustainable solar cell technology.

.

Cell Production News Focus

Roth & Rau's CAMiNI firing furnace qualifies for use in mass production processes

Roth & Rau's CAMiNI firing furnace was recently deployed for the first time in a production line for a major, but undisclosed, Taiwanese cell manufacturer,

Roth & Rau's CAMiNI furnace qualifies for mass production processes.

leading the company to state that CAMiNI has successfully qualified for use in mass production processes. By the end of the qualification stage, the furnace is said to have completed a 1,000,000 wafer endurance trial, with the cell manufacturer advising that better process results had been achieved with CAMiNI than when using competitor products. Roth & Rau noted that this success was because its furnace allows for processes to be flexibly adapted to different cell types and set new standards in temperature stability and repeatability. The cell manufacturer is said to have achieved a maximum cell efficiency rate of 19.14% during the qualification stage, with an average rate of 19%. Energy usage was said to have been cut by nearly 50%, with the company advising of low breakage rates.

bSolar to build 730kW ground-mounted solar project in Japan using bifacial PV cells

bSolar, through its strategic partner and Japanese distributor TSBM, has won a contract to construct a 730kW ground-mounted solar project in Nasukarasuyama city, Tochigi, Japan. The project is expected to go online in December and will feature bSolar's disruptive bifacial PV cells. bSolar also noted that its bifacial cells will be incorporated into several new solar modules by leading manufactures, including aleo solar, asola Solarpower, Solarnova Produktions-und Vertriebs and Solar-Fabrik.

Schott Solar announces surprise exit from c-Si manufacturing

Continuing market constraints and unattainable cost bases have conspired to force Schott Solar's management to withdraw from c-Si PV manufacturing completely. Although the company's thin-film and CSP activities are unaffected by this news, this exit from the c-Si sector will affect around 870 employees as well as its Mainz and Alzenau plants in Germany, Valasske Mezirici in the Czech Republic and Albuquerque in New Mexico.

As a glass manufacturer, Schott's remaining in the thin-film and BIPV applications market is one that needs little explanation. The company had also released a management statement last year that claimed that the CSP sector was strong for the company in terms of contracts.

The company's main focus has been on manufacturing wafer-based cells and modules, and in 2010 it had reached a global production capacity of 450MW per year of both cells and modules. In January this year, Schott announced the closure

Schott Solar's management to withdraw from c-Si manufacturing.

of its multicrystalline wafer operations in Jena, Germany, impacting 290 workers, but stressed that its monocrystalline wafer production in the same location would continue.

Management is said to have investigated several options in an attempt to maintain its crystalline PV production, all of which have compounded the company's opinion that remaining in this sector is no longer economically feasible.

Over the past two years, Schott has managed to shave up to 50% off its cost base; however, industry analysts have claimed that some competitors' cost bases – particularly those based in Asia – have seen closer to 60% reductions in costs over the space of one year. Prices of multicrystalline wafers have more than halved in 2011, after declining around 40% in the prior year as significant levels of new capacity in China, Korea and Taiwan were ramped.

Business News Focus

Applied Materials solar sales flat at US$77 million

Management at Applied Materials spent little time discussing the performance of its Energy and Environmental Solutions (EES) division results, which houses the majority of its solar sector equipment and services to the PV industry. The company reported EES sales in its financial third quarter that were almost flat with the previous quarter at US$77 million. However, new orders decreased significantly to only US$35 million, compared to US$62 million in the prior quarter.

Inventory write-downs (US$26 million) and restructuring charges of its EES division helped Applied produce a non-GAAP operating loss of US$64 million, up from US$57 million in the previous quarter. Non-GAAP operating losses from its EES Division for the current financial year have topped US$138 million.

Management also acknowledged that the downturn in capital spending due to industry overcapacity had been longer and deeper than previously expected. Concern was also raised over the lack of speed in the industry consolidation process, a prerequisite for a spending recovery.

centrotherm gains €50 million in bank loans: Taiwanese cell producers place new orders

centrotherm photovoltaics has received loans from an unidentified number of banks, amounting to approximately €50 million. Currently in insolvency proceedings, the cash injection was said to result in the company having around €90 million of liquidity, supporting ongoing operations such as equipment shipments, spare parts deliveries and general services. The company also announced that it had received orders from Taiwan-based c-Si solar cell manufacturers. Although the customers were not identified, centrotherm said that one customer was new to the company, having placed a multiple equipment order that included diffusion and anti-reflective coating tools. A long-standing Taiwanese customer was said to have placed an order for centrotherm's fast-firing furnace, c.FIRE.

Solar3D solar cell claims a US$6.2 billion impact on global market

Solar3D has released a statement claiming its three-dimensional solar cell could have delivered more than US$6.2 billion of additional electricity in the world last year. The company's analysis indicates that a typical 17% efficient solar cell performs more like a 5% efficient cell when light is shining 20 degrees from the side, such as during the morning or evening hours. The company estimates that its Solar3D cell can maintain a high 25% efficiency for a longer period of time, over the course of a day and year. Solar3D states that this translates into 200% more power than conventional solar cells and a system payback period that is approximately half the time of the current solar technologies.

Solar sales at Manz sink to 12% of total revenues; diversified markets limit sales decline

Supporting the need to have a diversified market approach, equipment supplier Manz reported first-half 2012 sales of €113.5 million and an operating profit of €1.1 million, despite solar equipment sales declining to only 12% of total revenues. Manz said that strong sales and orders in its display segment and entry into the battery market were key reasons for overall sales in the period only falling around 16%.

Manz reported a significant decline in sales within its solar segment, providing further proof of the collapse in capital spending from PV manufacturers as they continue to be impacted by severe


SCHMID
Let the Sun shine. Catch the Power.
Silver-free cell backside saves 6 US cent/wafer and increases efficiency by 0.2%abs.
Easy integration of TinPad into cell and module lines.
Payback time 7-9 months.
TinPad
www.schmid-group.com
No silver - more profit!


MIKRON
THE AUTOMATION SOLUTION
AS A WORLD LEADER IN AUTOMATED ASSEMBLY, MIKRON OFFERS HIGH PERFORMANCE SOLUTIONS FOR THE PHOTOVOLTAIC INDUSTRY.
WE MANAGE PRODUCTION PROCESSES IN SILLICON AND THINFILM TECHNOLOGIES.
WWW.MIKRON.COM
AMERICA: DENVER (USA) - ASIA: SINGAPORE, SHANGHAI (CHINA) - EUROPE: BOUDRY (SWITZERLAND), BERLIN (GERMANY)

News

overcapacity. Manz said that it had generated only €13.1 million in revenue from the solar segment, down from €46 million in the same period a year ago.

However, core competences in the fields of automation, laser process technology, vacuum coating, printing, metrology and wet chemical processes would continue to be invested in, though management warned that weak sales to the PV industry could still impact earnings for the full-year.

Meyer Burger makes a first time loss as new orders fall 84%

Citing continued reluctance of customers to place equipment orders in response to continued industry overcapacity and widespread quarterly losses, Meyer Burger still expects sales to top CHF600 million in 2012. Although management highlighted concern as to the overall industry conditions, improvements in equipment order intake are expected in 2013. The company made a loss for the period of CHF34.2 million, the first time it had reported a loss since its 2006 IPO.

With record sales and orders in 2011, Meyer Burger's sales for the first-half of 2012 look to have fallen drastically. Sales reached CHF307.8 million (US$316 million approx.), down from 575.0 million in the first-half of last year.

On a geographical basis, Meyer Burger reported that the Asia region generated 77% of net sales. Europe provided 18% of net sales while the USA accounted for 5% of net sales.

Order intake faired worse. The company noted that new orders fell 84% in the first six months of 2012 compared to the prior year period. However, new order intake actually increased 44% when compared to the second half of last year. New orders were CHF128.4 million (US$131 million approx.) in the first six months of 2012, compared to a record high of CHF787.6 million in the same period a year ago.

The all-important order backlog for the first six months stood at CHF672.6 million (US$691 million approx.), down from CHF909.9 million as of the end of December, 2011.

Meyer Burger said that it expected sales for the full year to be in the lower half of previous guidance (sales CHF600–800 million; EBITDA margin between 4 and 8%).

Q-Cells creditors approve sale of business operations to Hanwha

After filing for insolvency on April 3, 2012, Q-Cells creditors have approved the sale of the business operations to the Hanwha Group, whereby Hanwha will assume responsibility of 1,250 employees (from 1,550) and most parts of the total Q-Cells Group. Q-Cells Bitterfeld-Wolfen administration site in Berlin, a production site in Malaysia and some international sales companies are included in the transaction. Both companies noted that many of the job cuts in the Q-Cells organization will be from the administration side.

The purchase price is comprised of the takeover of operational liabilities and falls in the lower triple-digit millions, with a cash component in the mid double-digit millions. The purchase agreement is still subject to the approval of certain anti-trust authorities.

"In the current macroeconomic and political environment, which is extremely difficult for Q-Cells, it is a great success that we managed to maintain not only research and development, but also the production capacities at the Bitterfeld-Wolfen site," Schorisch emphasized today at the Q-Cells headquarters in Bitterfeld-Wolfen. "While I regret the fact that there are certain job losses, I am very happy that Q-Cells has found a strong partner in Hanwha, who has the necessary means to provide company, brand and staff with long-term perspectives again."

Schorisch noted that he has begun negotiations with the works council on reconciliation of interests and a social plan because of the required staff adjustments. Further, the insolvency administrator has brought up the issue of funds to establish a re-employment and training company where the employees affected will be able to receive training and support in order to find new jobs.

Q-Cells creditors accept Hanwha bid to take over the company: top 5 PV manufacturer created.

Amtech posts revenue of US$24 million: implements cost-cutting measures

Despite a 13% increase in sales for its fiscal third quarter, specialist PV equipment supplier Amtech Systems has implemented new cost-cutting measures to tackle the downturn that has proved to be longer and deeper than expected. The cost reductions include voluntary salary reductions by management, ranging from 10 to 20% and salary reductions of other corporate staff.

The cost savings were put at US$6-US$7 million in fiscal 2013, though the company reiterated that it would continue to invest in key R&D programs for the PV industry, including its ion implant technology, launched at SNEC in Shanghai earlier this year. Management said that the cost savings would not impact customer engagements.

Amtech reports net revenue for the third quarter of fiscal 2012 of US$24.3 million, up 13% sequentially from US$21.6 million for the preceding quarter. The increase in sales was primarily due to previously deferred revenue on shipped equipment to PV manufacturers.

New order intake was US$6.1 million but only US$0.7 million for its solar segment, which was down from total orders of US$18.0 million ($7.2 million solar) in its fiscal second quarter. Total order backlog stood at US$35.6 million, compared to total backlog of US$67.4 million at March 31, 2012. Amtech's solar segment order backlog stood at US$26.1 million, compared to US$54.1 million at the end of the fiscal second quarter.

Product Reviews

Manz

Manz enters wet-chemistry front-end process market

Product Outline: Manz has launched new equipment to address the wet-chemical processing of crystalline silicon solar cells. The IPSG CEI 4800 has a claimed throughput of 4,800 wafers per hour and integrates chemical edge isolation (CEI) and phosphor silicate glass (PSG) removal.

Problem: Cost-reduction strategies within c-Si processes remain a critical focus of PV manufacturers. Attention to wafer throughput while offering a lower cost tool is essential, which can be met by integrating multiple process steps in a single tool.

Solution: The IPSG CEI 4800 removes the highly doped layer from the back side and the edges of a wafer and creates a CEI step. In a second process the remaining PSG layer on the front side of the wafer that was created during the previous diffusion process step is removed. The newly developed soft sponge roller process concept enables faster inline transportation speeds and ensures higher process stability combined with gentle wafer handling at the same time. Due to a magnetic coupling system the gear wheels and drives are completely separated from the wet-chemical bath.

Applications: Phosphor silicate glass removal and edge isolation.

Platform: The IPSG CEI 4800 footprint is approximately 12,200 x 2,150 x 2,200mm in non-automated configuration and 16,250 x 3,050 x 2,600mm with automation. Throughput is claimed to be 4,800 wafer/h (with optimization giving up to 5,000 wafer/h). Performance uptime is said to be 95% and the wafer breakage rate delivered is <0.1% including the use of automation.

Availability: May 2012 onwards.

Digital Photonics

Digital Photonics offers scalable route from lab to fab

Product Outline: The Digital Photonics Corporation (DPC) has launched the SolarJet printer for selective emitter application of solar front contacts (c-Si). The SolarJet printer is claimed to simplify offline process feasibility by making it possible for labs to quickly, accurately and cost-effectively gauge real-world performance benefits before making larger inline investments.

Problem: Taking selective emitter processes cost effectively and within the shortest timescales can be problematic because of the significant variances in lab to fab equipment. Providing a scalable and reproducible process path is required.

Solution: The SolarJet simplifies feasibility testing by allowing for scalable and highly indicative test runs. Wafers are fed from underneath along a conveyer belt (as in typical production runs) to provide accurate production simulation. Up to three separate photovoltaic materials (such as etchants, dopants and dielectric layers) can be deposited in a single run – further simplifying and speeding up testing processes. The SolarJet has a vision capture system for quality control, consisting of three distinct CCD cameras that monitor the dispensed droplets and resulting lines. The system ensures adjustments can quickly and easily be made to guarantee reliable, reproducible print quality. The SolarJet has a throughput capability of 30 wafers per hour with manual loading and up to 200 wafers per hour with the auto-loading system.

Applications: Selective emitter processing.

Platform: The SolarJet system is the first in the industry to use the new VersaEtch Etchant / n-Dopant combination material from Trident Solar as a precursor to screen printing of front silver contacts.

Availability: May 2012 onwards.

2BG

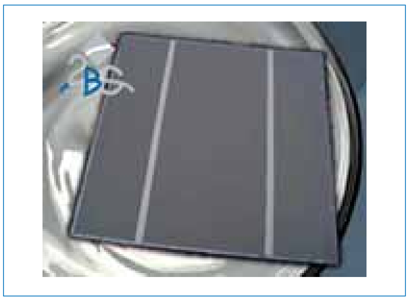

2BG employs Selective Plating technology for silver-free back-side contact cells

Product Outline: 2BG is introducing a new technology in order to completely remove the use of silver paste from crystalline silicon solar cell back sides, resulting in improved cell efficiency and a significant reduction in costs. The technology is a result of a partnership with Rise Technology, an Italian company founded by researchers from La Sapienza University, Rome.

Problem: All the main players of the PV market are focusing on increasing solar cell efficiency by combining significant reductions in the production cost. Although the industry has focused on silver paste consumption issues, enabling a host of new formulations entering the market that reduce usage, while improving cell efficiencies, the key next-generation step is to eliminate its use altogether. Back-side copper plating is seen as a key future technology.

Solution: The Selective Plating process makes it possible to directly deposit aluminium, copper and tin instead of silver pastes, achieving a claimed saving of up to €0.6 per wafer, with efficiency increases of up to 0.2%; the data relates to cells with 6" dimensions. Selective Plating also allows an adherence level four times higher than standard silver paste. This technology is claimed to allow a return of investment in less than one year and offers the opportunity to use it in working plants, without changing standard production processes.

Applications: All crystalline cell manufacturing lines, without relevant modifications to standard production processes.

Platform: Any further information will be disclosed directly to interested parties.

Availability: From October 2012 onwards.

Back-contacted high-efficiency silicon solar cells – opportunities for low-cost metallization and cell interconnection

Nils-Peter Harder, Agnes Merkle, Till Brendemühl, Fabian Kiefer, Ralf Gogolin, Martin Lehr, Frank Heinemeyer, Henning Schulte-Huxel, Bianca Lim, Verena Jung, Sarah Kajari-Schröder, Marc Köntges & **Rolf Brendel**, Institute for Solar Energy Research Hamelin (ISFH), Emmerthal, Germany

ABSTRACT

This paper presents ISFH's recent developments and advances in the field of back-contacted silicon solar cells. The efficiency potential of back-contacted solar cells is very high; nevertheless, in industrial production, back-contacted solar cells are decidedly the minority. In the field of back-contacted solar cells, ISFH has developed several cell concepts and new processing techniques, such as laser ablation for silicon structuring, contact opening through passivation layers, and hole drilling for emitter-wrap-through (EWT) solar cells. The latest results are presented regarding ISFH's work on back-junction back-contacted solar cells and EWT solar cells, as well as on back-contacted solar cells employing an amorphous/crystalline silicon heterojunction. Also discussed are the advances in high-throughput evaporation of aluminium as a low-cost option for the metallization of back-contacted solar cells. Finally, a novel, silver-free cell interconnection technique is presented, which is based on the direct laser welding of a highly conductive, low-cost Al foil, as a cell interconnect, onto the rear side of back-contacted solar cells.

Introduction

In 1977, Lammert and Schwartz [1] proposed the concept of the interdigitated back-contact solar cell for use in concentrated sunlight; since then, many different designs of back-contacted silicon solar cells have been proposed and further developed, as summarized in a review article by Kerschaver and Beaucarne [2]. In high-volume production, back-contacted silicon solar cells have already achieved efficiencies of more than 22% [3]. In addition, SunPower have reported an energy conversion efficiency of 24.2% on an area of 155.1cm^2, thus proving the potential of this solar cell structure [4].

Besides the back-junction back-contact (BJBC) concept, the field of back-contacted solar cells also includes the emitter-wrap-through (EWT) structure [5,6] and the metal-wrap-through (MWT) technology [7]. While the EWT concept is currently not commercialized, possibilities for industrial-scale production were investigated by the former Advent Solar (now owned by AMAT), yielding efficiencies of up to 19.0% on boron-doped p-type Czochralski-grown silicon (Cz-Si) [8]. MWT solar cells, meanwhile, have achieved 19.7% on n-type Cz-Si [9] and 20.1% on B-doped p-type Cz-Si [10].

The fact that back-contacted solar cells provide the metallization for both electrical polarities at the rear side has the potential to simplify the cell interconnection process in module manufacturing. In the past, several processes have been developed specifically for the interconnection of back-contacted solar cells. MWT cells, for example, are glued with conductive adhesives to a conductive backsheet [11,12]. Typical conductive adhesives contain silver [12] and are therefore cost intensive. In other, much more advanced or explorative, concepts the front side of the cell is processed first, after which the cells are bonded to a glass substrate [13,14]. The rear side of the cells is subsequently processed, and finally the cells are interconnected either by low-temperature Ag paste [13] or by a combination of Ag/Al metallization and a transparent conductive oxide [14].

This paper summarizes recent results obtained by ISFH on back-contacted wafer solar cells, including BJBC and EWT, as well as the combination of the back-junction concept with amorphous/crystalline silicon (a-Si:H/c-Si) heterojunction (SHJ) technology. Each of these three concepts has distinct advantages. While the BJBC concept using, for example, a front-surface field (FSF) has the higher efficiency potential, EWT cells (emitter at the front) are known for their higher robustness with respect to variations in the front-surface passivation. Heterojunction technology, on the other hand, minimizes recombination by combining surface passivation with the process of contacting the solar cell.

In general, back-contacted solar cells require a high ratio of minority-carrier diffusion length L (within the bulk) to device thickness W, as well as exceptionally low values for the front-surface recombination velocity. The latter can be achieved either with direct passivation of the front side, by using a FSF, or with a (floating) emitter at the front side. In order to ensure high minority-carrier diffusion lengths within the bulk, P-doped, n-type Czochralski-grown silicon (Cz-Si) is used as base material.

> "ISFH developed two different technologies for the interconnection of Al-metallized solar cells."

For the purpose of reducing the material cost, ISFH developed two different technologies for the interconnection of Al-metallized solar cells. Note that this metallization does not involve any masking steps, but instead a self-aligned separation of the contacts. Evaporation of Al has long been used for laboratory-type solar cells. However, this technique has so far not been implemented into industrial solar cell production on a large scale, in part due to the unavailability of a suitable cell interconnection technique for Al-metallized cells.

Two techniques for Al-based cell interconnection, as developed at ISFH, will therefore be presented in the last part of this paper. First, the deposition of solderable metal stacks, such as Al/Ni:V/Ag on Al-metallized stacks, is considered; importantly, these metal stacks can be deposited with the same equipment used to evaporate the Al. Second, a new interconnection technique recently developed at ISFH is presented, in which

the Al-metallized rear side of a solar cell is directly laser welded with an Al-layer to a transparent substrate (AMELI process).

Back-junction back-contact cells

For the fabrication of the BJBC solar cells, (100)-oriented phosphorus-doped 12.5×12.5cm^2 pseudo-square Cz-Si wafers were used, with a thickness of 200µm and a resistivity of 1.0Ωcm. A schematic cross section of the BJBC solar cells presented in this work is shown in Fig. 1. The front side of the cell is textured with random pyramids and passivated by plasma-enhanced chemical vapour deposited (PECVD) silicon nitride (SiN_x), which also acts as an anti-reflective coating. On the rear side, the boron-diffused p^+ emitter regions are interdigitated with phosphorus-diffused n^+ back-surface fields (BSFs) on two height levels. This structure is realized by laser ablation of silicon and an additional damage etching without any photolithographic patterning steps [15]. Both the emitter and the BSF are passivated with a thermally grown oxide layer (SiO_2). A picosecond laser is used for laser contact openings (LCO) by locally ablating the thermally grown SiO_2 [16].

The metallization of the cell is realized in a single mask-free vacuum evaporation process of aluminium and a thin layer of silicon oxide (SiO_x). The SiO_x layer acts as an etching barrier in the next wet chemical aluminium etching step to achieve a self-aligned separation of the emitter and base regions. The separation of the contacts occurs at the vertical flanks of the laser-generated structure [17,18]. Note that the Al at the rear side of the cell is sufficient for module integration with ISFH's aluminium-based mechanical and electrical laser interconnection (AMELI) process, which will be discussed later.

Table 1 summarizes the measured parameters of such a BJBC baseline solar cell under standard testing conditions (25°C, 100mW/cm^2, AM 1.5G). These measurements were carried out in-house using a LOANA system from pv-tools, with the total area of the cell (155.1 cm^2) being illuminated. Table 1 also includes the performance of an optimized cell of the same size. For this optimized cell, an improved passivation layer was used for the rear side.

The baseline solar cell has an efficiency η = 20.7% and the optimized cell 21.4%. Both of these performances refer to the total wafer area, including all edges and busbars. The open-circuit voltages (V_{oc}) of 668mV and 683mV demonstrate effective passivation of the front and rear sides, respectively. The short-circuit current densities (J_{sc}) of 40.6mA/cm^2 and 40.8mA/cm^2 also confirm front-surface passivation and preservation of the high carrier lifetimes during the cell processing. The high current is further promoted by a large emitter coverage area as well as high rear-side reflection at the silicon/thermally grown SiO_2/aluminium. The fill factor (*FF*) losses are mainly due to a high series resistance (R_s) of 1.5Ωcm^2.

Simulations of the busbar regions [19] show that these regions have a significant impact on cell efficiency. These results were confirmed by measurements of cell performance with busbars excluded. Losses in the emitter busbar lead to a reduction in the fill factor, while losses in the base busbar reduce the short-circuit current density [3,19]. Therefore, a re-design of the cell layout – where one or both busbars are omitted – has the potential to realize a cell efficiency of over 21% for the baseline cell. For the optimized cell structures, a designated area efficiency of 22.4% on 133cm^2 has been determined.

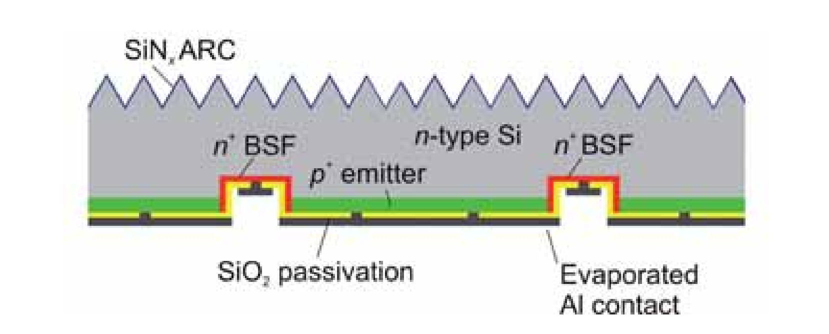

Figure 1. Cross section of the BJBC baseline cell presented in this work.

	A [cm^2]	η [%]	*FF* [%]	V_{oc} [mV]	J_{sc} [mA/cm^2]
Best baseline cell (Fig. 1)	155.1	20.7	76.4	668	40.6
Optimized process	155.1	21.4	76.9	683	40.8

Table 1. Cell parameters measured under standard testing conditions (STC) for a BJBC cell fabricated at ISFH.

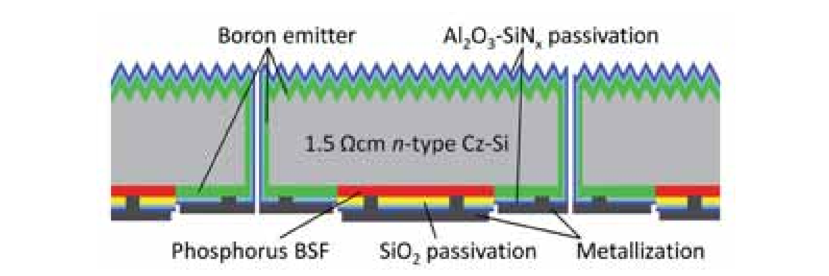

Figure 2. Schematic cross section of the EWT solar cell (adapted from Kiefer et al.).

High-efficiency emitter-wrap-through cells on n-type Cz-Si

For back-junction solar cells it is crucial to minimize the recombination at the front side, while EWT cells are far more tolerant. One possibility is the direct passivation of the base, as shown in Fig. 1; another, potentially more effective, way is the implementation of a FSF. However, when using a FSF it is imperative that both the control of the doping profile and the passivation are excellent. One way to overcome this issue is to use a front-side emitter instead of a FSF: the front-side emitter enhances the robustness of the cell structure to variations in front-surface passivation quality.

"For back-junction solar cells it is crucial to minimize the recombination at the front side, while EWT cells are far more tolerant."

As an alternative to a BJBC solar cell, a back-contacted solar cell can be realized using the concept of an EWT solar cell [6], connecting front and rear emitters by via holes. These via holes can be seen in the cross section of the EWT solar cells depicted in Fig. 2. Phosphorus-doped n-type silicon with a base resistivity of 1.5Ωcm was used. This design allows benefit to be gained from the combination of high lifetimes and high base conductivity. The layout of the rear side of our EWT cells has an interdigitated


FOLLOW
US ON
TWITTER!
@pv_tech

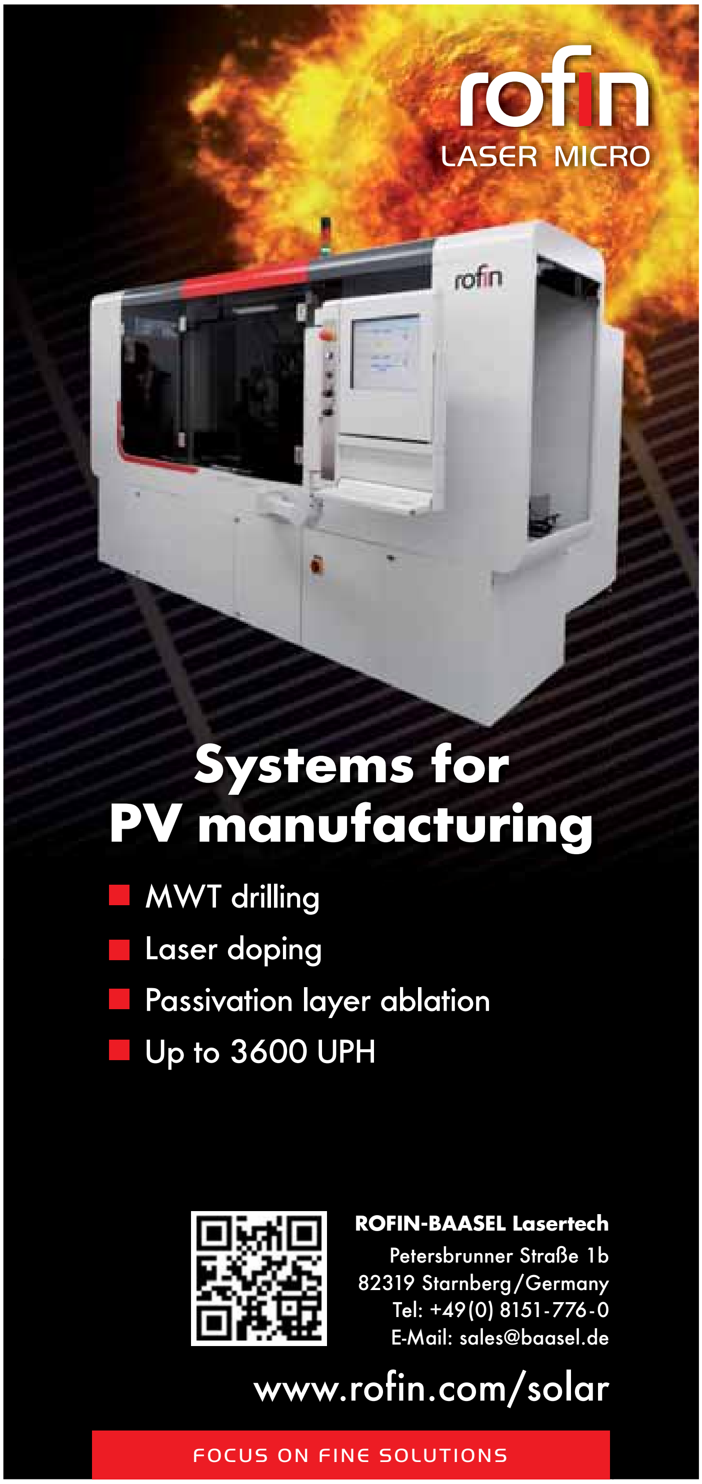
rofin
LASER MICRO
Systems for
PV manufacturing
MWT drilling
Laser doping
Passivation layer ablation
Up to 3600 UPH
ROFIN-BAASEL Lasertech
Petersbrunner Straße 1b
82319 Starnberg/Germany
Tel: +49(0) 8151-776-0
E-Mail: sales@baasel.de
www.rofin.com/solar
FOCUS ON FINE SOLUTIONS

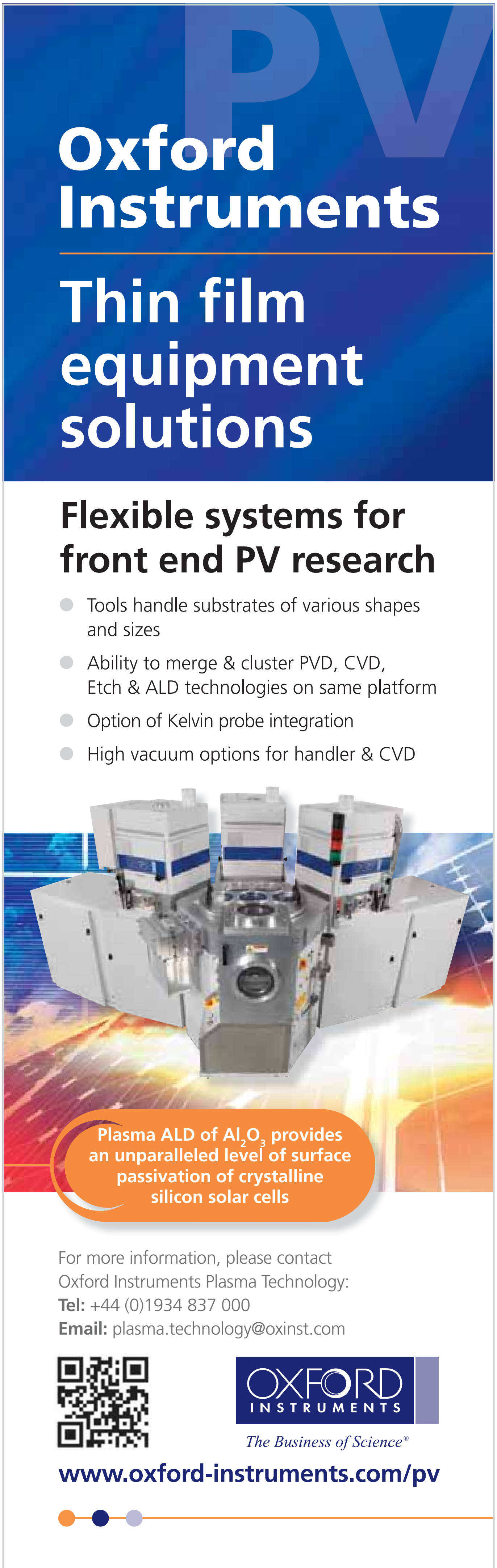
PV
Oxford
Instruments
Thin film
equipment
solutions
Flexible systems for
front end PV research
Tools handle substrates of various shapes and sizes
Ability to merge & cluster PVD, CVD, Etch & ALD technologies on same platform
Option of Kelvin probe integration
High vacuum options for handler & CVD
Plasma ALD of Al2O3 provides an unparalleled level of surface passivation of crystalline silicon solar cells
For more information, please contact
Oxford Instruments Plasma Technology:
Tel: +44 (0)1934 837 000
Email: plasma.technology@oxinst.com
OXFORD
INSTRUMENTS
The Business of Science®
www.oxford-instruments.com/pv

	A [cm^2]	η [%]	FF [%]	V_{oc} [mV]	J_{sc} [mA/cm^2]
Small area	4	21.6	80.8	661	40.4
Large area	243.4	21.0	77.7	667	40.5

Table 2. Cell parameters measured under STC for n-type EWT solar cells fabricated at ISFH.

	A [cm^2]	η [%]	FF [%]	V_{oc} [mV]	J_{sc} [mA/cm^2]
IBC-SHJ (ISFH + HZB)	1	20.2	75.7	673.0	39.7
Both-side-contacted (ISFH)	4	19.8	74.4	695.0	38.3
Both-side-contacted (ISFH)	100	19.6	77.1	706.8	36.0

Table 3. Cell parameters for the IBC-SHJ solar cells fabricated in cooperation with HZB and for both-side-contacted SHJ solar cells fabricated at ISFH.

contact structure, similar to BJBC solar cells with a phosphorus-diffused BSF and boron-diffused p^+ emitter. The emitter is also formed on the front side and inside the via holes.

To achieve high open-circuit voltages with the solar cells, a thermally grown SiO_2 passivation layer was used for the phosphorus-doped base, along with an aluminium-oxide and silicon-nitride (Al_2O_3-SiN_x) passivation stack for the boron-diffused emitter surfaces, as depicted in Fig. 2. For contact formation, LCOs [16,20] were generated, and aluminium and a dielectric layer subsequently deposited on the rear side of the solar cell by vacuum deposition. The contact separation is realized with a combination of laser ablation and wet chemical etching.

With this cell structure, cell efficiencies of up to 21.6% for small-area solar cells (4cm^2, designated area without busbars) [21] were achieved. Table 2 summarizes the measured parameters of the cell, including a high EWT solar cell fill factor of 80.8%.

For the large-area 15.6×15.6cm^2 cells, full square Si wafers were used; in-house measurements were performed using the LOANA system. Table 2 shows the *I-V* parameters of the best large-area EWT solar cell with an efficiency of 21.0%, measured on the full area, including the busbars. The loss in fill factor compared to the small-area cell is mainly due to a higher series resistance. Longer contact fingers and extended minority and majority current paths in the busbar regions lead to this increased series resistance.

Heterojunction back-junction back-contact cells

The potential of BJBC solar cells can be further increased by combining it with amorphous/crystalline silicon (a-Si:H/c-Si) heterojunction (SHJ) [22–25] technology [26]. a-Si:H/c-Si heterojunction solar cells with contacts on the front and rear sides have already achieved high conversion efficiencies of up to 23.7% and open-circuit voltages of up to 745mV [27] because of the excellent surface passivation provided by thin a-Si. These solar cells, however, suffer from optical losses in the front a-Si:H layer and front transparent conductive oxide (TCO), as well as from contact shading of the metallization grid. These losses would not be present in a back-junction back-contact a-Si:H/c-Si heterojunction (BJBC-SHJ) solar cell, because no a-Si:H and TCO would be necessary at the front. A BJBC-SHJ solar cell thus promises excellent open-circuit voltages as well as high short-circuit current densities. Recently, very high efficiencies above 23% have been achieved with this approach [28].

Interdigitated back-contacted silicon heterojunction (IBC-SHJ) solar cells [29] were fabricated in cooperation with the Helmholtz Zentrum Berlin (HZB). Fig. 3 shows a schematic cross section of the IBC-SHJ solar cell; 3Ωcm n-type float-zone silicon was used as base material. The front side is textured with random pyramids and comprises a phosphorus-diffused n^+ FSF, with a sheet resistance of about 200Ω/sq. Passivation and anti-reflective coating are provided by a stack of thin thermal SiO_2 and PECVD SiN_x [30]. This surface preparation produces very little optical loss and provides stable and excellent front-surface passivation.

At the rear side, the gap between the n- and p-type regions is also passivated with a stack of thin thermal SiO_2 and PECVD SiN_x, resulting in very low surface recombination velocities [31]. The (i/p) a-Si:H emitter covers 60% of the rear side, the (i/n)a-Si:H BSF covers 28% and the gap 12%. The solar cells have a 1×1cm^2 active cell area and are fabricated using photolithography.

The *I-V* characteristics were measured using a Wacom 'WXS-156S-L2, AM1.5GMM' dual-source (tungsten and halogen lamp) sun simulator with class AAA characteristics at a temperature of 25.0±0.2°C. The intensity was adjusted using a calibration cell with front-side phosphorus diffusion. The aperture cell area of 1×1cm^2 was defined by a shadow mask and did not include the busbar areas.

Table 3 shows the results for the best IBC-SHJ solar cell, with an efficiency of 20.2±0.4%. The high short-circuit current density of 39.7mA/cm^2 demonstrates the effective light-trapping and high-passivation quality of the solar cell's front

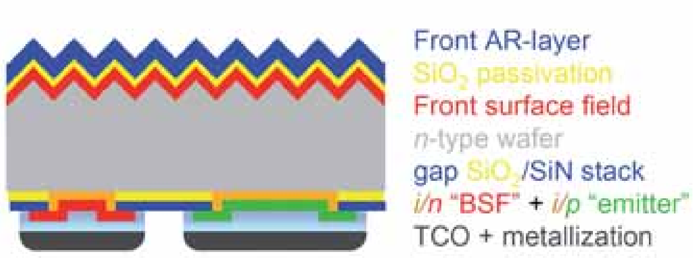

Figure 3. Schematic cross section of the IBC SHJ solar cell.

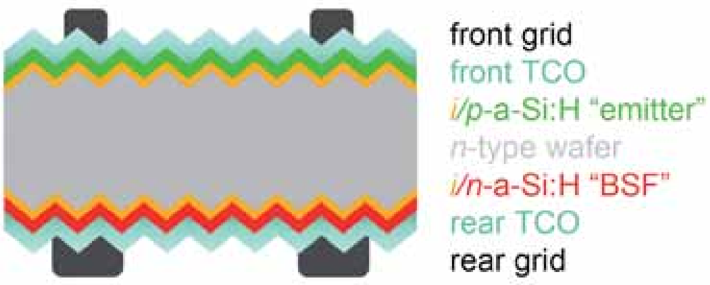

Figure 4. Schematic cross section of the both-side-contacted SHJ (HIT) solar cell.

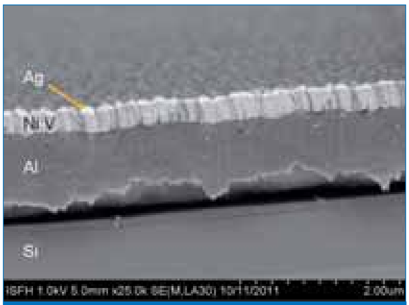

Figure 5. Cross-sectional SEM image of a metallization stack on a silicon wafer: 1µm evaporated Al (dark grey with breaking edge in the bottom of the layer), 250nm sputtered Ni:V (light grey) and 25nm sputtered Ag (white).

side. Although a relatively high voltage of 673mV was obtained, the potential of the solar cell concept is not exhausted.

In order to optimize the (i/p)a-Si:H emitter and (i/n)a-Si:H BSF stack, as well as the a-Si:H – TCO contact, a cell process for both-side-contacted SHJ solar cells was established at ISFH [32]. Fig. 4 shows a schematic cross section of one of these cells, which has a similar structure to the heterojunction with intrinsic thin layer (HIT) solar cell pioneered by Sanyo [22,27]. This relatively simple cell process allows a wide range of process parameter variations to be investigated without having to fabricate the complex IBC-SHJ solar cell structures. The metallization can be performed by aluminium evaporation or low-temperature, silver (Ag) screen printing. Table 3 shows the results for the best fully screen-printed 2.5×2.5cm² and 10×10cm² SHJ solar cells. *I–V* measurements were performed with a LOANA system from pv-tools.

Aluminium as contact material

A common step in producing all ISFH's solar cells is the evaporation of aluminium for the contact formation. This process has long been known as a laboratory technique for high-efficiency silicon solar cells [15]. With the exception of Schott Solar [33] and BP Solar [34], it has so far not been implemented into production lines on a large scale, even though the metal evaporation process is a well-known process from the coating industry. It is used on an industrial scale for various applications, for example to create protection layers in potato-crisp bags. Unfortunately, both the solar cell production lines have now closed down.

In recent years, however, high-throughput in-line evaporation systems have been investigated with regard to their applicability in silicon solar cell fabrication, and promising results have been obtained [35,36]. These systems (Applied Materials ATON500/ATON1600) allow a throughput of over 3000 wafers/h, with a flexible configuration of evaporation or sputter units. This enables a sequential deposition of different metals to create metal layer stacks without breaking the vacuum.

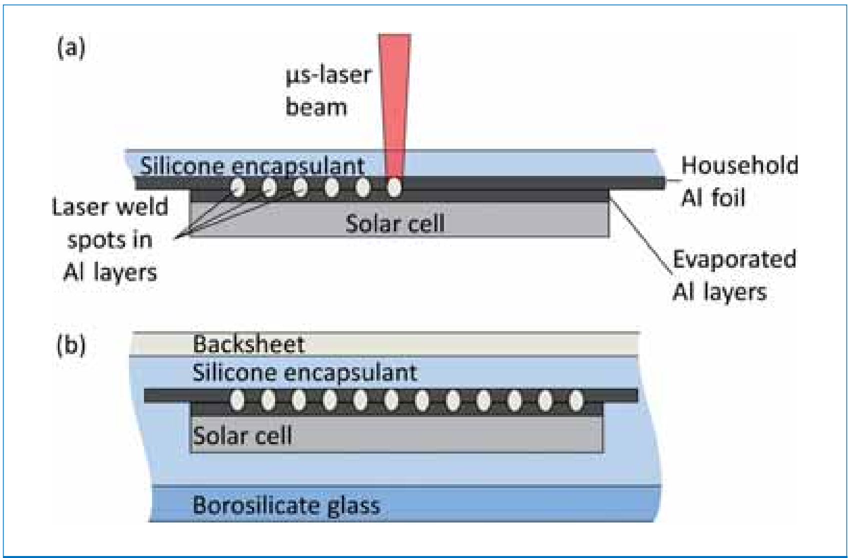

Figure 6. Schematics of (a) the laser weld process, and (b) the final lay-up of the module. (Adapted from [45].)

Evaporation of aluminium for contact formation on silicon solar cells offers distinct advantages over the standard metallization process (i.e. screen printing), such as the potential to reduce material costs, a higher throughput, lower process temperatures (and therefore less stress for the produced cells), a lower contact resistance (of the order of $10^{-3}\Omega cm^2$ [37]) between wafer and metal, and, most importantly, higher solar cell efficiencies (21.8% so far [38]).

The cost reductions arise because the need for expensive, potentially silver-containing, pastes is eliminated, and the amount of aluminium used is about 10% less than that currently required [36,39]. The process temperature depends on the deposition rate and the velocity of the carrier system transporting the wafer [39]. With the standard parameters, the deposition temperature is below 300°C, which results in wafer bows lower than 1mm on a standard 15.6cm wafer. However, it is also possible to form an Al-p⁺ BSF, which reduces the surface recombination velocity (SRV) if a deposition temperature is chosen that is sufficiently high [40].

Module integration with evaporated aluminium

In general, crystalline silicon solar cells are interconnected by soldering. Unfortunately, aluminium is not directly solderable owing to the formation of a stable native oxide. In screen-printed both-side-contacted solar cells, soldering pads made from silver-containing pastes are used to ensure solderability, which is a significant cost distribution in module production.

> "Evaporation of aluminium for contact formation on silicon solar cells offers distinct advantages over the standard metallization process."

The solderability of an evaporated aluminium layer can, however, be achieved by depositing a metal stack of, for example, Al/Ni:V/Ag, as shown in Fig. 5. This can be done without breaking the vacuum. The silver capping layer in this stack has a thickness of only 25nm, leading to a silver consumption of approximately 6mg per 15.6×15.6cm² wafer, which is a significant reduction compared to the 50–90mg/wafer that is required in standard rear-side screen-printing processes [41].

Positive results on solderability and long-term stability tests of this metal stack on solar cells have recently been published; in these tests, the peel force for a solder joint on solar cells was investigated after thermal treatment between 80 and 150°C for up to 720h. In every peel test, the peel

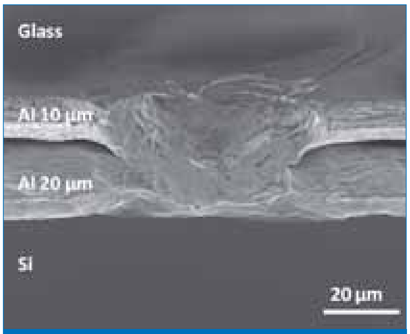

Figure 7. Cross-sectional SEM image of a laser weld spot of a sample with a 20µm-thick Al layer on the Si wafer, and a 10µm-thick Al layer on the glass substrate.

	A [cm²]	η [%]	FF [%]	V_{oc} [mV]	I_{sc} [mA]
Cell 1	34.4	20.4	78.3	663	1350
Cell 2	34.4	20.8	78.5	666	1368
Cell 3	34.4	20.7	78.1	666	1372
Cell 4	34.4	20.2	77.5	664	1349
Cell 5	34.4	20.7	77.8	666	1377
Module	172	20.4	78.2	3326	1348
Module laminated	172	19.3	78.3	3320	1275

Table 4. Module parameters measured under standard conditions. The given area *A* is either the total area of a cell or the designated area of a module (area of the five cells only). (Adapted from [45].)

force exceeded the minimum peel force (defined in DIN EN 50461 to be 1N/mm) by a factor of more than four. From the analysis of inter-metallic compound growth at the solder/Ni:V-interface, it was possible to derive a required Ni:V layer thickness of less than 200nm for a lifetime of 25 years under realistic conditions [42].

A suitable way to solder back-contacted solar cells, using the specific advantage of having both contacts accessible on the same side, is the ATLAS (on-laminate laser soldering) process [43]. Here, the soldering process takes place after the cells have been positioned on the module glass and encapsulant, making further handling steps with unsupported fragile strings unnecessary.

An interconnection technique that omits silver completely was recently developed at ISFH. The so-called aluminium-based mechanical and electrical laser interconnection, or AMELI, process [44,45] forms laser weld spots between the Al-metallized rear side of a solar cell and an Al layer on a transparent substrate. Fig. 6 shows the schematics of the process using a silicone encapsulant as transparent substrate carrying a 10µm-thick Al foil. A pulsed laser beam is focused through the transparent substrate into the interface between the Al layer on the substrate and the cell metallization; as a result, the Al layers melt and fuse, as shown in Fig. 7.

The laser welding is performed using a Rofin StarCut Disc 100ICQ laser source. The laser pulses have a pulse duration of 1µs at a wavelength of 1030nm. The laser spot welds are formed by single laser pulses with a pulse energy of 2.3mJ. After the laser welding, the solar cells are interconnected via the Al foil, and the resultant module is then ready for final lamination.

The laser weld spots used for interconnection are characterized by the following properties [45]:

- Strong mechanical interconnection, resulting in a perpendicular tear-off stress of 380kPa after lamination of the stack.
- Low contact resistance ρ_c of less than 1×10^{-2}mΩcm² for a contact area of 420×940µm² with a welded area fraction covered by weld spots of 20%.
- Degradation of less than 3% of the contact resistance during accelerated aging experiments (300 humidity-freeze cycles, from -40°C to +85°C at 85% rel. humidity).

A proof-of-concept module was fabricated using 12.5×12.5cm² BJBC solar cells, which were laser cut into stripes of width 2.75cm. The cell parameters of five of these cells (cells 1 to 5) are given in Table 4. The cell stripes were subsequently interconnected in series using the AMELI process.

The module on the transparent substrate was measured after the laser interconnection and before lamination ('Module' in Table 4). For this in-house measurement, a module flasher (Halm) with a flash duration of 13ms was used. After lamination with a white backsheet and a borosilicate front glass (see Fig. 6(b)), the module was measured once again ('Module laminated'). Note that a shadow mask was used for the *I-V* measurements of the module: this limited the illuminated area to the cell area.

The sum of the open-circuit voltages V_{oc} of the solar cells before welding was 3325mV, while the open-circuit voltage of the module before lamination was 3326mV. In addition, neither the fill factor *FF* nor the short-circuit current I_{sc} changes after laser welding, resulting in a module efficiency η of 20.4% (before lamination). It is thus concluded that the cell interconnection process does not induce any appreciable damage and that the Al weld has a very low contact resistance.

After lamination the efficiency decreases to 19.3% due to reflection and absorption in the front glass and the encapsulant, which notably decreases the short-circuit current. Modules fabricated by this interconnection process have shown to be stable under accelerated aging [46].

> "All of these cell structures have the potential for realizing efficiencies well above 22%."

Conclusions

An overview of back-contacted solar cells developed at ISFH has been presented, namely BJBC, EWT and IBC-SHJ. All of these cell structures have the potential for realizing efficiencies well above 22%, with a record efficiency of 24.2% having been achieved by SunPower in the case of BJBC cells [4].

All the back-contacted solar cells (BJBC, EWT and IBC-SHJ) at ISFH were metallized with evaporated aluminium, a method that offers very low material consumption cost. However, the practical utilization of Al-metallized cells requires novel cell interconnection techniques. Two processes for interconnecting solar cells with evaporated Al metallization were therefore presented: 1) the deposition of an additional metal stack using the same in-line system, such as Al/Ni:V/Ag, and subsequent soldering; and 2) direct laser welding of the Al on the solar cell rear side with an Al-layer on a transparent substrate (AMELI process). Both significantly reduce the silver usage per cell compared to state-of-the-art screen printing, while allowing the transfer of the solar cell results to the module level.

Acknowledgement

We would like to thank our colleagues at ISFH for fruitful discussions and support in solar cell processing. This work was partly funded by the German Ministry for the Environment, Nature Conservation and Nuclear Safety (BMU) under contract numbers 0327660 (VAMOS), 0325195A (VaCoC) and 0325192 (CrystalLine). This work was also funded in part by Q-Cells and the BMU under contract number 0329988C (ALBA II). Part of this work was carried out in cooperation with Helmholtz Zentrum Berlin (HZB) and funded by Bosch, Sunways, Schott and Stiebel Eltron, and the BMU under contract numbers 0325114A and 0325114B (TopShot).

References

[1] Lammert, M.D. & Schwartz, R.J. 1977, "The interdigitated back contact solar cell: A silicon solar cell for use in concentrated sunlight", *IEEE-TED*, Vol. 24, pp. 337–342.

[2] Van Kerschaver, E. & Beaucarne, G. 2006, "Back-contact solar cells: A review", *Prog. Photovolt.: Res. Appl.*, Vol. 14, pp. 107–123.

[3] De Ceuster, D. et al. 2007, "Low cost, high volume production of >22% efficiency silicon solar cells", *Proc. 22nd EU PVSEC*, Milan, Italy, pp. 816–819.

[4] Cousins, P.J. et al. 2010, "Generation 3: Improved performance at lower cost", *Proc. 35th IEEE PVSC*, Honolulu, Hawaii, USA, pp. 275–278.

[5] Hall, R.N. & Soltys, T.J. 1980, "Polka dot solar cell", *Proc. 14th IEEE PVSC*, San Diego, California, USA, pp. 550–553.

[6] Gee, J.M., Kent Schubert, W. & Basore, P.A. 1993, "Emitter wrap-through solar cell", *Proc. 23rd IEEE PVSC*, Louisville, Kentucky, USA, pp. 265–270.

[7] van Kerschaver, E. et al. 1998, "A novel silicon solar cell structure with both external polarity contacts on the back surface", *Proc. WCPEC-2*, Vienna, Austria, pp. 1479–1482.

[8] Gee, J.M. et al. 2011, "Development of industrial high-efficiency back-contact czochralski-silicon solar cells", *Prog. Photovolt.: Res. Appl.*, Vol. 19, pp. 887–893.

[9] Guillevin, N. et al. 2011, "Development towards 20% efficient n-type Si MWT solar cells for low-cost industrial production", *Proc. 26th EU PVSEC*, Hamburg, Germany, pp. 989–994.

[10] Lohmüller, E. et al. 2011, "20% efficient passivated large-area metal wrap through solar cells on boron-doped Cz silicon", *IEEE-TED*, Vol. 32, pp. 1719–1721.

[11] Lamers, M.W.P.E. et al. 2012, "17.9% metal-wrap-through mc-Si cells resulting in module efficiency of 17.0%", *Prog. Photovolt.: Res. Appl.*, Vol. 20, pp. 62–73.

[12] de Jong, P.C. et al. 2004, "Single-step lamination full-size PV module made with back-contact mc-Si cells and conductive adhesives", *Proc. 19th EU PVSEC*, Paris, France, pp. 2145–2148.

[13] Govaerts, J. et al. 2010, "A novel concept for advanced modules with back-contact solar cells", *Proc. 25th EU PVSEC/5th World Conf. PV Energy Convers.*, Valencia, Spain, pp. 3850–3853.

[14] van Roosmalen, J.A.M., Bronsveld, P.C.P. & Weeber, A.W. 2012, "Introducing XIS, a new integrated device and module concept", *Energy Procedia*, Vol. 27, pp. 604–609.

[15] Engelhart, P. et al. 2006, "Laser-processing of 22% efficient back-contacted silicon solar cells", *Proc. 21st EU PVSEC*, Dresden, Germany, pp. 773–776.

[16] Engelhart, P. et al. 2007, "Laser ablation of SiO_2 for locally contacted Si solar cells with ultra-short pulses", *Prog. Photovolt.: Res. Appl.*, Vol. 15, pp. 521–527.

[17] Sinton, R.A. et al. 1988, "Development efforts in silicon backside-contact solar cells", *Proc. 8th EU PVSEC*, Florence, Italy, 1988, p. 1472.

[18] Engelhart, P. et al. 2005, "The RISE-EWT solar cell – A new approach towards simple high efficiency silicon solar cells", *Proc. 15th Int. PV Solar Energy Conf.*, Shanghai, China, pp. 802–803.

[19] Hermle, M. et al. 2008, "Shading effects in back-junction back-contacted silicon solar cells", *Proc. 33rd IEEE PVSC*, San Diego, California, USA, p. 412.

[20] Hermann, S. et al. 2010, "Picosecond laser ablation of SiO_2 layers on silicon substrates", *Appl. Phys. A*, Vol. 99, pp. 151–158.

[21] Kiefer F. et al. 2011 "High efficiency n-type emitter-wrap-through silicon solar cells", *IEEE J. PV*, Vol. 1, pp. 49–53.

[22] Tanaka, M. et al. 1992, "Development of new a-Si/c-Si heterojunction solar cells: ACJ-HIT (artificially constructed junction-heterojunction with intrinsic thin-layer)", *Jpn. J. Appl. Phys.*, Vol. 31, pp. 3518–3522.

[23] Bätzner, D. et al. 2011, "Characterisation of over 21% efficient silicon heterojunction cells developed at Roth & Rau Switzerland", *Proc. 26th EU PVSEC*, Hamburg, Germany, p. 1073–1075.

[24] Descoeudres, A. et al. 2011, "21% efficiency silicon heterojunction solar cells produced with very high frequency PECVD", *Tech. Digest 21st Int. PV Sci. Engineer. Conf.*, Fukuoka, Japan, 3A-1O-02.

[25] Muñoz, D. et al. 2011, "Progress on high efficiency standard and interdigitated back contact silicon heterojunction solar cells", *Proc. 26th EU PVSEC*, Hamburg, Germany, pp. 861–864.

[26] Ji, K.S. et al. 2011, *Tech. Digest*

21st Int. PV Sci. Engineer. Conf., Fukuoka, Japan, 3A-1O-06.
[27] Kinoshita, T. et al. 2011, "The approaches for high efficiency HITTM solar cell with very thin (<100 μm) silicon wafer over 23%", *Proc. 26th EU PVSEC*, Hamburg, Germany, pp. 871–874.
[28] Jung-Hoon Choi et al. 2012, "Development of heterojunction back contact solar cell for 25% cell efficiency", *2nd nPV Worksh.*, Amsterdam, Netherlands.
[29] Lu, M. et al. 2007, "Interdigitated back contact silicon heterojunction solar cell and the effect of front surface passivation", *Appl. Phys. Lett.*, Vol. 91, p. 063507.
[30] Harder, N.-P., Mertens, V. & Brendel, R. 2008, "Buried emitter solar cell structures: Decoupling of metallisation geometry and carrier collection geometry of back-contacted solar cells", *physica status solidi (RRL)*, Vol. 2, pp. 148–150.
[31] Larionova, Y. et al. 2010, "Surface passivation of *n*-type Czochralski silicon substrates by thermal-SiO_2/plasma-enhanced chemical vapor deposition SiN stacks", *Appl. Phys. Lett.*, Vol. 96, p. 032105.
[32] Gogolin, R. et al. 2012, "Silicon heterojunction solar cells: Influence of H2-dilution on cell performance", *Solar Energy Mater. & Solar Cells*, Vol. 106, pp. 47–50.
[33] Hezel, R., Hoffmann, W. & Jaeger, K. 1991, "Recent advances in silicon inversion layer solar cells and their transfer to industrial pilot production", *Proc. 10th EU PVSEC*, Lisbon, Portugal, pp. 511–514.
[34] Bruton, T. et al. 2003, "Towards 20% efficient silicon solar cells manufactured at 60MWp per annum", *Proc. WCPEC-3*, Osaka, Japan, 4PL-E1-01.
[35] Nekarda, J. et al. 2009, "Industrial PVD metallization for high efficiency crystalline silicon solar cells", *Proc. 34th IEEE PVSC*, Philadelphia, Pennsylvania, USA, pp. 892–896.
[36] Heinemeyer, F. et al. 2010, "Inline-high-rate thermal evaporation of aluminum as a novel industrial solar cell metallization scheme", *Proc. 2nd Worksh. Metalliz.*, Constance, Germany, pp. 48–51.
[37] Mader, C. et al. 2010, "Rear-side point-contacts by inline thermal evaporation of aluminium", *Proc. 35th IEEE PVSC*, Honolulu, Hawaii, USA, pp. 1446–1449.
[38] Schramm, S. et al. 2010, "Large scale rear side metallization of c-Si solar cells by high rate evaporating of aluminium", *Proc. 25th EU PVSEC*, Valencia, Spain, pp. 1702–1705.
[39] Mader, C. et al. 2011, "Temperature of silicon wafers during in-line high-rate evaporation of aluminum", *Solar Energy Mater. & Solar Cells*, Vol. 95, pp. 3047–3053.
[40] Mader, C. et al. 2011, "Formation of locally aluminum-doped p-type silicion regions by in-line high-rate evaporation", *Energy Procedia*, Vol. 8, pp. 521–526.
[41] Buchner, C. 2012, "Production equipment for new cell architectures", talk given at 7th Europe Photon Equipment Conf., Berlin.
[42] Jung, V. & Köntges, M. 2012, "Al/Ni:V/Ag metal stacks as rear-side metallization for crystalline silicon solar cells", *Prog. Photovolt.*: Res. Appl., DOI: 10.1002/pip.2169.
[43] Köntges, M. et al. 2008, "A novel photovoltaic-module assembly system for back contact solar cells using laser soldering technique", *Proc. 23rd EU PVSEC*, Valencia, Spain, pp. 2709–2712.
[44] Schulte-Huxel, H. et al. 2012, "Aluminum-based mechanical and electrical laser interconnection process for module integration of silicon solar cells", *IEEE J. PV*, Vol. 2, pp. 16–21.
[45] Schulte-Huxel, H. et al. 2012, "Al-foil on encapsulant for the interconnection of Al-metalized silicon solar cells", *IEEE J. PV*, DOI: 10.1109/JPHOTOV.2012.2208096.
[46] Schulte-Huxel, H. et al. 2012, "Aging behavior of laser welded Al-interconnections in crystalline silicon modules", *Solar Energy Mater. Solar Cells*, Vol. 106, pp. 22–26.

About the Authors

Nils-Peter Harder is head of the high-efficiency silicon solar cells group at ISFH and a junior professor at the Leibniz University of Hanover. After studying physics in Cologne, Vancouver and Leipzig, he received his Ph.D. for his work at the UNSW in Sydney on thin-film Si solar cells and advanced photovoltaic concepts. Prior to joining ISFH he worked for Saint Gobain Glass as a product development engineer.

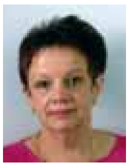

Agnes Merkle studied physics at the University of Bucharest, Romania, where she specialized in biophysics. She joined ISFH in 1995, carrying out research and development work on several high-efficiency solar cell concepts. Her current research focuses on the development of n-type BJBC solar cells for their application in novel module concepts.

Till Brendemühl received his diploma degree in 2005 in engineering physics from the University of Applied Science in Emden, Germany. From 2005 to 2008, he worked as an engineer, developing laser processes at ISFH. Since then he has been a project leader in the high-efficiency silicon solar cells group, with a focus on back-contact high-efficiency solar cell concepts.

Fabian Kiefer studied physics at the University of Freiburg, Germany, and the University of Warsaw, Poland. He received the diploma degree in physics from the University of Freiburg in 2010 for his research on epitaxially grown emitters on crystalline silicon solar cells and on crystalline silicon thin-film solar cells, carried out at the Fraunhofer Institute for Solar Energy Systems (ISE), Freiburg, Germany. In 2010, he joined ISFH, where he is working towards his Ph.D. degree. His research focuses on the understanding and development of back-contacted silicon solar cells, especially EWT solar cells.

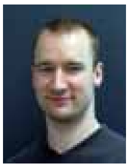

Ralf Gogolin studied physics at the University of Hanover, Germany, where he specialized in PV. He received the diploma in 2009, and his thesis centred on his work on trapping-related recombination in silicon, carried out at ISFH. Since 2009 he has been working as a Ph.D. student on the TopShot project, where he focuses on the development of amorphous-crystalline silicon heterojunction solar cells.

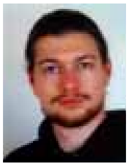

Martin Lehr studied physics at the Johannes Gutenberg University of Mainz, Germany, and received the diploma in 2011. For his diploma thesis he investigated magnetic circular dichroism in Co/Pd-multilayer systems. Since then has been working as a Ph.D. student at ISFH, focusing on the metallization of crystalline silicon solar cells.

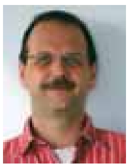

Frank Heinemeyer studied mineralogy at the Leibniz University of Hanover and received his diploma degree in 1997 on selenization of galvanic-deposited CuIn-layers for $CuInSe_2$ solar cells. He joined ISFH in 2001, working on CIGS solar cells on textile fibres. Since 2007 he has been a project leader in the process technology group, with a focus on the metallization of crystalline silicon solar cells.

Henning Schulte-Huxel studied in Leipzig, Germany, and in Bucharest, Romania. He received his B.Sc. and M.Sc. degrees in physics, in 2008 and 2010 respectively, from the University of Leipzig, for his work on characterization of CuInGaSe2 and on laser ablation of CuInSe2 with femtosecond laser pulses. Since 2010 he has been working towards his Ph.D. degree with ISFH. He is currently involved in the development of novel interconnection techniques and module concepts.

Bianca Lim studied physics at Freie Universität Berlin and did her diploma thesis at Hahn-Meitner-Institut Berlin. She then joined ISFH to pursue a doctorate, focusing on boron-oxygen-related recombination centres in silicon, and was awarded a Ph.D. (Dr. rer. nat.) by Leibniz Universität Hannover in 2012. She is currently working on n-type silicon concepts in the materials research group.

Verena Jung studied chemistry at the Johannes-Gutenberg University in Mainz, and received a Ph.D. degree for her Mössbauer spectroscopy investigation of the local surrounding and diffusion of tin in silicate glasses. In 2009 she joined the ISFH PV module group and now works in the field of metallization and interconnection technology.

Sarah Kajari-Schröder received her Ph.D. in 2009 from the University of Ulm, Germany, for her work in theoretical quantum optics. She then joined the PV module group at ISFH, where her research focused on the mechanics of PV modules with a particular emphasis on crack formation in solar cells and the influence of cracks on the reliability of PV modules. She is now the head of the silicon thin-film research group at ISFH, which covers the fabrication, handling and interconnection of ultra-thin crystalline silicon wafers and solar cells.

Marc Köntges received a Ph.D. degree in physics in 2002 from the University of Oldenburg, Germany, for his research on the characterization of CuInGaSe2 and CdTe thin-film solar cells. From 2002 he led the thin-film technology group at ISFH, and then became head of the PV module and interconnection group in 2005. He currently develops characterization and production methods for PV modules.

Rolf Brendel is the scientific director of ISFH. He received his Ph.D. in material science from the University of Erlangen, Germany, for his work on infrared spectroscopy. In 2004 he joined the Institute of Solid State Physics of the Leibniz University of Hanover as a full professor. His main research focuses on the physics and technology of crystalline silicon solar cells.

Enquiries

Nils-Peter Harder
Institute for Solar Energy Research Hamelin (ISFH)
Am Ohrberg 1
D-31860 Emmerthal
Germany
Tel: +49-5151-999-631
Fax: +49-5151-999-400
Email: harder@isfh.de

Current status of MWT silicon solar cell and module technology

Elmar Lohmüller, **Max Hendrichs**, **Benjamin Thaidigsmann**, **Ulrich Eitner**, **Florian Clement**, **Andreas Wolf**, **Daniel Biro** & **Ralf Preu**, Fraunhofer Institute for Solar Energy Systems (ISE), Freiburg, Germany

ABSTRACT

This paper reviews metal wrap through (MWT) solar cell and module technology. As MWT solar cells and modules have received more and more attention in recent years, many highly efficient MWT cell types have been presented by research institutes and industry and are summarized herein. The MWT cell structure benefits from a reduced silver consumption compared with a conventional H-pattern cell, and its realization can be easily combined with novel metallization technologies such as dispensing or stencil printing. The introduction of a rear-surface passivation into the MWT structure is feasible with the high-performance MWT (HIP-MWT) concept developed at Fraunhofer ISE. The resulting fabrication sequence includes only one additional process step – laser drilling of vias – compared with an H-pattern passivated emitter and rear cell (PERC). Furthermore, the synergistic effects of MWT and PERC boost the conversion efficiency gain of MWT-PERC-type cells beyond the expected sum of what could be achieved individually from these two approaches. According to the calculations made by Fraunhofer ISE, conversion efficiencies of up to 21.5% (annealed) are feasible for p-type Cz silicon MWT-PERC cells. Because via metallization is one of the challenges in the fabrication of MWT cells, different via pastes are investigated with regard to their series resistance and contact behaviour. With cell-to-module losses in conversion efficiency of only 0.9% abs., both the interconnector-based MWT module technology and the conductive backsheet concept show promising results.

Introduction

In terms of the competitiveness of PV compared with other energy sources, innovations in solar cell and module manufacturing technology are a prerequisite for further reductions in specific costs (€/Wp). The current crisis that is affecting a major part of the solar industry is putting more pressure on the requirement for technological innovations as instruments for increasing manufacturers' margins.

To date, most of the crystalline p-type silicon solar cells produced worldwide still feature the conventional and long-established double-side contacted solar cell structure, consisting of an H-pattern silver metallization grid on the front and a full-area aluminium metallization with a back surface field (BSF) on the rear (H-pattern BSF, Fig. 1(a)). This type of silicon solar cells suffers from high rear-surface recombination velocities, parasitic absorption at the rear contact and increased front-surface shading due to the presence of the external busbar contacts; thus the H-pattern BSF solar cell conversion efficiency potential is limited. Moreover, at the module level, the interconnection ribbons shade the front of the cell. Their optimization, with the aim of achieving lower series resistances, is limited by thermomechanical stresses resulting from larger cross-sections of the ribbon.

To overcome the drawbacks of H-pattern BSF solar cells, the introduction of a rear-surface passivation and/or the reduction of front-surface shading by using back-contact cell structures with both external polarities only on the rear are possible options. Furthermore, back-contact structures permit the optimization of series connection in the module for the lowest series resistance-related losses. So far, only modules with interdigitated back-contacted solar cells (IBC) from SunPower [1] have made their way into industrial production and are available on the PV market.

Another very promising back-contact cell and module concept close to market introduction is the metal wrap through (MWT) concept [2], shown in Fig. 1(c). Various solar cell manufacturers revealed ramp-up plans for MWT cell production during last year's MWT workshop in Freiburg, and presented pilot-line results at this year's Intersolar trade fairs in Europe and North America, as well as at the SNEC in Shanghai.

In our opinion, the MWT concept is one of the above-mentioned innovations which should be quickly brought into industrial production.

Advantages of MWT technology

MWT technology combines various advantages that allow high conversion efficiencies at both cell and module levels. As the MWT concept is part of back-contact solar cell technology, the external contacts of the device are located on the rear of the cell. This results in up to 50% less shading of active cell area on the front and therefore increases the conversion efficiency by around 0.5% abs. at the cell level compared with conventional H-pattern BSF solar cells [3]. In addition, the absence of front busbars allows a greater range of

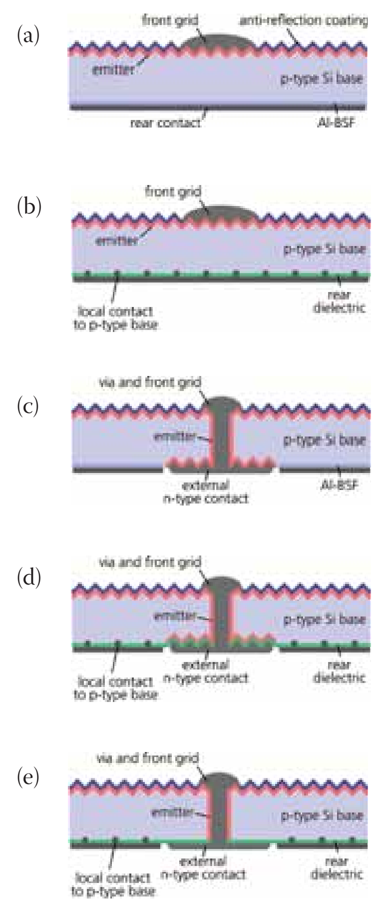

Figure 1. Schematic drawings of different p-type device structures considered in this paper [16]: (a) H-pattern BSF; (b) H-pattern PERC; (c) MWT-BSF; (d) MWT-PERC; (e) HIP-MWT.

Published by	Type of base doping	Base material	Cell concept	Edge length [mm]	Best η_{Cell} [%]
ITRI [45]	p	mc-Si	Al-BSF	125	16.65
Hyundai [46]	p	mc-Si	Al-BSF	156	17.60
Bosch [47]	p	Cz-Si	Al-BSF	156	19.39
Canadian Solar [48]	p	cast mono Si	Al-BSF	156	19.61
ECN & Yingli [49]	n	Cz-Si	phosphorus-BSF with passivation layer	156	19.70
Canadian Solar [50]	p	monocrystalline Si	?	156	21.10

Table 1. Recently published cell results for large-area silicon-based MWT solar cells from other research institutes and industry. Note that none of the results has been confirmed by a calibration laboratory.

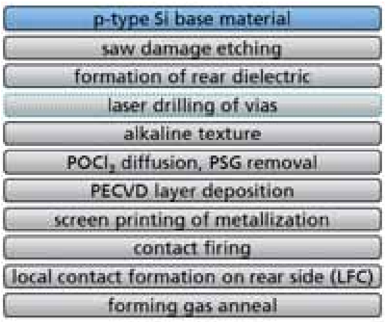

Figure 2. Typical process sequence for p-type HIP-MWT solar cells. Compared with a typical PERC-type solar cell process, a single additional process step (laser drilling of vias) makes the full benefit of the MWT concept accessible.

applicable deposition methods for the front grid, as well as enabling alternatives to the industrially common screen-printing process to be used. Novel innovations such as stencil printing [4,5] or dispensing [6,7] are promising technologies for realizing finger widths below 50µm while maintaining high electrical conductivity and low contact resistance.

> "Another major benefit of the MWT cell concept is the reduced silver consumption."

Another major benefit of the MWT cell concept is the reduced silver consumption. As the consumption of this material is one of the main cost drivers of cell production it should be kept to a minimum [8]. For MWT solar cells with an edge length of 156mm, a reduction in silver of ~50mg/cell (~30% of the total silver amount used) compared with a conventional H-pattern cell is expected because of the different designs of external n-type contacts [5]. Assuming a silver paste price of US$1.04/g (August 2012), this leads to a cost reduction of US$0.05/cell.

The fact that the module interconnection of MWT cells is performed on the rear of the cell broadens the possibilities for cell interconnection. Since the constraints related to conventional front-to-back tabbed interconnection are absent, it is possible to optimize the shape of the applied cell connectors with respect to electrical and thermomechanical features. This allows fill-factor losses and cell stress at the module level to be reduced. Within this optimization, the amount of conductive interconnection material to use on the rear simply becomes a question of material cost. Moreover, a higher packing density is feasible.

As mentioned above, improved surface passivation leads to highly efficient solar cells. By applying the passivated emitter and rear cell concept (PERC, [9], Fig. 1(b)), recombination losses are significantly reduced. Passivation is realized by forming a thin dielectric layer on the rear of the cell. Local contacts through the passivation layer ensure the electrical interconnection of the full-area aluminium to the silicon base. Additionally, the dielectric layer serves as an internal rear-surface reflector, improving the light-trapping of the solar cell, leading to increased short-circuit currents. The PERC approach allows a gain in conversion efficiency of up to 1% abs. compared with state-of-the-art H-pattern BSF technology [10].

Another concept to consider for boosting cell conversion efficiency is the application of a selective emitter on the front of the cell [11]. Here, a low contact resistance between silicon and front metallization is realized by heavy doping of the emitter underneath the metal grid. The more lightly doped emitter in the photoactive cell area leads to reduced Auger recombination and increased quantum efficiency, raising short-circuit current and open-circuit voltage [12].

In recent years, PERC technology has gained increasing recognition in the PV industry when it comes to the production of highly efficient solar cells [13]. In the field of MWT solar cells, the application of a conventional BSF passivation approach is still predominant (see Table 1).

The application of the PERC approach to the MWT cell concept results in a MWT-PERC device [14,15], shown in Fig. 1(d). By combining both technologies, the achieved conversion efficiency gain is even higher than expected from the sum of the two approaches because of synergistic effects [16], whereas the complexity of the process sequence is comparable to conventional PERC sequences.

With the high-performance MWT solar cell HIP-MWT [5,17] (see Fig. 1(e)), a simplified MWT-PERC design is available

Base material	Metallization technology	Edge length [mm]	Best η_{Cell} [%]	Publication reference
mc-Si	screen printing	156	18.2	[51]
Cz-Si	screen printing	125	19.7	
Cz-Si	dispensing	125	20.1	[7]
Ga-doped Cz-Si	stencil printing	156	19.9	[5]
mCz-Si	stencil printing	156	20.2	[5]
FZ-Si	screen printing	125	20.3	
FZ-Si	dispensing	125	20.6	[7]

Table 2. Conversion efficiencies (annealed) achieved at Fraunhofer ISE for large-area silicon-based p-type MWT-PERC solar cells (confirmed by Fraunhofer ISE CalLab PV Cells).

that requires only one additional process step, namely the laser drilling of vias, for the integration of the MWT structure in an industrial PERC cell fabrication line (Fig. 2). In the HIP-MWT structure there is no rear emitter, so rear structuring steps are not necessary in the production line.

Overview of recently published MWT solar cell results

Table 1 summarizes recent results of large-area silicon-based MWT solar cells from research institutes and industry. MWT research at Fraunhofer ISE focuses on the MWT-PERC approach. A wide range of metallization processes and base materials have recently been characterized. Table 2 shows the results of p-type MWT-PERC solar cells processed on the pilot line of the Photovoltaic Technology Evaluation Center (PV-TEC) [18] at Fraunhofer ISE.

The highest conversion efficiency so far of 20.6% is achieved by applying dispensed front fingers and using float-zone silicon (FZ-Si) base material [7]. The dispensing approach allows a decrease in width of the gridlines while maintaining a high aspect ratio of ~0.9 [19]. Dispensing and stencil printing offer an increased homogeneity of the gridlines compared with screen-printed fingers, leading to a lower series resistance contribution of the front grid [5]. Advanced printing technologies such as dispensing and stencil printing are especially suited to MWT cells because of the absence of front busbars; this eliminates the need for a second printing step. In the case of stencil printing, the stability of the stencil is increased owing to the simplified stencil design [5,19].

> "The highest conversion efficiency so far of 20.6% is achieved by applying dispensed front fingers and using float-zone silicon (FZ-Si) base material."

Besides the rather costly FZ-Si, other materials such as gallium-doped Cz-Si (Ga-doped Cz-Si) and boron-doped magnetically cast Cz-Si (mCz-Si) enable the production of solar cells with reduced, or even absent, light-induced degradation (LID) [20]. The best mCz-Si MWT cells presented so far achieve annealed conversion efficiencies of up to 20.2% and exhibit an efficiency drop of only 0.3% abs. after degradation. The reduced LID of the mCz-Si material originates from a lower oxygen content of mCz-Si compared with conventional Cz-Si. Because of the absence of boron in Ga-doped Cz-Si, this material does not show boron–oxygen-related degradation at all [5].

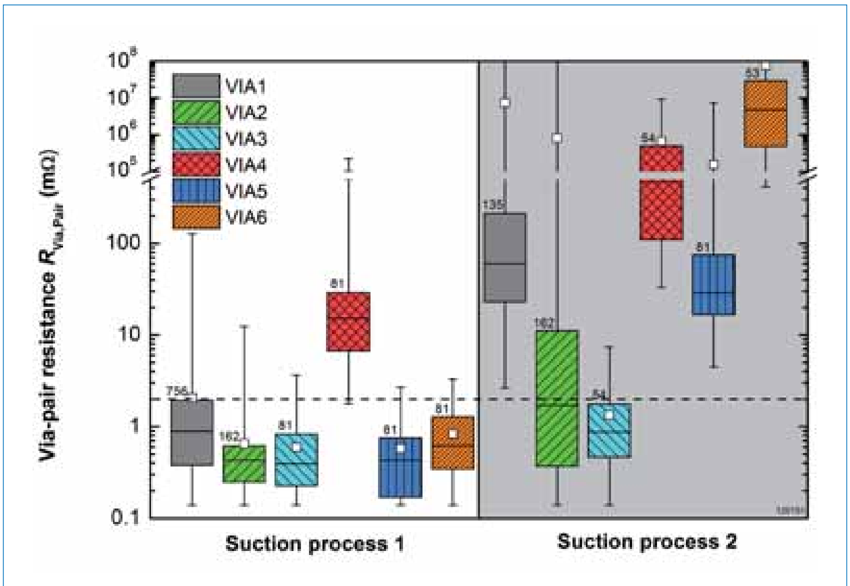

Figure 3. Measured series resistance values $R_{Via,Pair}$ (from four-point probe measurements [44]), for six different via pastes (VIA1–VIA6) and two different suction processes (different time and low-pressure value). The number of measured via-pairs is stated above the boxes. The horizontal dashed line indicates $R_{Via,Pair}$ = 2mΩ.

Via pastes for MWT solar cells

Since the external front contact in MWT solar cells is relocated to the rear, a reliable and continuous via metallization is essential, otherwise high via series resistances lead to decreased fill factors and thus to low conversion efficiencies [21].

Not only are the vias metallized using via pastes but the external rear contacts are as well (e.g. the external n-type contacts in Fig. 1(a),(d),(e)). Therefore, the via pastes should show low shunting behaviour in the crucial regions where the external n-type contact is located next to the p-type silicon base [14,22] (respectively the external p-type contact for n-type base doping).

This is of major importance especially for the HIP-MWT structure (Fig. 1(e)), since this type of solar cell does not have an emitter on the rear (thus the n-type via paste overlaps the p-type base), and therefore reliable forward and reverse bias behaviour is crucial. In forward bias up to the open-circuit voltage, no significant current flow should occur. As partial shading of a photovoltaic module may lead to reverse bias conditions for the shaded cells, reverse breakdown and hot-spot generation are issues that need to be addressed [23]. A low reverse breakdown voltage can lead to an application with an integrated bypass diode at the cell level allowing a controlled reverse current flow (fewer, or even no, external bypass diodes required). For conventional module configurations, a high reverse bias stability is the desired behaviour.

Both forward and reverse bias behaviours can be manipulated either by the use of an intermediate rear dielectric (Fig. 1(d),(e)), as already demonstrated on p-type silicon [24], or by choosing a suitable via paste. In the following section, six different via pastes are investigated with regard to their via series resistance values and their contact behaviour with p-type silicon without an intermediate dielectric in forward and reverse bias conditions.

Via series resistance

Since each external rear contact is connected to the front contact by two vias, the measured series resistance value $R_{Via,Pair}$ is a combination of two vias in parallel (via-pair). Fig. 3 shows the measured series resistance values $R_{Via,Pair}$ for six different via pastes (VIA1–VIA6), using two different suction processes performed after the screen-printing step [25]. Four-point probe measurements were carried out on MWT solar cells with a wafer thickness of ~160µm, fabricated according to a process sequence similar to that shown in Fig. 2. Via radii are ~90µm on the rear and ~60µm on the front. Note that the calculated [21] minimum via-pair resistance value is 0.14mΩ, assuming an optimally filled via and using $3 \cdot 10^{-8}$Ωm as a typical specific conductivity of a via paste. The lower measured values are attributed to measurement uncertainty and corrected to this value.

Application of the two-diode model reveals that a series resistance of 1Ωcm^2 causes a fill factor loss of ~5.5% abs. when calculating the dependency of fill factor from series resistance using latest cell parameters. If a fill factor loss smaller than 0.1% abs. is considered to be negligible for a MWT cell with an edge length of 156mm, and assuming 54 vias, the maximum tolerable series resistance value of a single

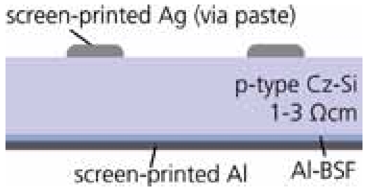

Figure 4. Test structure used for the investigation of the six via pastes.

via R_{Via} is calculated to be ~4mΩ. In our case, the value for $R_{Via,Pair}$ should therefore be lower than ~2mΩ (assuming that both vias in parallel contribute the same proportion to the measured value).

As can be seen for suction process 1 in Fig. 3, all via pastes (except via paste VIA4) show low series resistance values $R_{Via,Pair}$, with mean values below 2mΩ. Only a few outliers lead to higher maximum values. Nevertheless, suction process 1 provides a stable and reliable via-metallization process. Significantly greater via resistance values are measured when using the non-optimal suction process 2. Only via paste VIA3 exhibits comparable values for both suction processes. Suction process 1 is therefore selected for reliable via metallization.

Forward and reverse bias behaviour

To investigate the *I-V* characteristics of the six via pastes in forward and reverse bias conditions, p-type silicon test structures (Fig. 4) were fabricated. In order to examine the behaviour of the via pastes in the most challenging application (as for example in MWT-BSF cells without a rear/via emitter), the pastes are in direct contact with the silicon base material (no intermediate dielectric). The entire back is contacted by screen-printed aluminium. The two silver busbars (via pastes VIA1–VIA6), with a contact area of 3.7cm^2, are screen printed directly onto the front of p-type silicon wafers with a thickness of ~200µm and an edge length of 125mm without any dielectric in between.

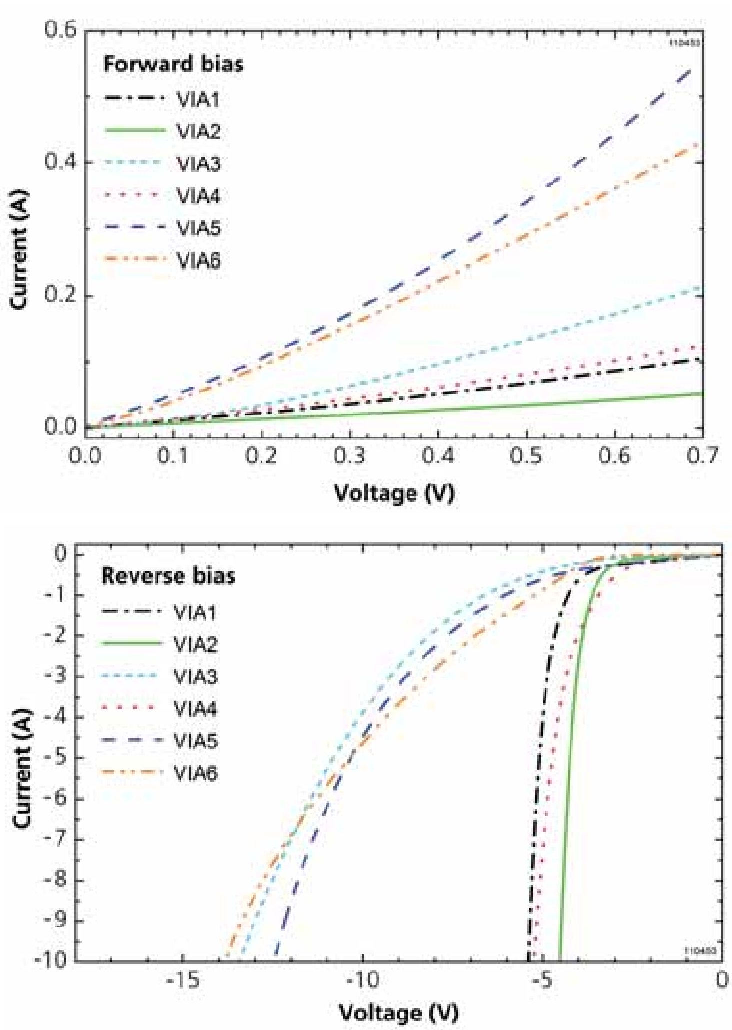

Figure 5. Forward (top) and reverse (bottom) bias dark *I-V* characteristics for the six via pastes (VIA1-VIA6) on p-type test structures shown in Fig. 4. The curves represent the mean values of three to five test structures for each via paste [25].

The measured dark *I-V* characteristics [25] are shown in Fig. 5; as can be easily seen, the six via pastes behave quite differently. The VIA2 paste exhibits the lowest current flow in the forward direction (~0.05A at 0.7V) and a low reverse breakdown voltage. VIA1 and VIA4 also show low reverse breakdown voltages, but somewhat higher forward currents. VIA3, VIA5 and VIA6 show even higher values of forward current, and the reverse breakdown voltage is markedly shifted to higher values. In conclusion, the VIA2 paste best meets the requirements of a non-contacting silver paste on p-type silicon.

Conversion efficiency potential of MWT-PERC solar cells

A loss analysis using analytical and numerical device modelling [26–29] reveals the most important loss mechanisms of p-type MWT-PERC cells [19]. Regarding the short-circuit current density, the major contributors to short-circuit current losses are shading caused by grid lines, non-ideal light trapping and rear recombination. Future technological improvements such as stencil printing, dispensing or more advanced seed and plate approaches are expected to further decrease the shading-related losses. Emitter recombination is another important loss mechanism, which reduces the blue response of the cell and thus the short-circuit current.

With decreasing rear-surface recombination – especially for PERC-like structures – the impact of emitter recombination on open-circuit voltage is increasingly pronounced. Emitter optimization should therefore be in the focus of future investigation. Recently, considerable progress in the development of novel diffusion processes and emitters with low dark saturation current densities was presented by several research institutes [30–32]. These results form the basis for future low-cost but high-performance industrially applicable emitter structures.

For solar cells with passivated rear-side and local base contacts, an adapted base doping is of major importance. The optimum dopant concentration required for maximum performance is higher than for conventional full-area aluminium rear contacts. Besides a gain in open-circuit voltage, a low base resistivity leads to a reduction in PERC-related spreading resistance and MWT-related series resistance contributions. Since Auger recombination and LID (in the case of boron-doped Cz-Si) increase with heavier base doping, the optimum base doping is a trade-off between series resistance and recombinative losses [5].

For high-efficiency MWT-PERC solar cells, device modelling reveals an

Double Laser System for Higher Productivity

- ILS TT: Machine designs that cover the needs for industrial processing of crystalline silicon wafers
- Innovative laser techniques for maximum cell efficiency: Metal Wrap Through, Selective Emitter, Junction Isolation, Laser Fired Contacts, Contact Opening
- Modular machine design. Selection of appropriate laser sources according to the application‘s requirements
- Available as standalone systems or as inline designs that can be easily integrated in existing and new production lines
- Exceptionally high throughput of up to 3.600 wafers/h

3600 wafers/h

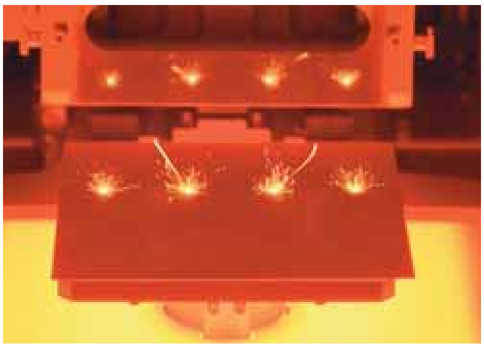

InnoLas Systems GmbH
Robert-Stirling-Ring 2
82152 Krailing
Germany
Tel.: +49 89 / 899 48 28-0
Fax: +49 89 / 899 48 28-1111
www.innolas-systems.com
info@innolas-systems.com

optimum resistivity of less than 1Ωcm [19]. The above-mentioned MWT-related series resistance arises in the region of the rear n-type contact, where the p-type bulk is not directly connected to the aluminium contact. Majority charge carriers generated in this area have to travel laterally to reach the p-type contact. This loss is reduced by an adaptation of the rear n-type contact geometry to small solder islands. One possible way to further reduce the n-type area on the base rear is to decouple the external solder pad from the base by applying an insulating layer while maintaining the solderability of the external n-type contact.

The use of front-grid printing technologies that allow the processing of thin lines with a high aspect ratio offers several advantages. Besides the reduction of shading, the emitter-related series resistance losses are decreased owing to reduced finger pitches. Furthermore, a smaller cell area is metallized, leading to a reduction in recombinative losses at the semiconductor–metal interface. By replacing screen printing with advanced metallization technologies, not only is a conversion efficiency gain achieved, but also the finger homogeneity is increased, making a further reduction in silver consumption per cell feasible [5].

> "Conversion efficiencies up to 21.5% (annealed) for p-type Cz-Si MWT-PERC cells are feasible in a short to medium time frame."

According to the calculations made by Fraunhofer ISE, conversion efficiencies up to 21.5% (annealed) for p-type Cz-Si MWT-PERC cells are feasible in a short to medium time frame, when combining the advances in cell layout and processing with adapted base material properties [19]. For PERC solar cells, the high conversion efficiencies of 19.5% obtained for multicrystalline silicon (mc-Si) [13] and 20.2% for Cz-Si (deactivated boron-oxygen complex) [13] support the reasoning that the simulated values for Cz-Si MWT-PERC cells are not far from being reached.

Most of the improvements presented for further exploiting the conversion efficiency potential of p-type MWT-PERC solar cells are likewise effective for corresponding n-type cells.

MWT modules

For the interconnection of MWT cells two different concepts have been developed and implemented by researchers and manufacturers [33]. In the first concept the conventional tabbing-stringing of standard H-pattern cells is modified so that only the rear of the cell is addressed, with interconnectors that reach over two neighbouring cells [34]. Depending on the design of the interconnector and on the layout of the contacts on the cell rear, an electrical insulation is required to avoid direct contact of the interconnector to opposite cell polarities. The subsequent manufacturing steps are identical to standard module manufacturing, as the interconnected cell strings are placed on the front glass with one layer of encapsulant, followed by cross connection of the strings.

The second concept is an adaptation of surface-mount technology concepts from microelectronics, whereby a conductive backsheet provides the electrical interconnection circuit [35,36]. The backsheet therefore exhibits a structured metallization layer, usually copper, on the side that faces the cell, along with a finish for electrical insulation. Following the process of Eurotron/ECN [37], the conductive adhesives or solder pastes are then applied to the contact points, and the encapsulant, with punched holes, is placed on the backsheet. Subsequently, all cells are assembled on the encapsulant with their sunny side pointing upwards, followed by the lay-up of the second encapsulant layer and the front glass. Prior to lamination the stack is flipped, and the module enters the laminator with the glass facing downwards.

Interconnection

The use of solder and of conductive adhesives has been demonstrated [38,39] for the interconnection of MWT cells. The advantages of conductive adhesives are: (i) lower processing temperature (below 180°C) and lower material stiffness compared with solder (resulting in low-stress interconnections [40]); (ii) the compatibility for heterojunction concepts [41]; and (iii) the option to cure the adhesive during the lamination process in the case of the conductive backsheet concept. On the other hand, silver-containing conductive adhesives are more expensive than soldering pastes and require high levels of accuracy in processing [42]. As well as being cost-effective, solders are well proven in the PV industry and provide high electrical conductivity.

To avoid high thermomechanical stress on the cell and excessive cell bow after soldering, the interconnection of MWT cells at Fraunhofer ISE is performed with structured interconnector ribbons. Their geometric design yields a high conductivity for low fill-factor losses and low mechanical stress after soldering. The most recent performance tests using this approach [43] have indicated a conversion efficiency loss from cell to module of 0.9% abs. and a module conversion efficiency (aperture area) of 17.0%. These results demonstrate the competitiveness of the interconnector-based MWT technology compared with the conductive backsheet concept, in which cell-to-module losses of 0.9% abs. and module conversion efficiencies of 17.0% have also been reported [38].

Conclusion

Clearly, the MWT approach is of major interest for research and industry, when low-cost production of highly efficient solar systems is an issue. The MWT-PERC solar cell in particular, which benefits from synergistic effects arising from the union of MWT and PERC technology, is a promising candidate for achieving high conversion efficiencies. For p-type MWT-PERC solar cells processed and measured at Fraunhofer ISE, the best conversion efficiency achieved is 20.6% with FZ-Si. Analytical and numerical simulations reveal the huge potential of Cz-Si p-type MWT-PERC cells, with conversion efficiencies of up to 21.5% forecast. With the HIP-MWT approach, a MWT-PERC cell process is available that can be easily adopted by existing PERC production lines, requiring only one additional process step, namely the laser drilling of vias.

> "With the HIP-MWT approach, a MWT-PERC cell process is available that can be easily adopted by existing PERC production lines, requiring only one additional process step, namely the laser drilling of vias."

It is noteworthy that the metallization process in particular offers the opportunity to further increase the conversion efficiency of MWT solar cells. Recent developments concerning advanced front-grid printing technologies such as dispensing and stencil printing have demonstrated promising results, where conversion efficiency is improved and silver consumption is reduced at the same time.

In the case of via metallization, special attention has to be given to the right choice of both metallization paste and suction process, in order to ensure a low via-related series resistance. The dark *I-V* characteristics in forward and reverse bias conditions show quite different behaviours for each of the via pastes tested.

Two different interconnection concepts for MWT solar cells are available:


SCHMID
Maximize your Competitiveness – with SCHMID.
Drastic reduction of silver consumption by up to 80%.
Potential of 0.3%abs efficiency gain.
Fully integrated | Contact-free | For highest efficiency
HiMeT
www.schmid-group.com


STRAMAMPS
DER Sondermaschinenbauer
Sun simulator ProMoSim®evo3 maximizes the value of your PV cells and modules
Key factors for your success
Highly accurate efficiency measurement
Precise Pmpp selection due to minimum non-uniformity (<0.4%) and excellent spectral match (+/- 10%).
Simulating real sun light
Class A+A+A+ simulator offering steady state mode in addition to flash mode. Intensity variation and programmable spectra allow for additional tests e.g. darkfield measurements at multi junction cells.
Very high throughput
No recharging necessary. Therefore extremly short repetition rate of <0.5 sec and short flash rate. Immediate and stable light, no shutter or trigger limits needed.
Very long LED life time
LED arrays last more than 50.000.000 flashes without degredation effects, continuously keeping long term temporal instability of irradiance below 0.5%, thus providing a constant and reliable spectrum.
ProMoSim®evo3 is the state-of-the-art test system for photo-voltaic cells as well as solar modules. The large-surface, multi-coloured LED array offers short pulsed flash and continuous light.
Testing solar cells with LED technology
Moving the limits together. Constantly.
Strama-MPS Maschinenbau GmbH & Co. KG
Ittlinger Straße 195 · 94315 Straubing
Tel.: +49 9421 739-0 • Fax: +49 9421 739-247 • solar@strama-mps.de • www.strama-mps.de

interconnector-based technology and a conductive backsheet concept. Both of these show promising results, demonstrating cell-to-module losses in conversion efficiency of only 0.9% abs.

Cell Processing

Acknowledgements

The authors would like to thank the Photovoltaic Technology Evaluation Center team for its support. Also many thanks to our project partners Bosch, Sunways, DuPont, Heraeus, Merck and SolarWorld for supporting our MWT activities. This work was partly funded by the German Federal Ministry of Environment, Nature Conservation and Nuclear Safety (Contract Number 0329849B).

References

[1] Cousins, P.J. et al. 2010, "Generation 3: Improved performance at lower cost", *Proc. 35th IEEE PVSC*, Honolulu, Hawaii, USA, pp. 275–278.

[2] Van Kerschaver, E. et al. 1998, "A novel silicon solar cell structure with both external polarity contacts on the back surface", *Proc. 2nd WCPEC*, Vienna, Austria, pp. 1479–1482.

[3] Meyer, K. et al. 2010, "Novel MWT cell design on monocrystalline silicon wafers", *Proc. 25th EU PVSEC*, Valencia, Spain, pp. 1774–1777.

[4] Heurtault, B. et al. 2010, "Towards industrial applications of stencil printing for crystalline silicon solar cells", *Proc. 25th EU PVSEC*, Valencia, Spain, pp. 1912–1916.

[5] Thaidigsmann, B. et al. 2012, "The path to industrial production of highly efficient metal wrap through silicon solar cells", *Green: Internat. J. SECS* [in press].

[6] Pospischil, M. et al. 2011, "Investigations of thick-film-paste rheology for dispensing applications", *Energy Procedia*, Vol. 8, pp. 449–454.

[7] Lohmüller, E. et al. 2011, "20% efficient passivated large-area metal wrap through solar cells on boron-doped Cz silicon", *IEEE Elect. Dev. Lett.*, Vol. 32, No. 12, pp. 1719–1721.

[8] Green, M.A. 2011, "Ag requirements for silicon wafer-based solar cells", *Prog. Photovolt.: Res. Appl.*, Vol. 19, No. 8, pp. 911–916.

[9] Blakers, A.W. et al. 1989, "22.8% efficient silicon solar cell", *Appl. Phys. Lett.*, Vol. 55, No. 13, pp. 1363–1365.

[10] Gatz, S. et al. 2011, "19.4%-efficient large-area fully screen-printed silicon solar cells", *physica status solidi (RRL)*, Vol. 5, No. 4, pp. 147–149.

[11] Ventura, L. et al. 1995, "Realization of selective emitters by rapid thermal and laser assisted techniques", *Proc. 13th EU PVSEC*, Nice, France, pp. 1578–1581.

[12] Hilali, M.M. et al. 2004, "A review and understanding of screen-printed contacts and selective-emitter formation", *Proc. 14th Worksh. CSSCM*, Winter Park, Colorado, USA, pp. 109–116.

[13] Engelhart, P. et al. 2011, "Q.ANTUM – Q-Cells next generation high-power silicon cell & module concept", *Proc. 26th EU PVSEC*, Hamburg, Germany, pp. 821–826.

[14] Dross, F. et al. 2006, "Impact of rear-surface passivation on MWT performances", *Proc. 4th IEEE WCPEC*, Waikoloa, Hawaii, USA, pp. 1291–1294.

[15] Romijn, I. et al. 2007, "Aspire: A new industrial MWT cell technology enabling high efficiencies on thin and large mc-Si wafers", *Proc. 22nd EU PVSEC*, Milan, Italy, pp. 1043–1049.

[16] Thaidigsmann, B. et al. 2012, "Synergistic effects of rear-surface passivation and the metal wrap through concept", *IEEE J. Photovolt.*, Vol. 2, No. 2, pp. 109–113.

[17] Thaidigsmann, B. et al. 2011, "Large-area p-type HIP-MWT silicon solar cells with screen printed contacts exceeding 20% efficiency", *physica status solidi (RRL)*, Vol. 5, No. 8, pp. 286–288.

[18] Biro, D. et al. 2006, "PV-Tec: Photovoltaic Technology Evaluation Center – design and implementation of a production research unit", *Proc. 21st EU PVSEC*, Dresden, Germany, pp. 621–624.

[19] Thaidigsmann, B. et al. 2012, "Loss analysis and efficiency potential of p-type MWT-PERC solar cells", *Solar Energy Mater. & Solar Cells* [in press].

[20] Schmidt, J. et al. 2001, "Impact of light-induced recombination centres on the current-voltage characteristic of Czochralski silicon solar cells", *Prog. Photovolt.: Res. Appl.*, Vol. 9, No. 4, pp. 249–255.

[21] Clement, F. et al. 2010, "High throughput via-metallization technique for multi-crystalline metal wrap through (MWT) silicon solar cells exceeding 16% efficiency", *Solar Energy Mater. & Solar Cells*, Vol. 94, No. 1, pp. 51–56.

[22] Clement, F. et al. 2007, "Processing and comprehensive characterisation of screen-printed mc-Si metal wrap through (MWT) solar cells", *Proc. 22nd EU PVSEC*, Milan, Italy, pp. 1399–1402.

[23] Fertig, F. et al. 2011, "Impact of junction breakdown in multi-crystalline silicon solar cells on hot spot formation and module performance", *Proc. 26th EU PVSEC*, Hamburg, Germany, pp. 1168–1178.

[24] Thaidigsmann, B. et al. 2011, "Manipulation of the reverse bias behaviour of silicon solar cells", *Proc. 21st PVSEC*, Fukuoka, Japan.

[25] Lohmüller, E. et al. 2012, "Evaluation of via pastes for p- and n-type metal wrap through (MWT) solar cells", *Proc. 27th EU PVSEC*, Frankfurt, Germany [in press].

[26] Wolf, A. et al. 2010, "Comprehensive analytical model for locally contacted rear surface passivated solar cells", *J. Appl. Phys.*, Vol. 108, No. 124510, pp. 1–13.

[27] Fischer, B. et al. 2002, "Scanning IQE-measurement for accurate current determination on very large area solar cells", *Proc. 29th IEEE PVSC*, New Orleans, Louisiana, USA, pp. 454–457.

[28] Fellmeth, T. et al. [forthcoming], *IEEE J. Photovolt.*

[29] Greulich, J. et al. 2012, "Optical modeling of the rear surface roughness of passivated silicon solar cells", *Energy Procedia* [in press].

[30] Jäger, U. et al. 2011, "Beam shaping for high throughput laser doped selective emitter solar cells", *Proc. 26th EU PVSEC*, Hamburg, Germany, pp. 1377–1380.

[31] Komatsu, Y. et al. 2010, "Sophistication of doping profile manipulation – emitter performance improvement without additional process step", *Proc. 25th EU PVSEC*, Valencia, Spain, pp. 1924–1929.

[32] Mack, S. et al. 2011, "Surface passivation of phosphorus-diffused emitters by inline thermal oxidation", *Energy Procedia*, Vol. 8, pp. 343–348.

[33] Wirth, H. et al. 2011, "Current status and future potential of back-contact (BC) module technology", *Photovoltaics International*, 14th Edn, pp. 166–173.

[34] Wirth, H. et al. 2010, "New technologies for back contact module assembly", *Proc. 25th EU PVSEC*, Valencia, Spain, pp. 3846–3849.

[35] Gee, J. M. et al. 1997, "Simplified module assembly using back-contact crystalline-silicon solar cells", *Proc. 26th IEEE PVSC*, Anaheim, California, USA.

[36] deJong, P. 2010, "Achievements and challenges in crystalline silicon back-contact module technology", *Photovoltaics International*, 7th Edn, pp. 138–144.

[37] Späth, M. et al. 2007, "A novel module assembly line using back contact solar cells", *Proc. 17th PVSEC*, Fukuoka, Japan, p. 436.

[38] Lamers, M.W.P.E. et al. 2012, "17.9% Metal-wrap-through mc-Si cells resulting in module efficiency of 17.0%", *Prog. Photovolt.: Res. Appl.*, Vol. 20, pp. 62–73.

[39] Wirth, H. et al. 2010, "Tabbing-stringing quality control challenges", *Photovoltaics International*, 5th

Edn, pp. 24–29.
[40] Bennett, I.J. et al. 2007, "Low-stress interconnection of solar cells", *Proc. 22nd EU PVSEC*, Milan, Italy, pp. 2674–2678.
[41] Scherff, M.L.D. et al. 2006, "10 × 10 cm^2 hit solar cells contacted with lead-free electrical conductive adhesives to solar cell interconnectors", *Proc. 21st EU PVSEC*, Dresden, Germany, pp. 1384–1387.
[42] Eitner, U. et al. 2012, "Characterization of electrically conductive adhesives", *Energy Procedia* [in press].
[43] Eitner, U. et al. 2012, "Interconnector-based module technology for thin MWT cells", *Proc. 27th EU PVSEC*, Frankfurt, Germany [in press].
[44] Menkoe, M. et al. 2010, "Fast and precise resistance characterisation of laser drilled and metallized vias", *Proc. 35th IEEE PVSC*, Honolulu, Hawaii, USA, pp. 1395-1400.
[45] Chen, S.-Y et al. 2011, "An industrially feasible processing for MWT solar cells", *Proc. 26th EU PVSEC*, Hamburg, Germany, pp. 2001–2003.
[46] Lim, J.K. et al. 2011, "Metal contact structure optimization for high efficiency mc-Si metal wrap-through (MWT) solar cells", *Proc. 26th EU PVSEC*, Hamburg, Germany, pp. 2236–2238.
[47] Meyer, K. et al. 2011, "MWT cells with Al-BSF on Cz silicon with efficiencies up to 19.4%", *Proc. 26th EU PVSEC*, Hamburg, Germany, pp. 984–988.
[48] Yin, W. et al. 2012, "19.6% cast mono MWT solar cells and 268W modules", *Proc. 38th IEEE PVSC*, Austin, Texas, USA.
[49] Guillevin, N. et al. 2011, "Development towards 20% efficient Si MWT solar cells for low-cost industrial production", *Energy Procedia*, Vol. 8, pp. 9–16.
[50] Canadian Solar 2012, "Canadian Solar ELPS PV cells reach 21.1% efficiency", press release.
[51] Thaidigsmann, B. et al. 2011, "HIP-MWT – a new cell concept for industrial processing of high-performance metal wrap through silicon solar cells", *Proc. 26th EU PVSEC*, Hamburg, Germany, pp. 817–820.

About the Authors

Elmar Lohmüller studied physics at the University of Tübingen, Germany, and received his diploma degree in 2010. For his diploma thesis, Elmar worked on the development of p-type MWT-PERC silicon solar cells at Fraunhofer ISE, and is now focusing on the development of n-type MWT solar cells for his Ph.D. thesis.

Max Hendrichs studied renewable energy engineering in Berlin, Germany, and completed his master's thesis on TCOs for HIT solar cells. Max began his Ph.D. dissertation at Fraunhofer ISE in 2012, with a research focus on the development of innovative concepts for module integration of back-contact solar cells.

Benjamin Thaidigsmann studied physics in Tübingen, Germany, and finished his diploma thesis on quantum efficiency analysis of crystalline silicon solar cells in 2009 at Fraunhofer ISE. Benjamin then started his Ph.D. dissertation with Fraunhofer ISE, focusing on the development and characterization of metal wrap through silicon solar cells with surface passivation.

Ulrich Eitner studied technical mathematics at the University of Karlsruhe. From 2006 to 2011 he worked on thermomechanics of PV modules at the Institute for Solar Energy Research Hamelin (ISFH) and obtained his Ph.D. from the University of Halle-Wittenberg. Ulrich has been managing the Photovoltaic Modules group at Fraunhofer ISE since 2011.

Florian Clement is head of the MWT Solar Cells and Printing Technology group at Fraunhofer ISE. He received his Ph.D. degree in 2009 from the University of Freiburg. Florian's research focuses on the development of highly efficient pilot-line processed MWT solar cells as well as on the development and evaluation of printing technologies.

Andreas Wolf studied physics at the Technical University of Darmstadt and at the KTH Royal Institute of Technology in Stockholm. He received his Ph.D. degree from the Leibniz University of Hanover in 2007. Andreas is head of the Thermal Processes/Passivated Solar Cells group at Fraunhofer ISE.

Daniel Biro studied physics at the University of Karlsruhe and at UMASS Amherst, USA; he completed his Ph.D. thesis at the University of Freiburg in 2003. Daniel coordinated the design and ramp-up of the Fraunhofer ISE production technology lab PV-TEC and is now department head in the field of thermal, PVD and printing technology/industrial cell structures.

Ralf Preu is director of the Division for PV Production Technology and Quality Assurance at Fraunhofer ISE. He received a diploma degree in physics in 1996 from the University of Freiburg, Germany, and a Ph.D. degree in electrical engineering in 2000. Ralf also has a diploma degree in economics, which he was awarded by the University of Hagen in 2003.

Enquiries

Fraunhofer Institute for Solar Energy Systems (ISE)
Heidenhofstrasse 2
79110 Freiburg
Germany
Tel.: +49 (0) 761 4588 0
Fax: +49 (0) 761 4588 9000
Email: info@ise.fraunhofer.de
Website: www.ise.fraunhofer.de

20.1%-efficient industrial-type PERC solar cells applying ICP AlO_x as rear passivation layer

Thorsten Dullweber, **Christopher Kranz**, **Birgit Beier**, **Boris Veith** & **Jan Schmidt**, Institute for Solar Energy Research Hamelin (ISFH), Emmerthal, & **Björn Roos**, **Oliver Hohn** & **Torsten Dippell**, Singulus Technologies AG, Kahl am Main, Germany

ABSTRACT

The passivated emitter and rear cell (PERC) is considered to be the next generation of industrial-type screen-printed silicon solar cell. However, only a few deposition methods currently exist for rear passivation layers which meet both the high-throughput and low-cost requirements of the PV industry while demonstrating high-quality surface passivation properties. This paper presents an evaluation and the optimization of a novel deposition technique for AlO_x passivation layers, applying an inductively coupled plasma (ICP) plasma-enhanced chemical vapour deposition (PECVD) process. High deposition rates of up to 5nm/s, as well as excellent surface recombination velocities below 10cm/s after firing, are possible using this ICP AlO_x deposition process. When applied to PERC solar cells the ICP AlO_x layer is capped with a PECVD SiN_y layer. Independently confirmed conversion efficiencies of up to 20.1% are achieved for large-area 15.6cm × 15.6cm PERC solar cells with screen-printed metal contacts and ICP AlO_x/SiN_y rear side passivation on standard boron-doped Czochralski-grown silicon wafers. The internal quantum efficiency (IQE) reveals an effective rear surface recombination velocity S_{rear} of 110±30cm/s and an internal rear reflectance R_b of 91±1%, which demonstrates the excellent rear surface passivation of the ICP AlO_x/SiN_y layer stack. Currently, the ICP AlO_x deposition process is being transferred from the ISFH laboratory-type tool to the Singular production tool of Singulus Technologies in order to commercialize this novel deposition process during 2012.

Introduction

The passivated emitter and rear cell (PERC) is a very promising candidate for next-generation industrial-type screen-printed silicon solar cells. The International Technology Roadmap for Photovoltaics (ITRPV) forecasts the introduction of rear-passivated cells into volume production within the next two years [1]. Numerical simulations using typical solar cell parameters indicate that the conversion efficiency of screen-printed PERC cells is up to 1.5% (absolute) higher than screen-printed solar cells with full-area aluminium back surface field (Al-BSF) owing to the reduced rear surface recombination velocity S_{rear} and an increased rear surface reflectance R_b [2,3]. Excellent conversion efficiencies above 20.0%, with record values of up to 20.2%, have been demonstrated by several companies and research institutes for large-area p-type PERC solar cells with screen-printed metal contacts [4,5,6,7]. Several production-type tools for the deposition of rear passivation layers are already available on the market [8,9] or under development [10,11]. In particular, rear passivation layers consisting of aluminium oxide (AlO_x) have attracted considerable attention because of their excellent surface passivation properties. Effective surface recombination velocities below 10cm/s have been demonstrated [12] for Al_2O_3 layers deposited by atomic layer deposition (ALD) after a high-temperature firing step which is typically carried out for screen-printed metal contacts.

> "In addition to excellent electrical properties, it is important that the AlO_x deposition process achieve high deposition rates."

However, in addition to excellent electrical properties, it is important that the AlO_x deposition process achieve high deposition rates and hence a high throughput, which enables a low cost of ownership. Plasma-enhanced chemical vapour deposition (PECVD) processes applying an inductively coupled plasma (ICP) form a high-density plasma (HDP), yielding electron densities of around $1×10^{12}cm^{-3}$ [13], and hence allow high deposition rates of up to several nanometres per second [14]. ICP PECVD processes have been extensively investigated for the deposition of dielectric insulation and encapsulation layers consisting of SiO_x [15,16] or SiN_x [16,17,18]. The focus at that time was on applications in microelectronic manufacturing, such as a final passivation layer or a diffusion barrier. One important feature of the ICP process is that the plasma density can be varied independently of the ion energy, which is typically lower than 30eV. Hence, an independent optimization of the deposition rate versus the reduction of surface damage of the silicon wafer is possible. In recent years, Singulus Technologies has commercialized the ICP process for the deposition of SiN_x anti-reflective layers of silicon solar cells using their Singular tool platform [14].

This paper presents an investigation of the application of the ICP process, to our knowledge for the first time, to the deposition of AlO_x layers. The ICP AlO_x layers are deposited using a laboratory-type tool at ISFH. The surface passivation properties of the resulting ICP AlO_x layers are analyzed, and the SiN_y capping layer deposition is optimized in order to improve the surface passivation quality after firing. For rear passivation, ICP AlO_x/SiN_y layer stacks are applied to large-area PERC solar cells with screen-printed metal contacts, resulting in excellent conversion efficiencies of up to 20.1%. Moreover, the electrical and optical properties of the ICP AlO_x/SiN_y layers are analyzed by measuring and modelling the internal quantum efficiency (IQE) and the reflectance of the resulting PERC solar cells.

AlO_x deposition using an ICP process

The ICP AlO_x layers are deposited in a laboratory-type cluster tool (Von Ardenne CS 400 P) at ISFH; the tool consists of a load lock chamber, a transfer chamber and several PECVD deposition chambers, including the ICP AlO_x

chamber as shown in the photograph in Fig. 1(a). A schematic drawing of the ICP AlO_x deposition chamber is given in Fig. 1(b). A coil outside the vacuum chamber inductively excites the plasma using a high-frequency generator set at a frequency of 13.56MHz. Trimethylaluminium (TMAl) is used as the precursor gas, and oxygen (O_2) as a reactive gas. The silicon wafer is transported on a carrier and electrically heated during the AlO_x deposition.

Depending on the process parameters, high static deposition rates of up to 5nm/s are obtained while maintaining low ion energies below 30eV. The thickness of the resulting ICP AlO_x layers is varied by adjusting the time of the deposition process. Afterwards, the ICP AlO_x passivation layers are covered with a PECVD SiN_y capping layer (SiNA/Roth & Rau or Singular/Singulus) in order to improve the firing stability and the optical reflectivity when applied to PERC solar cells.

Surface passivation properties of ICP AlO_x layers

In order to determine the surface passivation properties, ICP AlO_x layers capped with a PECVD SiN_y layer (SiNA/Roth & Rau) are deposited on both sides of p-type 1.4Ωcm float zone (FZ) wafers, and a typical firing process is carried out in a conveyor belt furnace with peak temperatures of 910°C. The minority charge carrier lifetime is then measured using the quasi-steady-state photoconductance (QSSPC) technique at a carrier density of $1\times10^{15}cm^{-3}$. Using the measured lifetime τ_{eff}, the maximum surface recombination velocity S_{max} (attributing the whole recombination to the wafer surface) can be calculated from the equation $S_{max} = W/(2 \times \tau_{eff})$, where W is the mean wafer thickness.

> “QSSPC measurements reveal excellent effective lifetimes of up to 2ms.”

The QSSPC measurements reveal excellent effective lifetimes of up to 2ms, corresponding to surface recombination velocities (SRVs) S_{max} below 10cm/s for ICP AlO_x/PECVD SiN_y layer stacks after firing, as shown in Fig. 2. The error bars in Fig. 2 refer to the minimum and maximum values of the effective lifetimes measured at different positions on the same wafer, revealing a good homogeneity of the surface passivation across the wafer. A moderate dependence of the SRV on the AlO_x layer thickness can be seen, with a minimum value of 7.5±1.5cm/s at an AlO_x thickness of 15nm.

The next step is to evaluate a SiN_y capping layer applied by the Singular tool

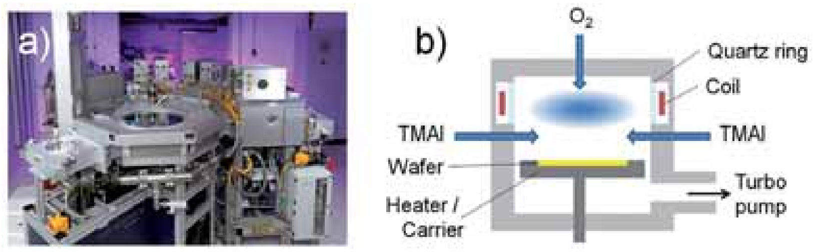

Figure 1. (a) The laboratory-type cluster tool (Von Ardenne CS 400 P), consisting of a load lock chamber, a transfer chamber and several process chambers, including the ICP AlO_x deposition chamber. (b) Schematic of the ICP AlO_x deposition chamber – plasma is inductively excited with a coil outside the vacuum chamber using TMAl and O_2 as process gases, and the wafer is transported on a carrier and heated during deposition.

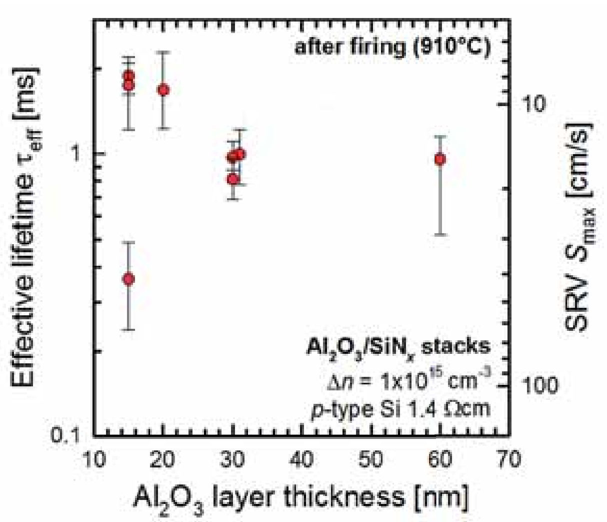

Figure 2. Effective carrier lifetimes and corresponding surface recombination velocities (SRVs) as a function of the ICP AlO_x layer thickness, measured for 1.4Ωcm float zone (FZ) wafers. The results indicate lifetimes of up to 2ms and SRVs below 10cm/s for ICP AlO_x layers covered with a PECVD SiN_y layer (SiNA/Roth & Rau) after firing.

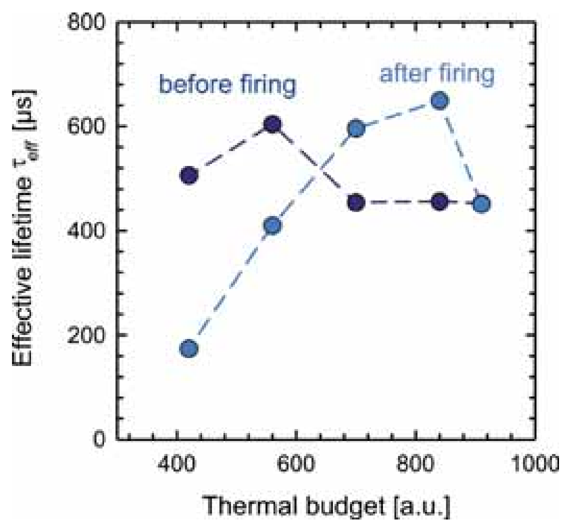

Figure 3. Effective lifetime of 20nm-thick ICP AlO_x layers capped with an ICP SiN_y layer (Singular/Singulus) on 156mm ×156mm, 2Ωcm Cz wafers. After firing, the effective lifetime strongly increases with increasing thermal budget prior to SiN_y deposition.

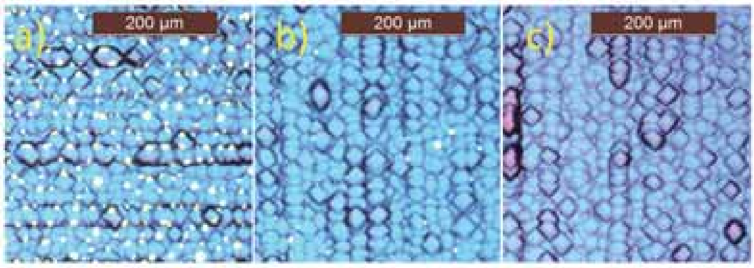

Figure 4. Light microscope images of the ICP AlO_x/ICP SiN_y-covered wafer surfaces of Fig. 3 after firing, for thermal budgets (prior to SiN_y deposition) of: (a) 420, (b) 560, and (c) 840. A greater thermal budget reduces the blistering (white dots) and hence improves the surface passivation after firing.

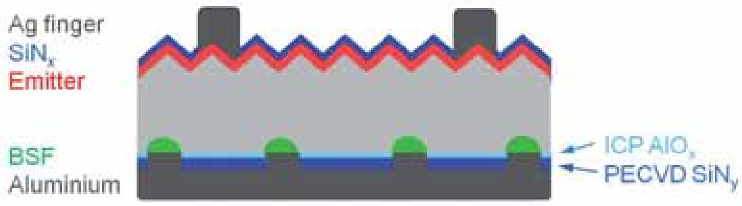

Figure 5. Schematic of the PERC solar cells with screen-printed front and rear contacts, and the application of an ICP AlO_x/SiN_y rear passivation stack.

[14] from Singulus Technologies, which uses an ICP plasma source. The ICP AlO_x layers applied in this study have a layer thickness of 20nm. It has previously been reported that an appropriate annealing of ALD Al_2O_3 layers prior to SiN_y deposition reduces blistering and hence improves the passivation quality after firing [19].

The Singular tool is designed so that a pre-heating chamber heats the silicon wafers prior to the ICP SiN_y deposition. Accordingly, the thermal budget of the pre-heating chamber prior to SiN_y deposition is varied in order to optimize the passivation quality of the ICP AlO_x/ICP SiN_y layers. The passivation layer stacks are deposited on both sides of 156mm × 156mm, 2Ωcm Czochralski (Cz) wafers. Industrial-type wafers are used in this case in order to allow a direct comparison of the resulting test wafer temperatures such as would occur in industrial cell processing.

Before firing, only a moderate dependence of the effective lifetime on the thermal budget is seen, as illustrated in Fig. 3. After firing at 900°C, however, the dependence changes: a strong increase of the effective lifetime with increasing thermal budget is found, and an optimum lifetime of around 600µs is observed. The light microscope images in Fig. 4 confirm that the increased thermal budget reduces the blistering of the ICP AlO_x/ICP SiN_y layers after firing, which explains the improvement of the effective lifetime resulting from the improved surface passivation of the ICP AlO_x/ICP SiN_y layer stack.

Application of ICP AlO_x/SiN_y layer stacks to high-efficiency screen-printed PERC cells

Rear surface passivation using ICP AlO_x/SiN_y

Cell Processing

layer stacks was implemented for industrial-type high-efficiency PERC solar cells with screen-printed metal front and rear contacts. The process sequence of the PERC solar cells is very similar to the process sequence reported in detail in Dullweber et al. [20], so only the most important process steps will be highlighted here.

Industry-standard 156mm × 156mm, boron-doped Cz silicon wafers with resistivities of 2–3Ωcm and starting thicknesses of 200µm are used. Before texturing and phosphorus diffusion, a dielectric protection layer is deposited on the rear side of the wafer, leaving the rear side planar and non-diffused. A homogeneously doped phosphorus emitter with a sheet resistance of about 60Ω/sq. is employed. Next, an AlO_x layer is deposited on the rear side by means of the ICP deposition process as described earlier. Two different ICP AlO_x layer thicknesses of 20nm and 30nm are evaluated and compared to a 10nm-thick ALD Al_2O_3 layer as the reference.

A PECVD SiN_y (SiNA/Roth & Rau) capping layer is then deposited on top of the AlO_x passivation layer at the rear in order to improve both the optical reflectivity and the surface passivation quality. Alternatively, an ICP SiN_y (Singular/Singulus) capping layer with a thermal budget of 900 is deposited. The emitter is covered with a SiN_x anti-reflective coating. The dielectric layer stacks at the rear are locally ablated by laser contact opening (LCO) in order to form local line openings [21,22]. Line contacts are chosen instead of point contacts, since line openings facilitate the formation of a deep and uniform local Al-BSF [23]. The Ag front contacts are deposited by a print-on-print (PoP) screen-printing process, resulting in a finger width of around 70µm and a shadowing loss (including bus bars) of around 6.2% [24]. The Al rear contact is formed by full-area Al screen printing, in which a commercially available Al paste designed for local contacts is applied.

A schematic drawing of the cross section of the resulting PERC solar cell is shown in Fig. 5, and photographs of the front and rear sides are shown in Fig. 6. The contact lines are clearly visible on the cell rear side as well as on the rear passivation layer.

"The PERC solar cell with a 30nm ICP AlO_x layer achieves an independently confirmed conversion efficiency of 20.1%."

Table 1 summarizes the *I-V* parameters of the best solar cells of each split group. The PERC solar cell with a 30nm ICP AlO_x layer achieves an independently

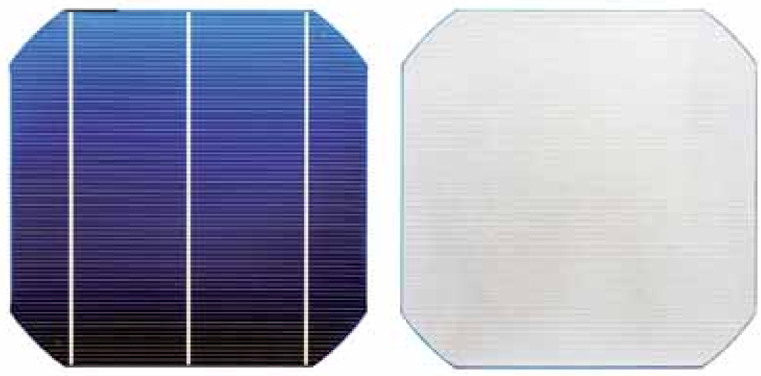

Figure 6. Photographs of the front and rear sides of a PERC solar cell with 20.1% conversion efficiency. Whereas the front side is very similar to industry-standard screen-printed solar cells, the rear side shows the ICP AlO_x/SiN_y passivation layer and the local line contacts.

Rear side passivation	AlO_x layer thickness [nm]	V_{oc} [mV]	J_{sc} [mA/cm^2]	*FF* [%]	η [%]
ICP AlO_x/PECVD SiN_y	30	655	39.0	78.8	20.1*
ICP AlO_x/PECVD SiN_y	20	657	39.1	77.8	20.0*
ICP AlO_x/ICP SiN_y	20	649	39.4	77.5	19.8
ALD Al_2O_3/PECVD SiN_y	10	656	39.2	76.9	19.8*
Al-BSF	N/A	638	37.1	79.1	18.7

* Independently confirmed at Fraunhofer ISE CalLab.

Table 1. *I-V* parameters measured under standard testing conditions (STC) of 156mm × 156mm p-type Cz PERC silicon solar cells. The ICP AlO_x/SiN_y-passivated cells achieve conversion efficiencies of up to 20.1%.

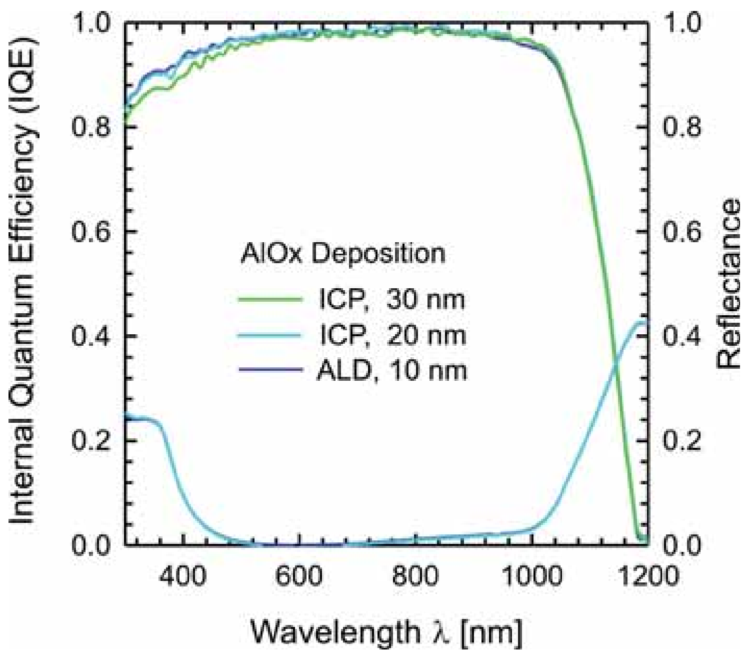

Figure 7. IQE and reflectance of the PERC solar cells of Table 1. S_{rear} values of 80–150cm/s and R_b values of 90–92% are obtained by analytical modelling, demonstrating the excellent electrical and optical parameters of the ICP AlO_x/SiN_y passivation stacks.

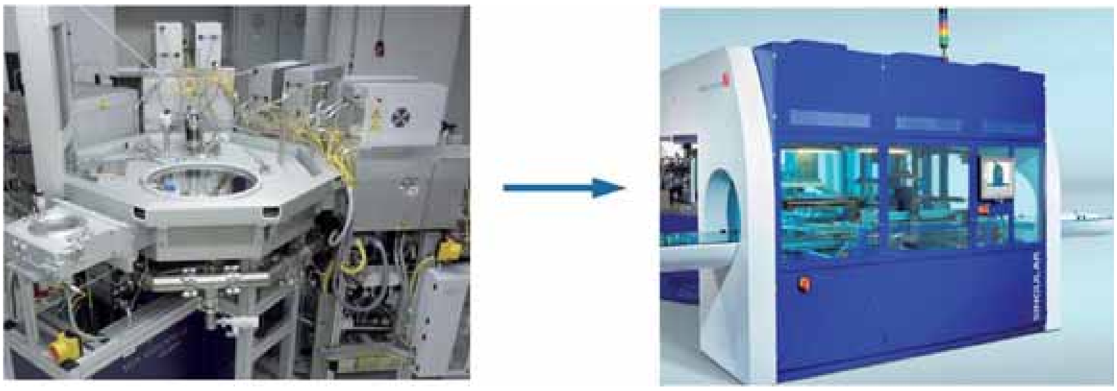

Figure 8. The ICP AlO_x process is currently being transferred from the ISFH lab tool (left) to the Singular production tool (right) for the commercialization of this novel passivation layer during 2012.

confirmed conversion efficiency of 20.1%, which is one of the highest efficiencies reported so far for industrial solar cells of this type. The high values of V_{oc} (655mV) and J_{sc} (39.0mA/cm^2) indicate the excellent rear side passivation by the ICP AlO_x/PECVD SiN_y stack. The PERC solar cells with the 20nm ICP AlO_x layer exhibit similar *I-V* parameters for both PECVD (SiNA/Roth & Rau) and ICP SiN_y (Singular/Singulus) capping layers. The reference PERC solar cell with ALD Al_2O_3/SiN_y rear passivation displays similar solar cell parameters as well.

Table 1 also includes the *I-V* parameters of an industry-standard screen-printed solar cell with full-area Al-BSF and a conversion efficiency of 18.7%. As can be seen by comparison, the significant efficiency improvement of the PERC solar cells compared to the full-area Al-BSF cell is mainly due to improved V_{oc} and J_{sc} values as a result of the improved electrical and optical properties of the rear side.

IQE analysis of screen-printed PERC cells with ICP AlO_x/SiN_y rear passivation

Fig. 7 shows the IQE and reflectance of the PERC solar cells in Table 1. The rear passivation layer mainly affects the reflectance and IQE in the wavelength range of 900nm to 1200nm. As can be seen in Fig. 6, the PERC solar cells show almost identical IQE and reflectance values in this particular range. By analytical modelling it is possible to obtain effective rear surface recombination velocities S_{rear} of 80–150cm/s and internal rear reflectances R_b of 90–92%, showing the excellent electrical and optical properties of the ICP AlO_x/SiN_y passivation stacks; these properties are almost identical to those of the ALD Al_2O_3/SiN_y stack.

> "The ICP process has been demonstrated to be very well suited to the deposition of high-quality AlO_x passivation layers."

Conclusions and outlook

A novel deposition technique has been developed for AlO_x layers, in which an ICP PECVD deposition process is applied, allowing high deposition rates of up to 5nm/s. Experiments on test wafers have demonstrated an excellent surface passivation quality of the resulting ICP AlO_x layers, with surface recombination velocities after firing reduced to 7.5cm/s when applying a SiN_y capping layer. A strong increase of the passivation quality was achieved by appropriate annealing of the ICP AlO_x layer in the pre-heating chamber of the Singular tool prior to SiN_y deposition. Industrial-type PERC solar cells with an ICP AlO_x/SiN_y rear passivation stack applied have exhibited conversion efficiencies of up to 20.1%, which is one of the highest conversion efficiencies reported so far for these types of solar cell.

An IQE analysis revealed an excellent rear surface recombination velocity of 110±30cm/s and a high internal optical reflectance of 91±1%. The rear surface recombination velocity S_{rear} of 100cm/s of the PERC cells was in good accordance with the effective surface recombination velocity S_{max} of 10cm/s for test wafers, taking into account the additional contribution of the local Al contacts with surface recombination velocities S_{met} of around 400cm/s [23]. To our knowledge, this is the first time that the ICP process has been demonstrated to be very well suited to the deposition of high-quality AlO_x passivation layers. The ICP AlO_x process is currently being transferred from the ISFH lab tool to the Singular production tool of Singulus Technologies in order to commercialize this novel passivation layer during 2012.

Acknowledgements

We thank our colleagues at ISFH for their support in solar cell processing, as well as Heraeus and Ferro for providing the screen-printing pastes. We also thank T. Falcon from DEK for the fruitful collaboration in improving the front side screen-printing process. This work was funded by the German Federal Ministry for the Environment, Nature Conservation and Nuclear Safety within the R&D projects HighScreen and ALBA II, and by our industry partners Singulus Technologies, Rena, Schott Solar, Solar World and Q-Cells.

References

[1] SEMI PV Group 2012, "International technology roadmap for photovoltaic (ITRPV.net): Results 2011" [available online at http://www.itrpv.net/doc/roadmap_itrpv_2012_full_web.pdf], p. 13.

[2] Dullweber, T. et al. 2011, "High-efficiency rear-passivated screen-printed silicon solar cells", *Photovoltaics International*, 13th Edn, pp. 77–84.

[3] Schmidt, J. et al. 2012, "Impurity-related limitations of next-generation industrial silicon solar cells", *Proc. 38th IEEE PVSC*, Austin, Texas, USA [in press].

[4] Schott Solar AG 2011, Press Release (August) [available online at http://www.ffpress.net/Kunde/SOL/PM/12592330/].

[5] Engelhart, P. et al. 2011, "Q.ANTUM – Q-Cells next generation high-power silicon cell and module concept", *Proc. 26th EU PVSEC*, Hamburg, Germany, pp. 821–826.

[6] Veith, B. et al. 2012, "Comparison of ICP-AlO_x and ALD-Al_2O_3 layers for the rear surface passivation of c-Si solar cells", *Proc. 2nd SiliconPV Conf.*, Leuven, Belgium [in press].

[7] Münzer, K.A. et al. 2011, "Development and implementation of 19% rear passivation and local contact Centaurus technology", *Proc. 26th EU PVSEC*, Hamburg, Germany, pp. 2292–2297.

[8] Sperlich, H.-P. et al. 2010, "High productive solar cell passivation on Roth & Rau MAiA® MW-PECVD inline machine – A comparison of Al_2O_3 , SiO_2 and SiN_x-H process conditions and performance", *Proc. 25th EU PVSEC*, Valencia, Spain, pp. 1352–1357.

[9] Münzer, A. et al. 2012, "Technical performance and industrial implementation in favour of Centaurus technology", *Proc. 2nd SiliconPV Conf.*, Leuven, Belgium [in press].

[10] Werner, F. et al. 2011, "High-rate atomic layer deposition of Al_2O_3 for the surface passivation of Si solar cells", *Energy Procedia*, Vol. 8, pp. 301–306.

[11] Vermont, P.G., Kuznetsov, V. & Granneman, E.H.A. 2011, "High-throughput solar cell passivation on in-line Levitrack ALD Al_2O_3 system – Demonstration of process performance", *Proc. 26th EU PVSEC*, Hamburg, Germany, pp. 1644–1647.

[12] Veith, B. et al. 2011, "Comparison of the thermal stability of single Al_2O_3 layers and Al_2O_3/SiN_x stacks for the surface passivation of silicon", *Energy Procedia*, Vol. 8, pp. 307–312.

[13] Kändler, E., Graßhoff, G. & Drescher, K. 1995, "Characterization of plasma in an inductively coupled high-dense plasma source", *Surf. & Coatings Technol.*, Vols. 74–75, Part 1, pp. 539–545.

[14] Roos, B.F.P. et al. 2009, "SINGULAR – A novel static inline PECVD-deposition concept for silicon-cell production", *Proc. 24th EU PVSEC*, Hamburg, Germany, pp. 1665–1668.

[15] Inoue, Y. & Takai, O. 1996, "Spectroscopic studies on preparation of silicon oxide films by PECVD using organosilicon compounds", *Plasma Sources Sci. Technol.*, Vol. 5, pp. 339–343.

[16] Lee, J.W. et al. 2000, "Low temperature silicon nitride and silicon dioxide film processing by inductively coupled plasma chemical vapour deposition", *J. Electrochem. Soc.*, Vol. 147, No. 4, pp. 1481–1486.

[17] Han, S.-S. et al. 1998, "Preparation of a-SiNx thin film with low hydrogen content by inductively coupled plasma enhanced chemical vapor deposition", *J. Electrochem. Soc.*, Vol. 145, No. 2, pp. 652–658.

[18] Yota, J., Hander, J. & Saleh, A.A. 2000, "A comparative study on inductively-coupled plasma high-density plasma, plasma-enhanced, and low pressure chemical vapor deposition silicon nitride films", *J. Vac. Sci. Technol. A*, Vol. 18, No. 2, pp. 372–376.

[19] Vermang, B. et al. 2011, "On the blistering of Al_2O_3 passivation layers for Si solar cells", *Proc. 26th EU PVSEC*, Hamburg, Germany, pp. 1129–1131.

[20] Dullweber, T. et al. 2011, "Towards 20% efficient large-area screen-printed rear-passivated silicon solar cells", *Prog. Photovolt: Res. Appl.*, DOI: 10.1002/pip.1198.

[21] Gatz, S. et al. 2011, "19.4%-efficient large-area fully screen-printed silicon solar cells", *physica status solidi (RRL)*, Vol. 5, pp. 147–149.

[22] Gatz, S. et al. 2012, "Analysis and optimization of the bulk and rear recombination of screen-printed PERC solar cells", *Proc. 2nd SiliconPV Conf.*, Leuven, Belgium [in press].

[23] Müller, J. et al. 2011, "Contact formation and recombination at screen-printed local aluminum-alloyed silicon solar cell base contacts", *IEEE Trans. Electron. Dev.*, Vol. 58, No. 10, pp. 3239–3245.

[24] Hannebauer, H. et al. 2011, "18.9%-efficient screen-printed solar cells applying a print-on-print process", *Proc. 26th EU PVSEC*, Hamburg, Germany, pp. 1607–1610.

About the Authors

Thorsten Dullweber received his Ph.D. from the University of Stuttgart in 2002. From 2001 to 2009 he worked as a project leader at Siemens, Infineon and

Qimonda. Since 2009 Thorsten has led the R&D solar cell production processes group at the Institute for Solar Energy Research Hamelin (ISFH), focusing on process and efficiency improvements of industrial-type screen-printed silicon solar cells.

Christopher Kranz received his diploma degree in physics from the University of Münster (WWU) in 2011, after which he started a Ph.D. programme at ISFH in the R&D group for solar cell production processes. Christopher currently carries out research on screen-printed solar cells with passivated emitter and rear side.

Birgit Beier is a process engineer in the solar cell production processes group at ISFH, where she is responsible for industrial-scale silicon solar cell passivation and anti-reflective coatings. Birgit received her degree in engineering physics from South Westphalia University of Applied Sciences in 1996.

Boris Veith is a scientist in the materials research group at ISFH. His current research interests include the evaluation of novel surface passivation methods for silicon solar cells. Boris received his diploma degree in physics from the Leibniz University Hanover (LUH) in 2010. His thesis topic was aluminium oxide as a passivation method for silicon solar cells.

Jan Schmidt is a professor in physics at the Leibniz University Hanover and heads the photovoltaics department at ISFH. Jan's current research interests include the manipulation of defects in silicon materials and the development of solar cell concepts and fabrication processes, with a focus on novel surface passivation techniques.

Björn Roos graduated with a Ph.D. from Kaiserslautern Technical University. He joined the R&D department at Singulus Technologies in 2003, working on PECVD and sputter processes for optical coatings. In 2007 Björn switched to the photovoltaic group and was involved with the development of the Singular PECVD tool; he has been the solar product manager since 2008.

Oliver Hohn earned his Ph.D. degree in physics from J.W. Goethe University in Frankfurt am Main. He has been working in the R&D department at Singulus Technologies AG since 2002. Besides participating in the development of sputtering cathodes and vacuum sources, Oliver is responsible for equipment and process development in PV.

Torsten Dippell received his Ph.D. from the Faculty of Chemistry of the Technical University of Darmstadt in 2001. From 2001 until 2007 he worked as a project manager in various R&D divisions at Interaxia AG (Switzerland) and STEAG Hamatech AG. Since 2007 Torsten has been working as a project leader in the R&D department of Singulus Technologies AG, where he currently focuses on the process development of silicon solar cells.

Enquiries

Thorsten Dullweber
Institute for Solar Energy Research Hamelin (ISFH)
Am Ohrberg 1
D-31860 Emmerthal
Germany
Tel: +49-5151-999-638
Fax: +49-5151-999-400
Email: t.dullweber@isfh.de

Development of cost-effective PERL-type Si solar cells with 19.5% average efficiency

Antonio Cacciato, **Filip Duerinckx**, **Kasper Baert**, **Matthieu Moors**, **Tom Caremans**, **Guido Leys**, **Milica Mrcarica**, **Erwann Picard** & **Jozef Szlufcik**, Photovoltech N.V., Tienen, Belgium

ABSTRACT

The development of a cost-effective and industrially up-scalable process for p-type Cz monocrystalline silicon solar cells of the passivated emitter, rear locally diffused (PERL) type requires a careful trade-off between the potential benefits that novel process steps can deliver (in terms of improved efficiency and/or process control) and the additional costs involved. The approach chosen by Photovoltech is to limit as much as possible the number of PERL-specific process steps and to fine-tune the processes already in use for our standard full Al back-surface field (Al-BSF) technology in order to satisfy the more stringent requirements of PERL technology. Some of the results of this development are reported in this paper. In particular, the impact of different local BSF pastes on our proprietary extended laser ablation (ELA) rear-contacting technique is investigated, as well as the effect of the wafer resistivity and emitter diffusion/oxidation processes on cell performance. This paper also reports the results of large-batch experiments in which the capability of our optimized PERL process was tested against that of a standard full Al-BSF process. An average efficiency of 19.5% and a top efficiency of 19.7% were demonstrated.

Introduction

Laboratory-scale passivated emitter, rear locally diffused (PERL) solar cells still hold the world record of 25% efficiency for monocrystalline silicon when using a single junction [1–3]. However, almost fifteen years after its first realization, the industrial production of this cell architecture remains challenging. One reason why the widespread industrialization of PERL technology is hampered is the immediate cost issue arising from an increased number of production steps and from the novel type of equipment needed compared to that for the mainstream full Al-BSF-type architecture. This imposes severe requirements not only on the minimum efficiency that PERL cells should have in order to be an economically viable alternative to full Al-BSF cells, but also on the stability throughput and controllability of the new equipment/processes required for PERL cell manufacturing.

> “PERL solar cells still hold the world record of 25% efficiency for monocrystalline silicon when using a single junction.”

Moors et al. [4] reviewed the efforts made by Photovoltech to speed up the industrialization of PERL-type cells. In particular, a new rear-contacting technique (called extended laser ablation, or ELA) was presented; the method results in a high-quality local back-surface field (BSF) around the rear contacts, allowing a best cell efficiency of above 19% to be realized for PERL cells. These results were obtained while keeping a standard design on the front side (homogeneous emitter; 75Ω/sq; SiN_x anti-reflective coating; screen-printed contacts), using only thin dielectric layers on the rear (~100nm AlO_x/SiN_x stack), and avoiding both the expensive cleaning steps and the final forming gas anneal treatment (FGA) often used for cells with a passivated rear side to heal laser damage and recover high V_{oc} values [5].

This paper reports on the further industrialization of Photovoltech's industrial PERL-type Si solar cells. In particular, a possible path towards higher efficiency and increased manufacturability will be explored by (i) fine-tuning the wafer resistivity; (ii) screening the local BSF paste most suitable for our ELA metallization scheme; and (iii) optimizing the emitter diffusion/oxidation processes. Finally, the capability of Photovoltech's optimized PERL process is tested against that of a standard full BSF process in large-batch experiments. A top efficiency of 19.7%, a 19.5% average efficiency and an efficiency increase of about 1% abs. with respect to Al-BSF cells are demonstrated.

Experimental

PERL cells were fabricated on 156mm×156mm, 200µm-thick, p-type Cz monocrystalline silicon wafers, with resistivity in the 1.5–2.2Ωcm range, according to the industrial process flow: alkaline texturing, single-side polishing, homogeneous emitter (65–77Ω/sq) and wet edge isolation (WEI). After emitter diffusion and WEI, a thin, dry oxide layer was grown in a classic tube furnace; this was immediately followed by AlO_x and SiN_x depositions on the rear (~100nm AlO_x/SiN_x stack) and SiN_x ARC deposition on the front. High-throughput deposition tools were used for this purpose (Roth & Rau PECVD for SiN_x and Levitech Spatial ALD for AlO_x [6]).

Screen printing was used for both front and rear metallization (commercial Ag and Al pastes), followed by a standard co-firing step in an IR belt furnace. A full Al layer was printed on the rear. Rear-side metallization was performed using the ELA process as described in Moors et al. [4]. No FGA was carried out after the ELA process. For the ELA process, a disk laser (60W and ~1µs pulse length) was used (λ = 1032nm). A matrix of dots with a pitch varying from 0.45mm to 0.55mm, depending on the wafer resistivity, was used as the rear-contact pattern for every cell.

Cells were finally characterized by photo- or electroluminescence and quantum efficiency measurements using commercially available systems. The electrical performance was measured using stabilized reference cells calibrated at ISE CalLab and a DC solar simulator under standard illumination conditions (AM 1.5G, 1000W/m^2, 25°C).

Results

Effect of the wafer resistivity

To increase the efficiency of PERL cells, one option is to reduce the wafer resistivity. For example, Fig. 1 shows that by decreasing the resistivity from 2.2Ωcm to 1.5Ωcm, with all the other parameters

remaining the same, there is an increase of 4.2mV in V_{oc}. Moreover, the lower resistivity allows a further optimization of the rear-contact pitch, which results in a higher fill factor *FF* (Fig. 2).

"To increase the efficiency of PERL cells, one option is to reduce the wafer resistivity."

A disadvantage of the lower resistivity, however, is that the higher boron concentration can enhance the light-induced degradation (LID) of the cell. For example, at a resistivity of 1.5Ωcm, a drop in efficiency of up to 0.7% is caused by LID, as can be seen in Fig. 3. However, as demonstrated in this figure, a 30-minute anneal at 170°C under 1 sun illumination is sufficient to almost completely recover the cell performance, bringing the boron–oxygen-related complex to the inactive state as described in Rein et al. [7].

Screening of local BSF pastes for the ELA metallization scheme

A critical aspect of PERL architecture is the quality of the local BSF formed around the rear contacts. An insufficient local BSF formation would in fact cause increased recombination and parasitic shunting in the presence of inversion layer passivation at the rear contacts [7]. The selection of the most appropriate local BSF paste is therefore of primary importance for achieving a stable and efficient PERL process. As an example, three different pastes are compared in Fig. 4. From the data reported in the figure it is clear that the best choice for our ELA process would be paste B, which provides the highest values of both V_{oc} (Fig. 4(a)) and J_{sc} (Fig. 4(b)), thus resulting in an overall better efficiency (Fig. 4(c)).

It is interesting to note that paste C performs just as well as paste B with respect to local BSF formation (both achieve a similar V_{oc}), but it is significantly worse in terms of internal reflectance (Fig. 5) and therefore in terms of short-circuit current (Fig. 4(b)). Additional experiments suggest that such deterioration of

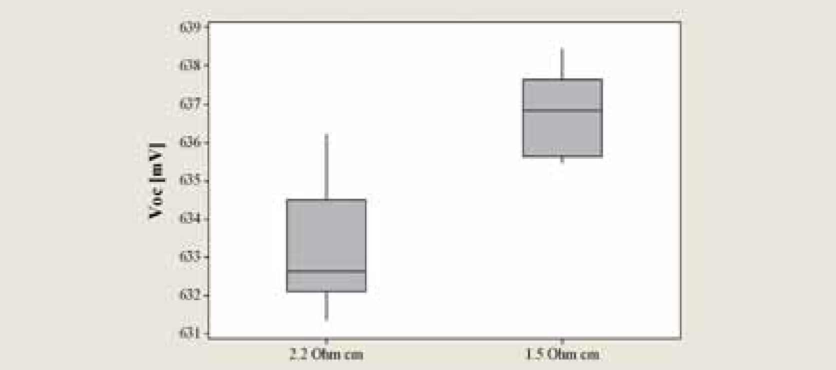

Figure 1. Comparison of the open-circuit voltage for PERL-type Si solar cells fabricated on 2.2Ωcm and 1.5Ωcm substrates. The rear-contact pitch is 0.4mm.

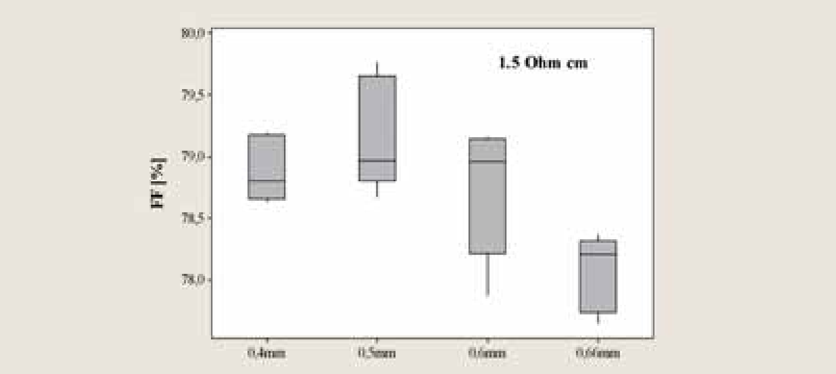

Figure 2. Fill factor as a function of rear-contact pitch, for PERL-type Si solar cells fabricated on 1.5Ωcm substrates.

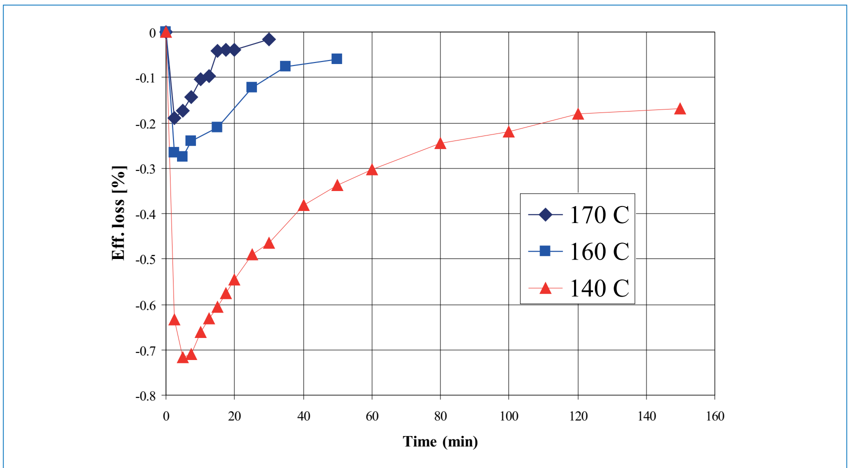

Figure 3. Efficiency loss as a function of exposure time and substrate temperature, during light-soaking (1 sun) for PERL-type Si solar cells. Cells are fabricated on 1.5Ωcm substrates.

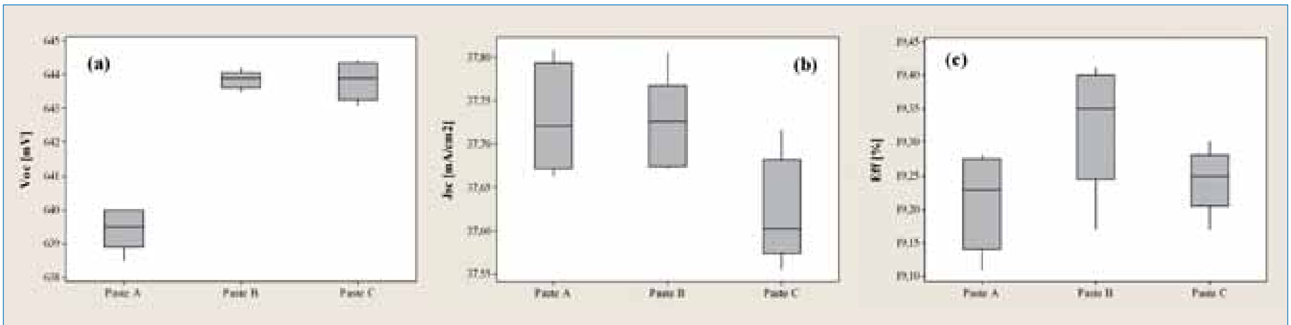

Figure 4. Comparison of PERL-type Si solar cells with three different local BSF pastes: (a) open-circuit voltage; (b) short-circuit current density; and (c) efficiency. The rear-contact pitch is 0.5mm.

internal reflectance would not occur if rear-passivation stacks thicker than our ~100nm-thick AlO_x/SiN_x stack were used, indicating that thin rear-passivation stacks are more demanding with respect to local BSF pastes than thicker ones.

Optimization of emitter diffusion/oxidation

In Photovoltech's process flow a short oxidation is carried out after the wet edge isolation step. This oxidation step increases the stability and manufacturability of the PERL process, but at the expense of a reduced cell current if the oxide at the front surface is grown too thick [8]. A trade-off between oxide thickness and good rear-side passivation could improve the cell efficiency without jeopardizing the manufacturability of the PERL process. An example of this optimization is shown in Fig. 6. In this figure the effects on the short-circuit current of two different diffusion processes for different oxidation conditions are compared. Clearly, by changing the diffusion process and by reducing the oxidation time, both an increase in J_{sc} (Fig. 6(a)) and good rear-side passivation (higher V_{oc} values in Fig. 6(b)) can be obtained.

Al-BSF versus PERL

After integrating the process optimizations described in the previous sections in the reference PERL-type process flow, large-batch experiments were carried out to benchmark the optimized PERL process with the reference full Al-BSF flow. The results of these experiments are given in Fig. 7 and Table 1. An average efficiency of 19.5% (with 30% of the manufactured cells having an efficiency greater than 19.5% and a maximum of 19.7%) was obtained for the PERL-type Si solar cells. This is about 1% higher than the efficiency obtained for full Al-BSF cells. Moreover – and this is very important for large-scale manufacturing – the spread of the cumulative distribution of PERL and BSF cells is similar, demonstrating a good control of the extra process steps required to manufacture the PERL-type cells.

> "Photovoltech's industrial PERL process was shown to be capable of achieving an average efficiency of 19.5% and a top efficiency of 19.7%."

Conclusions

This paper has reviewed some of the optimizations done at Photovoltech that aim to accelerate the industrialization of PERL-type monocrystalline silicon solar cells. The integration of these optimizations in Photovoltech's reference PERL process flow has been tested in

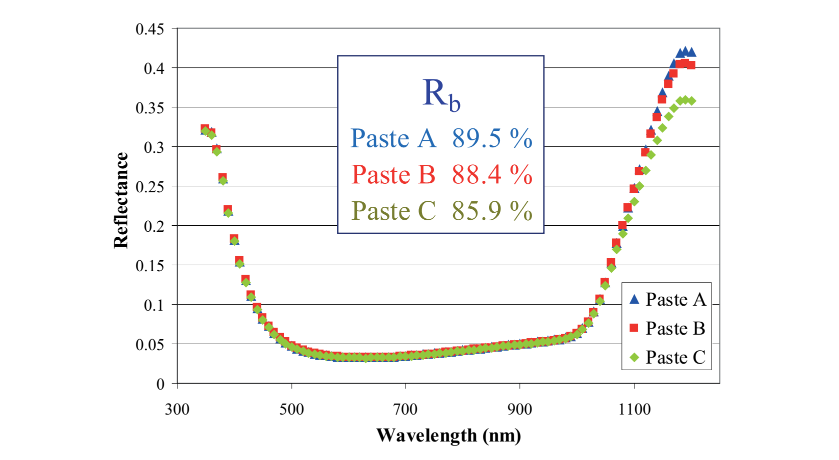

Figure 5. External reflectance measured on the same cells as in Fig. 4. The insert shows the internal reflectance (R_b) of the Si/dielectric/metal system for the three pastes.

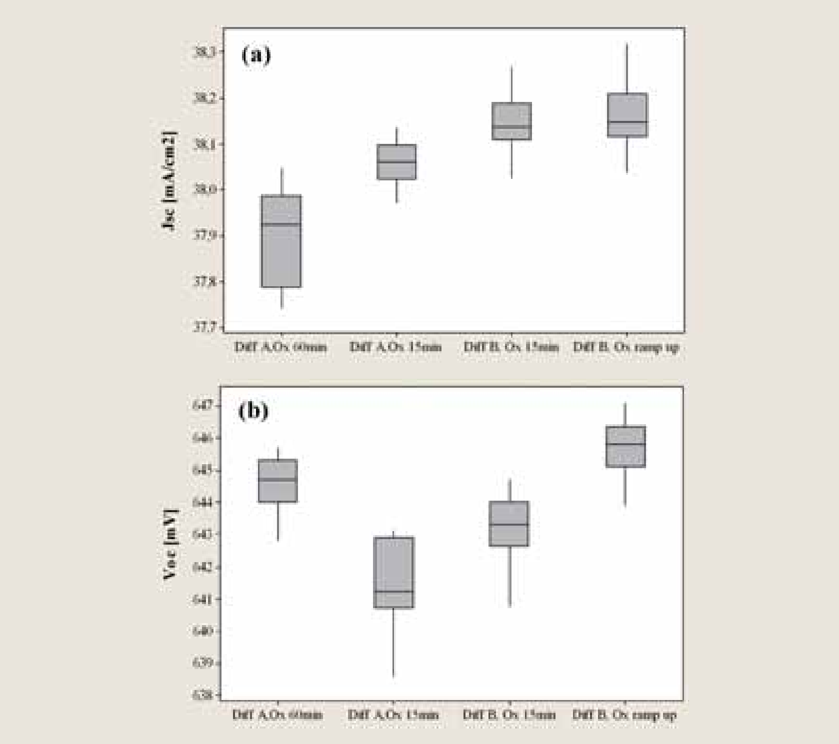

Figure 6. Comparison of PERL-type Si solar cells with different emitter diffusions and oxidation steps: (a) short-circuit current density; and (b) open-circuit voltage. ('60 min' = 60-minute dry oxidation at 800°C, '15 min' = 15-minute dry oxidation at 800°C, 'ramp up' = oxygen flow only during temperature ramp-up.)

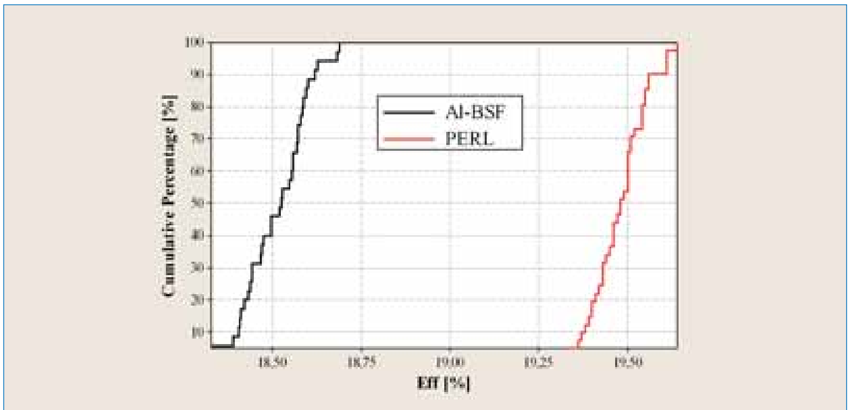

Figure 7. Cumulative percentage distribution of efficiency for full Al-BSF and optimized PERL-type Si solar cells.

	J_{sc} [mA/cm²]	V_{oc} [mV]	*FF* [%]	Eff [%]
PERL	38.35	648	78.5	19.48
Al-BSF	37.30	633	78.7	18.52

Table 1. Average electrical parameters for optimized PERL-type and full Al-BSF Si solar cells, measured at standard test conditions (AM 1.5G, 1000W/m², 25°C).

large-batch experiments and benchmarked with the reference full Al-BSF process. Photovoltech's industrial PERL process was shown to be capable of achieving an average efficiency of 19.5% and a top efficiency of 19.7%. Moreover, the spread of the cumulative distributions of PERL and BSF solar cells was similar, demonstrating good control of the PERL-specific process steps – a very important advantage in large-scale manufacturing.

Acknowledgements

This work was partly funded by the European Commission under the FP7 collaborative project '20plμs' (contract number 256695). The authors would also like to thank the imec photovoltaic group in general, and Dr. J. Horzel in particular, for useful discussions and feedback within the imec industrial affiliation programme (IIAP).

References

[1] Wang, A., Zhao, J. & Green, M.A. 1990, "24% efficient silicon solar cells", *Appl. Phys. Lett.*, Vol. 57, No. 6, p. 602.

[2] Zhao, J., Wang, A. & Green, M.A. 1999, "24.5% efficiency silicon PERT cells on MCZ substrates and 24.7% efficiency PERL cells on FZ substrates", *Prog. Photovolt.: Res. Appl.*, Vol. 7, p. 471.

[3] Kazmerski, L.L. 2012, "Best research solar cell efficiencies from 1976 to 2012", National Renewable Energy Laboratory (NREL), Golden, Colorado, USA [available online at http://www.nrel.gov].

[4] Moors, M. et al. 2012, "Industrial PERL-type solar cells exceeding 19% with screen-printed contacts and homogeneous emitter", *Solar Energy Mater. & Solar Cells* [in press].

[5] Schwab, C. et al. 2011, "Screen-printed Al-pastes for LFC solar cells", *Proc. 3rd Metalliz. Worksh. Cryst. Solar Cells*, Charleroi, Belgium.

[6] Duerinckx, F. et al. 2012, "Accumulation versus inversion layer passivation on +19% screen-printed industrial crystalline silicon solar cells", *Proc. 27th EU PVSEC*, Frankfurt, Germany.

[7] Rein, S. et al. 2003, "Quantitative correlation of the metastable defect in Cz-silicon with different impurities", *Proc. 3rd WCPEC*, Osaka, Japan, pp. 1048–1051.

[8] Cacciato, A. et al. [manuscript in preparation].

About the Authors

Antonio Cacciato received his M.S. degree in solid state physics from the University of Catania, Italy, and his Ph.D. degree (also in physics) from the University of Utrecht, the Netherlands. After receiving his Ph.D., he worked as a metal contamination engineer, process integration engineer, project manager and transfer officer at Philips Semiconductors and imec. He is currently the manager of the R&D Advanced Processes group at Photovoltech.

Filip Duerinckx received his Ph.D. in 1999 from the Katholieke Universiteit Leuven, Belgium, on the subject of industrial silicon solar cell processing with an emphasis on the application of silicon nitride passivation in screen-printing processes. He then worked on efficiency improvement for multicrystalline and thin-film epitaxial silicon solar cells in the Solar Cell Technology group at imec. He joined Photovoltech in 2008, where he is responsible for process step integration for PERL-type silicon solar cells.

Kasper Baert received his Ph.D. in chemistry in 2010 from the Katholieke Universiteit Leuven, where he worked on photonics, more particularly on fluorescence in colloidal photonic crystals. After that he switched to the field of photovoltaics and now works as an R&D engineer for Photovoltech, where his specific interest is the rear metallization of PERL-type solar cells.

Matthieu Moors received an M.S. degree in chemistry in 2005 and a Ph.D. in materials science and nanotechnology in 2010, both from the Université libre de Bruxelles (ULB). He then worked as an R&D engineer at Photovoltech, specializing in rear-contacting technologies. Since July 2012 he has been working as an R&D engineer at Total in Belgium.

Tom Caremans received his Ph.D. degree from the Katholieke Universiteit Leuven in 2009. He subsequently joined Photovoltech as a research engineer, working on the improvement of wet chemical processes in production lines. Since 2010 Tom has been responsible for the development and optimization of all wet chemical processes of Photovoltech's high-efficiency solar cells.

Guido Leys joined Photovoltech in 2003 and was responsible for cell and module manufacturing during the company's start-up. Since 2008 he has been a member of the R&D department, within which he has become a recognized expert on metallization.

Milica Mrcarica holds an M.S. degree in photovoltaics from UNSW. From 1995 to 2009 she was with Solarex/BP Solar, working on a broad range of cell and module engineering and R&D projects, process integration and the transfer of new technology to production. In 2009 she joined Roth&Rau as a process manager for screen-printing and LDSE technology. She has been with Photovoltech since 2011 and is responsible for standard and advanced emitter development for silicon solar cell concepts.

Erwann Picard is the Production Technologies Group Leader at Photovoltech, in charge of the short-term development and continuous improvement of standard processes. He has extensive experience in semiconductor technology, having worked at Philips for six years, where he focused on passive technologies, and as a technology transfer engineer for various Chinese semiconductor companies. He holds a Ph.D. in physics and materials science, and master's degrees in applied physics and in microelectronics devices.

Jozef Szlufcik received his M.S degree in electronic engineering in 1981 and his Ph.D. degree in 1989, both from Wrocław University of Technology in Poland. From 1981 to 1990 he studied at the Silesian University of Technology, Gliwice, Poland, with a research focus on thick-film microcircuits and photovoltaics. He then joined Interuniversity Microelectronics Centre (imec), Leuven, Belgium, in 1990, where he led research on low-cost crystalline silicon solar cells. He has been an R&D and technology manager at Photovoltech since 2003.

Enquiries

Photovoltech N.V.
Industrial Area West Grijpen
Grijpenlaan 18
B-3300 Tienen
Belgium
Tel: +32.16.804.462
Email: antonio.cacciato@photovoltech.be

Thin Film

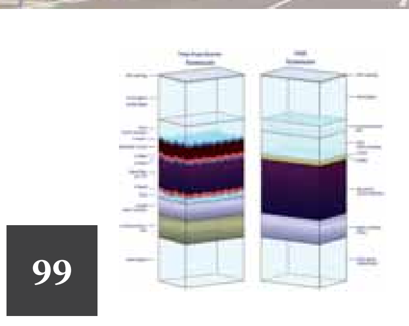

Indian solar industry suffocated by US thin-film manufacturers

Non-governmental organization, the Centre for Science and Environment (CSE), is accusing US thin-film manufacturers of using a loophole in the Indian government's renewable energy scheme to "ruin the Indian domestic PV industry". The Jawaharlal Nehru National Solar Mission (JNNSM) initiative mandates a domestic content requirement, only for crystalline PV, however, and not for thin-film. Chandra Bhushan, CSE's deputy director general, said, "The US has been very disingenuously using this fund to promote its own solar manufacturing. The US Export-Import Bank of the United States [Ex-Im] and the Overseas Private Investment Corporation [OPIC] have been offering low-interest loans to Indian solar project developers on the mandatory condition that they buy the equipment, solar panels and cells from US companies. This has distorted the market completely in favour of US companies." The CSE claims the Ex-Im and OPIC are seducing Indian companies by offering low interest rates of approximately 3%, payable over an 18-year period. Loans from Indian banks come with an interest rate of close to 14% or more.

The JNNSM initiative mandates a domestic content requirement for crystalline PV but not for thin-film.

Judith Pryor, vice-president of external affairs at OPIC, told *Environmental Finance*, "OPIC provides financing that is unavailable from local or foreign private-sector financial institutions. In other words, we don't compete with the local markets. And before OPIC supports a project, we determine whether that project will be subject to any trade-related performance requirements".

A spokesman for Ex-Im stated, "Any OECD member country can offer financing for up to 18 years – this is not special to the US. We don't set the interest rates, [those are] negotiated between the borrower and the lender."

R & D News Focus

Heliatek trials solar film technology production

Heliatek has started a pilot production programme for its new solar film technology. Production is being carried out at its facility in Dresden, Germany, which was inaugurated in March 2011. Heliatek is a specialist in the manufacture of energy-harvesting components made from flexible solar films based on organic semiconductor materials. According to the company's CEO, Thibaud Le Séguillon, it is operating the "world's first production line in which organic solar films are manufactured in a roll-to-roll process using vacuum deposition".

Dyesol's DSC technology excels in performance testing

Dyesol announced that its biomimetic Dye Sensitized Solar Cell (DSC) has been doing exceedingly well in external performance testing, leading the company to begin plans for the next phase of the technology's commercial development.

Newport Corporation's Technology and Application Centre's PV (TAC-PV) Laboratory tested Dyesol's DSC strip cell active area at 7.48% efficiency with one-third sun, a typical lower light, real-world condition. After performance was confirmed, Dyesol acknowledged that with its initial proof-of-concept phase reaching completion, it was time for its Ohio-based joint venture, DyeTec Solar, to relocate and expand its workshop in order to allow the company to enter the testing-validation and prototype development phase. This will be the last phase before the venture anticipates beginning product development of a DSC-enabled glass building façade product for commercial demonstration. Ohio Third Frontier's continued funding allows the company's testing-validation and prototype development phase to take between 12 and 18 months. This period will see the DyeTec Solar team focus on material evaluation, design, finalization of low-cost manufacturing procedures, and the production of a limited number of the façade product.

Thin-film research project receives €10m EU grant

A coalition of thirteen different organizations has secured an EU-funded €10 million research grant for the development of low-cost thin-film technologies.

The 'Scalenano' project aims to develop and scale up an innovative chalcogenide photovoltaic technology by using environmentally friendly and sustainable processes to deliver lower costs and higher efficiencies. The scheme will become one of the largest research and development projects in the field of energy generation in Europe.

The full list of organizations taking part in the research includes groups from five Research Institutes, four Universities and four companies from various different sectors.

Currently, expensive necessities in the manufacturing process of advanced thin-film photovoltaics, such as vacuum processes and high temperatures, have meant that the associated costs have often been prohibitive. In addition, issues surrounding uniformity and the limited supply of Indium have also pushed up the cost.

The project intends to exploit the potential of non-vacuum processes based on nanostructured materials as electrochemical synthesis of nanocrystalline precursors and printing of nanoparticle-based inks, as well as novel chemical-based deposition processes for the development of modules on large-area substrates, with improved uniformity and at lower production costs.

Breakthroughs unearthed from the collaborative research between the thirteen different organisations will be tested on a pilot production line in the hopes of pioneering methods for manufacturing solar cells with higher efficiencies and at lower costs.

Business News Focus

Sharp posts US$58m loss for solar division: Katsuragi thin-film plant to ramp down

Tough times across Sharp Corporation's electronics sectors filtered down into

Sharp is relocating thin-film staff to advanced plant in Sakai, Osaka.

its solar manufacturing arm in its first quarter sales for the current financial year. Overall, Sharp posted quarterly losses of ¥138.4 billion (US$1.76 billion) on net sales of ¥458.6 billion. Sales within its solar cells segment were down 18.2%, compared to the same period in the previous year at ¥41.9 billion (US$534 million), generating an operating loss of ¥6.9 billion (US$57.5 million).

Because of the weakness in its core LCD business, the company is to undertake major restructuring. Its Solar Systems Group will be merged into its Health and Environmental Systems Group and renamed the Health, Environment and Energy Solutions Group.

Administration and headquarter functions of its Solar System Group, which currently operate out of its Katsuragi solar plant, are to be relocated to its advanced LCD and solar production site in Sakai, Osaka.

The 160MW a-Si thin-film-based Katsuragi solar plant will also scale down operations going forward. The plant started production in 2005 and the company has two other advanced plants in Japan and Sicily.

Schüco to permanently close all thin-film facilities

Sustained operational losses due to weak demand in core end-markets and continued aggressive price declines of conventional crystalline silicon modules has forced Schüco International to exit the thin-film PV market. The German-based PV manufacturer will close both its production facilities over the next few months as well as its R&D facility by year end, with the loss of approximately 270 jobs.

The company said that its production facility in Grossröhrsdorf, Dresden, Germany, would be permanently closed at the end of August, while its plant in Osterweddingen, Magdeburg, Germany, would be closed by the end of September this year. The R&D centre in Bielefeld, Germany, would be closed by the end of the year.

The company highlighted that its New Energy division had seen its annual sales decline significantly since 2010, when sales reached over €1 billion, but declined 19% to €850 million in 2011. Schüco said that sales in the first half of 2012 had already declined a further 'double-digit' amount.

Singulus sales slump but targeting investments in thin-film and c-Si technologies

Singulus Technologies reported sales of €43.6 million for the first six months of the year, down from €64.6 million in the same period of 2011. Solar segment equipment sales were 27.5% of revenue in the first half of 2012, or approximately €12 million, down from 33.1% of sales in the prior-year period.

Not expecting a recovering in equipment sales to the solar industry any time soon, Singulus Technologies said it would be investing in new technologies and products within both the CIGS thin-film and crystalline silicon (c-Si) sectors to become a key technology partner. Management also hinted at potential acquisitions as part of the strategy.

Singulus announced at the end of July 2012 that it had received an order worth more than €7 million from Photovoltaic Technology Intellectual Property Limited (PTIP), a spin-off from the University of Johannesburg undertaking research into CIGS thin-film cells. Orders

were placed with Singulus for its vacuum coating, selenization and wet-chemical process tools.

Management noted that it did expect to receive new orders in the second half of the year but didn't expect to turn a profit for the full year.

News

First Solar raises production targets on renewed demand

First Solar reported net sales in the second quarter of 2012 of US$957 million, up from US$497 million last quarter, while revenue guidance was raised for 2012 to US$3.6-US$3.9 billion, up from a range of US$3.5 billion to US$3.8 billion.

Merchant module sales guidance was raised to between 500MW and 600MW, up from a range between 300MW and 500MW. To meet demand, management said that module production would be raised to between 1.8GW and 1.9GW, up from previous guidance of between 1.4GW and 1.7GW.

First Solar also reported an operating income of US$140 million compared to an operating loss of US$456 million in the first quarter of 2012. The second quarter net income was US$111 million.

With increased demand through the rest of the year, First Solar said it would raise production targets. However, plant utilization was only 63% in the second quarter, down from 85% in the first quarter. Total module output was 369MW in the recently completed quarter.

Management noted that in the second half of the year, capacity utilization was expected to be around the 90% mark, which supports improved cost-per-watt.

Module manufacturing cost-per-watt in the second quarter was US$0.72, up US$0.02 quarter on quarter. First Solar noted that its core cost-per-watt was US$0.53.

Management said that its best plant was manufacturing modules at a cost of US$0.63 per watt, with the assumption of full capacity utilization.

The average production line module conversion efficiency was 12.6% in the second quarter, whereas the best performing line was producing modules with 13.1% conversion efficiency, 0.1% up on the previous quarter.

NexPower enters Japanese solar market with 10MW of thin-film shipments

Taiwan-based a-Si thin-film manufacturer NexPower Technology has used three different channels to market in an effort to capture business from the burgeoning Japanese PV market. The company said that, though it did not break down the quantities, it had shipped 10MW of modules to Japan in the first half of 2012 to local distributors, EPC firms and PV project developers.

The company claimed that its expected pipeline in Japan this year could result in more than 1,000 rooftop installations using its thin-film modules.

Solar Shakeout: AQT Solar begins search for partner to buy its assets

The CIGS industry can add another notch to the wall as VentureWire reports that AQT Solar has announced its quest to sell off its assets. The CIGS company is looking for a partner or an acquirer and "has retained Gerbsman Partners to handle the sale of its assets and intellectual property."

Based in Sunnyvale, California, AQT announced in early January that it had received an US$18.7 million investment to double production at its California headquarters, increasing the plant's capacity to 30MW per year. VentureWire noted that since AQT's founding, the company has raised around US$32 million in equity.

MiaSolé restructuring to preserve cash: strategic partnership expected within 90 days

MiaSolé is cutting its workforce dedicated to manufacturing and operations to preserve cash as a 'strategic partnership' deal is expected within the next 60-90 days, according to a statement from the CIGS thin-film module start-up. Jobs are being retained in the technology and commercial areas as well as in its flexible thin-film product areas. The company said that a partnership would enable it to carry out its technology roadmap, which includes the launch of its flexible laminate product offering as well as meeting execution goals on its 1GW-plus commercial pipeline.

The rapid and significant cost reductions of conventional crystalline silicon technologies, due primarily to the drastic decline in polysilicon prices and larger-scale operations of c-Si PV manufacturers, has meant all thin-film start-ups face huge challenges in becoming cost competitive.

Other News

Solar Frontier becomes first to obtain new JETPVm certification

Solar Frontier has become the first company to receive the new JETPVm certification (Trust Assurance) (JIS Q 8901) from Japan Electrical Safety & Environment Technology Laboratories (JET), a Japanese registered certifier of

Source: Green Tech Advocates

AQT Solar looking to sell its assets.

electrical products and other goods. Solar Frontier submitted its certification request for its CIS thin-film modules in July and officially received the JETPVm Certification on August 9. The certification verifies the reliability of a manufacturer's PV modules as well as the organization's customer-support system. Prior to certifying a PV module, JET examines and approves the quality of the product design, its production process and the PV manufacturer's ability to provide long-term product warranty and customer support. The certification was established in June by JET to coincide with the launch of Japan's new FiT programme in July. With this new programme in place, the industry is expecting a boom in investments and activities in the solar industry. Indeed, the Japanese PV market is expected to surge 64% year on year in 2012 to 2.05 GW, independent research firm Solarbuzz predicts.

Former Solyndra employees reach US$3.5m settlement with bankrupt company

A report by Bloomberg has brought Solyndra back into the spotlight. The now defunct company reached a US$3.5 million settlement with former workers, who filed suit against Solyndra, alleging that they had not received adequate lay-off notices. The settlement resolves the issue that the company did not give employees 60 days notice under the Workers Adjustment and Retraining Notification Act when it fired most of its workforce on August 31, 2011.

Solyndra plans to set up the US$3.5 million fund, which will be distributed to the workers two weeks after the settlement is effective. Bloomberg pointed out that both sides proposed the settlement, which is still subject to court approval. Fired employees can choose to opt out of the settlement while the court approval is finalized. The first of two hearings will be held on September 7.

NexPower 160W thin-film modules UL and CEC registered

Taiwan-based thin-film manufacturer NexPower Technology has had its 160W thin-film modules both UL and CEC registered. According to the company, its a-Si thin-film modules were first used in its project in Kansai, Japan, which has started construction.

In the first half of this year, NexPower shipped over 10MW to the USA. Most of these modules were used for a utility project near the area of New Jersey, while the rest were distributed for residential rooftop installations.

The company also states that in early 2012, NexPower modules were tested and listed as the world top three modules by the industry-recognized Photon Module Test 2011.

Most of Energy Conversion Devices assets now sold

According to the US court dealing with the bankruptcy of Energy Conversion Devices and its wholly-owned subsidiary United Solar Ovonic, the majority of assets have been successfully sold, meaning the companies affairs can begin winding up. Eligible voting creditors were said to have approved the actions.

In a statement from ECD, the company said that it had completed the sale of substantially all of the machinery, equipment and inventory held by both companies.

The sale of intellectual property, real-estate holdings and interest in Ovonyx were said to be underway.

Conversion Devices, thin-film plant and machinery sold.

Product Reviews

PLANSEE

PLANSEE develops special alloys for higher performance CIGS layers

Product Outline: PLANSEE has developed two special alloys that are designed to improve the molybdenum layers used in thin-film solar cells via sputtering. The molybdenum-sodium (MoNa) alloy is used for precise sodium doping, while the molybdenum-tantalum (MoTa) is used for a better corrosion resistance.

Problem: Small amounts of sodium in the CIGS absorber improve the efficiency of the solar cell. In the case of glass-based CIGS modules, the soda-lime glass usually also acts as the sodium source. During the production process, sodium from the glass diffuses through the molybdenum back contact into the absorber layer. Unfortunately, this process is not easy to control and the sodium is often unevenly distributed.

Solution: Sputtering targets made from sodium-doped molybdenum (MoNa) offer a simpler alternative. A thin MoNa layer is sputtered above or below the molybdenum back contact. This MoNa layer is then responsible for the controlled release of sodium that occurs as the CIGS absorber is being formed. The concentration of sodium in the absorber can be precisely adjusted by varying the thickness of the layer. Secondly, molybdenum can oxidize in corrosive atmospheres so targets made from molybdenum-tantalum have been proven in numerous tests to offer superior corrosion resistance.

Applications: Molybdenum layers used in CIGS thin-film solar cells via sputtering.

Platform: PLANSEE monolithic targets can be used without backing tubes. They can be sputtered at power densities of >30 kW/m. For improved yield, u-shaped and dogbone targets can be built for material utilization levels of even more than 75 % and thus longer target lifetimes.

Availability: September 2012 onwards.

ECM

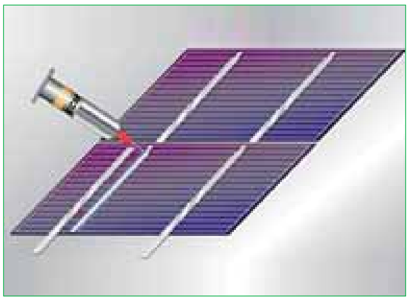

ECM provides fast-curing high-Tg conductive adhesive for CIGS modules

Product Outline: Engineered Conductive Materials (ECM) has developed a new fast-curing conductive adhesive CA-100 for stringing and bussing next-generation CIGS solar modules. This material formulation is optimized for improved conductivity and stability on molybdenum and other substrates used in thin-film manufacturing.

Problem: Next-generation CIGS thin-film modules are challenged to compete with conventional c-Si technologies on both cost and performance. Shorter cycle-times coupled to improved yields and throughput are required.

Solution: CA-100 is designed for thermal cycling and damp heat stability on molybdenum and other substrates used in the CIGS manufacturing process. The high Tg of CA-100 is suitable for manufacturing semi-rigid glass-backed modules and is not designed for flexible modules utilizing reel-to-reel manufacturing. The material can be partially cured for 60 to 90 seconds, providing enough 'green strength' to withstand induced stresses from the manufacturing process until the adhesive cure is completed during the encapsulant lamination process. CA-100 has optimized rheology for dispensing, improved damp heat resistance and conductivity stability on molybdenum, tin, tin-silver and silver-plated ribbons.

Applications: Only suitable for manufacturing semi-rigid glass-backed CIGS modules.

Platform: CA-100 is the latest addition to Engineered Conductive Material's full line of conductive stringer attach adhesives, conductive adhesives for back-contact crystalline silicon, thin-film and via fill applications, as well as conductive grid inks for PV applications.

Availability: June 2012 onwards.

LPKF

Versatile LPKF Presto laser scriber meets lab and production system functions

Product Outline: LPKF SolarQuipment, a subsidiary of LPKF Laser & Electronics, has developed the LPKF Presto laser scriber for structuring thin-film coatings of CdTe, aSi/µSi and CIS/CIGS for laboratory applications but employs the same functions as production systems.

Problem: To improve the efficiency of thin-film solar modules it is necessary to optimize production processes. In the past, users had to utilize large production systems to find out new parameter settings. This causes high costs when disrupting the production process or there is a need for a production-sized laser scriber.

Solution: The LPKF Presto laser scriber is developed for laboratory use and process development. It offers the same functions as the production systems, but comes with increased flexibility. The LPKF Presto has been developed to handle all steps within the laser structuring of thin-film substrates: scribing the pattern in P1, P2 and P3. It is able to scribe at up to 2m/s and to handle glass substrates of up to 6mm thickness. An imaging system is integrated to measure the coordinates for P2 and P3, as well as for an optical inspection. The construction allows structuring both the coated side and through the glass substrate.

Applications: The laser system is made for structuring thin-film coatings of CdTe, aSi/µSi and CIS/CIGS.

Platform: The LPKF Presto uses the same laser sources as the larger production systems of the LPKF Allegro series. The LPKF Presto combines all technical advantages of the high-volume production system LPKF Allegro, but is much smaller and more affordable.

Availability: Currently available.

Laser structuring of thin films for flexible CIGS solar cells

Gediminas Račiukaitis, **Paulius Gečys** & **Simonas Grubinskas**, Department of Laser Technologies, Center for Physical Sciences and Technology (CPST), Vilnius, Lithuania, **Klaus Zimmer**, **Martin Ehrhardt** & **Anja Wehrmann**, Leibniz Institute of Surface Modification, Leipzig, Germany, & **Alexander Braun**, Solarion AG, Leipzig, Germany

ABSTRACT

Thin-film solar cells (TFSCs) still hold unlocked potential for achieving both high efficiency and low manufacturing costs. The formation of integrated interconnects is a useful way of maintaining high efficiency in small-scale solar cells by their connection in series to form a module. Laser scribing is widely used for scribing a-Si- and CdTe-based TFSCs to form interconnects. The optical properties of the ternary copper-indium-gallium (di)selenide (CIGS) compound are well suited to the solar spectrum, with the potential to achieve a high photoelectrical efficiency. However, since it is a thermally sensitive material, new approaches for the laser-scribing process are required, to eliminate any remaining heating effects. For flexible CIGS solar cells on non-transparent substrates (metal foils or polymer), the scribing process faces additional challenges. This is one reason why ultrashort laser pulses yield better results in terms of scribing quality and selectivity. The modelling of laser energy coupling and an extensive characterization of laser scribes allow approaches to be developed for laser scribing of CIGS solar cells on flexible polymer substrates. The measured high efficiency of the resulting high-speed laser-scribed, integrated CIGS mini-modules proved the capability of this approach.

Introduction

Thin-film solar cells (TFSCs) based on copper, indium, gallium and selenium – abbreviated $Cu(In,Ga)Se_2$, or CIGS – have received increasing attention because of achievable photoelectrical conversion efficiencies as high as 27% [1], which is the highest among the different TFSC types. Experimentally verified efficiencies are 20.1% for rigid CIGS solar cells [2] and 17.1% for flexible ones on polyimide [3]. Despite the currently lower efficiency, there is a lot of interest in flexible CIGS solar cells because of the cost-saving roll-to-roll processing and the lower thermal budget for fabrication. Further advantages of flexible CIGS solar cells with relevance to applications are their excellent power-to-weight ratio, a good resistance to radiation (space application [4]) and their flexibility, allowing building integration.

Within the CIGS solar module fabrication process by monolithic integrated interconnection (MII), the efficiency is lower, currently reaching values from 12.1% to 15.9% [5]. Low-loss series interconnections therefore hold significant potential for the fabrication of high-efficiency solar modules. Among other aspects, precise and damage-free scribing of thin films for the interconnections is necessary in order to maximize the effective area and to minimize the losses due to contact resistances and shunts at the interconnections.

Industrial processes for module fabrication call for high speed, low cost, high throughput and high reliability. Scaling up the CIGS thin-film solar cell production and reducing the production costs below US$1/$W_p$ are essential requirements for the future development of the entire fabrication process of CIGS modules. Laser processing is one of the key technologies in reaching this goal [6].

To achieve the high module efficiency over large areas, the module area must be divided into small segments that are interconnected in series in order to maintain a low current while limiting the serial resistance losses within the thin films and the interconnections. The standard way of producing MIIs includes alternating steps of layer deposition and layer patterning. Structuring is accomplished by three scribing processes called P1, P2 and P3, which perform the definition of the length of the solar cell, the formation of the contact area, and the disconnection of the front contact. However, in the alternative approach of external integrated interconnection (EII), the whole film stack is fabricated first and is scribed afterwards. In consequence, the challenges are different for MII and EII.

Currently the scribing of the films is often performed by mechanical tools that provide a rather limited performance in

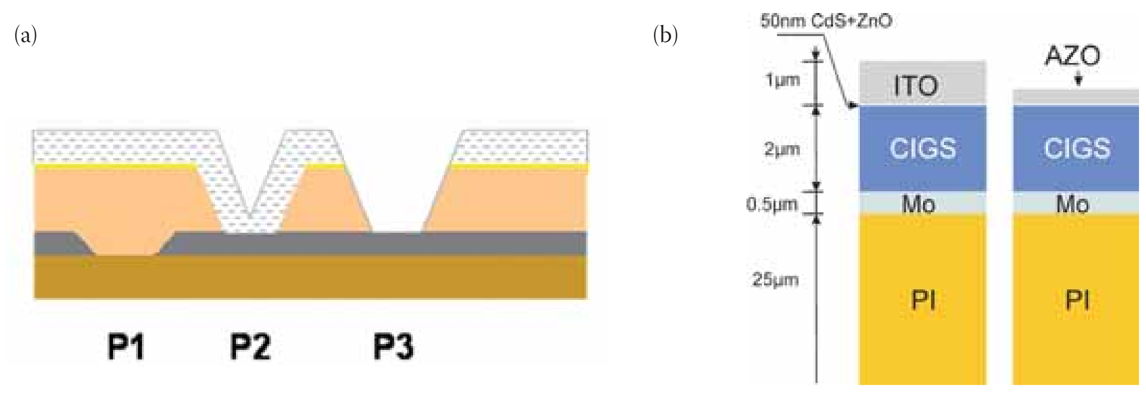

Figure 1. (a) Standard monolithic integrated interconnect (MII) scheme, with P1, P2 and P3 scribing processes performed between deposition steps. (b) Typical layer structure of a CIGS solar cell with a transparent top contact made of ITO or AZO (ZnO:Al).

terms of the scribing width, chipping of the films, tool degradation and scribing speed. However, this technique is still in use, especially for scribing thermally sensitive CIGS films with the processes P2 and P3 [5]. Hence, the use of mechanical tools, despite their shortcomings, provides evidence that laser scribing of such thin-film stacks is still challenging for current laser technology. Different approaches for the development of laser-scribing processes in CIGS solar module fabrication by MII are known. The scribing of the molybdenum film (P1) by laser is widely accepted [7,8]. However, a nanosecond laser may produce cracks in the molybdenum and this must be avoided.

> "Only ultrashort pulsed lasers appear to be capable of patterning CIGS films without any undesirable thermal effects."

There are no established processes for the laser scribing of all the films of CIGS solar cells owing to the thermal sensitivity of the material involved. Because of this sensitivity, laser processing may lead to material modification or cause interface damage by, for instance, the phase transition of semiconducting $CuInSe_2$ to a metallic state. Nanosecond lasers have been used in trials, but only ultrashort pulsed lasers appear to be capable of patterning CIGS films without any undesirable thermal effects [9], although p-n junction damage during the scribing process, even with ultrashort laser pulses, has been reported [10]. On the other hand, the laser-induced conversion of semiconducting CIGS to a metallic phase has been utilized for the fabrication of P2 interconnects using nanosecond lasers with the so-called 'welding' process [11].

Most of the research into the use of picosecond lasers for scribing CIGS solar cells has been carried out using layers deposited on a rigid glass substrate [12,13]. For solar cells based on glass substrates, laser scribing can be performed by irradiation through the glass substrate due to the micro-explosive effect [14]. The use of molybdenum both as a back contact and as the polyimide substrate in CIGS solar cell manufacturing makes it impossible to scribe through the substrate side because of the optical characteristics of the support. The laser-scribing processes of CIGS on flexible metal [11] and polymer substrates [10,15,16] are still challenging. The development of front side laser scribing is therefore essential for the implementation of industrial module fabrication. Fig. 1(a) depicts a schematic cross section of the interconnection area of an MII; the typical layer structure of a CIGS solar cell is shown in Fig. 1(b).

The goal of this study was to develop a flexible and rapid laser technology that is compatible with a roll-to-roll production line for the precise structuring of CIGS solar cells. Modelling of laser light absorption, energy coupling and heat distribution dynamics was realized after a

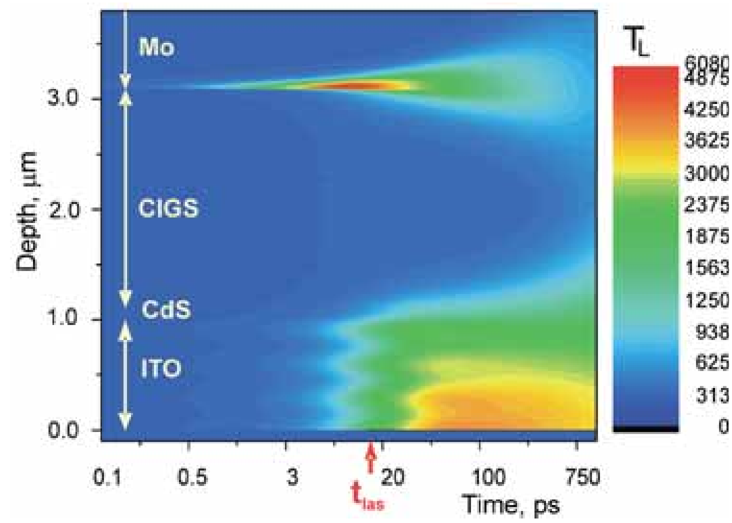

Figure 2. Spatial (bottom to top) and temporal (left to right) evolution of the lattice temperature inside the CIGS structure. A laser pulse with a duration of 10ps (indicated in red on the axis) struck the CIGS PV structure from the bottom (laser fluence = 1J/cm^2; wavelength = 1064nm).

(a) (b)

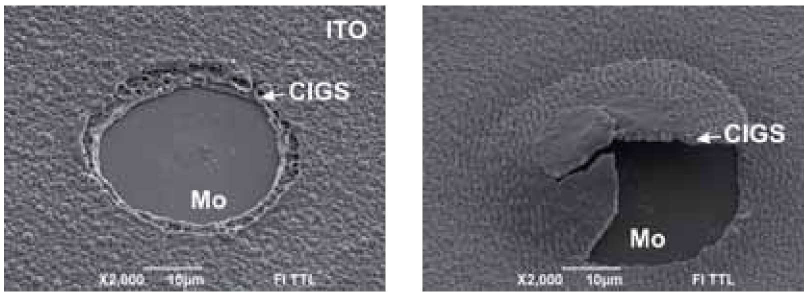

Figure 3. SEM images of craters ablated in (a) ITO/CIGS/Mo/PI and (b) ZnO/CIGS/Mo/PI solar cell structures. The effect of selectivity in energy coupling with the material removal quality is illustrated: CIGS can be cleanly removed using 1064nm in (a), but it is not fully removed using 1572nm in (b).

(a) (b)

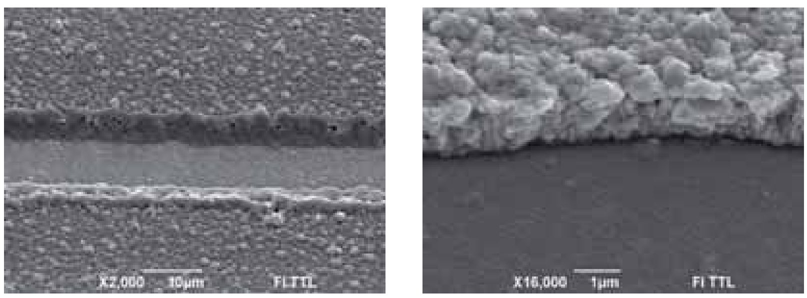

Figure 4. P3-type laser scribes in a CIGS PV structure: a single pass at 200mm/s has been performed using a wavelength of 1064nm in (a), and 1572nm in (b).

picosecond laser pulse was applied to the thin-film structure. Lasers with the picosecond and femtosecond pulse durations were used in the scribing of the CIGS TFSCs deposited on a flexible polymer substrate. An evaluation of the laser-scribe quality, an elemental analysis, and investigations of the local electrical properties of solar cells near the laser-scribing zone, together with efficiency and parallel resistance measurements, are presented for both pulse durations.

Modelling of energy coupling and laser-induced stress

Modelling of the laser-induced processes is important for interpreting the experimental results. Since different physical processes are involved, the finite-element method provided by COMSOL Multiphysics packages was utilized to simulate the process.

The quantity of laser energy coupled inside the films can be found by solving the Helmholtz beam propagation equation, which takes into account absorption and reflection of electromagnetic waves [8]. The wavelength and the complex refractive index $\overline{n}$ (given by $\overline{n} = n + ik_{ext}$, where n is the real part of the refraction index and k_{ext} is the extinction coefficient) mainly define the energy coupling from the laser-generated photons within the thin-film stack. Reflection at the thin-film interfaces causes periodical modulation of the absorbed laser energy along the beam propagation direction, especially for wavelengths where the films are partially transparent, for instance 1064nm. The selectivity of the laser-scribing process can be controlled as a result of the localization of the coupled laser energy at the inner interfaces.

By using the two-temperature model and the calculated absorption of a laser pulse, a numerical simulation of the temperature distribution in the CIGS solar cell structures was performed as a function of the wavelength of the laser radiation in order to determine the removal mechanisms of the transparent conductor and CIGS layers. Simulation results for CIGS solar cells with an ITO top contact are presented in Fig. 2.

Visible light is absorbed by the absorber layer itself. For infrared wavelengths, the high temperature at the CIGS–molybdenum interface remains for a few hundred picoseconds, while the CIGS layer itself is kept cold. This can prevent thermal degradation of the CIGS material.

Because the laser-induced stress increases in proportion to the thermal gradient, the large temperature gradients ΔT of up to 6000K can result in strain values of the order of tens of GPa within the different layers. The irradiated area of the sample experiences plastic deformations and can be fractured under laser-induced thermal strain [14]. Because localization of the strain by local absorption near the interfaces is beneficial, the infrared laser beams can be very useful for scribing thermally sensitive thin-film stacks by using spallation. The SEM images in Fig. 3, showing experimental CIGS ablation with wavelengths of 1064nm and 1572nm, present evidence of the laser-induced mechanical removal processes.

In the case of Fig. 3(a), laser pulses of 1064nm wavelength were sufficiently absorbed at the CIGS/Mo interface, and a clean exposure of the Mo layer was observed. In the case of Fig. 3(b), using a 1572nm wavelength, the laser pulse energy was not sufficient to fully remove the CIGS layer.

Scribing and laser wavelength

Scribing of the CIGS structure with the thick ITO top contact was performed using the picosecond laser (pulse duration 10ps) with different wavelengths. Scribing with a 1064nm wavelength caused clean exposure of the Mo layer (Fig. 4). This result agrees with theoretical assumptions that a large amount of the 1064nm irradiation is absorbed at the CIGS-Mo interface, enabling good layer removal selectivity. The 532nm wavelength induced the formation of a melt area at the edges of the scribe due to the high absorption of this wavelength at the CdS-CIGS interface. The CIGS material was

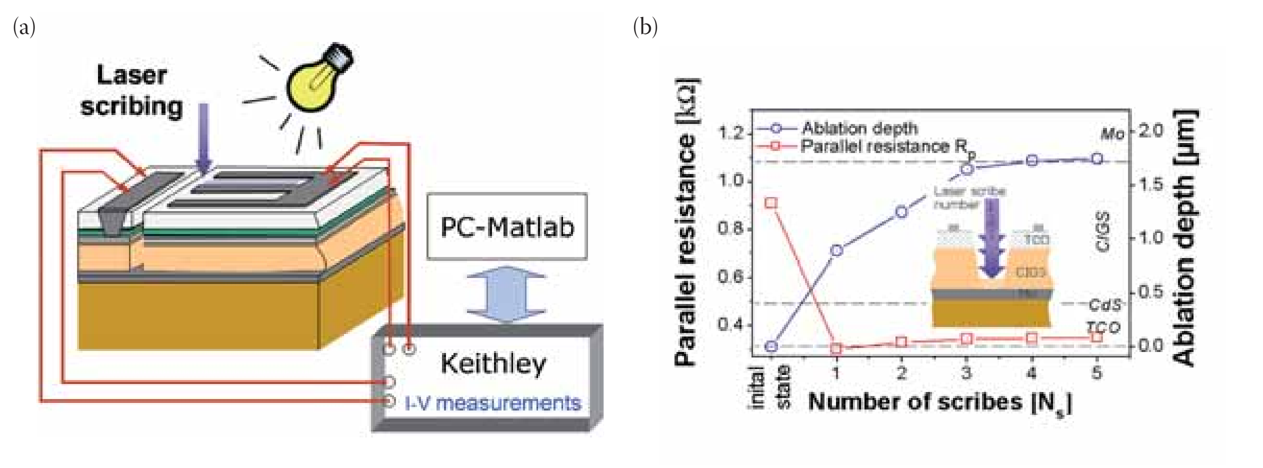

Figure 5. Quasi in situ measurements of a CIGS TFSC for the optimization of the scribing process with an ultrashort pulse laser ($t_p \approx$ 150fs): (a) experimental set-up; and (b) parallel resistance during sequential laser scribing (laser fluence of 0.786J/cm² and a pulse overlap of 77%).

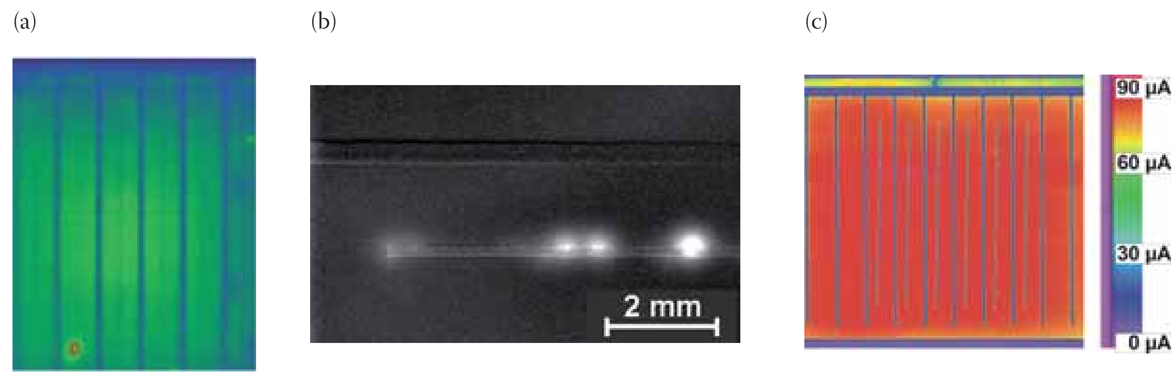

Figure 6. (a) LIT image of the laser-scribed area of a CIGS solar cell. The bright spots indicate film deposition defects, and the blue lines are the contact grid; laser scribes are located in between the vertical contact grid. (b) DLIT image of the overlapping laser scribes near a contact finger of a CIGS solar cell. (c) LBIC photocurrent map of the solar cell area after picosecond laser scribing.

removed by a direct laser ablation process, causing an increase in thermal effects. A 355nm radiation can produce high-quality scribes; however, gentle ablation with low pulse energy is required and multiple scans are necessary.

> "Scribing with a 1064nm wavelength caused clean exposure of the Mo layer."

A laser wavelength of 1064nm was found to be optimal for the P3-type scribe formation in the thin-film CIGS structure. By increasing the scanning speed to 900mm/s, it was possible to selectively remove only the ITO layer without noticeably affecting the absorber layer underneath.

Layer selectivity and depth control are crucial for the high-quality scribing of complex TFSCs. To investigate the remaining layer structure after picosecond and femtosecond laser scribing, SEM and X-ray energy dispersion spectrometer (EDS) analyses were applied [17]. EDS analysis did not detect any splashes of molten molybdenum on the edges of the scribed trench, and all the layers still had sharp interfaces. This demonstrates the potential of ultrashort lasers for high-quality selective thin-layer structuring.

Raman spectroscopy of the laser-affected area

CIGS is a thermally sensitive material, and laser scribing can induce structural changes close to the scribes. The formation of a metallic phase in the CIGS material may cause an internal shunt formation and a reduction in solar cell performance [18]. Raman spectroscopy is a sensitive tool for measuring local disorder in solid materials. Raman spectra were acquired by spatial resolution of 2μm at different locations relative to a laser scribe. Alterations in Raman spectra were obvious in the melt area (walls) as well as outside the trench, where the film was irradiated with wings of the Gaussian beam. However, those changes in spectra did not reveal any evidence of the secondary metallic phase $CuSe_x$ formation during the picosecond laser scribing, as no new lines appeared in Raman spectra close to 262cm^{-1}. These measurements confirmed the ability of picosecond lasers to scribe CIGS TFSCs with low thermally-induced structural changes of the material near the scribing zone.

Photoelectrical characterization of laser-scribed CIGS solar cells

To optimize the laser scribing of CIGS solar cells, measurements of the laser-induced modifications of the electrical characteristic are needed; ex situ and in situ characterization techniques should therefore be applied. The main objective is to evaluate the alterations in solar cell photoelectrical properties after laser scribing.

Electrical measurements of laser-scribed CIGS TFSCs

Fig 5(a) shows the experimental set-up utilized for quasi in situ measurements during the laser scribing. This allowed the rapid collection of reliable information

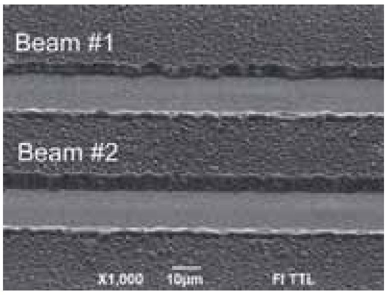

Figure 7. SEM image of parallel P3 scribes in a CIGS PV cell. Distance between them can easily be controlled by optics.

about the changes of the solar cell characteristics due to the laser scribing. Together with the capabilities of the laser-scribing workstation, the scribe geometry and the optical image of the scribe, as well as the electrical properties extracted from the *I-V* curves, can now be evaluated quasi in situ for the assessment of the laser and thin-film interactions and for optimization of the laser-scribing process of TFSCs.

The sequential multi-pass scribing of the CIGS TFSC with ultrashort laser pulses (λ = 775nm, t_p = 150fs) caused a sudden drop in the parallel resistance (R_p) due to shunt formation, as shown in Fig. 5(b). This happened during the first scribe, which resulted in a laser ablation depth of nearly one micron. However, further scribes did not change R_p greatly, as further laser pulses hit only the modified CIGS material. The results show that even femtosecond pulses can introduce thermal modification of CIGS if the film is absorbing energy and is not completely removed during scribing.

Electrical measurements of the solar cell characteristics give no information about the reasons for the laser-induced modifications or about their distribution. Thus, localized studies using electro-optical techniques can help in understanding the laser-induced defect formation, and are required to study the correlations of electrical defects to chemical, physical and topographical properties at the scribing edge. Suitable techniques for high-resolution electro-optical measurements are laser beam-induced current (LBIC) mapping, electroluminescence (EL) imaging and dark lock-in thermography (DLIT) in the reverse current direction.

Lock-in thermography (LIT) has proved to be a valuable technique for non-uniformity diagnostics in crystalline and polycrystalline solar cells [19]. It utilizes AC infrared imaging of a device, where the temperature is affected by an external AC voltage of the same lock-in frequency. The thermography images represent the local current losses.

To detect any short-circuiting caused by laser ablation, LIT measurements were performed in the area close to the scribes. A typical LIT image for the CIGS cell scribed using the infrared 1064nm radiation of a picosecond laser is shown in Fig. 6(a). The film deposition defects are clearly visible and cause a short-circuit current leak at the examined surface. However, no change in the surface temperature was observed for the picosecond or femtosecond scribing regimes. No significant internal shunt formation was detected during laser scribing with either pulse duration. The IR camera was optimized for large-area observation; the resolution was too low to observe an area of the order of a scribe width, and small defects may not have been detected.

The high-resolution DLIT technique in the reverse current direction is well suited to analyzing localize shunts at the edge of laser scribes [10]. The DLIT image in Fig. 6(b) clearly shows that the laser-induced defects are located only on one side of the scribe, and that no defects, for example due to speed reduction, occur at the end of the scribe. The localization of the defects might be due to inadequate overlapping (hatching) in making a wide scribe or to the non-symmetric beam profile. Both localized and distributed shunts are found at the laser-scribe edges. Current investigations show, however, that the efficiency of thin-film $Cu(In,Ga)Se_2$ modules can also be reduced as a result of laser scribing with ultrashort laser pulses.

Laser beam-induced current is a non-destructive optical technique used for defect detection in semiconductors. The LBIC image consists of measurements of the total local current, flowing out through contacts, that is induced by the local laser beam irradiation. The diode laser beam was focused into a 50μm spot and this defined the spatial resolution of the technique. Laser scribing was performed between the fingers of the front contact. The LBIC map of the areas close to the laser scribe (see Fig. 6(c)) showed a uniform distribution of current in the area close to the scribe lines made with the picosecond laser. The dead area near the scribe was minimal, although the resolution of the measurements did not allow an investigation of the defect formation on a micro-scale at the edge of the ablated trench.

PV performance after laser scribing

Complete working solar cells from a prefabrication stage, with an average efficiency of 10.7% and an active surface area of $32cm^2$, were scribed using optimal process parameters. The total length of the laser scribes was 360mm in all cases. The photoelectrical efficiency and parallel resistance measurements were taken before and after laser scribing to evaluate the influence of the laser scribing on the solar cell performance. Reference cells not subjected to laser scribing were also used to monitor degradation of the experimental cells. The measurements were performed using irradiance of the standard global spectrum AM 1.5 and $1000W/m^2$ intensity. The initial photoelectrical efficiency of the CIGS solar cells used in experiments was about 10.7%.

The photovoltaic efficiency tests after laser scribing revealed a minor decrease in the solar cell performance and parallel resistance during optimized laser scribing with picosecond and femtosecond pulse durations. The average drop in efficiency of the CIGS solar cells after laser scribing was 0.35%, which also included the effect of a reduction in active area due to scribe width.

Issues in the industrial implementation of CIGS laser scribing

The industrial implementation of the laser-scribing technologies developed is not yet practical, because of issues concerning reliability, process speed and the realization of flexible substrates in the R2R concept. The reliability issue relates to the remaining effects of laser scribing on the PV performance of the cells, even using ultrashort lasers, and the acceptance of the variation in film thickness and composition. To produce rolls of flexible cells in a single run, a high scribing speed is necessary from an economic point of view. The separate locations of the laser scribing processes (P1, P2, P3) for MIIs along the production line cause an obstruction or a stoppage in the technology implementation. Further progress in flexible CIGS solar cells may therefore benefit from new interconnect architectures. Those issues will be addressed next.

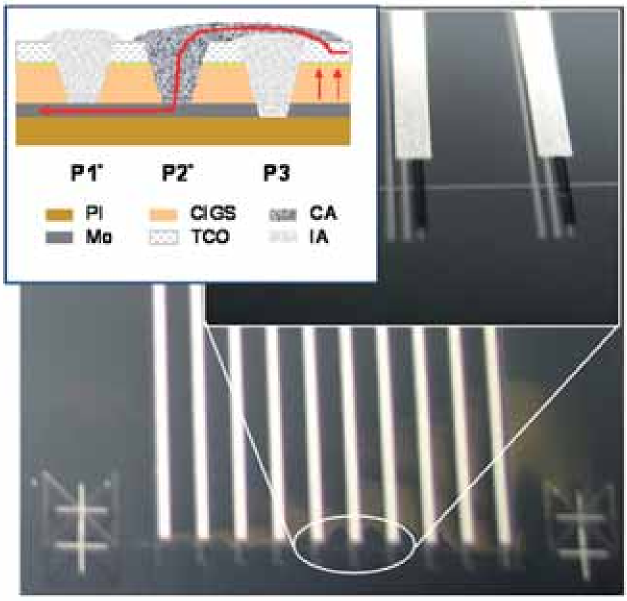

Figure 8. CIGS modules fabricated by the external integrated interconnection (EII) scheme using the R2R laser-scribing process.

> "Laser scribing in the multi-layered structures of modern TFSCs requires high selectivity in the ablation of the films."

Reducing the modified area by the use of shaped laser beams for scribing

Laser scribing in the multi-layered structures of modern TFSCs requires high selectivity in the ablation of the films, without adjacent material being affected. The focused spot of a Gaussian beam that is limited by a beam diameter contains only 86.5% of the laser beam power, and the intensity on the boundary is only 13.5% of the peak intensity. The energy in the wings causes modification of the surrounding material. This type of spatial beam profile does not therefore permit a distinct boundary of the scribes to be achieved. Specialized optical elements are able to transform the smooth Gaussian profile into the square-shaped flat-top beam [20]. The utilization of a top-hat profile beam reduced the laser-modified area on the edges of the ablated scribe by 34% because of uniform irradiation within a limited area, with sharp edges on the boundaries. Moreover, the width of the scribe was less sensitive to instability in the laser pulse energy for the flat-top profile beam. Reliability of the scribing process with regard to the material variation was improved.

Utilization of the full laser power by parallel scribing

Industrial scribing applications demand cost-effective, high-speed processes that are able to be easily integrated into existing production lines. In most cases the best scribing results were achieved when the laser power was a fraction of the total available power of the source. One way to increase productivity and exploit the full power of the laser is to split the beam and then scribe, in parallel, a few lines simultaneously with the same system. The typical distance between integrated interconnects in TFSCs is 5–10mm, which means that several segments of the solar cell fit into the working field of the galvo scanner, and a common beam-guiding system can be used. Moreover, simultaneous scribes for advanced external interconnects can be realized in a single pass, keeping a tight distance control between separate scribes of the same interconnect. The 'dead area' can be reduced significantly with this approach.

The scribing of CIGS TFSCs with four parallel beams was realized by working with a single scanner head and installing a beam splitter in the experimental set-up [21]. The overall power required for the scribing is much lower than the maximum power of the laser used, and the processing can be easily realized using four or more parallel beams. The distance between focused parallel laser beams was adjusted by the splitting angle, which depended on the optical set-up. The same scribing conditions (focusing, power) were maintained for parallel beams, with an excellent repeatability of the laser-scribed trenches (Fig. 7). This illustrates the potential for optimizing laser-scribing processes for CIGS solar cells while meeting the demands of an industrial implementation in terms of process speed and economics.

The process parameters were very close to those obtained for the single-beam configuration. As only about one-tenth of the full laser power was required for the P3 scribing in CIGS solar cells, the approach can be expanded to the ten-beam processing using a picosecond laser. By using a single laser for multiple simultaneously scribed lines, a substantial reduction in the processing cost may be realized.

External integrated interconnections and CIGS modules

By using the EII approach [22], CIGS TFSCs on flexible substrates were interconnected by laser scribing and screen printing of conductive adhesive to fabricate mini-modules. For the interconnection, EII (a cross section is shown in Fig. 8) requires three parallel scribes, which can be made simultaneously as discussed above. However, the requirements of the laser-scribing process for EII are even more demanding than those of the scribing process for MII, as damage to all films and interfaces of the TFSC must be avoided for all scribes from P1 to P3. This is a challenge because the full CIGS stack has to be scribed and requires specific optimized laser-scribing processes.

The complete EII process for CIGS module fabrication comprises:

1. Deposition of the complete stack of CIGS solar cell material.
2. Laser scribing with ultrashort laser pulses.
3. Formation of the interconnection by screen printing of a silver-containing conductive adhesive.

The benefits of this EII technology are: (1) the reduced demand on the scribing procedure concerning the requested overlay accuracy; (2) the division of the fabrication process into thin-film deposition and laser-scribing steps, whereby both the thin-film deposition and the laser scribing can be optimized without interference; and (3) the opportunity to use the same process for CIGS thin-film deposition as for CIGS solar cell fabrication. The laser-scribing procedure in particular can be improved by developing parallel scribing schemes with adapted laser fluences, scribing widths and number of scribe repetitions.

Laser-scribed flexible CIGS thin-film modules, illustrated in Fig. 8, with an output voltage of ~4.5V and an efficiency of ~10% were fabricated. A relative precision and overlay accuracy to external markers of better than 5μm and 10μm, respectively, have been measured within the module area of 20×20cm^2. The rather extended interconnection area is a result of the limited precision of the screen printing, which potentially offers scope for further increases to be made in module efficiency in the future.

Conclusions

The modelling of laser energy coupling and an extensive characterization of laser scribes have facilitated the development of a high-speed laser scribing of CIGS solar cells on flexible polymer substrates. The selection of the appropriate laser wavelength allowed the energy coupling to be kept in a well-defined region at the interface between layers. The high absorption at the inner interface of the layers triggered a localized temperature increase. The transient stress caused by the rapid temperature rise led to peeling of the films rather than evaporation.

Although the quality of laser scribes is promising, most of the processes are too slow in real production lines. The reliability of the scribing process is still an open issue as well. However, to address these issues, a parallel-processing approach has been developed, and the beam-shaping technique was applied to increase the quality of scribes.

> "A new interconnect architecture similar to the external integrated interconnection may make it easier to adapt the laser-scribing technology to the roll-to-roll production of flexible solar cells."

Thin Film

The picosecond lasers used in scribing the thin-film CIGS solar cells exhibited high potential for industrial applications. A new interconnect architecture similar to the external integrated interconnection may make it easier to adapt the laser-scribing technology to the roll-to-roll production of flexible solar cells.

References

[1] Cheyney, T. 2008, "Thin-film CIGS starts to come of age", *Photovoltaics International*, 1st Edn, pp. 86–92.

[2] Jackson, P. et al. 2011, "New world record efficiency for Cu(In,Ga)Se_2 thin-film solar cells beyond 20%", *Prog. Photovolt: Res. Appl.*, Vol. 19, pp. 894–897.

[3] Chirilă, A. et al. 2011, "Cu(In,Ga)Se2 solar cell grown on flexible polymer substrate with efficiency exceeding 17%", *Prog. Photovolt: Res. Appl.*, Vol. 19, pp. 560–564.

[4] Otte K. et al. 2006, "Flexible Cu(In,Ga)Se_2 thin-film solar cells for space application", *Thin Solid Films*, Vol. 511–512, pp. 613–622.

[5] Ishizuka, S. et al. 2010, "Monolithically integrated flexible Cu(In,Ga)Se_2 solar cell submodules", *Solar Energy Mater. & Solar Cells*, Vol. 94, pp. 2052–2056.

[6] Dhere, N.G. 2007, "Toward GW/year of CIGS production within the next decade", *Solar Energy Mater. & Solar Cells*, Vol. 91, pp. 1376–1382.

[7] Westin, P.O. et. al. 2011, "Next generation interconnective laser patterning of CIGS thin film modules", *Solar Energy Mater. & Solar Cells*, Vol. 95, pp. 1062–1068.

[8] Zoppel, S., Huber, H. & Reider, G.A. 2007, "Selective ablation of thin Mo and TCO films with femtosecond laser pulses for structuring thin film solar cells", *Appl. Phys. A*, Vol. 89, pp. 161–163.

[9] Hermann, J. et al. 2006, "Comparative investigation of solar cell thin film processing using nanosecond and femtosecond lasers", *J. Phys. D: Appl. Phys.*, Vol. 39, pp. 453–460.

[10] Wehrmann, A. et al. 2011, "Change of electrical properties of CIGS thin-film solar cells after structuring with ultrashort laser pulses", *Proc. SPIE*, Vol. 7921, p. 79210T.

[11] Kessler, F., Herrmann, D. & Powaila, M. 2005, "Approaches to flexible CIGS thin-film solar cells", *Thin Solid Films*, Vol. 480–481, pp. 491–498.

[12] Heise, G. et al. 2011, "Monolithical serial interconnects of large CIS solar cells with picosecond laser pulses", *Phys. Procedia*, Vol. 12B, pp. 149–155.

[13] Westin, P.-O., Zimmermann U. & Edoff, M. 2008, "Laser patterning of P2 interconnect via in thin-film CIGS PV modules", *Solar Energy Mater. & Solar Cells*, Vol. 92, pp. 1230–1235.

[14] Bovatsek, J. et al. 2010, "Thin film removal mechanisms in ns-laser processing of photovoltaic materials", *Thin Solid Films*, Vol. 518, pp. 2897–2904.

[15] Gečys, P. et al. 2010, "Ps-laser scribing of CIGS films at different wavelengths", *Appl. Phys. A*, Vol. 101, pp. 373–378.

[16] Račiukaitis, G. et al. 2012, "Selectiveness of laser processing due to energy coupling localization: Case of thin film solar cell scribing", *Appl. Phys. A* [in press].

[17] Gečys, P. et al. 2012, "Scribing of thin-film solar cells with picosecond and femtosecond lasers", *J. Laser Micro/Nanoeng.*, Vol. 7, pp. 33–37.

[18] Miyazaki, H. et al. 2003, "Cu(InGa) Se_2 thin film absorber with high Ga contents and its application to the solar cells", *J. Phys. Chem. Solids*, Vol. 64, pp. 2055–2058.

[19] Breitenstein, O. et al. 2001, "Shunts due to laser scribing of solar cells evaluated by highly sensitive lock-in thermography", *Solar Energy Mater. & Solar Cells*, Vol. 65, pp. 55–62.

[20] Račiukaitis G. et al. 2011, "Laser processing by using diffractive optical laser beam shaping technique", *J. Laser Micro/Nanoeng.*, Vol. 6, pp. 37–431.

[21] Gečys P. et al. 2011, "Scribing of thin-film solar cells with picosecond laser pulses", *Phys. Procedia*, Vol. 12, pp. 141–148.

[22] Zimmer, K. et al. 2012, "Laser processing for CIGS thin-film photovoltaics", Biannual Reports 2010/11, IOM Leipzig, pp. 10–13.

About the Authors

Gediminas Račiukaitis studied physics at Vilnius University, Lithuania, and received a Ph.D. for his research on nonlinear spectroscopy of semiconductors. He is the head of the Department of Laser Technologies at the Center for Physical Sciences and Technology (CPST), where he specializes in laser technology development using ultrashort pulsed lasers. Gediminas is a consultant on laser technologies for the laser company EKSPLA; he is also the CEO of ELAS, a spin-off company of EKSPLA, specializing in laser system integration.

Paulius Gečys studied physics at Vilnius University and is currently in the final stages of completing his Ph.D. thesis on the laser scribing of thin-film CIGS solar cells. He has been a research fellow at the CPST since 2008.

Simonas Grubinskas studied theoretical physics at Vilnius University and is now continuing his studies at the University of Utrecht, the Netherlands. He formerly worked in the Department of Laser Technologies at CPST, where his responsibilities included the simulation of laser-induced processes.

Klaus Zimmer studied microelectronic engineering at the University of Applied Science Mittweida, Germany, and received his Ph.D. in thin-film deposition by lasers. His specialities include micro and nano patterning, laser technology and micron technology. Klaus is a senior scientist and group leader at the Leibniz Institute of Surface Modification, where he focuses on laser technology.

Martin Ehrhardt holds degrees in physical engineering and physics from, respectively, the University of Applied Science Wildau, Germany, and the Clausthal University of Technology, Germany. He is currently working on his Ph.D. thesis on laser micro and nano patterning at the Leibniz Institute of Surface Modification in Leipzig.

Anja Wehrmann studied microsystem engineering at the University of Applied Science Mittweida. She investigated laser scribing of thin-film solar cells at the Leibniz Institute of Surface Modification in Leipzig and is now with the German company First Solar Manufacturing.

Alexander Braun holds degrees in physics from Leipzig University, Germany, and Portland State University, USA, and received his Ph.D. in laser physics. He has specialized in thin-film technology, laser physics and surface science since 1996, and is now a CTO at Solarion AG in Leipzig, where he has been a board member since 2006.

Enquiries

Dr. Gediminas Račiukaitis
Head of Department of Laser Technology
Center for Physical Sciences and Technology (CPST)
Savanoriu Ave. 231
LT-02300 Vilnius
Lithuania
Tel: +370-5-2644868
Fax: +370-5-2602317
Email: graciukaitis@ar.fi.lt

Baseline meets innovation: Technology transfer for high-efficiency thin-film Si and CIGS modules at PVcomB

Björn Rau[1], Felice Friedrich[2], Niklas Papathanasiou[1], Christof Schultz[3], Bernd Stannowski[1], Bernd Szyszka[2] & Rutger Schlatmann[1,3]
[1]Helmholtz-Zentrum Berlin für Materialien und Energie GmbH/PVcomB, Berlin; [2]Technical University Berlin/PVcomB, Berlin; [3]University of Applied Sciences Berlin (HTW)/PVcomB, Berlin, Germany

ABSTRACT
Thin-film PV modules are one of the most sustainable options for the generation of electricity, with low material consumption and short energy-payback times. Both of these factors are essential for paving the way towards a terawatt PV market. However, the cost-competitive production of PV modules has become extremely difficult, and module producers are facing huge challenges. A rapid technology transfer from research to industry is therefore required in order to introduce innovations for lower production costs and higher conversion efficiencies. At the Competence Centre Thin-Film- and Nanotechnology for Photovoltaics Berlin (PVcomB), founded by the Helmholtz-Zentrum Berlin (HZB) and the Technical University Berlin, two R&D lines for 30×30cm² modules based on thin-film silicon and copper indium gallium (di)selenide (CIGS) respectively are operated. Robust baseline processes on a high efficiency level, combined with advanced process and device analytics, have been established as a basis for the introduction and development of further innovative technology steps, and their transfer to industry.

PVcomB's mission

Over the last few years, thin-film (TF) PV has been successfully established on the PV market. Large-area production technologies and the use of substrates such as glass or foil are just two means of achieving low-cost production. Different material concepts – such as thin-film silicon, CIGS (compounds based on copper, indium, gallium, sulphur and/or selenium) and cadmium-telluride – are currently in mass production; they have already shown their potential and ability to realize low costs and high volumes in industrial production. But the current market crisis has considerably increased the pressure both on conventional PV production of crystalline Si modules and on TF technologies. The need for significant cost reductions and higher conversion efficiencies is greater than ever.

> "The need for significant cost reductions and higher conversion efficiencies is greater than ever."

The Competence Center Thin-Film- and Nanotechnology for Photovoltaics Berlin (PVcomB) expressly addresses these topics by bridging the gap between fundamental research and industrial application. PVcomB is therefore focusing on the following topics: 1) technology transfer from the lab to a cost-effective production line; 2) R&D in all aspects of production of thin-film PV modules; and 3) education and training of highly skilled, thin-film PV professionals.

To this end, PVcomB has set up in the last three years two R&D TF PV reference lines (TF Si and CIGS) on an intermediate module size of 30×30cm². The whole process chain from glass-substrate washing to the encapsulation of fully processed solar modules is covered, complemented by advanced analytical tools for in situ and ex situ process analytics and high-level device characterization. A truly unique feature of PVcomB's reference lines is that both technologies (TF Si and CIGS) are studied within a single laboratory. This arrangement offers the potential to unlock significant synergies in many topics common to all thin-film-based technologies.

PVcomB – as part of the Helmholtz-Zentrum Berlin (HZB) and in close cooperation with the Technical University Berlin (TUB), the University of Applied Sciences Berlin (HTW) and industrial partners – combines competences in fundamental materials research and device development on the one hand, with industrial experience and technology on the other.

Work at PVcomB concentrates not only on upscaling of promising device concepts from fundamental research, but also on existing industrial processes. For this, PVcomB has created a semi-industrial-like environment to also address aspects of throughput, statistics, reliability and 'easy-to-transfer processes.' The two production 'baselines' for TF PV modules offer the ideal references for new materials, process steps and methods: new device concepts can be directly compared to state-of-the-art technology. In the same way, technological questions from industry (e.g. producers of solar modules as well as manufacturers of production equipment) can be handled by implementing alternative materials, layers or process steps and compared to the reference process.

The two reference lines – PVcomB's backbone

In 2009 PVcomB was recognized as the leading PV cluster in Germany. Over a five-year period (2010–2014), PVcomB will receive €15 million in funding from the BMBF (German Federal Ministry of Education and Research) and the state of Berlin. An advanced research infrastructure has been set up with this support.

Fig. 1 shows a schematic of the two baselines. The heart of the TF Si line is a plasma-enhanced chemical vapour deposition (PECVD) cluster tool – the AKT 1600 from Applied Materials. This tool is equipped with three deposition chambers and a vacuum magazine for up to six 30×30cm² glass substrates. A throughput of up to ten tandem stacks per day is achieved from 12 hours' average operation. An in-line sputter tool (A600V7) from Leybold Optics Dresden is used to develop transparent conducting oxide (TCO) front contacts and to prepare TCO/metal back contacts.

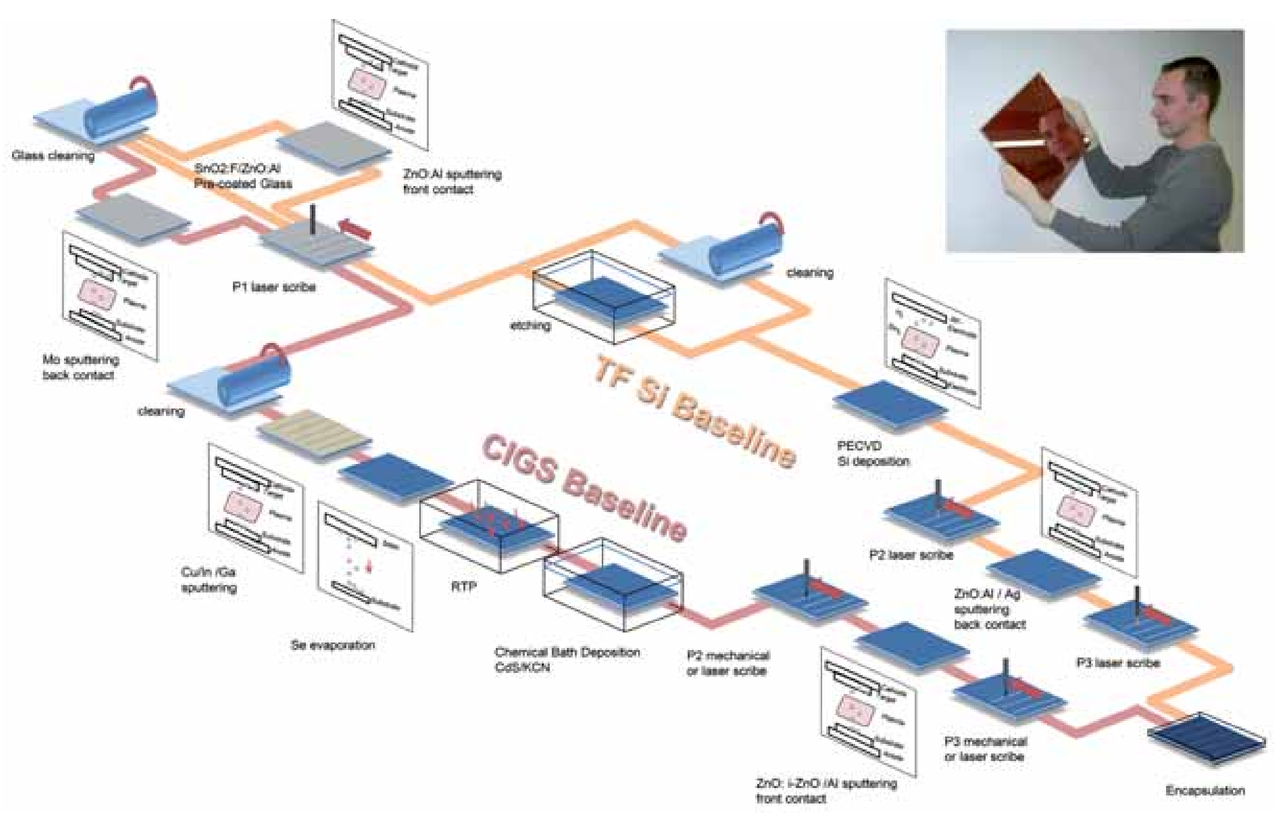

Figure 1. Schematic representation of the two 30×30cm[2] reference lines for TF Si (a-Si/µc-Si) and CIGS modules.

Four magnetron positions (two planar, two rotatable) can be used for various materials. A sixfold carrier magazine for changing substrates and having the ability to coat two substrates simultaneously ensures that automated processes can be run with a high throughput and a high level of reproducibility.

A high-performance laser-scribing tool from Rofin Baasel Lasertech is used to prepare baseline laser scribing as well as for developing novel concepts of laser patterning. Its configuration with nano- and picosecond lasers is optimized for both applications.

The CIGS baseline follows the sequential processing concept. A second A600V7 in-line sputtering tool (four planar and two rotatable magnetrons) is used to deposit the back contact (Mo, SiO_x) and the precursor layers of the absorber (CuGa, In). After a subsequent deposition of selenium, the layer stack is annealed in a rapid thermal processing furnace from Centrotherm. Advanced chemical labs are set up to perform the automatic chemical processing (chemical bath deposition and etching) before the TCO front contact is deposited in a VIS300 sputtering tool from Von Ardenne Anlagentechnik. The above-mentioned Rofin laser tool is also used for all scribes within the CIGS line. It is also equipped with a mechanical scribing tool in order to be comparable to the industrial standards for patterning.

To optimize preparation processes and device behaviour, PVcomB has set up a comprehensive data management system. Real-time investigations of processes (e.g. plasma analysis, residual gas analysis) are combined with tool-side process parameters (e.g. temperatures, gas flows): this allows short feedback times and an excellent understanding of deposition processes. Process tools as well as test sites are attached to an electronic lab book system; with this, operators and

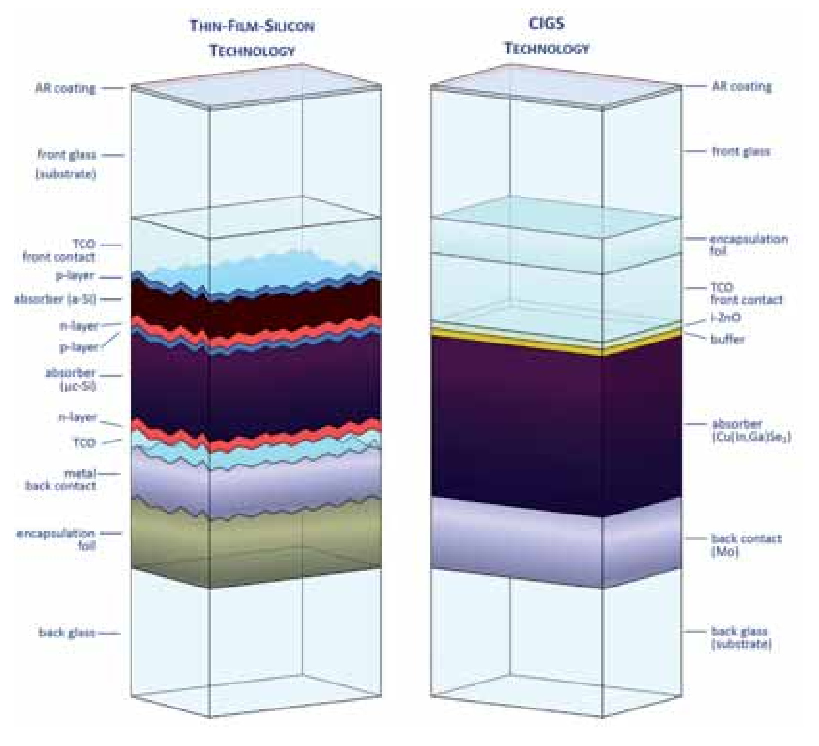

Figure 2. Layer structure of the solar cells developed at PVcomB: a-Si/µc-Si tandem cell (left) and CIGS (right). The entire layer stack, excluding glass and encapsulation, is typically 2–3µm thick.

researchers have fast access to all relevant parameters and results. To ensure a strictly confidential workflow, all selected data are protected by a reliable access control system.

Thin-film silicon solar cells and modules

Thin-film silicon solar cells are dominated by amorphous silicon (a-Si) p-i-n single junctions and amorphous/microcrystalline silicon (a-Si/µc-Si) p-i-n/p-i-n tandem junctions (Micromorph). With a tandem junction (see Fig. 2), an a-Si top cell of thickness 0.2–0.3µm is followed by a µc-Si bottom cell of thickness 1–2µm. While the top cell transforms the visual (VIS) fraction of the sun spectrum at a high voltage of ~900mV, the bottom cell transforms the longer wavelength fraction (near-infrared, NIR) at ~500mV. Because of light-induced defect generation in a-Si, the initial conversion efficiency η of tandem cells drops by typically 10–12% (relative) upon light-soaking before it stabilizes. For lab cells, η_{stable} = 12.3% for a tandem junction and η_{stable} = 10.1% for a single junction have been demonstrated by Oerlikon [1,2]. Owing to the higher conversion efficiency compared to a-Si single junctions, the tandem junction is becoming increasingly dominant in the thin-film silicon PV industry. Large-scale tandem modules achieve η_{stable} of 10–11% [3,4]. One of the main challenges in increasing η further is the limited light absorption in the thin µc-Si layer because of the low absorption coefficient of crystalline silicon. Sophisticated light-trapping schemes and textured substrates are therefore being developed. Here, the correct property of the TCO is crucial. At PVcomB, tandem cell processes have been established for all commonly used TCO substrates (SnO_2:F, ZnO:Al, ZnO:B). New transparent materials and better light-scattering substrates and back contacts are currently being developed.

"One of the main challenges in increasing η further is the limited light absorption in the thin µc-Si layer because of the low absorption coefficient of crystalline silicon."

Fig. 3 shows the results obtained at PVcomB for the initial efficiency over time of a-Si/µc-Si cells deposited on two different large-scale TCO substrates: commercial SnO_2:F (FTO) (blue) and DC magnetron sputtered and texture-etched ZnO:Al (AZO) (red). Both TCOs are on low-iron

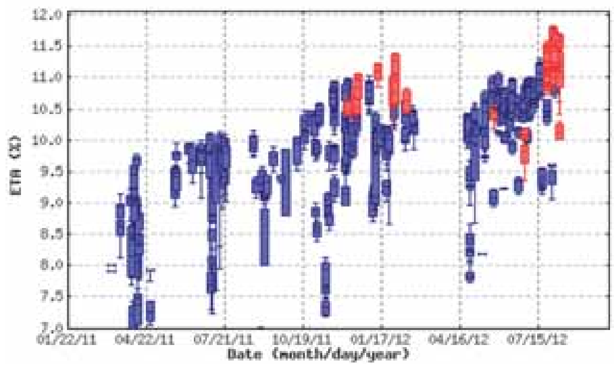

Figure 3. Box plot with a timeline of a-Si/µc-Si (initial) tandem cell efficiency values realized at PVcomB for different TCO substrates: FTO (blue) and AZO (red). A two-month downtime for maintenance and hardware modifications can be seen in spring 2012.

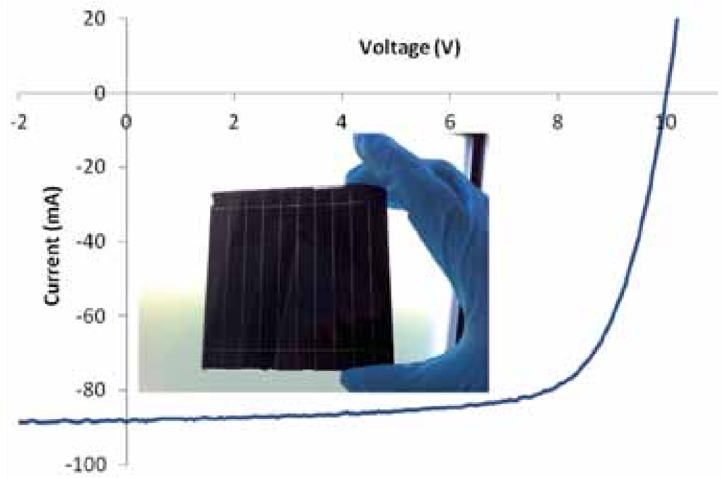

Figure 4. *I-V* characteristics of an a-Si/µc-Si mini-module (seven cells, 56cm² aperture area) from the PVcomB baseline, with 11.3% (initial) efficiency.

3.2mm-thick float glass without anti-reflection (AR) coating. During the last year of operation, the efficiency was increased by more than 2% absolute. So far, the best cell has achieved 12% (initial) and 10.8% (after 168 hours of light-soaking at AM1.5, 50°C), both on ZnO:Al. For recent 10×10cm² mini-modules (180µm interconnection width dead area), an initial efficiency of 11.3% was achieved (Fig. 4) – this is expected to stabilize at well over 10%.

Much higher efficiencies, however, are required. Most research groups currently working on a-Si/µc-Si tandems are therefore focusing on three topics:

1. Highly transparent (and reflecting) doped p- and n-layers, e.g. based on µc-SiO_x.
2. Low-defect growth of µc-Si:H on highly textured substrates.
3. Highly transparent, multi-scale, textured TCO substrates.

These three topics are being addressed at PVcomB, and the improved processes have been developed to be implemented in our baseline, demonstrating robustness, scalability and compatibility with industrial production. The latter is done in cooperation with our industry partners. It is aimed to demonstrate mini-modules with a stable efficiency of 12%. Examples of this work are given next.

New doped layers

In the most recent tandem cell shown in Fig. 2, all doped layers are based on µc-SiO_x, a mixed-phase material consisting of a (doped) µc-Si phase embedded in a-SiO_x as matrix material. Originally proposed and implemented by Kaneka Corp., it has been developed for cells over the last few years [5,6]. Besides the reduced parasitic absorption as compared to a-Si or µc-Si doped layers, the refractive index n can be varied in a wide range, which allows µc-SiO_x layers with low $n \approx 1.7$–2 to be employed as reflective layers (at the internal n/p contact)), or, with high $n \approx 2.5$, as an anti-reflective front p layer. Furthermore, the negative influence of local micro shunts on the cell's FF and V_{oc} is believed to be suppressed as a result of limited lateral conductivity.

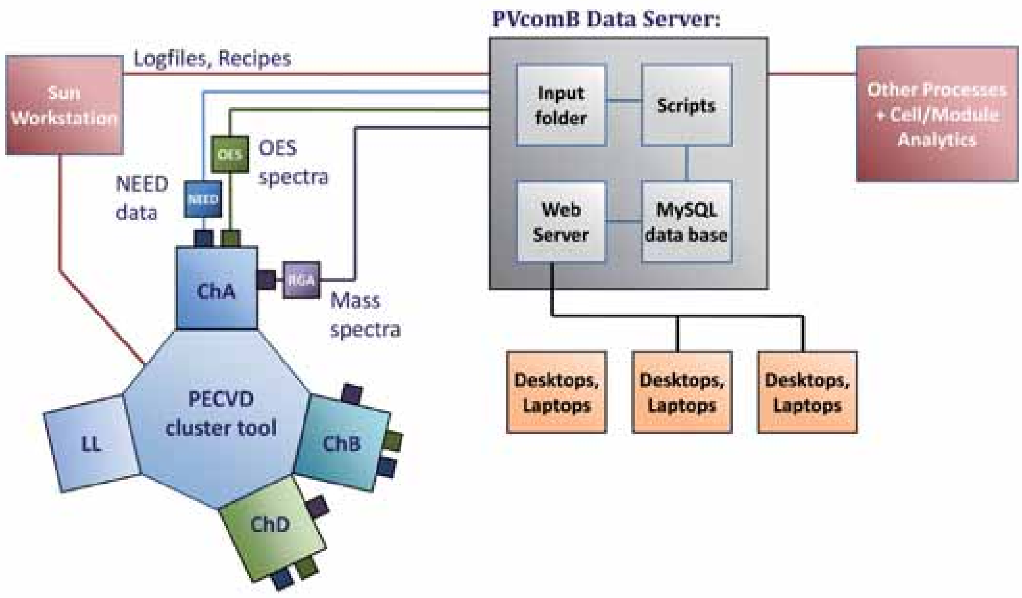

Figure 5. Schematic of the PECVD cluster tool (AKT), with in situ diagnostics and connection to the in-house database system.

The focus is on further development of that material in addition to establishing and transferring a robust process to large-scale production in collaboration with our industrial partners (Masdar PV and Inventux). Moreover, within the Helmholtz-Zentrum Berlin, research is being carried out on new materials based on SiO_x, SiC_x and SiN_x to be used as functional layers, for example doped layers, or as barrier layers for high-T applications, such as polycrystalline Si cells [7,8].

Highly transparent TCO

As can be clearly seen in Fig. 3, the cells based on ZnO:Al TCO outperform the cells on SnO_2:F, which partially results from better AZO transparency and light scattering, and partially from an optimized and more transparent AZO/p design based on the above-mentioned μc-SiO_x. A method for significantly improving the properties of ZnO:Al by annealing the TCO at 500–600°C under a thin a-Si capping [9,10] has been developed at Helmholtz-Zentrum Berlin. The free-carrier mobility was thus increased from about 35 to more than 70cm^2/Vs, helping to reduce absorption in the NIR. Moreover, transmission in the VIS is improved as a result of the annealing of structural defects at the grain boundaries. It was recently demonstrated at PVcomB that this leads to an improved short-circuit current. The quantum efficiency of initial cells on annealed ZnO:Al has already shown a 5% increase in current compared to the best cells on standard ZnO:Al TCO [11].

PECVD in situ diagnostics & in-house database

As mentioned above, PVcomB operates a PECVD cluster tool that is specifically designed for industrial applications; high throughput and reliability are key properties of this tool. This is crucial in order to optimize and control the baseline and to run the various R&D projects with enough statistics on one tool. To gain an understanding of growth processes, such as μc-Si or μc-SiO_x, as well as NF_3 etching and chamber conditioning, PECVD in situ diagnostics were implemented: OES (optical emission spectroscopy), RGA (residual gas analyzer, mass spectrometry) and a Hercules sensor by Plasmetrex for measuring the electron dynamics (NEED) of the plasma. These three techniques are complementary to, as well as compatible with, industrial production. With a database system developed in-house, all PECVD recipes and deposition parameters, in addition to the in situ diagnostics data, are logged, with easy access via a user interface (shown schematically in Fig. 5) [12]. Moreover, the database contains *I-V* and EQE (external quantum efficiency) measurement results from cells and modules. This facilitates the easy correlation of process data and plasma properties with cell parameters. Data mining and statistical process control, as well as fast troubleshooting, is also made possible.

CIGS solar cells and modules

Cu(In,Ga)$(S,Se)_2$ (CIGS) solar cells hold the technology world record in efficiency in the field of thin-film photovoltaics, with cell efficiencies of up to 20.3% [13]. There are several approaches to manufacturing CIGS solar modules: they can be classified as *sequential processing* and *co-evaporation*. In the case of co-evaporation, all elements are evaporated in a single vacuum chamber to form the CIGS layer; sequential processing, on the other hand, begins with a Cu/In/Ga precursor layer, which is converted in an annealing step into CIGS. Nevertheless, for both of these technologies, it has not yet been possible to transfer the record efficiencies into mass production, as the homogeneity in terms of composition and thickness of the CIGS layer plays a crucial role.

> "It has not yet been possible to transfer the record efficiencies into mass production, as the homogeneity in terms of composition and thickness of the CIGS layer plays a crucial role."

As of July 2012, all baseline equipment for CIGS solar cell processing has now been delivered and production has started. Results from the first solar cells are presented in the following section. As described earlier, the CIGS baseline applies a typical sequential processing sequence [14]. A substrate soda-lime glass is coated with an 800nm single-layer molybdenum (Mo) back-contact layer. Subsequently, a stacked elemental layer (SEL) of 370nm Cu:Ga, 500nm In (by magnetron sputtering) and Se (by thermal evaporation in a vacuum chamber) is deposited. This SEL is converted into the CIGS absorber layer within 90 seconds in a rapid thermal processing (RTP) furnace with radiation heating at 570°C. The temperature ramp is about 4K/s within the CFC carrier box. The whole process time is approximately 4 minutes (without pump- and cool-down times). After the p-type CIGS absorber layer is formed, the

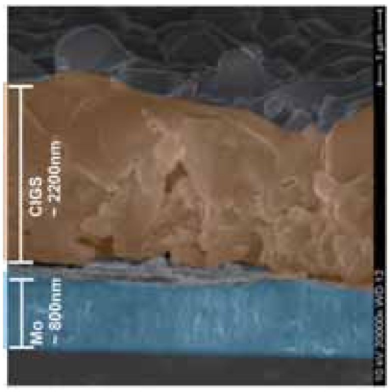

Figure 6. SEM cross section of a CIGS absorber layer.

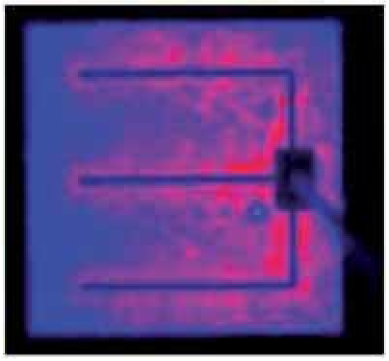

Figure 7. IR thermography image of a CIGS solar cell.

n-type CdS buffer layer is deposited in a chemical bath deposition (CBD). The cell is finished by the application of an intrinsic ZnO (i-ZnO)/ZnO:Al double layer. To produce a simple sample preparation, the 30×30cm^2 substrates are first cut into nine 10×10cm^2 coupons. These coupons are divided into 49 cells of 1.4cm^2. The cells are then contacted via a Ni/Al/Ni contact grid deposited by electron-beam evaporation.

The initial layers are thoroughly analyzed with respect to their compositional and thickness homogeneity, morphology and solar cell parameters. Absorber composition and thickness of precursor and absorber layers are determined by X-ray fluorescence spectroscopy (XRF), measured by a Rigaku XRF Primus II instrument, using a first-principles method without a calibration sample. The homogeneity is calculated by taking nine measurement points equally distributed on the 30×30cm^2 substrate. The thickness inhomogeneity of the sputtered precursor layers is about 2% for Mo and Cu:Ga, and 3.6% for In. Selenium is deposited with a thickness variation of about 10%. The resulting absorber layers have a Cu/(In+Ga) ratio of 0.82, with a variation of only 5.1%, while the absorber thickness varies between 1.94µm at the edge and 2.25µm in the centre (roughly 12% variation).

The best solar cell from our first run yielded a conversion efficiency of 8.7%, with a short-circuit current density (J_{sc}) of 40.2mA/cm^2, an open-circuit voltage (V_{oc}) of 400mV and a fill factor (*FF*) of 54%. The low fill factor can be explained by a high series resistance (R_{oc}) of 4Ωcm^2, which is mainly caused by the use of a ZnO window layer that was optimized for another CIGS device, not for the PVcomB stack. The low V_{oc} indicates that no gallium is at the top of the absorber layer, as gallium increases the band gap of CIGS and therefore the open-circuit voltage.

Scanning electron microscope (SEM) cross-section imaging reveals a compact and dense layer with no large holes (Fig. 6). Nevertheless, the polycrystalline CIGS has larger grains at the top and smaller grains at the bottom. Energy dispersive X-ray spectroscopy (EDX) line scans detect a large quantity of Ga in the small grains at the Mo/CIGS interface, indicating that these are Ga-rich crystallites. The agglomerate of gallium at the Mo back contact is typical for a sequential CIGS process. Pushing the Ga to the top is the biggest challenge in future process development. Quantum efficiency (QE) measurements also indicate that the top layer is pure $CuInSe_2$, since QE is still above 50% at 1200nm, which correlates to a band gap of 1eV, as expected for $CuInSe_2$. This is also the reason why the best initial solar cells have a V_{oc} of only 400mV.

Infrared (IR) lock-in thermography imaging shows only a few shunts in the solar cells (Fig. 7). This supports the image of a dense and homogeneous CIGS layer structure produced in the first experiments within the CIGS baseline.

In parallel with the optimization of CIGS solar cell processing, PVcomB is also targeting new concepts to improve the solar cell quality. Three major topics will be investigated:

1. A barrier layer to prevent uncontrolled sodium diffusion from the glass substrate, plus the application of additional sodium diffusion, such as a Mo back contact doped with sodium.
2. A Cd-free buffer layer using dry processes, such as atomic layer deposition (ALD).
3. The development of elemental selenium and sulphur sources for the RTP process in order to achieve a better control of the CIGS growth process.

The joint laser laboratory of HTW and PVcomB

In thin-film solar cell manufacturing, further reduction in cost, as well as increase in yield efficiency, requires the most innovative concepts. The application of laser technologies is already well established in the industrial production process (for example for monolithic series interconnection) and helps to drive down the cost per W_p. The three scribing steps P1, P2 and P3, alternating with thin-film deposition, are necessary for creating a serial interconnection of many cells on a single substrate.

For further increases in module efficiency and production yield, high precision patterning is required. To meet these challenges, HTW (with its very strong laser background) and HZB have joined forces in PVcomB to set up a state-of-the-art laser processing system and to develop new solar cell concepts.

> "For further increases in module efficiency and production yield, high precision patterning is required."

The laser-based patterning tool of HTW, directly integrated in PVcomB's laboratory environment, is equipped with a high-speed motion system and two different

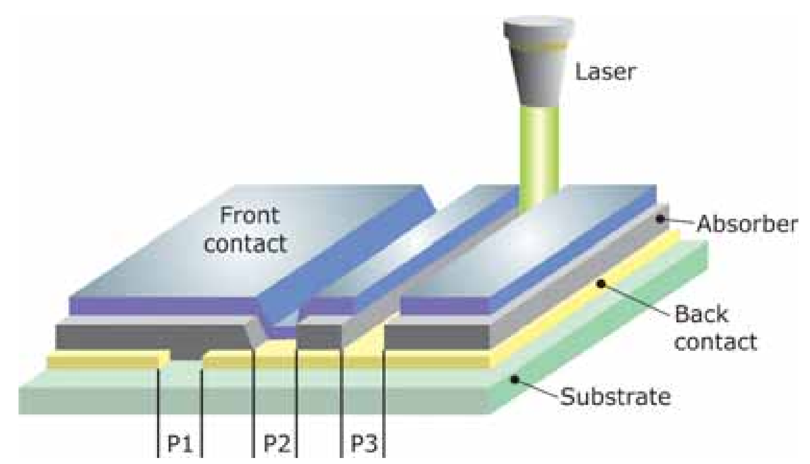

Figure 8. Schematic of a typical monolithic series interconnection of TF solar cells.

laser sources. The motion system facilitates accurate patterning with deviations of less than 5μm at velocities of up to 1200mm/s. This high accuracy allows us to reduce the area losses resulting from serial interconnection. Well-established standard patterning is performed using a nanosecond laser source with a wavelength of 532nm. For the purposes of developing novel concepts as well as heat-sensitive patterning, a picosecond laser source with a wavelength of 1064nm, in addition to second- and third-harmonic generation of laser pulses with 532nm and 355nm wavelengths, is integrated. For reference purposes, a scribing needle is available.

This innovative set-up allows novel laser-based patterning concepts to be developed and established for industrial solar cell fabrication as well as for the upscaling of these processes. It is also possible for solutions to be developed for external partners for their industrial laser applications, such as wafer marking, or for evaluating suitable parameters for patterning these materials.

At present, research topics include complete laser patterning of CIGS cells, especially patterning with a single nanosecond wavelength [15], and simulation of the laser–matter interaction in stacked layer systems [16]. Further investigations to seek a fundamental understanding of laser–matter interaction, such as the molybdenum ablation behaviour, are in progress.

Advanced analytics for device and process optimization

The analytics baseline at PVcomB comprises a number of standard characterization methods that are applied to, and documented online for, each processed sample. The equipment is calibrated on a regular basis to ensure highly reliable results in conformance with international standards. The backbone of the standard methods is formed of the AAA dual-source WACOM Solar Simulator and the AAA dual-source h.a.l.m. Flasher. These are complemented by a dual-source EQE set-up and a detailed optical characterization by means of a Perkin Elmer high-performance Lambda 1050 spectrophotometer. Apart from the standard tests, the continuous further development of analytical equipment, along with the implementation of new tools, is of high importance. Currently the integration of a lock-in thermography system (by Thermosensorik) and an electroluminescence set-up (by Great Eyes) in the baseline analytics process is the centre of attention (see Fig. 7). In addition, a number of methods – such as angle-resolved scattering (ARS), Raman spectroscopy, Hall effect and illuminated lock-in thermography – are available on site for basic research of materials.

With regard to advanced thin-film photovoltaic device analytics, a close cooperation has been established between the initial PVcomB partners and the Joint Lab (JL) of IHP Frankfurt/O and BTU Cottbus. As a result, a wide range of sophisticated analytical techniques suitable for PV materials is accessible for PVcomB research.

The PVcomB research at JL focuses on the adaptation and application of transmission electron microscopy (TEM) methods, in addition to spatially and spectrally resolved photoluminescence (PL) [17] techniques, each of which requires an approach to compete with the side effects of the glass substrate and low signal intensity. These methods are complemented by the Hamamatsu PHEMOS 1000 set-up at TU Berlin for spatially and spectrally resolved electroluminescence (EL) as well as light-beam-induced current (LBIC) investigations. In particular the latter can give valuable information on light-scattering effects in thin-film photovoltaic devices [18].

Among the methods available at TU Berlin, X-ray fluorescence techniques – such as grazing incidence XRF (GIXRF) – have already been successfully applied to both chalcopyrite and silicon absorber systems [19,20]. Here, a non-destructive depth-resolved analysis of the chemical composition is obtained by varying the X-ray angle of incidence, thus making it possible to extract information about, for example, composition gradients or buried interface properties. As mentioned earlier, PVcomB is equipped on site with a Rigaku WD-XRF ZSX Primus II. Because of the wavelength dispersive detection set-up, elements down to boron (Z=5) can be detected with high sensitivity and reproducibility. The implemented layer model is well adapted to a fundamental parameter-based analysis of the typical precursor stacks in chalcopyrite technology, yielding the thickness as well as the composition of individual layers. Last, but not least, the Primus II system comes with a mapping facility that provides information on lateral compositional non-uniformities.

In order to understand and distinguish the manifold effects caused by the thin-film nature of thin-film photovoltaics, PVcomB has finally entered the field of 2D/3D device modelling. There are several suitable commercial and non-commercial simulation tools available on the market, each offering a wide variety of physical models and pre-selected parameter sets (usually in regard to crystalline silicon). However, in order to obtain reliable information, the relevant models and parameters have to be chosen very carefully. PVcomB's approach is to use the knowledge gained by years of 1D modelling for a step-wise expansion of the 1D solar cell model into space. This extension is essential for a proper description of the complex optoelectronic interaction in current thin-film devices. Light-management phenomena [21] and functional non-uniformities, for example in intermediate reflector concepts, accompany advanced contacting schemes that can be effectively optimized by device modelling [22].

"The mission is to bridge the gap between innovative lab-sized solar cell concepts and industrially produced modules."

Summary

PVcomB is a joint initiative of HZB and the Technical University Berlin. Together with HTW and other partners from research and industry, a unique institution has been set up for applied research and development in the field of thin-film PV. The mission is to bridge the gap between innovative lab-sized solar cell concepts and industrially produced modules. To this end, PVcomB has set up two dedicated reference lines for research in thin-film Si- and CIGS-based modules with an area of 30×30cm^2; this module size is well suited to addressing various issues arising in industrial production. State-of-the-art TF modules from both of these technological routes are developed and produced in a semi-industrial environment, for investigating issues such as process stability, throughput, statistics and reliability. Advanced analytical methods for in situ and ex situ characterization of materials and devices have been established to support the whole range, from baseline characterization to advanced fundamental research. An ideal reference has therefore been created for the implementation of new materials, process steps and technologies.

Acknowledgements

We would like to acknowledge the invaluable contribution of all persons involved in building up PVcomB, from the initial idea generation to establishing full functionality. We also wish to express our appreciation for the support from our partner companies and institutions. This work was supported by the Federal Ministry of Education and Research (BMBF) and the state government of Berlin (SENBWF) in the framework of the 'Spitzenforschung und Innovation in den Neuen Ländern' programme (grant no. 03IS2151).

References

[1] Benagli, S. et al. 2009, "High-efficiency

amorphous silicon devices on LPCVD-ZnO TCO prepared in industrial KAI-M R&D reactor", *Proc. 24th EU PVSEC*, Hamburg, Germany.

[2] Kroll, U. et al. 2011, "Recent development of high efficiency micromorph tandem solar cells in KAI-M/Plasmabox PECVD reactors", *Proc. 26th EU PVSEC*, Hamburg, Germany.

[3] Kluth, O. et al. 2011, "The way to 11% stabilized module efficiency based on 1.4m^2 Micromorph® tandem", *Proc. 26th EU PVSEC*, Hamburg, Germany.

[4] Klein, S. et al. 2011, "Large area thin film silicon modules with 10% efficiency for production", *physica status solidi C*, Vol. 8, No. 10, pp. 2978–2981.

[5] Lambertz, A., Grundler, T. & Finger, F. 2011, "Hydrogenated amorphous silicon oxide containing a microcrystalline silicon phase and usage as an intermediate reflector in thin-film silicon solar cells", *J. Appl. Phys.*, Vol. 109, p. 113109.

[6] Cuony, P. et al. 2012, "Silicon filaments in silicon oxide for next-generation photovoltaics", *Adv. Mater.*, Vol. 24, pp. 1182–1186.

[7] Amkreutz, D. et al. 2011, "Electron-beam crystallized large grained silicon solar cell on glass substrate", *Prog. Photovolt.: Res. Appl.*, Vol. 19, No. 8, pp. 937–945.

[8] Sontheimer, T. et al. 2010, "Challenges and opportunities of electron beam evaporation in the preparation of poly-Si thin film solar cells", *Proc. 35th IEEE PVSC*, Honolulu, Hawaii, USA.

[9] Ruske, F. et al. 2010, "Improved electrical transport in Al-doped zinc oxide by thermal treatment", *J. Appl. Phys.*, Vol. 107, p. 013708.

[10] Wimmer, M. et al. 2012, "Improving the electrical and optical properties of DC-sputtered ZnO:Al by thermal post deposition treatments", *Thin Solid Films*, Vol. 520, p. 4203.

[11] Neubert, S. et al. 2012, "High-mobility Al-doped zinc oxide front electrodes: A perspective for improved conversion efficiency in Si thin-film solar cells", submitted to *Prog. Photovolt.: Res. Appl.*

[12] Gabriel, O. et al. 2011, "Time resolved process monitoring during the deposition of amorphous and micro-crystalline silicon", *Proc. 26th EU PVSEC*, Hamburg, Germany.

[13] Jackson, P. et al. 2011, "New world record efficiency for Cu(In,Ga)Se_2 thin-film solar cells beyond 20%", *Prog. Photovolt.: Res. Appl.*, Vol. 19, No. 7, pp. 894–897.

[14] Scheer, R. & Schock, H.W. 2011. *Chalcogenide Photovoltaics: Physics, technologies, and thin film devices.* Weinheim, Germany: Wiley-VCH.

[15] Schultz, C. et al. 2011, "P1, P2 and P3 structuring of CIGSe solar cells with a single laser wavelength", *Proc. 26th EU PVSEC*, Hamburg, Germany, pp. 2943–2946.

[16] Richter, M. et al. 2011, "Laser-ablation behavior of thin-film materials used in silicon and CIGSe based solar cells", *Proc. 26th EU PVSEC*, Hamburg, Germany, pp. 2540–2543.

[17] Klossek, A. et al. 2012, "PL, EDX, EBIC investigations on a-Si/µc-Si tandem cells", presented at EMRS 2012 spring meeting, submitted to *Mater. Sci. & Eng. B.*

[18] Boostandoost M. et al. 2011, "Characterization of poly-Si thin-film solar cell functions and parameters with IR optical interaction techniques", *J. Mater. Sci.: Mater. in Electron.*, pp. 1553–1579.

[19] Streeck, C. et al. 2010, "Elemental depth profiling of Cu(In,Ga)Se_2 thin films by reference-free grazing incidence X-ray fluorescence analysis", *Nucl. Instr. Meth. B*, Vol. 268, pp. 277–281.

[20] Pagels, M. et al. 2010, "GIXRF-NEXAFS investigations on buried ZnO/Si interfaces: A first insight in changes of chemical states due to annealing of the specimen", *Nucl. Instr. Meth. B*, Vol. 268, pp. 370–373.

[21] Lockau, D. 2012, "Optical modeling of thin-film silicon solar cells with random and periodic light management textures", Ph.D. thesis, Humboldt Universität zu Berlin.

[22] Teodoreanu, A.-M. et al. 2012, "2D modeling of polycrystalline silicon thin film solar cells", PV Technical Conf., Aix en Provence, France, submitted to *EPJ Photovoltaics*.

About the Authors

Björn Rau is the technology manager and the deputy director at PVcomB. He started PV research at the Helmholtz-Zentrum Berlin (the former Hahn-Meitner-Institut) in 2001, working on poly-Si TF solar cells. He received his Ph.D. in physics from the Humboldt Universität zu Berlin in 2003, and joined PVcomB in 2009 to coordinate PVcomB's scientific infrastructure and the baseline ramp-up.

Felice Friedrich is head of the analytics group at PVcomB. She received her Ph.D. in physics from the Technical University Berlin in 2009. After a short postdoctoral appointment at the Helmholtz-Zentrum Berlin, she joined PVcomB in 2010, where she coordinates the analytics infrastructure and the interplay with the PVcomB advanced analytics network.

Niklas Papathanasiou is head of the CIGS solar cell development at PVcomB. He received his Ph.D. in physics in 2004 from the Free University of Berlin. He studied CIGS solar cells for his Ph.D. and during his postdoctoral time at the Helmholtz-Zentrum Berlin (former Hahn-Meitner-Institut). Before joining PVcomB, he was head of R&D TF technology at Inventux Technologies AG, working on a-Si and µc-Si tandem PV modules.

Christof Schultz is an engineer in the HTW laser research group at PVcomB. He received his diploma degree in renewable energies in 2008 from the University of Applied Sciences Berlin. He formerly worked for PVflex Solar GmbH in the R&D department, where he specialized in laser patterning and technology.

Bernd Stannowski joined PVcomB in 2010 and is head of the TF Si R&D group. He received his Ph.D. in 2002 from Utrecht University, the Netherlands, for his research on TF Si transistors. He worked as a research engineer for four years on a TF Si PV project at Akzo Nobel. He subsequently built up and headed a development department at the PV module manufacturer Sontor GmbH (later Sunfilm AG).

Bernd Szyzska obtained his Ph.D. while working at the Fraunhofer Institut IST in Braunschweig. In 2003 he subsequently built up and led the large-area coatings department within the institute. Since July 2012 he has held a full professorship at the Technical University Berlin, a post which was created specifically in connection with PVcomB.

Rutger Schlatmann received his Ph.D. from the FOM Institute in Amsterdam and has been the director of PVcomB since 2008. From 1999 to 2008 he worked as an R&D manager at Helianthos, developing flexible thin-film Si solar modules. He will also hold a full professorship at the University of Applied Sciences Berlin (HTW) from October 2012.

Enquiries

Björn Rau
Email: bjoern.rau@pvcomb.de
Tel: +49 30 8062 18153
Fax: +49 30 8062 15677

PV Modules

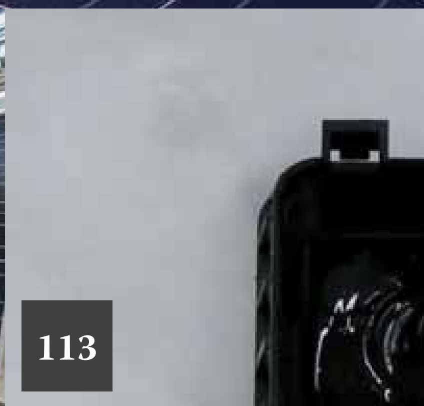

News

Suntech Power Holdings delivers more than 1GW of solar panels to the Americas

Suntech Power Holdings revealed that in July 2012 it had achieved the milestone of delivering more than 1GW of solar panels to customers in North and South America. The company noted that it is one of the first global solar companies with a 1GW delivery record for the region. Worldwide, Suntech has shipped more than 7GW of its solar panels to over 1,000 customers in more than 80 countries.

Altogether, deployed Suntech solar panels generate an estimated nine terawatt hours of clean electricity per year, greater than the power consumption of Costa Rica, or Paraguay, according to data from the CIA World Factbook.

In 2010, Suntech opened a 30MW solar module production facility in Goodyear, Arizona, which has since expanded to 50MW and now runs around-the-clock.

Suntech delivers over 1GW of solar panels to customers in North and South America.

Business News Focus

IMS Research: PV module prices declined by 44% annually

PV module prices had enjoyed a short period of stability in June because of high demand in Germany and Italy, but began to decline again in July. Over June, average prices fell by more than 2% and by 44% annually, according to the latest monthly module price report from IMS Research.

Despite module prices consistently declining throughout the last year, IMS Research found the outlook for prices for August to be more positive, and on average, industry buyers and sellers expected prices to increase by 0.3% in August.

However, expectations varied clearly by company type, with module suppliers and integrators forecasting a further small decrease, whilst distributors expect a small increase.

ReneSola strikes solar product insurance agreement with PowerGuard

ReneSola, a China-based specialist in the manufacture of solar wafers and modules, has signed a solar products insurance agreement with PowerGuard Specialty Insurance Services, a specialist in insurance and risk management solutions for solar and other alternative energy companies.

MPrime announces investment in innovation programme for PV module production line

MPrime, a subsidiary of Martifer Solar, has announced its investment in an innovation programme for its photovoltaic module production line at the company's factory in Oliveira de Frades, Portugal. The factory, which had already received ISO 9001, ISO 14001 and OSHAS 18001 quality certification, now has an EL Tester to ensure greater quality control of the final product.

The company claims that this new technology, developed in partnership with MBJ Solutions, makes it possible to discover hidden defects, ensuring a high quality standard of the products the company sells. In June, MBJ Solutions won an award in the photovoltaic category at Intersolar for its Mobile PV test centre.

Testing and Certification News Focus

DelSolar modules pass salt mist corrosion test conducted by TÜV Rheinland

TÜV Rheinland confirmed that DelSolar's solar modules have passed the new salt mist corrosion test with a severity level of 6, the highest stress rating for the test. Modules included in the testing were DelSolar's D6M_B3A, D6P-B3A and D6Q_B3A.

The company noted that its modules passed the ammonia test in March, performed by TÜV SÜD in compliance with IRC 62716. The modules were certified as being suitable for agricultural areas where high amounts of ammonia are found.

Canadian Solar, Mecosun, achieve Pass' Innovation certification from the CTSB

Canadian Solar and its French PV integrator partner Mecosun have achieved Pass'Innovation certification from the French Centre Scientifique et Technique du Bâtiment (CSTB).The testing confirms Canadian Solar's PV panels integration with Mecosun's MV€ system and aims to enable attainment of insurances and funding from French government authorities. The Pass'Innovation certification means to guarantee the quality of the integration of Canadian Solar panels with Mecosun's MV€ system for industrial and agricultural roofs. Panels certified include the CS6-P, poly- and monocrystalline modules as well as Canadian Solar's ELPS modules.

Upsolar receives two IEC certifications for modules with Schweizer Solrif frames

Upsolar announced that the International Electrotechnical Commission (IEC), in conjunction with ICIM, issued two new certifications for its 60-cell modules, which feature Schweizer Solrif (SOLar Roof Integration Frame) frames. IEC certifications through ICIM, are considered by Upsolar as a step towards obtaining certification from the French Centre Scientifique et Technique du Bâtiment (CSTB), which will allow customers to access FiTs available in the country. Upsolar notes that other products in its portfolio have already received CSTB certifications.

Yingli modules pass PID testing conducted by Intertek

Yingli Green Energy Holdings advised that its multicrystalline PV modules had undergone, and successfully passed, potential induced degradation (PID) testing, which was conducted by Intertek Group. The test analysed the power output of Yingli Solar's PV modules under severe conditions of high voltage, temperature and humidity. The company stated that its modules passed PID testing with high marks. The PID test was carried out under 85 degree conditions, with 85%

relative humidity and 1,000V of system voltage bias for a duration of 48 hours. According to Intertek results, Yingli Solar modules had a power degradation of less than 1%. Furthermore, Intertek also tested the modules for 96 hours and found that they still remained under a 1% degradation level.

Tigo Energy receives industry's first certification for SmartModule technology from TÜV Rheinland

TÜV Rheinland awarded Tigo Energy the industry's first ever certification for SmartModules, recognizing the company for embedding its junction box in PV modules for the North American and European solar markets. Since Tigo Energy is the first to go through this certification process, it states that it actually helped develop testing standards for SmartModules.

Senersun modules pass salt mist corrosion testing

Senersun advised that its polycrystalline modules had passed testing performed by SGS for compliance with IEC 61701 standards for salt mist corrosion. The solar panels underwent four test cycles spread over 28 days. Each module was sprayed with a salt mist solution and then stored for seven days at 40° C and 93% relative humidity. Testing confirmed that the panels were visually, dimensionally and functionally compliant with the IEC standards.

Kyocera modules pass Fraunhofer PID test

Kyocera's PV modules have passed the Fraunhofer Center for Silicon Photovoltaics CSP's PID test, the company has announced. The potential induced degradation (PID) test subjects the modules to high voltage stress to test the performance of individual modules, which can be negatively affected by PID, consequently affecting the power output of the entire system. Fraunhofer CSP has anonymously tested PV modules and Kyocera was among four types that passed the test, not showing degradation.

JA Solar products receive Intertek's Green Leaf Mark

JA Solar's emphasis on module production appears to have paid off. The company has announced that three of its cell models and three of its module models have successfully completed Intertek's Carbon Footprint Evaluation program and have been granted the Green Leaf Mark by Intertek. JA Solar is the first solar company in China to receive Green Leaf Mark verification for its products. In the second quarter of 2012, China saw a surge in investment to US$18.3 billion, up 92% from the previous quarter.

Intertek's Green Leaf Mark is a consumer product systems certification used to demonstrate that environmental claims have been independently verified. The evaluation process integrates both on-site audits and life cycle assessment (LCA) measures. The Green Leaf Mark is currently available for use outside of North America on product packaging and in point-of-purchase displays, product advertising and literature, to explain a product's environmental credentials.

Canadian Solar modules receive high ratings in ammonia resistance testing

Canadian Solar's modules were recently tested in the IEC 62716 draft C ammonia (NH_3) corrosion test by TÜV Rheinland and also in the DLG standard test for solar modules in agricultural environments. Testing concluded that the company's modules passed with the highest possible ratings and included power loss, visual inspection and insulation resistance.

Both TÜV Rheinland and DLG tested the solar modules for their resistance to NH_3 corrosion, with a maximum allowed power loss of 5%. Canadian Solar modules passed both tests without

Suniva modules verified by PV Evolution Labs to be PID-free

showing any performance degradation. TÜV Rheinland's ammonia corrosion test exposed the modules to extreme conditions for a 20-day test cycle, undergoing exposure to 6,667ppm of NH_3 under 8 hours of 140°F (60°C) with 100% relative humidity and then 16 hours of drying in standard atmosphere without ammonia under 73°F (23°C) and a maximum of 75% relative humidity.

Suniva receives PID-free certification from PVEL

PV Evolution Labs (PVEL) confirmed that Suniva received the highest level of certification as a PID-free module manufacturer under PVEL's potential-induced degradation testing programme. PVEL created the PID certification programme as a way to give manufacturers and project investors insight into how PV products withstand common causes of performance degradation and module failure.

"Suniva's PVEL PID certification is a testament to the quality and reliability we build into our high-powered cells and modules, assuring our customers of consistent power output," said Jon O'Neill, senior module engineer at Suniva.

PVEL noted that its engineers measured the stability of the Suniva panels electrical output when exposed to high system voltages (positive and negative 1kV) under harsh environmental conditions (85°C at 85% relative humidity) for 600 hours. According to results, Suniva's modules performed better than the allowable degradation limit.

ReneSola's solar modules obtain SII certification

ReneSola, a China-based manufacturer of solar modules and wafers, has received certification from the Standards Institution of Israel (SII) for its solar modules — including its Virtus, monocrystalline and multicrystalline series of solar modules.

The certification confirms that the company's solar modules meet Israel's equipment safety standards. But more importantly, its modules are now allowed to be used for on-grid installation in Israel, as the Israeli government requires all solar modules to be certified as complying with SII's certification before their use.

BYD Solar receives A class certification from Inmetro

BYD Solar announced that the National Institute of Metrology, Quality and Technology of Brazil had awarded its PV module products with A class certification.

BYD solar products are sold in various global locales, including Germany, Italy, Spain and the USA. The company notes that its Inmetro certification follows and supports its previous TÜV and UL certifications.

Supply Deal News Focus

ReneSola to sell 4.6MW of its modules to Solar Planet Power

ReneSola announced that it has agreed to sell 4.6MW of its 255W poly modules to Solar Planet Power. The company will ship the modules to Solar Planet during the third quarter of 2012. Solar Planet noted that it plans to order up to 15MW of additional solar modules within six months following the first delivery.

ReneSola is supplying its 60-cell and 72-cell multicrystalline and monocrystalline to Solar Planet for use in their PV systems.

Canadian Solar supplies over 8MW of solar modules to groSolar projects

Canadian Solar has been busy supplying over 8MW of its CS6P solar modules to groSolar, which have been utilized for three utility and commercial PV projects in the USA. The largest installation is a 6MW plant under construction in Lancaster County, Pennsylvania.

Canadian Solar will be the sole provider of solar modules for the Pennsylvania plant,

Source: A Shade Greener

JA Solar has signed a 47MW agreement with the PV installer A Shade Greener.

ReneSola supplying its Virtus PV modules to Greek Big Solar and Solargain PV.

which will produce 7.5 million kWh of solar energy per year under a 15-year PPA. Upon completion, it is expected to be the largest PV installation in the state.

The other two PV projects have recently reached completion: a 1.8MW solar project for the Camden County Municipal Utility Authority's wastewater treatment plant in New Jersey and a 1.5MW PV system at Longwood Gardens in Kennett Square, Pennsylvania. Combined, the two plants will generate nearly 4.95 million kWh of solar energy per year.

JA Solar signs 47MW supply agreement with UK's A Shade Greener

JA Solar Holdings advised that it had recently entered into a supply agreement with UK-based PV installer A Shade Greener, which will see the company deliver 47MW of its crystalline solar modules. Shipments are expected to begin this month. The deal was said to be one of the largest sales agreements to date in the UK for JA Solar.

JinkoSolar wins 30MW contract from China Guangdong Nuclear

JinkoSolar Holding has been awarded a 30MW supply contract by China Guangdong Nuclear Solar Energy Development. The modules will be used for a PV power plant that is being developed in Hami City, Xinjiang Province, China. Details regarding a delivery timeline were not disclosed.

Ledico to sell Yingli Solar modules in Israel

Yingli Green Energy has signed an agreement with Ledico in order to make the company its exclusive sales partner in Israel. Under the terms of the agreement, Ledico will sell and promote Yingli Solar modules in Israel. Ledico noted that the rooftop market was growing and had opened a dedicated operation to meet this demand. No details were provided on the module quantities applicable to the deal.

China Sunergy to supply 50MW of PV modules to V2M and affiliates

China Sunergy advised that it has agreed to provide Bulgarian partner V2M, and its affiliates, with 50MW of multicrystalline PV modules for projects in Romania and Macedonia. The modules will be delivered in the third and fourth quarters of 2012. V2M will be responsible for the project development and EPC contracting for the 50MW projects in Romania and Macedonia.

China Sunergy claimed it held a market share of over 11% and 32%, respectively, in Bulgaria and the Czech Republic in 2011. At this point in 2012, the company has shipped a cumulative total of 24.38MW of PV modules to Bulgaria for solar parks and rooftop systems.

Talesun Solar enters Japanese market with 26MW supply deal

As the Japanese market gets going after attractive feed-in tariffs were introduced at the beginning of July, 2012, Talesun Solar has signed a 26MW module supply deal with Nice Corporation, a Japanese construction materials company, which focuses on the residential market. The module supply deal included Talesun's polycrystalline Module TP660P and monocrystalline Module TP572M.

ReneSola does Virtus module deals with Solargain PV and Greek Big Solar

ReneSola advised that it has sold 5.95MW of its Virtus modules to Australian distributor Solargain PV. The agreement calls for ReneSola to ship 5.95MW of its 250W modules directly to Solargain. The company noted that it expects to ship more modules to Solargain in the future.

ReneSola has also entered into a supply agreement with Greek Big Solar, the company has announced. Under the agreement, ReneSola will provide Big Solar with 100MW of its Virtus PV modules.

Senersun appoints Spanish distributor and signs 6MW supply deal

France-based PV module specialist Senersun has appointed Spanish distributor Revosolar as its official distributor for the Spanish market. As part of the arrangement Senersun will supply 6MW of modules to the company.

Product Reviews

Sika

Sikasil AS-787 SL potting agent from Sika offers fast curing times

Product Outline: Sika AG, supplier of specialty chemicals and application knowledge has launched a new PV potting agent Sikasil AS-787 SL. The new two-component silicone potting agent is claimed to offer a fast curing time that enables shorter cycle times and a high automation index for junction box potting for crystalline and thin-film PV technologies.

Problem: Excellent adhesion of the PV module junction box is required for longevity and safety. However, shorter assembly times are required to reduce manufacturing costs.

Solution: The Sikasil AS-787 SL features, despite the improved flowing behaviour, a very short non-flow time to shorten and secure the storing time before handling and packaging. Because of the two-component technology, the fast and uniform curing is independent of humidity and can even be accelerated by slight heating, while maintaining long-term weatherability and adhesion to backsheet materials and glass.

Applications: Used for potting and sealing of the junction boxes of PV modules

Platform: Sikasil AS-787 SL is claimed to offer a balance of raw materials that negates sedimentation occurring and therefore no mixing is needed prior to usage compared with other potting materials. The material (colours are black and white) can be applied with most of the common dispensing systems for potting materials. With a UL 94 V-0 certification the product meets the highest flammability rating.

Availability: July 2012 onwards.

Honeywell

Honeywell's PowerShield 3W backsheet offers high durability

Product Outline: Honeywell has launched its third-generation laminate film, PowerShield 3W, which is designed to protect PV modules from harsh environments while helping them maintain power output over their 25-year life spans.

Problem: PV module manufacturers require cost-effective and reliable protection for cells and circuitry, while meeting the cost-reduction challenges.

Solution: PowerShield 3W is claimed to be a cost-effective backsheet preventing moisture from entering the module and keeping electrical charges within the module. These features help the module retain maximum power output while maintaining electrical safety. The new laminate is bound by a proprietary adhesive specifically designed for PV applications. The adhesive helps make the laminate the most durable backsheet available from Honeywell to date. Independent PV-industry laboratory tests were said to show that PowerShield 3W can withstand more than 3,000 hours of accelerated-aging exposure at 85°C (185°F) and 85% relative humidity without losing structural integrity.

Applications: PV module encapsulation.

Platform: The backsheet's superior adhesive offers excellent resistance to discoloration due to aging, which helps solar modules retain their appearance and reflectivity. Like all PowerShield backsheets, PowerShield 3W offers high resistance to environmental degradation from sunlight, heat, cold and humidity; strong resistance to acids, bases, solvents, salts and other chemicals; and resistance to excessive moisture infiltration within a module. The Honeywell PowerShield supply chain is said to provide module makers with a single point of contact for every component of their backsheet, helping ensure a reliable supply and quality.

Availability: May 2012 onwards.

Lapp Group

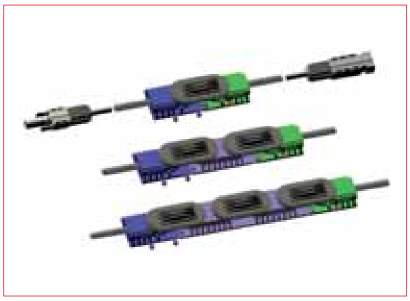

Lapp Group and FPE Fischer makes PV module junction box redundant

Product Outline: Lapp Group and FPE Fischer have introduced prototypes for a new connection system that is claimed to significantly increase efficiency, both for module manufacturers and for PV system operators. EPIC MAP SET represents a new approach by the two partners, which consists of a range of components such as diodes that can be combined as required to create connections between PV modules, rendering conventional junction boxes redundant.

Problem: Offering intelligent functionality combined with low costs throughout the value chain is becoming increasingly important for product differentiation.

Solution: EPIC MAP SET uses standardized components that can be mounted and welded onto modules automatically. The new design means connector components can be equipped with various types of diodes or electronic components. It also allows finished systems to be modified or retrofitted with minimal effort, according to the companies. Functional electronic components, such as electronic cut-off systems for individual modules and performance monitors, can be accessed and exchanged quickly and cost-effectively in the event of service or maintenance work. New technologies such as MPP trackers can be retrofitted. PV module maintenance costs are claimed to be reduced, compared with the use of conventional junction boxes, keeping them fully up to date and ensuring optimum performance.

Applications: The system is suitable for connecting crystalline, thin-film and organic PV modules.

Platform: The EPIC MAP SET consists of a range of components made of top-quality weatherproof, impact-resistant plastic. All components comply with protection class IP68.

Availability: Commercial availability by the end of 2012.

Product Reviews

Isovoltaic

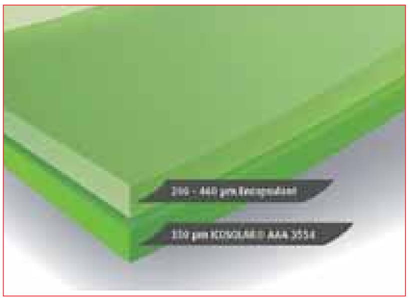

Icosolar encapsulant from Isovoltaic simplifies assembly process

Product Outline: Isovoltaic is offering a new encapsulating material which is combined directly with its production-proven Icosolar backsheets and completely replaces a layer of encapsulating material in the module.

Problem: Reducing material costs, especially in the area of module assembly, is critical. However, attention should be given to the effect on overall product reliability factors by lower cost or reduction in material layers, especially in the critical backsheet area.

Solution: Icosolar encapsulant is manufactured from a new material (TPO – thermoplastic polyolefin) and is claimed to have advantages over various materials used previously. A layer of encapsulant material between the cell and the backsheet is replaced completely, simplifying the manufacturing process of PV modules. Combined with the established Icosolar backsheets, the encapsulating layer is claimed to exhibit excellent adhesion to all common encapsulating materials and does not form any acetic acid in the damp heat test. By comparison with EVA, the Icosolar encapsulant exhibits less water absorption and water vapour permeability as well as improved damp heat and UV stability.

Applications: c-Si PV module encapsulation.

Platform: With Icosolar 4002 (Icosolar AAA3554 with encapsulating material), Icosolar 4006 (Icosolar APA 4004 with encapsulating material) and Icosolar APA 3G plus (Icosolar APA 3G with encapsulating material), Isovoltaic enables more efficient production of photovoltaic modules. Icosolar backsheets with encapsulant can also be ordered cut-to-size, thus creating less waste in downstream processing.

Availability: Currently available.

Komax Solar

Komax Solar offers new stringer for six-inch back-contact solar cells

Product Outline: Komax Solar has developed a new, fully automatic stringer for six-inch back-contact cells. The contactless soldering technology as well as the ribbon handling technology was designed to minimize the thermomechanical stress introduced into the solar cell. The stringer also adds electrical isolation between cells and ribbons.

Problem: Typically, five-inch back-contact cells are contacted at the edges and interconnected with tabs. However six-inch back-contact cells (MWT and EWT as well as IBC) need to be connected over the whole area in order to minimize resistive losses.

Solution: Komax Solar has developed a low-stress cell interconnection technology for back-contact cells by further optimizing their contactless soldering technology in combination with a special treatment of the ribbon which minimizes the thermomechanical stress introduced into the cell. In addition, the back-contact stringer from Komax adds the electrical isolation between the ribbons and the cell. For high aesthetic values, the electrical isolation material is available in transparent or white or black coloured. The newly developed interconnection technology takes care of environmental aspects as well, since it works also with lead-free solder.

Applications: Ribbon-based interconnection of five- and six-inch MWT, EWT and IBC solar cells.

Platform: The new back-contact stringer is based on back-contact stringing technology from Komax Solar, with more than 1GW of back-contact stringers (Xcell 3000 platform) installed in the market. The new back-contact stringer uses the same key technologies (closed-loop induction soldering, ribbon handling and handling of the isolating materials) as the Xcell 3000.

Availability: Currently available.

Saint-Gobain

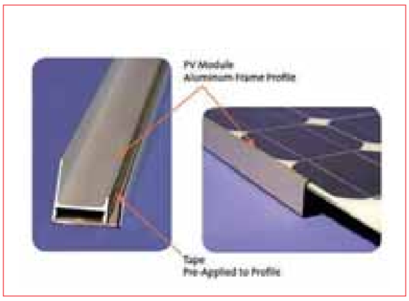

Saint-Gobain SolarBond ReadyFrame offers streamlining of module-framing process

Product Outline: Saint-Gobain has introduced the SolarBond ReadyFrame, a custom tape-in-frame solution designed to streamline the module-framing process by removing the extra steps needed to add a sealant or a tape to the frame.

Problem: Eliminating process steps at the module assembly stage, especially for small-to-medium-sized manufacturers is a key strategy to remain competitive. However, providing high-quality sealing for long-life weatherability is also required.

Solution: SolarBond ReadyFrame was designed to provide small-to-medium module manufacturers with a cost-effective framing solution that delivers a high-quality product quickly, easily and without making changes to their existing production line. Module aluminium frames to the customers, requirements are delivered with correctly pre-applied V7700UL SolarBond frame tape (UL listed). With the liner already removed, the tape is accurately bonded in the correct location using existing framing equipment and processes. Cost reductions include no inventory of tape, rolls, spools or wet sealants. Because of the simplified steps, throughput is claimed to increase, without a reduction in quality control.

Applications: Module framing.

Platform: Saint-Gobain works directly with the module manufacturer's aluminium extruder to ensure frame profiles and frame tape are correctly bonded and pre-packaged. SolarBond ReadyFrame, provides a clean application compared with removal of conventional sealant from the module.

Availability: June 2012 onwards.

An overview of module fabrication technologies for back-contact solar cells

Jonathan Govaerts, **Kris Baert** & **Jef Poortmans**, imec, Leuven, & **Tom Borgers** & **Wouter Ruythooren**, Photovoltech, Tienen, Belgium

ABSTRACT

Apart from aesthetics, the gain in electrical performance of back-contact solar cells and modules is particularly attractive compared to conventional PV modules. This major benefit results from getting rid of (the majority of) the metallization at the front, and providing all the cell contacts at the back. An overview is presented here of the different concepts put forward by different institutes and companies around the world for such back-contact modules. The different types of state-of-the-art back-contact cell are first introduced, together with their corresponding contacting and interconnection schemes. Keeping in mind the reference module technology for two-side-contacted cells as a starting point, each module concept is then briefly discussed in terms of technology and level of maturity. Finally, the main technological differences are summarized.

Introduction

The conventional approach that has been widely adopted for manufacturing modules, based on two-side-contacted cells, is the one described, for example, in Wohlgemuth & Narayanan [1]. The technique consists of first interconnecting the separate cells into strings by soldering ribbons from one cell's contacts to the next (so-called 'tabbing-stringing'). The strings are then laminated between a transparent glass or polymer frontsheet and a glass, metal or polymer backsheet using the cross-linking material ethylene-vinyl acetate (EVA). This is a very mature technology, and was developed for cells requiring out-of-plane interconnection between the front of one cell and the back of the neighbouring cell. The typical process flow diagram is shown in Fig. 1.

"The application of back-contact cell and module technology is expected to increase significantly."

However, with the drive towards higher efficiencies, several different concepts for crystalline silicon back-contact solar cells have been proposed, investigated and developed [2]. This direction of research and development is also in line with the ITRPV roadmap, where the application of back-contact cell and module technology is expected to increase significantly, both in absolute and relative terms. For such cells, it is worth questioning whether conventional module technology is still optimal and preferable.

Back-contact solar cell contacting and interconnection scheme

Current back-contact solar cells can be broadly divided into two types on the basis of the conduction mechanism for drawing the current out of the active area. On the one hand, the technologies closest to conventional two-side-contacted solar cells, widely referred to as metal wrap-through (MWT) and emitter wrap-through (EWT), rely on the same mechanism for extracting the generated carriers, namely cross-sectional conduction. In these cases the carriers collected at the front still need to be transferred to the contacts at

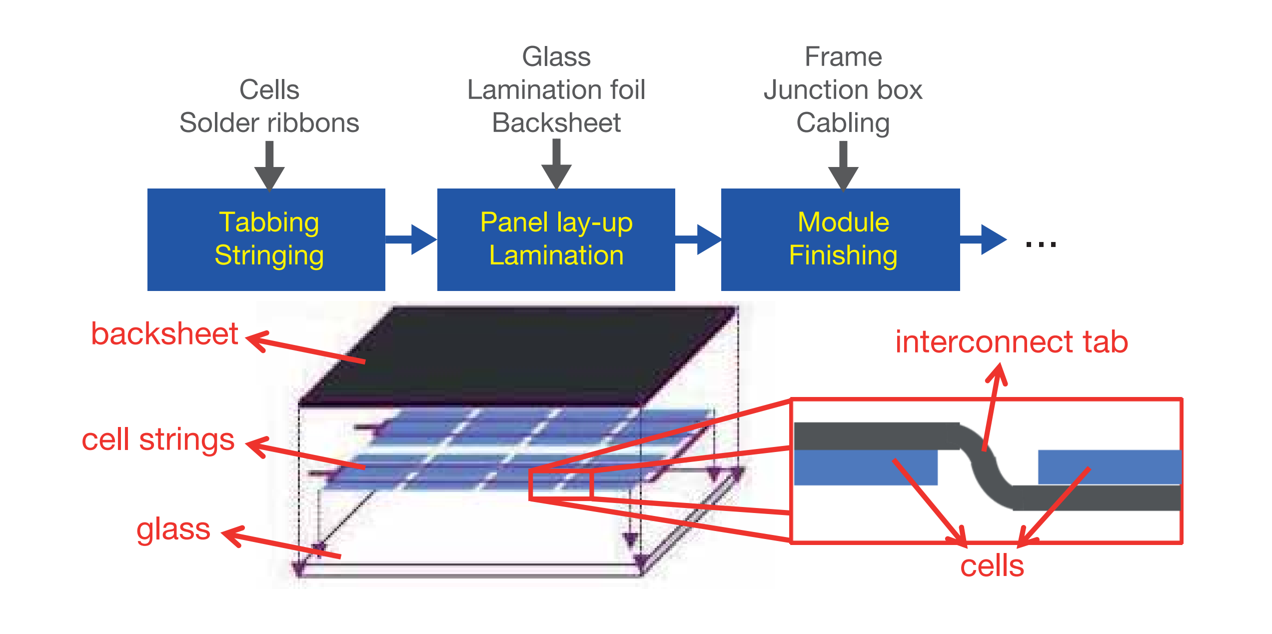

Figure 1. Typical flow diagram of conventional module fabrication.

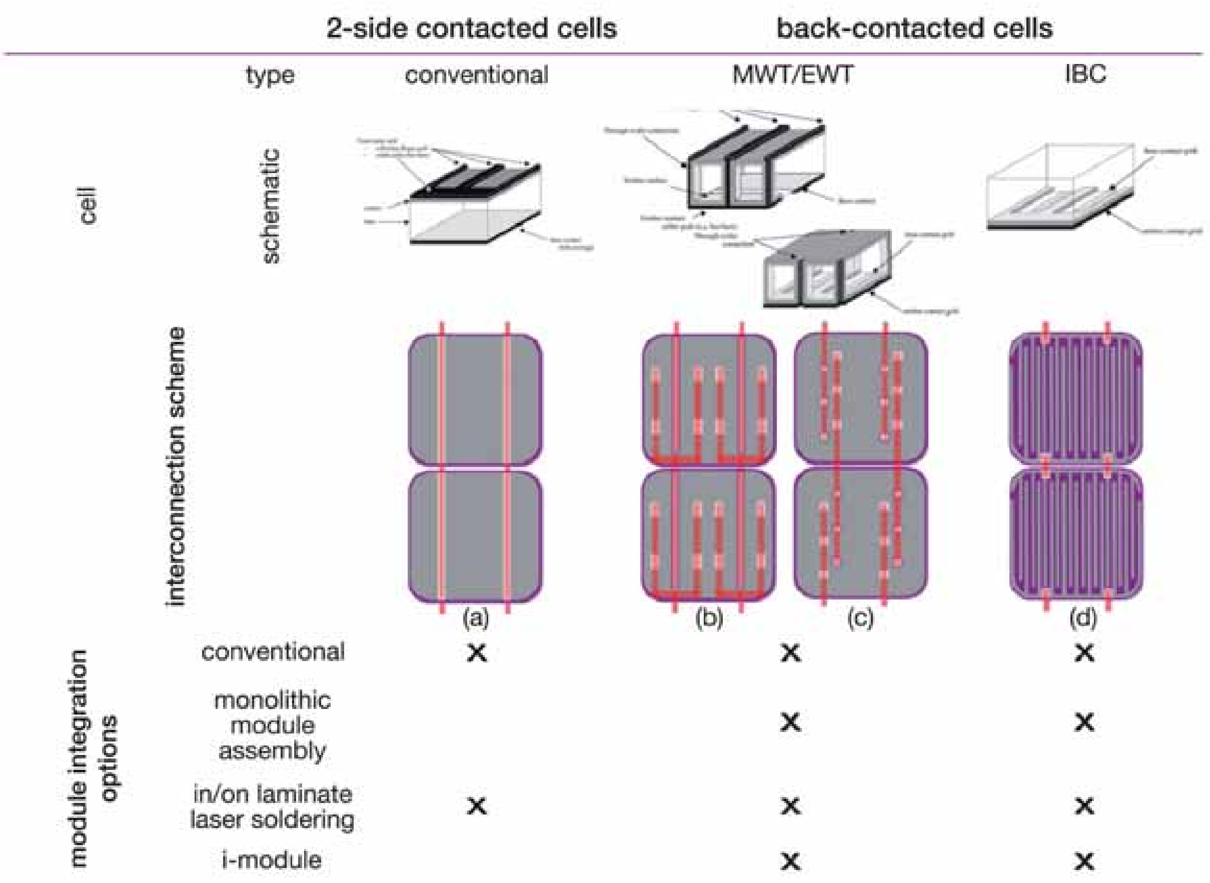

Figure 2. State-of-the-art back-contact cell concepts and module interconnection schemes (the red lines indicate the interconnect routing but its actual shape can be very different).

the back, which is done through vias in the silicon (hence 'wrap-through'). On the other hand, the interdigitated back-contact (IBC) cells do not extract carriers on the front, but instead both polarities are contacted at the back through an interdigitated grid. A schematic of the above cell concepts is shown in Fig. 2 (from Van Kerschaver and Beaucarne [2], where more details can also be found). For the interconnection of such finished cells, the routing schemes that are typically used are also indicated in the figure.

Interconnection can be achieved by tabs on the rear side only, or by using a conductive backsheet foil. Both have benefits compared to two-sided tabs. In the overview in Fig. 2, some important differences in module technology between conventional two-side-contacted and back-contacted cells are of interest. First, as there are no longer tabs at the front (so the topography and metal coverage is reduced), the encapsulation material for bonding the strings to the front sheet can be thinner (reduced material usage and reduced absorption losses). Second, the interconnections from one cell to the next are no longer kinked (from front to back) but are in-plane. This is advantageous since it means cells can be positioned closer to one another, but, at the same time, because the kink provides some stress relief during thermal cycling, the interconnect design should also take into account such stress-relief considerations. Third, by having all interconnections (using either tabs or a foil) at the rear there is more freedom of design: the interconnects can be designed (e.g. widened, tapered) to reduce series resistance and hence fill factor (*FF*) losses, and optimally distribute the current running through the interconnects. In this way, the interconnection scheme can be electrically optimized for module output, material usage and cost. Indeed, using MWT cells and an interconnection foil has resulted in a world record for multicrystalline modules [3,4].

In a design such as in Fig. 2(b), one set of busbars can be kept, and it is in this sense closer to conventional technology; however, rerouting of the interconnects from one cell to the next is required for this scheme. In a design such as in Fig. 2(c) or (d), a straight-line interconnection may be kept (although for the layout given in Fig. 2(c), the cells have to be rotated 180 degrees relative to the preceding and following cells). In addition, for the layouts of Fig. 2, in order to avoid shunting the cell an insulation layer is required wherever the interconnect crosses the metallization with opposite polarity on the back side of the cell. This extra insulation layer can be avoided in the layout of Fig. 2(d), as the interconnects do not need to cross the other polarity of the cell, owing to the interdigitated structure of the cell metallization.

Adaptation of conventional technology to back-contact solar cells [5,6,7,8,9]

The back-contact cell and module technology most closely related to conventional technology (based on two-side-contacted cells) is based on soldering the back-contact cells into strings, followed by lamination between the front glass and the backsheet using EVA.

> "Module-to-cell power ratios of over 98% have been obtained."

Photovoltech has developed such a stringing technology for its MWT cells. The main design goals of the approach were to avoid product reliability concerns by using materials that were as close as possible to those of existing module

So... There IS Something New Under the Sun

The Square Wave™ dispense valve applies liquid flux on bus bars and solder-coated ribbon at up to 500Hz, in volumes as small as .015 µL.

- Controlled flux application maximizes cell efficiency
- Non-contact dispensing won't damage wafers
- Industrial, compact, low-maintenance design
- Adjustable flow and drip-free shutoff

Nordson EFD

www.nordsonefd.com/ads/pvi-0912

East Providence, RI USA 800.556.3484; +1.401.431.7000 info@nordsonefd.com www.nordsonefd.com

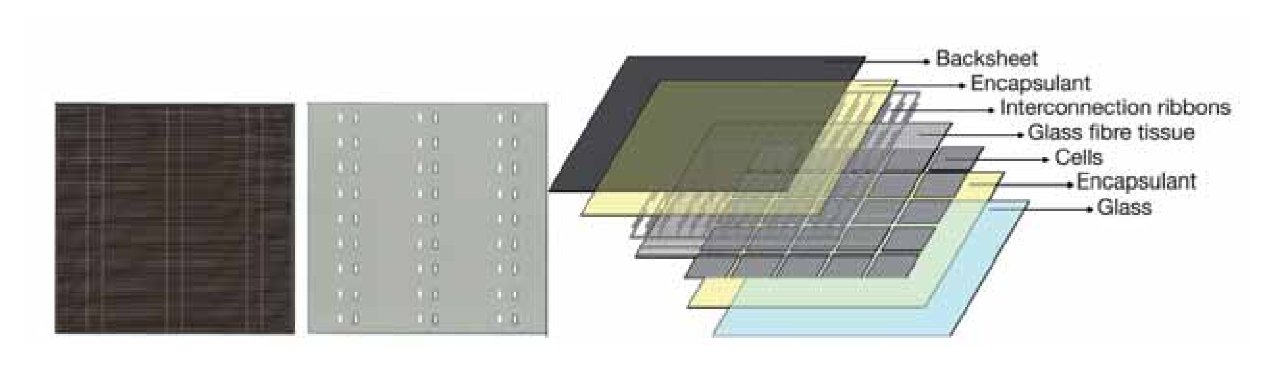

Figure 3. Front and back pattern of a Photovoltech MWT cell and the make-up of a module.

technology, and keeping the costs low by using commodity materials. The interconnection is based on the geometry described in Fig. 2(c) and thus requires an insulation layer between the cells and the ribbon conductors. The insulating layer is an open-structured glass fabric that does not require any alignment to the cells. To bridge the fabric between the ribbons and the cells, solder paste is applied. Module-to-cell power ratios of over 98% have been obtained. The width of the ribbons can be chosen to optimize the resistive losses in relation to the copper market price. The tabber-stringer equipment had to be modified to handle the fabric and paste dispensing. Details of the implementation of this approach and the tests carried out will be published in due course.

SunPower, widely acknowledged for its high-performance cells and modules, produces high-efficiency back-contact cells based on 'low-cost' alternatives for a lithography-based process flow on wafers with a high minority-carrier lifetime. As illustrated in Fig. 4, the cell relies on an IBC structure, and modules are fabricated using specifically designed straight-line interconnected strings (as in Fig. 2(d)), laminated between the front glass and the backsheet using EVA.

Monolithic module assembly [10,11,12,13,14,15]

The technology based on conductive backsheet foils has been developed by ECN and allows for an integrated cell and module approach. The conductive backsheet consists of PVF-PET-Cu foil, and the Cu foil is patterned according to the required interconnection scheme. Electrical contact between the cells and the foil is made by printing a conductive adhesive on the foil. The cells can be placed on the foil with adhesive by a gentle pick-and-place process. The adhesive is cured simultaneously in the lamination process of the encapsulant and thus does not require any additional processing, which means that this process is also suitable for thin wafers. Because of the simplified interconnection procedure, the monolithic module assembly process is up to six times as fast as conventional module manufacturing requiring tabber-stringer and lay-up stages. The manufacturing process of this type of MWT module has been developed in collaboration with the Dutch company Eurotron, and fully automated production lines with a capacity of up to 150MWp per line are now operational. MWT modules using this concept have obtained IEC 61215 and IEC 61730 certification [11]. A similar module fabrication technology is also under development at Applied Materials, but for EWT cells.

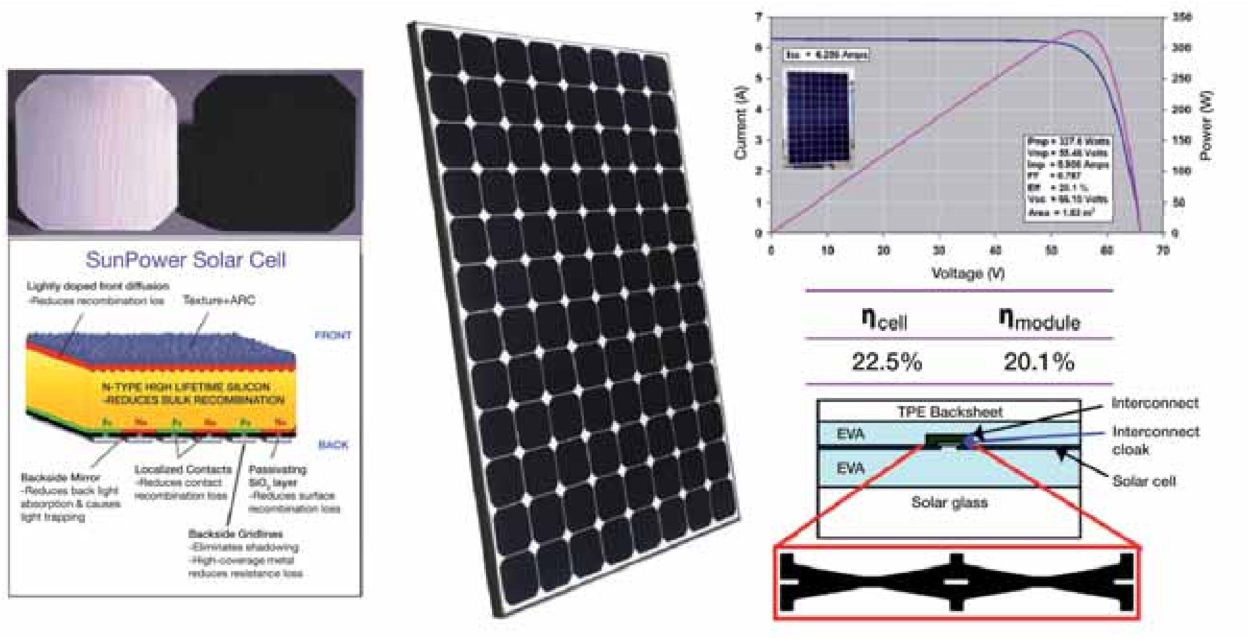

Figure 4. Make-up and performance of a SunPower (IBC) cell and module.

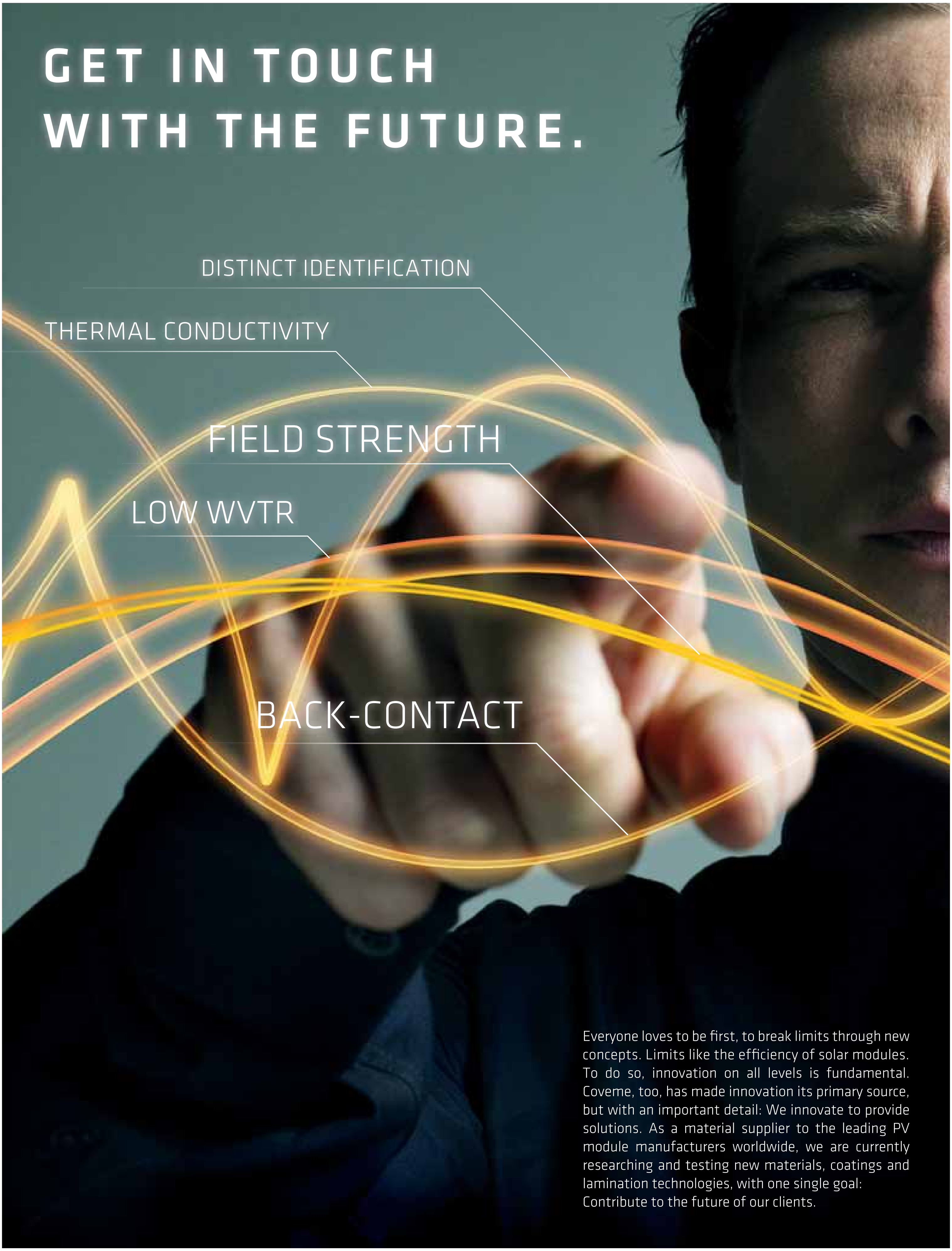
GET IN TOUCH
WITH THE FUTURE.
DISTINCT IDENTIFICATION
THERMAL CONDUCTIVITY
FIELD STRENGTH
LOW WVTR
BACK-CONTACT
Everyone loves to be first, to break limits through new concepts. Limits like the efficiency of solar modules. To do so, innovation on all levels is fundamental. Coveme, too, has made innovation its primary source, but with an important detail: We innovate to provide solutions. As a material supplier to the leading PV module manufacturers worldwide, we are currently researching and testing new materials, coatings and lamination technologies, with one single goal: Contribute to the future of our clients.

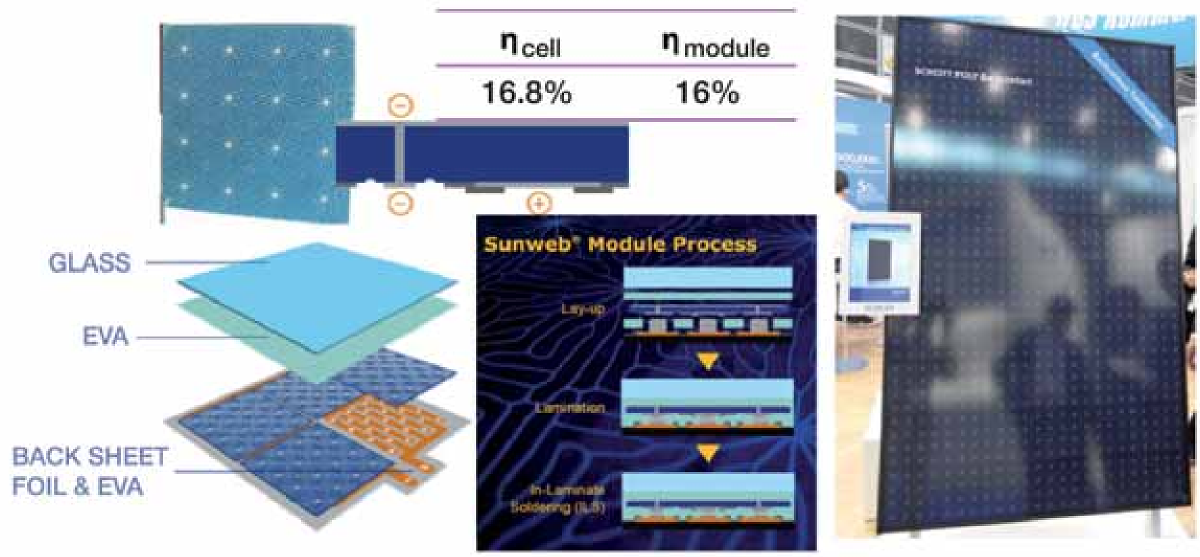

Figure 5. Make-up and performance of a Sunweb (MWT) cell and module.

"The monolithic module assembly process is up to six times as fast as conventional module manufacturing requiring tabber-stringer and lay-up stages."

In-laminate laser soldering [16,17,18,19,20]

At a time when the long-term reliability of conductive adhesives had not yet been proved in the field, a similar concept was proposed and developed on the basis of the industrially accepted soldering benchmark. In this case the construction closely resembles the above monolithic module assembly approach, but instead of conductive adhesive, a solder paste is dispensed on the patterned conductor backsheet. The cells are then placed and laminated as before on a front glass superstrate.

Since the lamination is typically carried out at around 150°C for EVA, and standard soldering requires temperatures of around 230°C, the interconnect tabs are not yet properly soldered during lamination. Therefore, after lamination, the tabs are soldered by laser to the backsheet contacts through the front glass. Alternatively, the tabs could be soldered prior to the lamination stage, but the laminated stack ensures a better defined contact pressure during laser soldering, which improves the reproducibility of the resulting joint. The concept is illustrated in Fig. 5. A potential simplification of this scheme, by making use of Al–Al direct laser welding, is currently also under development [21].

i-module [22,23,24]

As mentioned earlier, the conventional module fabrication approach requires the soldering of standalone cells and

(a)

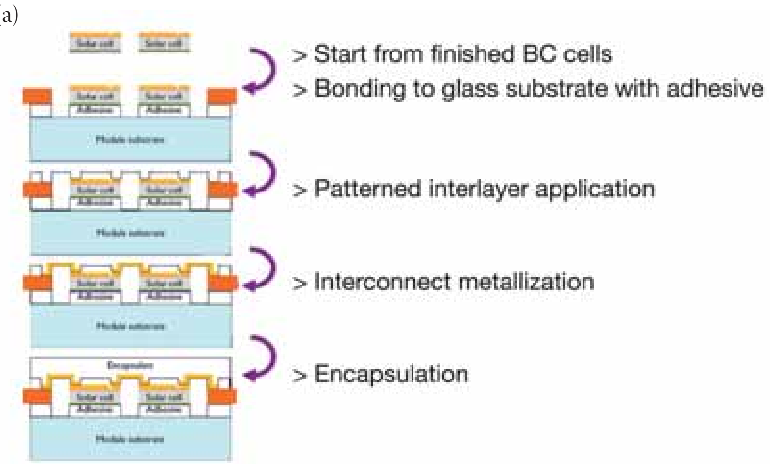

(b)

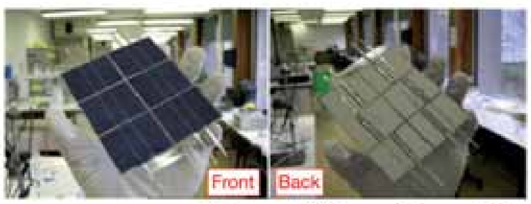

	Jsc (mA/cm²)	Voc (mV)	FF (%)	Eta (%)
cell 4	35.8	607	76.8	16.7
cell 5	35.8	609	76.3	16.6
cell 6	36.2	603	76.5	16.7
series 456	35.7	1823	76.9	16.7

Figure 6. (a) Schematic overview of the i-module concept; (b) an i-module based on MWT cells interconnected by soldering.


Now the sun light
is simulated with LEDs
ECOSUN10L
AAA sun simulator
The right choiche for:
- crystalline modules;
- back-contact modules;
- thin-film module;
TÜV Certified
ECOSUN 10L

		Conventional adapted for back-contact cells	Monolithic Module Assembly	In-laminate Laser soldering (ILS)	i-module
Technology	Encapsulation method	Full-stack lamination	Full-stack lamination	Full-stack lamination	Sequential layer buildup
	Encapsulation material	EVA sheets	Sheet-based encapsulants (EVA, thermoplastic, silicone)	Sheet-based encapsulants (EVA, thermoplastic, silicone)	Gel-based encapsulants
	Interconnection method	Soldering, conductive adhesives	Conductive foil and adhesives	Laser soldering	Soldering, thin-film metallization, printing
	Interconnection level	Cells/string-level before lamination	Module-level during lamination	Module-level after lamination	Module-level (intermediate)
Performance	Module-to-cell power ratio [%]	Photovoltech (MWT) 98 SunPower (IBC) 103	ECN (MWT) 97 Kyocera (MWT) 96 Photovoltech (MWT) 96	Solland (MWT) 102	Imec (MWT) 104 (small area)
	Reliability	lifetime guarantee 25 years	IEC certified	lifetime guarantee 25 years	Tbd
	Level of maturity	in mass production	industrial pilot-line production	industrial pilot-line production	R&D phase

Figure 7. Overview of the differences in technology and performance for the different back-contact module concepts (ratio values obtained by calculations based on public information).

the handling of long strings of cells prior to lamination, two steps in which (micro) cracks may easily be introduced, especially in the case of very thin cells (e.g. thicknesses of 100µm and below). The i-module (interconnect-module) approach aims to minimize the risk of cracks by providing a module-level interconnection that is created only after attaching the cells to the module substrate (glass). This is of course only possible if all of the cells' contacts are still available at this stage, and thus the approach requires back-contact cells.

An adhesive layer (typically silicone such as reported in Ketola et al. [25]) is applied to a clean glass module superstrate, and the solar cells are placed with the front ('sunny') side towards the glass, so that the contacts remain available for processing on the rear side. To isolate the emitter and base contacts, a dielectric layer is subsequently deposited, with holes so that the cells' contacts remain available. A metallization is applied to interconnect (e.g. serially) the different cells in the module; outside contacts are then provided and the stack is encapsulated to protect the metallization and reinforce the assembly. The process flow diagram is shown in Fig. 6(a).

For each of the different steps, several technology options can be (and already have been) considered, as reported in Govaerts et al. [22–24]. Attention is focused on a demonstration module that is the one closest to being industrially adopted in the short term. This proof of concept is based on MWT cells (provided by Photovoltech) with a typical thickness of 180µm. The dielectric layer on the back side of these cells has been selectively deposited (screen printing and dispensing – both are feasible) to isolate the front interconnects from the back side, and soldering has been chosen as the method of interconnection. Fig. 6(b) shows the results for such a demonstration module.

Summary and outlook

In overview, the different module fabrication concepts could be classified, for example, according to the moment when the cell interconnection is established. At one end of the spectrum lies conventional module technology, where cells are soldered (standalone) prior to lamination. At the other end, there is the in-laminate laser-soldering concept, which only finishes the interconnection after the full stack has been laminated. In between these two, monolithic module assembly provides interconnection during lamination. The i-module approach splits the full stack lamination, providing an intermediate level, closer to the sequential build-up of layers common in the fabrication of printed circuit boards. Fig. 7 highlights the classification of the concepts, along with the characteristics of each one.

The viability of several of the above basic concepts has been proved; some are in production, or close to production, and many hybrids of these can still be conceived. However, the existence of many different layouts for the contacts of back-contact cells (justified or not) implies that no standard interconnect routing scheme has so far been widely accepted in the industry. This is a drawback in the sense that it does not allow a straightforward comparison to be made between the different cell technologies with the same module technology, or between the different module technologies with the same cells.

In a broader perspective, however, if cell and module technology cannot be decoupled, this interdependency implies that companies in this area will have to vertically integrate to ensure the quality of their products. In this way, the back-contact c-Si module technology is likely to converge more and more on thin-film organic or inorganic technology. Both c-Si and thin-film technologies are increasingly targeted towards module-level performance (and processing), with the former evolving towards lower cost, and the latter evolving towards higher efficiencies and reliability.

Acknowledgements

Thanks are extended to all partners of imec's Wafer-based Si-PV Industrial Affiliation Program, and in particular to Dow Corning, who developed the silicone material for the i-module. We also thank W. Eerenstein from ECN for valuable contributions to this work.

References

[1] Wohlgemuth, J. & Narayanan, M. 2005, "Large-scale PV module manufacturing using ultrathin polycrystalline silicon solar cells", Dept. Energy Lab., NREL, Annual Report ZDO-2-30628-03.

[2] Van Kerschaver, E. & Beaucarne, G. 2006, "Back-contact solar cells: A review", *Prog. Photovolt.: Res. Appl.*, Vol. 14, No. 2, pp. 107–123.

[3] Bennett, I.J. et al. 2009, "World record module efficiency for large and thin mc-Si MWT cells", *Proc. 24th EU PVSEC*, Hamburg, Germany.


VISIT US AT:
SOLAR POWER INTERNATIONAL
Orange County Convention Center,
Orlando FL, Sept 11 - 13th 2012
Booth 917
27TH EU PVSEC
Messe Frankfurt, Germany
Sept 25 - 28th 2012
Hall / Stand 3.0/B32
XLAM 21/34E
LAMINATORS
• Highest Process Quality
• Attractive Cost/Performance Ratio
• High Reliability
XINSPECT 2800I
TESTERS
• EL testers from cost effective high throughput to laboratory process development solutions
• Reinforce EL with IV Curve measurement or Thermography imaging
• Automatic defect detection, Defect tracking system & Data analyzer software
XCELL X2 PLUS
STRINGERS
• High throughput • High Yield
• Enhanced state of the art process technology
• Maintenance free, patented, servo controlled transfer system AcuuTrack, produces perfect strings with a gentle motion for cell handling
THE WAY TO MAKE IT | TO GRID PARITY
To find out more about the way to make it,
visit us at: www.komaxsolar.com
Komax Solar Inc.
20 Innovation Drive, York, PA 17402 (USA)
+1 717.755.6800 | info.yok@komaxsolar.com
komax SOLAR

[4] Tjengdrawira, C. et al. 2010, "World first 17% efficient multi-crystalline silicon module", *Proc. 35th IEEE PVSC*, Honolulu, Hawaii, USA.

[5] Borgers, T. & Szlufcik, J. 2011, "Use of a uniform layer of insulating material in back-contact solar cells", Patent WO2012059534.

[6] van der Heide, A. & Ruythooren, W. 2010, "Optimisation of MWT cell design & module fabrication process for economical implementation of MWT technology", 2nd MWT Workshop, Amsterdam, Netherlands.

[7] Rose, D. & Daroczi, S. 2005, "Development and manufacture of reliable PV modules with >17% efficiency", *Proc. 20th EU PVSEC*, Barcelona, Spain, pp. 2670–2673.

[8] Rose, D., Jester, T. & Bunea, G. 2008, "Automated manufacturing of high efficiency modules", Final Report NREL/SR-520-42767.

[9] SunPower 2011, Datasheet "E20/327 Solar Panel".

[10] Spath, M. et al. 2008, "A novel module assembly line using back contact solar cells", *Proc. 33rd IEEE PVSC*, San Diego, California, USA.

[11] Eerenstein, W. et al. 2012, "Back contact module technology", SOLARCON/CPTIC, Shanghai, China.

[12] Guichoux, M. et al. 2010, "Impact of materials on back-contact module reliability", *Proc. 35th IEEE PVSC*, Honolulu, Hawaii, USA.

[13] Eerenstein, W. et al. 2010, "Climate chamber test results of MWT back contact modules", *Proc. 25th EU PVSEC*, Valencia, Spain.

[14] Gee, J.M., Garrett, S.E. & Morgan, W.P. 1997, "Simplified module assembly using back-contact crystalline-silicon solar cells", *Proc. 26th IEEE PVSC*, Anaheim, California, USA, pp. 1085–1088.

[15] Meakin, D.H. et al. 2010, "Development and Qualification of Monolithically Assembled Modules for Back Contact PV Cells", *Proc. 25th EU PVSEC*, Valencia, Spain, pp. 3858–3862.

[16] Gast, M., Köntges, M. & Brendel, R. 2008, "Lead free laser soldering for a new module manufacturing concept", *Prog. Photovolt.: Res. Appl.*, Vol. 16, p. 151–157.

[17] Köntges, M. et al. 2008, "A novel photovoltaic-module assembly system for back contact solar cells using laser soldering technique", *Proc. 23rd EU PVSEC*, Valencia, Spain [available online at http://www.isfh.de/institut_solarforschung/files/val08_koentges.pdf].

[18] Löffler, J. et al. 2010, "Laser processing for advanced solar cells", *Proc. 11th Int. Symp. Laser Prec. Microfab.*, Stuttgart, Germany.

[19] Solland 2011, Datasheet – Sunweb cells.

[20] Solland 2011, Datasheet – Sunweb modules.

[21] Merkle, A. et al. 2012, "From high-efficiency n-type solar cells to aluminum-based modules exceeding 20% efficiency", *Proc. 27th EU PVSEC*, Frankfurt, Germany [in press].

[22] Govaerts, J. et al. 2010, "A novel concept for advanced modules with back-contact solar cells", *Proc. 25th EU PVSEC*, Valencia, Spain, pp. 3850–3853.

[23] Govaerts, J. et al. 2011, "Developing an advanced module for back-contact solar cells", *IEEE Trans. Compon., Packag. Manuf. Technol.*, Vol. 1, No. 9, pp. 1319–1327.

[24] Govaerts, J. et al. 2011, "The i-module approach: Towards improved performance and reliability of photovoltaic modules", *Proc. 18th EMPC*, Brighton, UK.

[25] Ketola, B. et al. 2010, "Demonstration of the benefits of silicone encapsulation of PV modules in a large scale outdoor array", *Proc. 25th EU PVSEC*, Valencia, Spain [available online at http://www.dowcorning.com/content/publishedlit/06-1065-01.pdf].

About the Authors

Jonathan Govaerts received his Ph.D. degree from Ghent University, Belgium, in 2009 on packaging and interconnection technology for (flexible) electronics. Since then he has been working with the Solar Cell Technology group at imec, focusing on cell–module integration of silicon solar cells.

Kris Baert obtained his Ph.D. on PECVD of thin-film c-Si from the Katholieke Universiteit Leuven in Leuven, Belgium, in 1990. He joined imec in 1992 and managed research and development in various areas of MEMS and integrated microsystems. Since 2008 Kris has been programme manager of solar cells in the SOLO department.

Jef Poortmans received his degree in electronic engineering from the Katholieke Universiteit of Leuven, Belgium, in 1985, and his Ph.D. degree in June 1993. He is the director of the Solar and Organic Technologies Department at imec, and is currently director of the SOLAR+ strategic programme, which comprises all the photovoltaic technology development activities within imec. Jef has also been a part-time professor at the Katholieke Universiteit since 2008.

Tom Borgers joined imec in 2000, working on III-V detector technologies and developing a flip-chip approach for megapixel infrared sensors. From 2004 he was involved in the development of 3D integration and packaging for microsystems. Tom switched to the field of photovoltaics in 2008, when he began working for Photovoltech. His interests lie in back-contact solar cell concepts, specifically the development of module technology.

Wouter Ruythooren received a Ph.D. in 2002 from the Katholieke Universiteit Leuven, Belgium, for his study on the electro-deposition of magnetic materials for integrated components. He then developed GaN device processing technology at imec until 2005, after which he became manager of the R&D teams, focusing on 3D packaging and electrochemical deposition. Wouter has led the back-contact technology group at Photovoltech since 2010.

Enquiries

Jonathan Govaerts
imec
Kapeldreef 75
B-3001 Leuven
Belgium
Email: jonathan.govaerts@imec.be

Fab & Facilities

Materials

Cell Processing

Thin Film

PV Modules

Power Generation

Market Watch

Evaluation of creep in thermoplastic encapsulant materials deployed outdoors

Michael D. Kempe[1], **David C. Miller**[1], **John H. Wohlgemuth**[1], **Sarah R. Kurtz**[1], **John M. Moseley**[1], **Qurat (Annie) Shah**[2], **Govindasamy Tamizhmani**[2], **Keiichiro Sakurai**[1,3], **Masanao Inoue**[4], **Takuya Doi**[4], **Atsushi Masuda**[4], **Sam L. Samuels**[5] & **Crystal E. Vanderpan**[6]

[1]National Renewable Energy Laboratory, Golden, Colorado, USA
[2]Arizona State University Polytechnic, Mesa, Arizona, USA
[3]National Institute of Advanced Industrial Science and Technology, Ibaraki, Japan
[4]National Institute of Advanced Industrial Science and Technology, Saga, Japan
[5]DuPont Company, Wilmington, Delaware, USA
[6]Underwriters Laboratories, San Jose, California, USA

ABSTRACT

There has been recent interest in the use of thermoplastic encapsulant materials in photovoltaic modules to replace chemically cross-linked materials, for example ethylene-vinyl acetate. The related motivations include the desire to reduce lamination time or temperature, to use less moisture-permeable materials, and to use materials with better corrosion characteristics or improved electrical resistance. However, the use of any thermoplastic material in a high-temperature environment raises safety and performance concerns, as the standardized tests do not currently include exposure of the modules to temperatures in excess of 85°C, even though fielded modules may experience temperatures above 100°C. Eight pairs of crystalline silicon modules and eight pairs of glass/encapsulation/glass thin-film mock modules were constructed using different encapsulant materials, of which only two were designed to chemically cross-link. One module set with insulation on the back side was exposed outdoors in Arizona in the summer, and an identical set was exposed in environmental chambers. High-precision creep measurements (±20µm) and performance measurements indicated that, despite many of these polymeric materials being in the melt state during outdoor deployment, there was very little creep because of the high viscosity of the materials, the temperature heterogeneity across the modules, and the formation of chemical cross-links in many of the encapsulants as they aged. In the case of the crystalline silicon modules, the physical restraint of the backsheet reduced the creep further.

Introduction

With the recent interest in thermoplastic photovoltaic (PV) encapsulants and adhesives, there have been increasing concerns in the standards community regarding the potential for viscoelastic creep of these materials. The current qualification and safety tests (IEC 61215, IEC 61646, IEC 61730, UL 1703) [1–4] stress modules up to a maximum temperature of only 85°C in the 'damp heat', 'thermal cycling' and 'humidity freeze' tests. Additionally, small areas of a module may reach much higher temperatures during the 'hot spot' test [5], but the localized nature of this test does not examine the conditions inherent in the hottest operating environments and mounting conditions of modules. In very hot environments, modules are known to reach temperatures in excess of 100°C [6,7]. One could envision a material with a melting point near 85°C undergoing a highly thermally activated drop in viscosity, resulting in significant creep at 100°C. To evaluate this potential scenario, modules with eight different encapsulant types were assembled using two different module constructions and exposed outdoors in Mesa, Arizona, for the summer of 2011. A replicate module set was also exposed to high temperatures in indoor environmental chambers. The results of those tests are presented in this paper, along with a discussion of the implications for qualification testing, safety standards and manufacturing practices.

"In very hot environments, modules are known to reach temperatures in excess of 100°C."

Experimental

The encapsulant materials used (or under investigation for use) in PV modules were obtained from industrial manufacturers. Under an agreement with these manufacturers, we may disclose the general class of the polymeric resin and the physical properties we have measured (see Table 1). For the poly(dimethylsiloxane) (PDMS) encapsulation, a different formulation was used for the thin-film mock modules than for the crystalline silicon modules, but both are similar sparsely cross-linked gels. The PDMS values in Table 1 apply to the thin-film mock modules. Notably, a non-curing poly(ethylene-vinyl acetate) (NC-EVA) was formulated identically to a standard EVA formulation but without the inclusion of a peroxide to promote curing during lamination.

The set of silicon modules was made using forty-two 156mm upgraded metallurgical silicon cells with a final average aperture-area efficiency of 14.6%. The PDMS modules used sixty 156mm multicrystalline cells and were 13.9% efficient. The thin-film mock modules were constructed using two pieces of 3.18mm-thick, 61cm × 122cm glass. The rear surface of the back plate was painted black to simulate the optical absorption of a thin-film module. The inside of the front glass had a thin transparent conductive oxide (TCO) layer, which was removed in a 12.7mm region of the perimeter using laser ablation. The TCO was electrically connected to a ribbon passing through a hole cut in the back plate. This allowed the wet high-pot test to be carried out, to assess if creep would pose a safety or performance concern. Thin-film mock modules were mounted by adhesively attaching fibreglass

Encapsulant material type		DSC determined transitions			DMA determined transitions at 0.1 rad/s	
		T_g (°C)	T_m (°C)	T_f (°C)	T_g (°C)	T_m (°C)
Commercial PV EVA resin	EVA	-31	55	45	-30	47
Commercial PV EVA resin with all components but the peroxide	NC-EVA	-31	65	45	-28	69
Polyvinyl butyral	PVB	15	N/A	N/A	17	N/A
Aliphatic thermoplastic polyurethane	TPU	2	N/A	N/A	3	N/A
Part-catalyzed, addition cure polydimethyl silioxane gel	PDMS	-160	-40	-80		
Thermoplastic polyolefin #1	TPO-1	-43	93	81	-35	105
Thermoplastic polyolefin #3	TPO-3	-44	61	55	-41	79
Thermoplastic polyolefin #4	TPO-4	-34	106	99	-21	115

Table 1. Phase transitions determined by differential scanning calorimetry (DSC) and dynamic mechanical analysis (DMA). DMA glass transitions (T_g) were determined at the peak of the phase angle, and the DMA melting transitions (T_m) were determined when the phase angle was 45 degrees, except for the cross-linked PDMS and EVA, for which an inflection point in the modulus was used.

channels to the back, allowing the front piece of glass to move freely.

For the thin-film mock modules, the creep (displacement of the front glass relative to the back glass) was measured using a high-precision depth gauge with ±1µm increments. This gauge was mounted to a flat plate to ensure that it was positioned perpendicular to the side of the module and in the plane of the glass. By using this set-up, creep measurement reproducibility was better than ±20µm.

Modules were deployed in Mesa, Arizona, from May to September 2011 on a rack at a 33-degree latitude tilt and azimuth of 255 degrees so that they would face the sun more directly at the hottest part of the day. Additionally, a single NC-EVA thin-film mock module was exposed in Golden, Colorado, at a 40-degree tilt and 180-degree azimuth [8]. For both the thin-film and silicon module types, insulation was placed on the back side to simulate a rooftop installation (resulting in maximum measured temperatures between 102 and 104°C in Mesa, Arizona). The temperature of the modules was monitored by placing thermocouples underneath the insulation on the back side of each module. One thermocouple was placed in the centre of each module, and the other about 7.5cm diagonally inward from one corner of the module.

Following deployment in the field, the formation of polymer chain cross-links on the Arizona-fielded, NC-EVA, thin-film mock module was evaluated using size-exclusion chromatography (SEC) in conjunction with multi-angle laser light scattering (MALLS, Waters Corporation GPCV 2000 instrument) and viscometric detection (using a capillary viscometer detector CV from Waters). Samples were cut using a ceramic saw blade, which allowed them to be taken

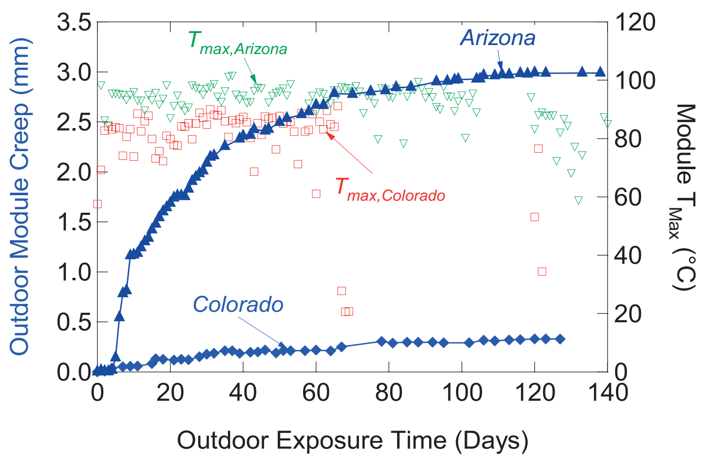

Figure 1. Measurement of thin-film mock module creep during outdoor exposure: module displacement and daily maximum module temperature for the NC-EVA modules deployed in Arizona and Colorado.

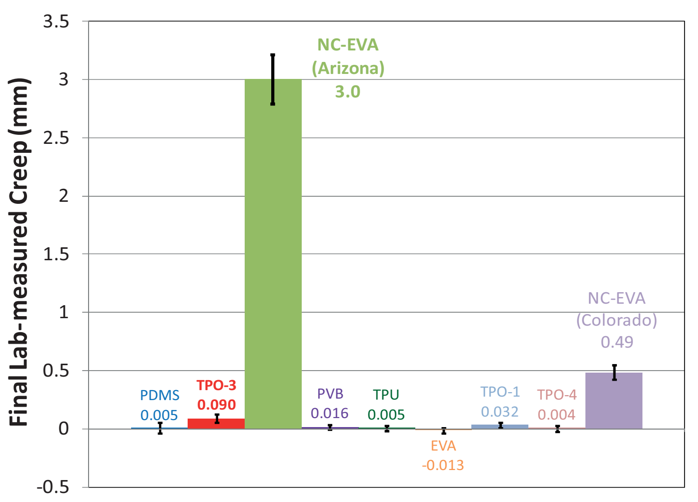

Figure 2. Detailed indoor measurement of thin-film mock module creep after field deployment in Arizona and Colorado.

at different distances from the edge. Polymer was removed from the glass by extraction in a solution of tetrahydrofuran (THF) for 72 hours; however, this left behind approximately 60% of the EVA as an insoluble fraction. The residual glass-EVA specimens were soaked in trichlorobenzene (TCB) overnight at 150°C to solubilize the remaining EVA. Samples of 'virgin' (unexposed) NC-EVA film were dissolved in THF and TCB at room temperature and 150°C, respectively, to serve as controls. Solutions were made with approximately 1mg/ml concentrations.

Results

Outdoor testing

Of the outdoor exposed modules, only the thin-film mock modules constructed using NC-EVA experienced significant creepage, moving 3.0±0.2mm over the course of the summer (Fig. 1). Despite this, the NC-EVA modules still passed the wet high-pot test. A more detailed indoor measurement after the exposure indicated that the TPO-3 module crept 0.090±0.036mm and the TPO-1 module crept 0.032±0.024mm (Fig. 2). Even though most of these thermoplastic encapsulants reached either the melt or rubbery state during exposure, no significant movement was observed.

> "Of the outdoor exposed modules, only the thin-film mock modules constructed using NC-EVA experienced significant creepage."

In Fig. 1 note the absence of creep beyond day 110 in Arizona and the general reduced creep rate when the maximum temperature is lower during the first 60 days or so; moreover, the Colorado-deployed module barely crept and rarely reached temperatures above 90°C. These observations indicate that creep is possible for uncured EVA when the maximum module temperature approaches around 90°C. Because the modules were mounted individually (i.e. so as to allow air to flow between them), as opposed to a closely packed installation, the temperature was between 10 and 15°C cooler at the edges of the modules during the hottest part of the day. The temperature differential appeared in both the thin-film mock and the crystalline Si modules, but the presence of an Al frame in the crystalline silicon modules is expected to make it more difficult, though not impossible, to realize an installation configuration that would significantly reduce this temperature heterogeneity. It is this temperature differential that helps to reduce the creep considerably, despite the fact that most of the module is well above its melting point of around 65 to 69°C.

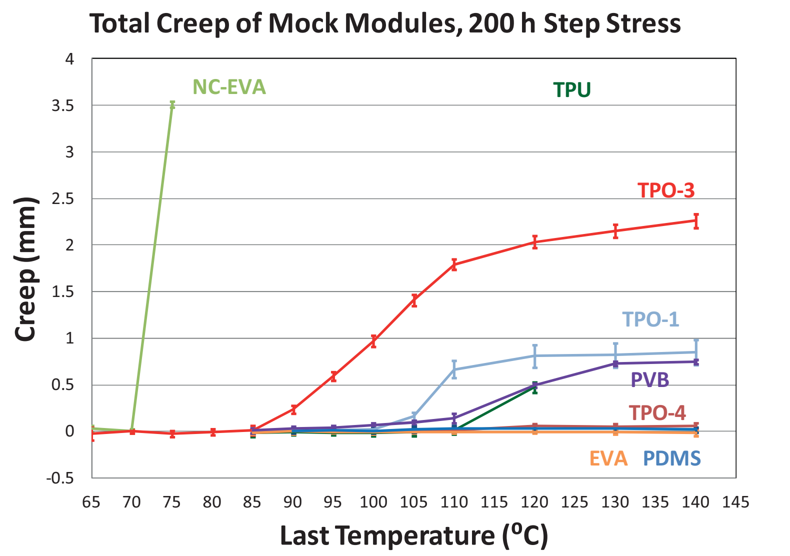

Figure 3. Relative displacement of glass sheets in the thin-film mock modules after step-stress tests, each lasting 200 hours.

Over the first 30 days, creep increased more quickly in the Arizona module, but slowed down in mid-summer even though the temperature did not fall appreciably. Typical EVA formulations are known to cross-link as they age in the field [9]. This reduction in creep rate suggests that, even without the peroxide additive, NC-EVA is cross-linking at these high temperatures.

Indoor testing

The modules were also examined indoors in a step-stress experiment. Modules were mounted vertically, with the crystalline Si modules simply resting on their frames, and the thin-film mock modules mounted vertically using adhesive on their back sides, allowing the front glass to move (Fig. 3). More creep is seen in indoor testing than in outdoor experiments at lower temperatures, where the cool perimeter of the outdoor modules limits motion. The NC-EVA began creeping detectably at 75°C in the thin-film mock module construction, and at 80°C in the crystalline Si construction. Similarly, the TPO-3 and TPO-1 thin-film mock modules began to creep detectably at 90 and 105°C respectively. Furthermore, the slope of the creep vs. temperature curve for TPO-3 does not continue to increase rapidly beyond 95°C, suggesting that it is chemically cross-linking at temperatures above 90°C. At even higher temperatures, above 120°C, the amount of creep in each cycle begins to plateau for TPO-3. Similar behaviour is also observed for TPO-1, TPO-4 and polyvinyl butyral (PVB). The only thermoplastic material that did not appear to cross-link as it aged was the thermoplastic polyurethane (TPU). In this case, after exposure at 130°C, the module plates were displaced by more than 1cm where they contacted the chamber floor. In addition, starting at 105°C a large number of bubbles began to appear within the module, and became present throughout the module after exposure to 110°C.

> "The only thermoplastic material that did not appear to cross-link as it aged was the thermoplastic polyurethane (TPU)."

Molecular weight changes

The cross-linking of the NC-EVA in the fielded module was verified using SEC in conjunction with MALLS and viscometry detection. Three samples were removed from the modules: one was cut from the edge of the module, one from about 2cm in from the edge, and one from about 4cm in. Fig. 4 shows that the THF-insoluble, TCB-solubilized sample taken from the edge of the NC-EVA module deployed in Arizona has a lower molecular weight distribution than the unaged TCB-solubilized control sample, indicating that chain scission has dominated over polymer cross-linking. In contrast, the samples taken at distances of 2cm and 4cm in from the edge have a higher molecular weight than the control, indicating that cross-linking has dominated over chain scission. However, all the aged samples show changes in intrinsic viscosity relative to the control, which is a sign of some degradation, causing changes in the degree of branching of the polymer chains.

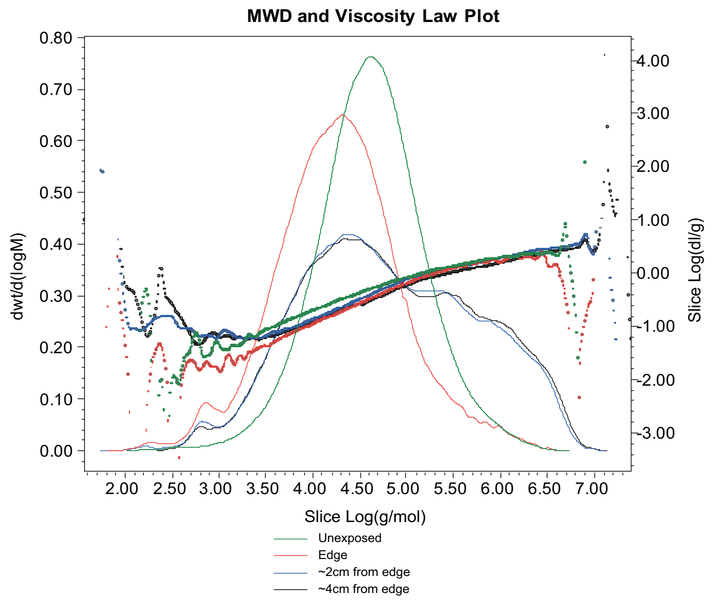

Figure 4. SEC-MALLS and viscometry results from the NC-EVA thin-film mock modules after exposure in Arizona. Samples were dissolved in trichlorobenzene (TCB) by extraction at 150°C overnight. The thin curves show the weight fraction of slices (left axis); the thick curves show the intrinsic viscosity of slices (right axis).

This result is supported by numerous observations of fielded modules in which discoloration of EVA is observed in the centre area of a cell, and yet greater oxygen incorporation is seen around the cell perimeter [10]. Similarly, it has been observed in aged samples that the gel content in the more highly yellowed EVA at the centre of the cell is higher than in the EVA at the perimeter [9]. Thus, yellowing and cross-linking are correlated to lower oxygen incorporation, and oxidative bleaching and lower cross-link densities are correlated to higher oxygen incorporation.

For the THF soluble fraction, very little difference in the molecular weight distribution was seen between the EVA samples extracted from the fielded modules and from the unstressed EVA (Table 2). The THF solution was only able to dissolve about 40% of the polymer. It therefore appears that any degradation causing chain scission or cross-linking renders EVA significantly less soluble in THF.

Discussion

Oxidation and cross-linking

There are many different chemical pathways possible for producing cross-linking in polymer chains. For NC-EVA, the fact that the formation of cross-links varies with position in the sample indicates that some chemical species must be entering or leaving the module package, thus affecting the kinetics. Starting from the edge and proceeding inwards, there are gradients in temperature, water content and oxygen content. The temperature gradient from the edge to the centre is at most around 20°C at the hottest part of the day (as indicated by infrared imaging). This would not be expected to create by itself large differences in the reaction kinetics over a 2cm distance. The diffusivity of water in EVA has an activation energy of about 38kJ/mol (0.40eV) [11], which was used to estimate an Arrhenius activation energy-weighted effective module temperature of 50°C for the corner and 60°C for the centre thermocouples [12,13]. At 50°C, the diffusivity of water in EVA is $1.6\times10^{-6}cm^2/s$. For the deployment time of 140 days, the characteristic penetration depth (x) was around 4.1cm ($x=\sqrt{Dt}$) [11]. In contrast, for a distance of 2cm the characteristic time is 29 days.

Marias et al. [14] compared the permeation characteristics of H_2O and O_2 in 33 wt% VA EVA at 25°C and found it to be selectively permeated by water 350× as fast as by oxygen, at the same vapour pressures, principally because of differences in solubility. If we use 10% RH in Arizona at 25°C for the water content, the partial pressure of water is about 0.24cmHg, as compared to 21% oxygen with 16cmHg, which means that water permeates EVA about 5.2× as fast as oxygen does. This makes it more likely that oxygen is the limiting reagent enabling the shift from cross-linking dominated reactions to chain-scission dominated reactions. However, more research is necessary to verify the kinetic pathways to confirm which component is limiting the reaction.

The reduction in creep rate of field-exposed modules and the formation of cross-links as shown by SEC-MALLS indicate that in anaerobic and anhydrous conditions, EVA will cross-link when exposed to heat and UV light, even without the addition of peroxide-based cross-linkers to the formulation. Because the thin-film mock modules were constructed so that light passed through the polymer, it is not known if these effects are driven by heat, UV light or a combination of the two. However, it does indicate that typical EVA formulations would be expected to cross-link with time, reducing the potential for thermally induced creep.

Creep and its consequences

Because the three TPOs and PVB did not have exponential-like increases in creep with temperature, it is concluded that exposure to high temperatures caused cross-linking reactions to dominate over chain scission. Therefore, as in the case

Sample		Mn [g/mol]	Mw [g/mol]	Mz [g/mol]	PDI	MP [g/mol]
THF soluble fraction	Unexposed	20,400	97,800	448,000	4.8	42,800
	Edge	19,900	89,100	379,000	4.5	40,300
	~2cm from edge	19,900	84,600	326,000	4.2	37,900
	~4cm from edge	21,300	104,000	437,000	4.9	40,900
TCB soluble fraction	Unexposed	15,600	97,800	512,000	6.3	44,400
	Edge	5,540	66,800	632,000	12	21,100
	~2cm from edge	8,720	394,000	2,220,000	45	25,000
	~4cm from edge	10,600	382,800	2,050,000	36	22,000

Table 2. SEC-MALLS results.

of EVA, it is probable that they too would cross-link with time in field exposure. In contrast, the TPU thin-film mock module began to creep at 100°C, and a large number of bubbles formed in the interior of the module. At higher temperatures the effective viscosity dropped dramatically and the front plate contacted the bottom of the chamber, causing creep that was too high to be measured in these chambers (see the dashed arrow in Fig. 3 for TPU). The TPU seemed to degrade dramatically at elevated temperatures. On the other hand, all the polymers with only carbon–carbon bonds in the backbone (EVA, TPOs and PVB) appear to cross-link when exposed to high temperatures. This will help to mitigate the potential for creep in these thermoplastic encapsulant materials.

The onset of creep correlates reasonably well with the melting points determined by DMA using the phase angle of 45 degrees (Table 1). The three TPOs showed much greater creep than PVB, despite the glass transition of the latter at 16°C because of its greater viscosity [8]. However, DMA measurements indicate the phase angle of PVB reaches 45 degrees, when measured at 0.01 rad/s and at a temperature of 115°C, which correlates better with the onset of its creep.

"None of the crystalline Si modules exhibited measurable creep when deployed outdoors."

None of the crystalline Si modules exhibited measurable creep when deployed outdoors. Only the TPO-3 module demonstrated a statistically significant performance loss, which was due to a cracked cell, presumably weakened or cracked during lamination because of TPO-3's higher viscosity relative to EVA [8]. Despite reaching what could be considered nearly the highest temperatures possible for a fielded module, none of the crystalline Si modules experienced a detectable safety or performance failure as a result of using a thermoplastic encapsulant. However, the modules were mounted with the cell strings arranged vertically. If the NC-EVA module had been mounted with the cell strings horizontal, it is more likely that some creep would have occurred in the cells in the centre of the module. Subsequent accelerated stress tests (humidity freeze) will be performed on these modules to investigate if longer term deployment results in deformation and/or performance degradation.

In indoor studies, the onset of creep for the NC-EVA silicon module occurred at 75°C. In this case, despite the fact that the sides of adjacent rows of cells were touching, there was no discernible performance loss with step-stress tests up to 100°C (Fig. 5). Although this significant cell movement did not directly create a performance issue, it is likely that extended exposure to thermal cycling after this amount of creep would increase the mechanical stress on the tabbing and solder bonds, leading to higher failure rates in the long term.

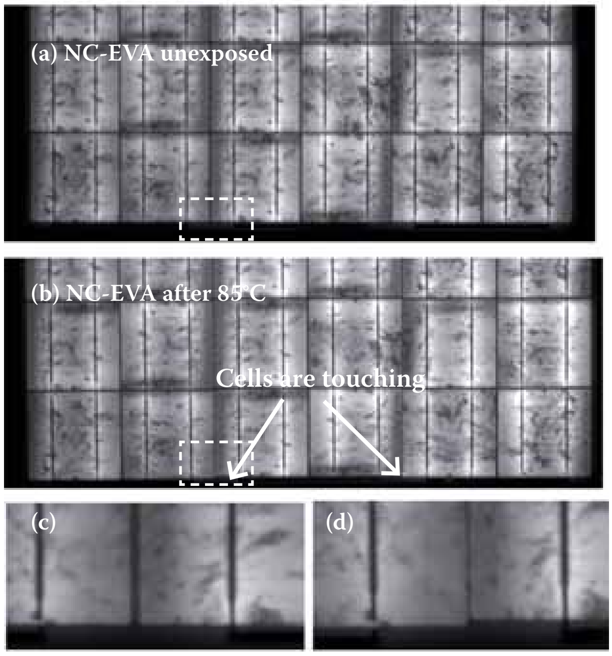

Figure 5. Electroluminescent images of the NC-EVA crystalline Si: (a) before thermal exposure; (b) after the 85°C exposure step of the indoor step-stress test; (c,d) close-ups of the bottom cells indicated by the boxes in (a) and (b) respectively.

Conclusions

The results presented here indicate that the potential for creep of the examined thermoplastic materials is negligible for the majority of PV installations. When a typical polymer-backed crystalline Si module was exposed outdoors in Arizona during the summer, with insulation on the back to simulate a rooftop mounting configuration, the module did not creep, even when made with EVA containing no cure chemistry. Thus, it was not possible to detect any short-term durability or safety issues likely to result from completely uncured EVA.

"To assess the potential for creep, manufacturers should consider not only the location of phase transitions and the viscosity at temperatures between 85 and 100°C, but also the effects of degradation on those material properties."

Only modules with an unrestrained front glass made of glass were shown to have any propensity to creep outdoors. This is due in part to the non-uniformity of temperature, resulting in small areas that significantly resist creep. Evidence that NC-EVA, TPO-1 and TPO-3 thermally cross-link, despite the absence of peroxide, was also presented. This unintended cross-linking actually serves to mitigate the potential for creep in some materials.

The use of 85°C in IEC standards necessitates cross-linking of EVA to achieve gel contents in excess of around 60%. However, even if the EVA of a framed, polymer-backed Si PV module had a very low gel content, it would have to be deployed in an extreme environment during the hottest time of the year, in close contact to a mounting structure that restricts heat transfer, for there to be a significant chance of creeping before it eventually thermally cross-linked on its own [9]. Therefore, to assess the potential for creep, manufacturers should consider not only the location of phase transitions and the viscosity at temperatures between 85 and 100°C, but also the effects of degradation (chain scission or cross-linking) on those material properties.

Acknowledgements

This work was part of a large collaborative effort by a number of people working on standards development at many institutions. The authors gratefully acknowledge the support of the following individuals: A. Stokes, A. Blosse, A. Norris, B. Koll, B. Adams, C. Kotarba (Chad), D. Trudell, D. Nobles, E. Gelak, G. Perrin, H.

Zenkoh, J. Galica, J. Bokria, J. Pern, J. Cano, K. Koka, K. Stika, K. Emery, K. Terwilliger, K. Olakonu, M. Yamamichi, M. Al-Jassim, N. Powell, N. Nickel, P. Gonzales, P. Hacke, R. Smith, R. Tucker, S. Glick, S. Rummel, T. Shioda and Y. Brun.

This work was supported by the U.S. Department of Energy under Contract No. DE-AC36-08-GO28308 with the National Renewable Energy Laboratory.

PV Modules

References

[1] UL 1703, "UL standard for safety for flat-plate photovoltaic modules and panels".

[2] IEC 61730 (2004, edn 1.0), "Photovoltaic (PV) module safety qualification – Part 1: Requirements for construction".

[3] IEC 61215 (2005), "Crystalline silicon terrestrial photovoltaic (PV) modules – Design qualification and type approval".

[4] IEC 61646 (2008), "Thin-film terrestrial photovoltaic (PV) modules – Design qualification and type approval".

[5] Wohlgemuth, J. & Herrmann, W. 2005, "Hot spot tests for crystalline silicon modules", *Proc. 31st IEEE PVSC*, Lake Buena Vista, Florida, USA, pp. 1062–1063.

[6] Miller, D. et al. 2010, "Creep in photovoltaic modules: Examining the stability of polymeric materials and components", *Proc. 35th IEEE PVSC*, Honolulu, Hawaii, USA.

[7] Kurtz, S. et al. 2009, "Evaluation of high-temperature exposure of rack-mounted photovoltaic modules", *Proc. 34th IEEE PVSC*, Philadelphia, Pennsylvania, USA.

[8] Moseley, J.M. et al. 2011, "The melt flow rate test in a reliability study of thermoplastic encapsulation materials in photovoltaic modules", NREL Report No. TP-5200-52586, pp. 1–20.

[9] Pern, F.J. & Czanderna, A.W. 1992, "Characterization of ethylene vinyl acetate (EVA) encapsulant: Effects of thermal processing and weathering degradation on its discoloration", *Solar Energy Mater. & Solar Cells*, Vol. 25, pp. 3–23.

[10] Klemchuk, P. et al. 1997, "Investigation of the degradation and stabilization of EVA-based encapsulant in field-aged solar energy modules", *Polym. Degrad. Stabil.*, Vol. 55, pp. 347–365.

[11] Kempe, M.D. 2006, "Modeling of rates of moisture ingress into photovoltaic modules", *Solar Energy Mater. & Solar Cells*, Vol. 90, pp. 2720–2738.

[12] Kurtz, S. et al. 2011, "Evaluation of high-temperature exposure of photovoltaic modules", *Prog. Photovolt.: Res. Appl.*, DOI 10.1002/pip. 1103.

[13] Pickett, J.E. & Sargent, J.R. 2009, "Sample temperatures during outdoor and laboratory weathering exposures", *Polym. Degrad. Stabil.*, Vol. 94, pp. 189–195.

[14] Marais, S. et al. 2000, "Permeation of water through polar and nonpolar polymers and copolymers: Determination of the concentration-dependent diffusion coefficient", *J. Polym. Sci. Part B: Polym. Phys.*, Vol. 38, pp. 1998–2008.

About the Authors

Michael Kempe has a Ph.D. in chemical engineering from the California Institute of Technology. He is currently a scientist at NREL, where he focuses on the modelling and measuring of moisture ingress into PV modules.

David Miller specializes in materials characterization for the purpose of durability assessment, reliability prediction and standardization of PV modules. This includes encapsulation and Fresnel lenses for CPV, as well as encapsulation and adhesives for flat-panel PV.

John Wohlgemuth joined NREL as principle scientist in PV reliability in 2010, where he is responsible for establishing and conducting research programmes for improving the reliability and safety of PV modules. He holds a Ph.D. in solid state physics from Rensselaer Polytechnic Institute.

Sarah Kurtz has a Ph.D. in chemical physics from Harvard University. She has worked at NREL since 1985, developing high-efficiency multijunction solar cells and studying the reliability of PV modules.

John Moseley is a graduate student at the Colorado School of Mines and NREL. His research involves the characterization of the microstructure and opto-electronic properties of CdTe thin films.

Qurat (Annie) Shah graduated from Arizona State University with a master's in alternative energy technologies. Having worked at the Photovoltaic Reliability Laboratory (PRL) on various applied projects related to PV, she is currently a solar engineer with a private company.

Govindasamy Tamizhmani is a professor at Arizona State University and the president of TUV Rheinland PTL. He has been involved in research into, and testing and certification of, PV devices for 29 years.

Keiichiro Sakurai has a Ph.D. in electrical engineering from Kyoto University. He is currently a researcher in AIST, working on deployment policies as well as on reliability of PV modules and systems.

Masanao Inoue has a B.S. from Ibaraki University. He specializes in PV module fabrication machines and characterization of PV modules.

Takuya Doi has a Ph.D. in engineering from the University of Tsukuba. He is currently a senior researcher in AIST, working on reliability of PV modules.

Atsushi Masuda received his Ph.D. degree in engineering from Kanazawa University in 1996. He is currently a team leader of the collaborative module-reliability research team at AIST. His main research field concerns solar-cell materials and reliability of PV modules.

Sam Samuels has a B.S. in chemical engineering from Carnegie-Mellon University and a Ph.D. in chemical engineering and polymer materials science and engineering from Princeton University. With over 39 years' experience in polymer and fibre development at DuPont, his recent focus has been on developing new packaging materials for the PV industry.

Crystal Vanderpan has a B.S. in chemical engineering and materials science from the University of California at Davis. She has worked at Underwriters Laboratories since 1995, and is currently the principal engineer for PV materials and printed circuit technologies.

Enquiries

Michael D. Kempe
National Renewable Energy Laboratory
15013 Denver West Parkway
Golden
Colorado 80401
USA

Testing times to bring down the costs of solar

Felicity Carus, USA correspondent, PV-Tech.org

A 100lb punch bag, sandbags and a ball bearing the size of your fist are not necessarily what you would associate with state-of-the-art testing for solar panels.

But at UL's solar laboratories in San Jose, California, these experiments that look like they were cooked up in an eccentric inventor's garden shed, put panels of all flavours through their paces on safety testing before they reach the US market.

The boxer's punch bag is dropped side-on like a wrecking ball onto an upright panel in a simulation of what could happen in a real-world installation if, say, a tree fell against it. Panels always shatter in the impact test, but small chunks are better than tiny shards, Chris Paxton, engineering leader of product safety, told me.

Sandbags weighing up to 55lb are placed on the front and back of panels to simulate snowfall and wind uplift on a roof. The ball bearing mimics what would happen should a monkey wrench fall from an installer's tool belt.

Manufacturer's cherished panels endure the full cycle of testing that includes being baked to 90°C and frozen to minus 40°C in huge ovens up to 1,000 times over and being shot at by a high-pressure gun that fires round ice bullets designed to mimic hail.

These are the experiments that can cause visible damage. But there are the more scientific experiments for standards such as flash tests, the continuous simulator for light-soaking, indoor temperature testing and hotspot endurance tests that burn through substrates like a cigarette in simulations of shading.

The only test that UL doesn't carry out in San Jose is setting fire to panels because of objections from the city council.

UL, a global safety testing and certification company, opened its solar testing lab in July 2008. Thin film and CPV are also tested at UL, some of them still only in prototype form and kept heavily under wraps. On the day of my visit, Stion and Suntrix appeared to have still-boxed samples to test.

It takes a minimum of 40-42 days to cycle through the testing system, a far cry from five years ago when testing could take as long as a year.

Thanks to its overnight success in San Jose, UL had to add five other testing labs around the world – India, China and Germany were obvious choices.

"We offer market access and provide an opportunity to understand product performance which helps investors, banks and utilities," said Butler. "There is a general expectation that these products are going to last 15, 20, 25 years. Insurers need to know how to underwrite the warranty and safety and performance standards are crucial for companies that have only been around for a couple of years."

Today's testing times are about to get even more intense as the solar industry undergoes dramatic consolidation.

"Consolidation was expected," said Butler, "but it started happening sooner than expected and is more rapid. That means some companies have decided not to be part of the industry and focus on other technologies."

"But we remain optimistic as solar is estimated to grow."

Meanwhile, down in New Mexico, mega-minds at Sandia National Labs are developing a network of testing labs to help prove to investors that the products that they lay down cash for are going to give them the return as advertised by project developers and manufacturers.

Regional Test Centres (RTCs) in Albuquerque, New Mexico, Denver, Colorado and Orlando, Florida, are about to get the green light from the US Department of Energy to put identical PV installations through their paces in different climates.

Denver was chosen for its Steppe climate – hot in summer, cold in winter; Albuquerque is a hot-dry climate and Orlando has a hot-humid climate.

The idea to develop three RTCs was hatched during a DoE PV Manufacturing

UL module testing lab, San Jose

Workshop at Lawrence Berkeley National Laboratory (LBNL) last March to supplement SunShot programmes.

"The aim will be to validate the performance of PV systems, verify and validate models used to predict performance, collect detailed operations and maintenance (O&M) data and investigate the role of various environmental (climatic) factors on reliability, durability and safety of PV technologies," said the DoE.

"Project developers will be able to use this data to go to the bank and potentially raise financing more easily," said Joshua Stein, a distinguished member of the technical staff at Sandia.

"But the ultimate goal of these is to really come up with a set of standards whereby other private labs could then participate and be RTCs."

He added: "There has been talk about designing modules for a specific region to match the spectral content of the light. I don't think the industry is mature enough yet to do that."

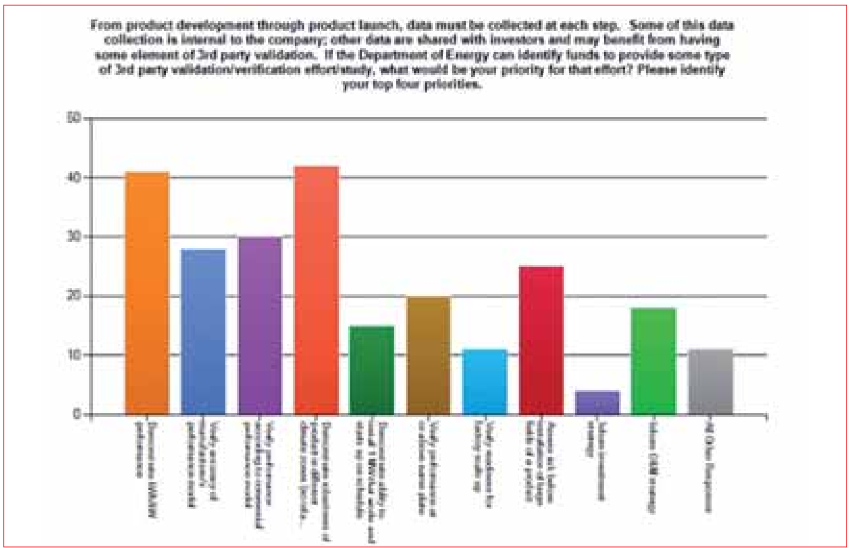

Power Generation

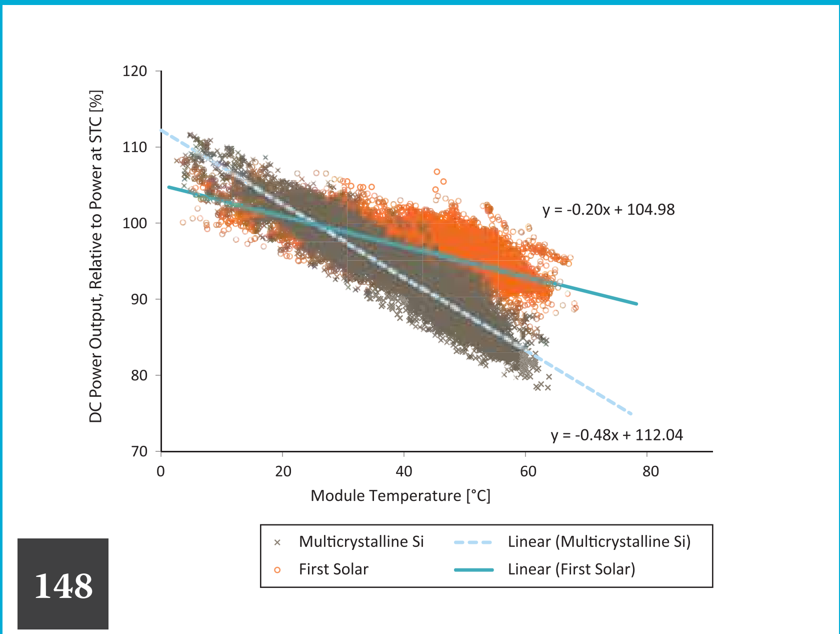

148

141

144

First Solar builds PV project pipeline

Major restructuring efforts at First Solar took a backseat during the company's second quarter conference call as management focused on a significant increase in its PV project pipeline. First Solar said it had added almost 1GW of new projects to a pipeline that previously stood at 2.9GW. Net sales were US$957 million, up from US$497 million last quarter, while revenue guidance was raised for 2012 to US$3.6-US$3.9 billion, up from a range of US$3.5 billion to US$3.8 billion.

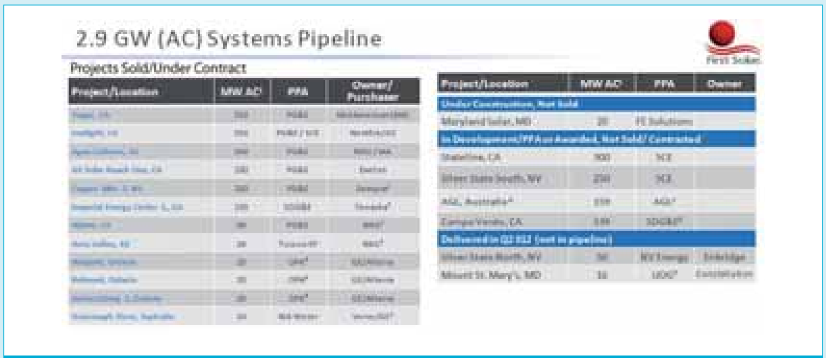

First Solar adds almost 1GW of new projects.

First Solar highlighted new project wins in Australia and India as well as projects in the company's main market, the USA. Improved module demand from third-party customers came from both Europe and India. The company had been successful in the first two major competitive bids for utility-scale projects in Australia, highlighting that the utility-scale market there was just starting to take off and that First Solar could be on track to take a 30% market share as a result.

First Solar management also noted that it was in the process of negotiating on a number of PV power plant projects in India, primarily in relation to third-party module sales. Hughes said that he expected the company to win around 20% of the Indian market in 2012 and retain that share going forward.

Asia & Oceania News Focus

Schanti Partners invests in 50MW Indian PV project

Schanti Partners, a US-based asset management company, has put aside INR5.8 billion (US$105.1 million) for the development of a 50MW solar power project in the district of Kaimur, Bihar, India, Energy Business Review has revealed. The company's subsidiary Sparkle Solar Bihar I will implement the project, which will be developed in five phases. Each phase will involve the installation of 10MW. The project will utilize PV equipment based on CPV technology provided by Sol Focus. The company has submitted a proposal for a 25-year PPA to the state-owned utility Bihar State Electricity Board (BSEB). The proposed PPA rate, as stated by The Times of India, is INR12.50 (US$0.225) per kWh.

Having already secured finance worth US$30 million from the US Ex-Im Bank for the project, Schanti Partners is hoping to secure a 30-year land lease contract for the project site. However, the loan deal requires the firm to source its solar equipment from the USA.

First Solar to develop Indian solar farms to counter grid blackouts

On the back of a two-day blackout in India which caused tragedy, chaos and loss of face at the end of July, Bloomberg has revealed that US solar giant First Solar is drawing out plans to develop solar farms in India as repeated power outages spur on demand for solar power. Citing Sujoy Ghosh, the new India manager at First Solar who assumed his position in May, Bloomberg revealed that the solar behemoth is targeting a 20% share of India's PV sales by becoming more than just a supplier. Demand is expected to come from industrial and commercial businesses. The company is expected to be involved in building, arranging finance and supplying modules.

Europe News Focus

TerniEnergia constructs 16MW of PV plants in Greece and South Africa

TerniEnergia, an Italian developer of PV projects, has begun the construction of a 10MW solar power plant in South Africa, the company has announced. The company has been chosen by an undisclosed European utility company to build the project, which is estimated to be connected to the grid later this year. TerniEnergia has further begun constructing a 6MW PV park in Greece. The project is being developed for a local utility. No further information was disclosed.

Solar Shakeout: PV project developer SunStrom goes bankrupt

The Germany-based PV project developer SunStrom has filed for bankruptcy at the Wienberg Dresden court, according to the provisional liquidator HWW Wienberg Wilhelm. The firm was a subsidiary of Solarwatt, which filed for creditor protection in June 2012. SunStrom has been in operation for 12 years and had been known for some high-profile PV projects in Germany, such as the rooftop installation at BMW-World. "The SunStrom GmbH has been in the market for over twelve years and has first-class know-how and excellent references," stated lawyer, Rudiger Wienberg.

Wages and salaries of employees are protected from the insolvency payments until the end of September 2012.

General Motors builds 8.15MW PV rooftop system in Germany

General Motors, a specialist in the automotive sector based in the USA, has announced that it has installed an 8.15MW PV system on the rooftop of its Opel Rüsselsheim facility in Rüsselsheim, Germany. According to GM, the PV system is one of the largest of its kind in Germany, covering an area equivalent to 32 football pitches. It will generate an output of approximately 7.3 million kWh. The solar electricity produced at Rüsselsheim feeds directly into the grid of the plant for use in vehicle production. Excess solar power is fed into the public grid of Stadtwerke Mainz, an energy provider in Germany. The addition of the 8.15MW system is in line with the company's target to double its global output of solar power by 2015, which it announced last year. This target is part of the company's broader plans to increase its use of renewable energy to 125MW by 2020.

As demonstrated by its targets, GM is committed to increasing the use of solar power at its facilities worldwide. The company has already installed similar rooftop PV systems on top of its Zaragoza and Kaiserslautern facilities. The Rüsselsheim system plus the systems at its Zaragoza and Kaiserslautern facilities generate enough electricity to power 5,800 households.

Belectric France inaugurates first PV plant in Provence Alpes Côte d'Azur, France

Belectric's French subsidiary has inaugurated a 1.8MWp PV plant in Valderoure in the Provence Alpes Côte d'Azur region in southern France. The inauguration ceremony was attended by various regional politicians as well as Belectric employees involved in the design and implementation of the power plant.

According to Belectric, a developer of ground-mounted and roof-mounted PV systems, the 1.8MWp power plant is the first ground-mounted solar power plant in the region and "a good example of Franco-German co-operation". The system was built on an area covering 5.5 hectares and utilizes 24,000 First Solar modules, which generate around 2.8 million kWh on an annual basis.

Suntech claims to be victim of massive fraud over GSF investment

Suntech Power Holdings said it had started multiple legal proceedings against a number of unidentified parties regarding investment guarantees it provided for a joint venture with PV power plant project developer, Global Solar Fund, S.C.A., Sicar (GSF). However, Suntech has claimed that a pledge of €560 million of German government bonds by a third-party investor of GSF, GSF Capital Pte Ltd., may never have existed. Suntech said that it may have to delay second-quarter financial reporting as a result. According to Suntech, recent efforts to "monetize" its investment in GSF led to the discovery that the "collateral related to the security interest may not have existed and the company may have been a victim of fraud."

Dr. Zhengrong Shi, Suntech's chairman and CEO, said, "We are very disappointed that this has occurred and it has the highest level of attention from the company and the board, including the audit committee. There is no indication that management had any involvement and we are vigorously pursuing all avenues to resolve this matter and ensure that we protect the interests of our shareholders."

Dr. Zhengrong Shi said he was very disappointed that Suntech may have been a victim of fraud.

Americas News Focus

Ingenostrum plans to build another large-scale PV project in Chile

Ingenostrum, a Spanish developer of PV projects, is planning to build another large-scale solar power plant in Antofagasta, Chile.

According to Photon, the capacity of the project has not been disclosed but the proposed plant is expected to cover an area of 531 hectares — which would make it one of the company's largest projects in the country. Martifer Solar, a manufacturer of PV modules based in Portugal, will supply all equipment and provide construction, maintenance and monitoring services. Ingenostrum will hold the responsibility for managing the project and for the engineering work. In July, the Spanish developer confirmed that it would construct six solar power plants in Antofagasta with a combined capacity of 706MW. The projects require a total investment of US$1.9 billion. Of these six projects, the most significant one is the Crucero Oeste project located in the Sierra Gorda sector of Antofagasta. The Crucero Oeste project will cost US$449 million and have an installed generating capacity of 160.3MW.

Two of the six projects were approved by the Commission for Environmental Assessment (CEA) in August 2012. These were the 76.7MW Laberinto Este project and the 69.8MW Laberinto Oeste project.

Africa & the Middle East

JinkoSolar establishes Solar Club, plans to offer members training and priority service

JinkoSolar Holding's will debut its new JinkoSolar Priority Solar Club sometime in August. The Solar Club plans to be an exclusive partner programme for its strategic customers and offer various benefits to its members. The Solar Club will have different levels of membership and offer different perks, including JinkoSolar updates, creative marketing support, professional product training, prioritized technical service, and Jink-branded promotional materials and sales tools. Members will earn points automatically with every qualifying purchase.

Eight19 expands Indigo off-grid solar scheme; launches Azuri Technologies Limited

Cambridge University spin-off Eight19 has revealed the launch of Azuri Technologies Limited, which will be used to develop the company's Indigo 'pay-as-you-go' solar technology for off-grid markets. Indigo, which has been developed over the last year, works by offering a pay-as-you-go solar option for customers in emerging markets. Users pay US$1 a week using scratch cards for the system, which consists of a battery, a solar panel, LED lights and a mobile phone charger. Although the technology is already deployed in Kenya, Malawi, Zambia, South Sudan, Uganda and South Africa, Azuri will now work to expand the Indigo product family and market reach while Eight19 continues to concentrate on development of its printed plastic solar technology. All Indigo activity has transferred to Azuri, and Simon Bransfield-Garth will remain chief executive officer of both companies at the headquarters in Cambridge, UK.

SolarWorld reports €144 million loss on increased shipments

Continued claims of solar modules being dumped on the market below manufacturing cost were cited as the key reason why SolarWorld reported a loss of €143.8 million for the first half of 2012. The PV manufacturer posted sales of €340.1 million, compared to €533.6 million in the first half of 2011. Continued price erosion meant the company made an inventory impairment charge of €33.5 million as well as an €80 million impairment on advance payments. Changes in regional demand due to feed-in tariff revisions provided inconsistent sales in key markets quarter on quarter. Noting pull-forward effects in the German market during the first quarter, SolarWorld said that demand in Germany softened in the second quarter. The Italian market was said to have been good, but not good enough to offset demand softness in Germany in the second quarter.

Demand from outside Germany contributed 60% of shipments in the first half of the year, yet was down from 69.1% in the same period a year ago.

SolarWorld said that shipments of modules and kits grew to 316MW, up from 269MW in the first half of 2011.

US Ex-Im bank to help finance US$2B worth of US technologies in South African energy sector

The US Export-Import bank signed a declaration of intent (DOI) with the Industrial Development Corporation of South Africa. The DOI aims to progress the South African government's Integrated Resource Plan and the South African Renewable Initiative. The agreement will see the Ex-Im bank provide financing up to US$2 billion worth of US technologies, products and services to South Africa's energy sector, with a focus on clean-energy development. The DOI was signed by Fred Hochberg, Ex-Im Bank chairman and president, Geoffrey Quena, CEO of the IDC and Gert Gouws, CFO of the IDC. The agreement was signed during the South Africa-United States Strategic Dialogue, which was hosted by US Secretary of State, Hillary Clinton.

Saudi company ACWA Power buys 42% stake in Karadzhalovo, Bulgaria, solar plant

SunEdison has advised that it has sold 98MW of European PV projects, including the 60MW Karadzhalovo, Bulgaria, plant, which became operational in March. It has been reported that Saudi Arabia-based ACWA Power advised that it had partnered with an associate of First Reserve Energy Infrastructure Fund and Clean Energy Transition Fund to buy the 60MW Bulgarian plant.

Once the transaction is completed, ACWA Power will have a 42% stake in the solar plant, which was funded with equity and debt capital. The debt was funded on a non-recourse basis by the International Finance Corporation, the US Overseas Private Investment Corporation and UniCredit. The plant will be operated by a new company formed in Bulgaria by ACWA Power's subsidiary NOMAC.

JA Solar sets up Japanese office to help drive growth

On the back of the introduction of attractive feed-in tariffs in the Japanese market in July 2012, JA Solar has announced that it has established an office in Tokyo in order to provide marketing and sales support as well as technical support services to its Japan-based customers. JA Solar, a key player in the solar products manufacturing sector, has established a strong presence in Japan. In the first quarter of its financial year, the company marked a record quarterly shipment to Japan, making it one of the top suppliers to the country. In the light of this, the new office has been set up in order to help drive its continued growth in the market.

Kyocera opens new warehouse in New Jersey

Kyocera has opened a new warehouse for its solar products in the USA, the company has announced. The warehouse is located in Cherry Hill, New Jersey, and the company chose this location, in collaboration with logistics provider NFI, to support its distribution centres in Scottsdale, Arizona, and San Diego, California. The building that functions as Kyocera's new warehouse has a 1.3MW PV rooftop array, equipped with 6,100 Kyocera PV modules, which was installed in 2010.

Product Reviews

AEG Power Solutions

AEG Power Solutions Protect PV.630 enables efficient use of thin-film modules

Product Outline: AEG Power Solutions has announced the expansion of its product portfolio with a new central inverter with 630kW capability. Protect PV.630 has an efficiency factor of 98.4%. With an appropriate transformer, it can also be adapted to the medium voltage grid (e.g. 10kV, 20kV, 33kV). The company has said the new inverter is the next step in offering high-end utility-class inverters.

Problem: Increased focus on overall yield from utility-scale and commercial-scale PV power plants requires improved inverter optimization. Flexibility in capabilities is required to limit product and installation costs, while matching the continued wide-range selection of solar module technologies for projects.

Solution: The technical highlight of the new inverter is its power stack PV core, designed in-house with a special control system, enabling an input DC voltage of up to 1,000V and providing high efficiency levels because of its optimized pulse pattern. This enables the efficient use of thin-film modules and cost-efficient overall equipment planning. The total concept is flexible and adjustable to many requirements as well as being applicable for almost all grid codes worldwide.

Applications: PV power plants and large-scale commercial PV power plants.

Platform: PV.630 has received numerous certifications and is compliant with the national grid regulations of several countries. Protect PV.630 is also available as a turnkey container solution. TKS-C 1250 is equipped with two inverters, a transformer and switchgear.

Availability: Protect PV 630 is immediately available as an indoor version. The outdoor solution will shortly be introduced to the market.

Clenergy

Clenergy offers PV-ezRack mounting system for trapezoidal sheet roofs

Product Outline: Clenergy has launched the PV-ezRack Trapezoidal module-mounting system, which is claimed to be a new high-quality universal mounting system designed for PV systems on trapezoidal sheet roofs with thicknesses of 0.4mm and above.

Problem: Trapezoidal sheet roofs provide specific problems for mounting PV modules. Key is the sheet roof thickness and weatherproofing after the securing guide rail and fixing bolts are installed.

Solution: PV-ezRack Trapezoidal is suitable for fixing frame modules onto all common trapezoidal sheet roofs with thicknesses of 0.4mm and at angles of 10° and above. It consists of a short guide rail and can be installed on raised beads that are as little as just 20mm wide thanks to its mounting form. The system material consists of weatherproof- and corrosion-resistant anodised aluminium rails. The EVA coating on the underside of the system and three pre-drilled fixing holes guarantee fully rainproof mounting and an optimally high load capacity. Depending on the thickness of the sheet roof, stainless steel screws with special cutter heads can be used to enable the system to be screwed in without chipping.

Applications: Trapezoidal sheet roof mounting system.

Platform: The system, which is supplied in its finished pre-assembled form, also comes with Clenergy's patented Z-module clips that can be simply clipped on from above. The small number of components that come with the system enables it to be rapidly mounted

Availability: June 2012 onwards.

PolyOne

PolyOne's Syncure Solar wire cable solution supports overall BOS cost reduction

Product Outline: PolyOne has introduced a new technology for PV systems wire and cable called Syncure Solar. Available globally, this UV-resistant, cross-linked polyethylene (XLPE) system is claimed to meet UL 4703 and VW 1 compliance in one material, eliminating the need to use two separate insulation and jacketing formulations.

Problem: Increased emphasis on simplifying the wiring of PV systems is required to reduce BOS costs. Providing electrical wiring insulation and jacketing in one format could simplify logistics, reduce cycle times and support overall system cost reductions.

Solution: Syncure Solar is claimed to provide multiple environmental benefits. First, it promotes the use of alternative energy by simplifying the wiring of PV systems. Because it complies with the stringent UL 4703 standard for PV wire as well as the UL 44 standard for interior wiring, it can be used seamlessly from the outside to the inside of a building in USE-2 (underground service entrance) applications, thereby streamlining installation and eliminating the need to create a junction between interior and exterior wiring or cabling. Second, as a one-material solution, it requires only one pass through the extruder (versus the industry norm of two) for simplified logistics, reducing cycle time and overall system cost.

Applications: Electrical cable and wire for wide-range of PV system installations.

Platform: Syncure Solar comes in two colours, natural and black, with comparable performance. Colour concentrates from PolyOne can also provide a range of colour options, allowing an easy, visual differentiation of wire and cable.

Availability: April 2012 onwards.

Product Reviews

Power-One

Power-One's second-gen micro-inverters have 96.5% efficiency rating

Product Outline: Power-One has launched the second generation of its micro-inverters, the improved Aurora Micro-0.3-I and Aurora Micro-0.25-I. The new version is claimed to offer a broader DC input voltage range with a maximum of 65Vdc, an extended MPP DC voltage range and an enhanced MPPT control with reduced DC input current ripple.

Problem: One of the main benefits of equipping each module with its own micro-inverter is that each panel benefits from a separate MPPT, which creates the optimum power curve for any light conditions. This minimizes efficiency losses not only from partial or temporary shading, but also from panel mismatching.

Solution: The Aurora Micro-0.3-I and Aurora Micro-0.25-I micro-inverters have a broader DC input voltage range with a maximum of 65Vdc, an extended MPP DC voltage range with and an enhanced MPPT control supporting a reduction in the DC input current ripple. As the devices are directly connected to each individual solar panel, there is no need for string sizing nor is there any constraint in terms of topology and orientation of the PV modules, not to mention the reduction of the effect of module aging. Moreover, Power-One's Aurora Micro micro-inverters offer many benefits to small rooftop installations, including the speed and ease of installation, increased control of individual panels and maximized energy harvesting for every installation – regardless of its size.

Applications: Residential PV installations.

Platform: The Aurora Micro micro-inverters include a rugged outdoor enclosure and HF isolation, allowing installation in any application which requires the grounding of either one of the DC input terminals.

Availability: June 2012 onwards.

Sika

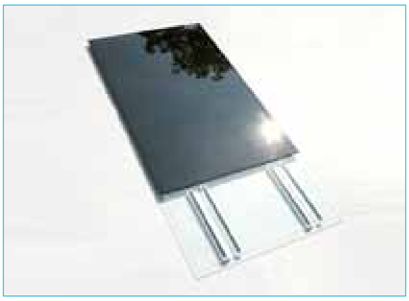

Sika claims a 40% reduction in module installation time

Product Outline: Sika has developed a two-component silicone-based bonding agent for fixing backrails or other mounting devices to PV modules. Sikasil AS-780 enables the PV module and system providers to move forward with the desired cost and material savings in fixation solutions with a secured long-term performance and simplified process integration.

Problem: Many new solutions for PV module backrails or point-holding systems have been introduced into the market as the focus on BOS costs increases. However, no bonding technology could provide all the characteristics to meet the demands for optimal in-process applications and long-term durability over decades of use.

Solution: Sikasil AS-780 is claimed to combine the long-term performance of a structural silicone used in the façade industry with the process ability of a high tack and high green-strength adhesive. The initial green strength and strength development is much higher than existing silicone technologies, according to the company, enabling bonding of the mounting devices without the need for any large buffer zones or pre-fixation devices. The company claims that savings in material and labour of up to 25% compared to common framing and mechanical installation systems can be achieved and a reduction in installation time by up to 40%

Applications: Fixation of point-holding systems and PV modules for residential and industrial rooftops.

Platform: Sikasil AS-780 meets the requirements of the most severe structural glazing standard for façades, the EOTA ETAG 002. This standard has a lifetime expectation of at least 25 years.

Availability: September 2012.

Siliken

Siliken's energyBox offers complete rooftop optimization solutions

Product Outline: Siliken has developed the energyBox PV system that offers more than 100 structural solutions for the design of any type of residential and industrial rooftop. The kit is scalable and therefore allows covering any rooftop size by connecting several energyBoxes in tandem. Siliken has also developed a 72-cell module, which yields the same power with 20% fewer modules, therefore saving components and cutting operating costs and installation time.

Problem: With continued module price declines making up less and less of the total BOS cost of a PV system, as well as falling feed-in tariffs, improving the yield while reducing BOS costs is required in order to enable expected customer ROI.

Solution: Developing the energyBox, Siliken selected each element to ensure the best performance, which results in a fully optimized system, both electrically and mechanically. The kit includes all of the necessary components for any residential and industrial rooftop PV installation, such as modules, structure and inverters as well as electrical components (AC/DC connection boxes, counter, cables and connectors). Siliken also developed an online configuration tool, enabling installers to design and optimize rooftop installations, using the energyBox kit.

Applications: Residential and industrial rooftops.

Platform: Siliken's 72-cell modules are available in Europe and the USA, which is in line with the company's policy to release its new technology in the countries in which it is active. The maximum power generated by the multicrystalline modules is 305Wp with +3/0% tolerance. They are UL, TÜV and Intertek certified for worldwide applications.

Availability: July 2012 onwards.

Solectria

Solectria's SGI 500XT utility-scale inverter claims 98% efficiency

Product Outline: Solectria Renewables has introduced the new SGI 500XT, a 500 kilowatt (kW), 600V DC inverter. The SGI 500XT is a 208V AC transformer-less, direct to medium voltage, utility-scale inverter. It is claimed to have the highest inverter efficiency at 98% (CEC) in the industry.

Problem: Utility-scale PV systems owners and operators not benefiting from conventional feed-in tariff payments, such as in North America, require fully optimized high-uptime operations to maximize yield.

Solution: Solectria Renewables' external transformer Smartgrid 500XT inverters are designed to maximize return on investment (ROI) through high efficiencies, easy installation, a wide operating voltage range and integrated customized options. The product boasts an industry-leading 98% CEC weighted efficiency, translating into increased energy generation for utility-scale PV systems.

Applications: North American-based utility-scale PV systems

Platform: The inverter is claimed to offer utility options such as real power curtailment, reactive power control, and voltage and frequency ride through, providing the lowest night-time tare loss in the industry to date, according to the company. Safety listings and certifications include: UL 1741/IEEE 1547, IEEE 1547.1, IEEE 62.41.2, IEEE 62.45, IEEE C37.90.2, CSA C22.2#107.1, FCC part 15 B (Certification Agency: ETL).

Availability: July 2012 onwards. US market only.

Sputnik Engineering

SolarMax 8MT2 string inverter from Sputnik, designed for smaller PV plants

Product Outline: Sputnik Engineering has added to its SolarMax MT series by developing the new 8MT2 string inverter with an output power of 8kW. The three-phase inverter is said to be particularly suitable for flexible use in the field for detached houses and multiple dwellings. The SolarMax MT series was displayed at Intersolar Europe 2012.

Problem: For private domestic plants, the module strings must often be distributed in an asymmetrical manner owing to multiple orientation roofs. This normally results in one large and one or several small module fields. Quite often, module areas are also partially shadowed by roof architecture or antennae.

Solution: The new 8MT2 string inverter comprises two trackers that are designed asymmetrically. This way, for example, the tracker with the higher input current can be connected to a large solar generator with uniformly oriented modules, thus optimizing the main yield of the plant. For this, there are two string connections. The second tracker, with only one string connection is, used for smaller module fields and/or module fields that are partially shaded or orientated differently. The SolarMax MT inverters come with efficiencies of up to 98%. The light and compact design, as well as the easily accessible connections, allows for quick and simple installation.

Applications: Detached houses and multiple dwellings

Platform: The SolarMax MT inverters meet all currently applicable standards and grid connection directives and, thus, are suitable for use in numerous European (Germany, Italy, France, Austria or Switzerland) and non-European countries.

Availability: Provisionally available in the third quarter of 2012 onwards.

REC

REC's Peak Energy Plus Series module is first to use back-side passivation technology

Product Outline: Renewable Energy Corporation (REC) has made commercially available its REC Peak Energy Plus Series module, based on cells with back-side passivation technology, which improves module performance by enhancing the solar cell's response to red light.

Problem: Diminishing feed-in tariff rates are shifting the need towards higher yielding modules to provide adequate returns on investment. Maximizing yield through low-light conditions, typically in early morning and early evening cycles, is important.

Solution: The introduction of back-side passivation increases cell efficiency in two ways. First, the backside passivation layer reflects light that has travelled through the cell without generating electrons and reached the back side. The reflected light will pass through the cell a second time, which generates additional current. Second, the layer passivates the crystal defects associated with the back surface of the silicon wafer better than a conventional cell. This means that electrons that are generated near the back side of the cell are less likely to be captured and lost. The new module is claimed to perform well in low-light conditions and at high temperatures.

Applications: Residential and commercial rooftops.

Platform: The new REC Peak Energy Plus Series delivers an additional 5W compared to the earlier generation product. The module has a nominal power output in watt classes ranging from 245Wp to 255Wp, with higher watt classes possible in the future. It is certified by TÜV to IEC 61215 and IEC 61730 standards, passing damp heat, mechanical load, thermal cycling and humidity freeze tests.

Availability: June 2012 onwards.

Performance characterization and superior energy yield of First Solar PV power plants in high-temperature conditions

N. Strevel, **L. Trippel** & **M. Gloeckler**, First Solar, Perrysburg, Ohio, USA

ABSTRACT

Like all semiconductor photovoltaic devices, cadmium telluride (CdTe) modules have a characteristic response to temperature changes. This paper describes the effects of the temperature coefficient of power, using operational system data to quantify the First Solar CdTe technology energy-yield advantage over typical crystalline silicon technology in high-temperature conditions. This paper also describes the underlying mechanisms of initial stabilization and long-term degradation that influence module efficiency. The processes used to characterize and rate module power output, given these effects, are further discussed. First Solar's significant experience in building and operating power plants in high-temperature conditions, along with associated system performance data and accelerated lab test data, is reviewed to substantiate the warranty considerations and long-term capability of power plants using CdTe PV modules.

Introduction

First Solar has successfully designed, built and operated utility-scale solar power plants in many diverse climates. In high-temperature climates, both initial and long-term module performances are critical to lifetime energy production. The purpose of this paper is to explain the fundamentals of high-temperature operation that influence energy output, module efficiency and module reliability over the power plant's life. First Solar cadmium telluride (CdTe) technology, like all PV modules, has device-specific characteristics which drive observable output changes over time that are taken into account during module rating and future energy predictions.

Instantaneous response – temperature coefficient

First Solar's thin-film CdTe solar modules have a proven high-temperature performance advantage over typical crystalline silicon solar modules. The leading contributor to this performance advantage is the lower temperature coefficient of CdTe semiconductor material, which delivers higher energy yields at elevated temperatures. Module performance has been thoroughly characterized over time to establish power ratings and energy prediction models that are used to set system performance expectations in various climate conditions. PV modules receive their nameplate power rating at standard test conditions (STC) of 1000W/m^2 solar irradiance, AM 1.5 and 25°C module temperature.

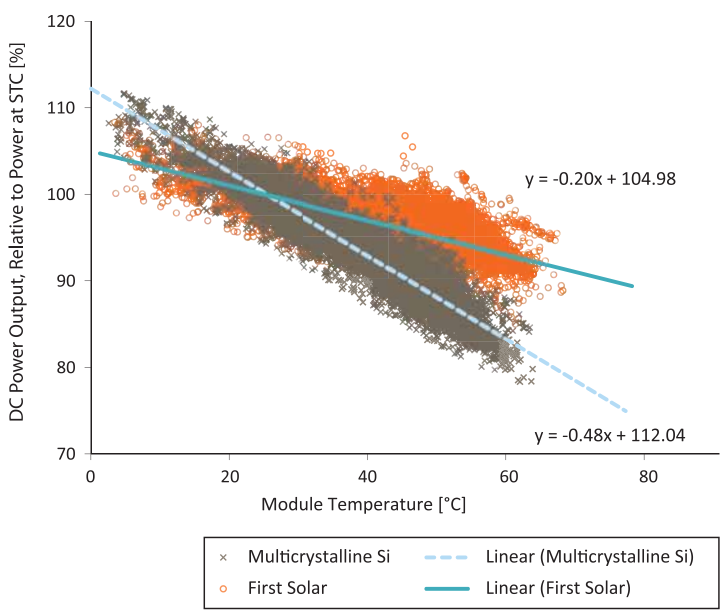

Figure 1. First Solar and multicrystalline DC power output vs. temperature [4].

> "As module temperature rises, all PV semiconductor technologies incur increasing losses in performance."

As module temperature rises, all PV semiconductor technologies incur increasing losses in performance, primarily due to the drop in open-circuit voltage of the PV cell. The temperature coefficient expresses the rate of change of power output as a function of module operating temperature. Crystalline silicon solar modules typically have a temperature coefficient of –0.45 to –0.5% per degree Celsius [1,2]. First Solar's CdTe PV modules have a temperature coefficient of –0.25% per degree Celsius, resulting in about half the incremental power loss compared to conventional solar modules [3]. Fig. 1 shows the DC power of two PV systems consisting of CdTe and multicrystalline silicon (mc-Si) modules. As module temperatures rise above 25°C, CdTe solar modules experience an increasing performance advantage.

In a typical region of high solar irradiance, module temperatures in peak operating conditions often reach 65°C (40°C above STC) or higher. At 65°C, the power output of conventional solar modules is reduced by up to 20%, while the power output of First Solar modules is reduced by approximately 10%. For example, on a day with an ambient temperature of 37°C and a module temperature of 65°C, a 50 megawatt peak (MWp) multicrystalline silicon solar system will produce approximately 40 megawatts (MW) at 1000W/m^2 irradiance, while an equivalent First Solar power plant will produce approximately 45MW, resulting in 10% more power output. As this effect continues over time for a typical hot-climate power plant, the result is an increase in annual energy output of 5–9% for the same nameplate-rated plant. Consistent with this performance range, a comparison performed by a major system integrator concluded that, in southern Italy, CdTe modules outperformed mc-Si in annual specific yield by 5.7% [5]. Energy prediction simulations performed using industry-standard tools such as PV SYST further illustrate the behaviour.

"The majority of solar energy production occurs when module cell temperature is greater than ambient temperature."

The majority of solar energy production occurs when module cell temperature is greater than ambient temperature. Fig. 2 shows the annual distribution of ambient temperature and of the temperature measured on the back surface of a solar module for an operational First Solar power plant in the US desert Southwest. The figure shows the frequency distribution of module temperature over a full year period. Note that the distribution of ambient temperature ranges from 0 to 45°C, and is centred on approximately 25°C, while the distribution of back-surface temperature ranges from 0 to 70°C, and is centred on approximately 40°C. The back-surface temperature is a good approximation of the actual cell temperature, and studies have shown that cells typically run 3°C warmer than back-surface temperatures for glass–glass laminate construction [6].

The majority of solar energy production occurs when the module operating temperature is much greater than 25°C. Fig. 3 overlays the distribution of energy production at high (≥ 25°C) and low (<25°C) temperatures for the same operational PV plant described in Fig. 2. The availability of irradiance represented by the energy production in Fig. 3 indicates that the relevant energy-weighted average temperature is approximately 45°C.

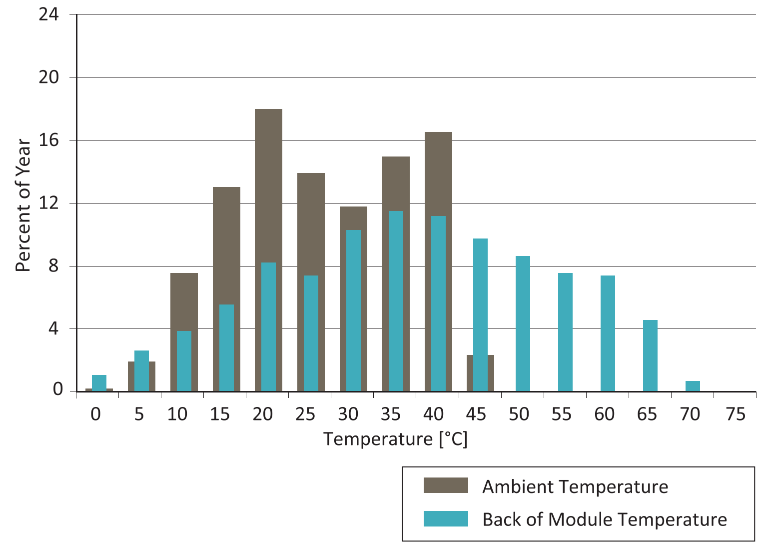

Figure 2. Distribution of ambient and back-surface temperatures, measured in a First Solar constructed US desert Southwest array.

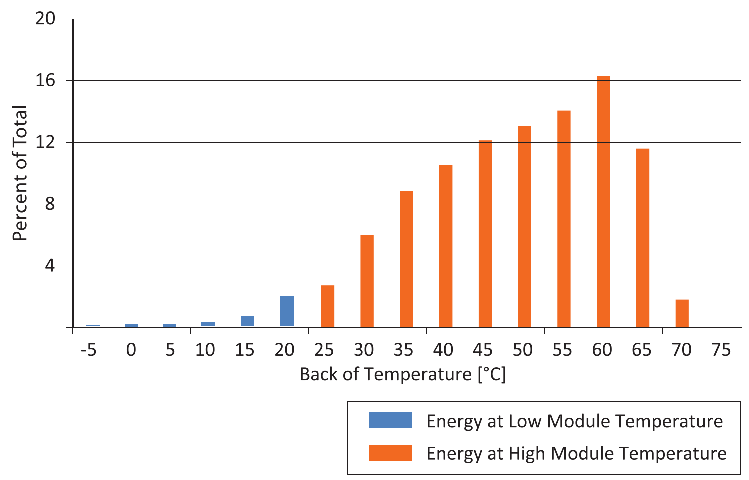

Figure 3. Distribution of power production vs. back-surface module temperatures [7].

"Solar power plants in high-temperature climates spend the majority of their operational lives above 25°C, where CdTe modules have a proven performance advantage over crystalline silicon solar modules."

For this operational First Solar power plant in the US desert Southwest, 94% of total energy was produced when the panels were operating at module temperatures of 25°C or higher. It is concluded that solar power plants in high-temperature climates spend the majority of their operational lives above 25°C, where CdTe modules have a proven performance advantage over crystalline silicon solar modules, producing more kilowatt hours of energy per installed kilowatt of capacity. The fundamental advantage of the low temperature coefficient of thin-film CdTe modules in high-temperature climates results in more energy output and therefore higher financial returns for system owners.

Short-term response – initial stabilization

Most PV technologies exhibit some form of non-linear initial efficiency loss, for several reasons. P-type monocrystalline silicon may experience light-induced degradation

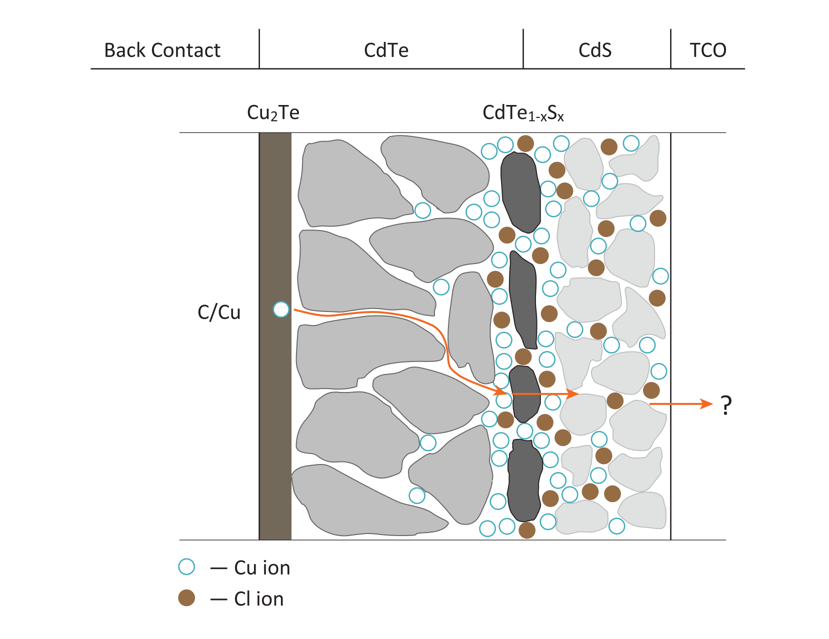

Figure 4. Copper migration through a CdTe device model (after Cahen et al. [10]).

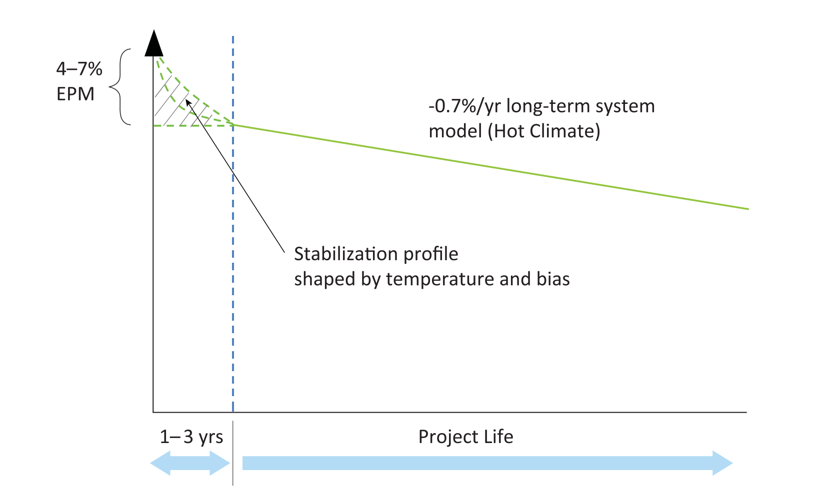

Figure 5. First Solar CdTe PV system degradation profile.

of approximately 2.5 to 3.5%, which varies as a function of the oxygen content of the wafers [8]. This is clearly reflected in tier 1 crystalline silicon manufacturers' warranties that discount module power output by 3% in year one [9]. Thin-film CdTe modules exhibit a similar phenomenon, but as a result of a different fundamental mechanism. The CdTe semiconductor device stabilizes because of the grain boundary diffusion of copper (Cu) from the back contact [10]. Although some details of the mechanisms remain elusive owing to the nanoscopic nature of the changes, it is generally accepted that Cu diffuses from a Cu-rich back-contact area through the CdTe absorber along grain boundaries and can accumulate at the CdTe/cadmium sulphide (CdS) interface. This is graphically depicted in Fig. 4, reproduced from Cahen et al. [10]. First Solar has optimized its product through the reduction and tighter control of the Cu introduced into the device and by reducing the sensitivity of the CdTe/CdS interface to the presence of Cu.

The process of diffusion can be accelerated in the laboratory by performing accelerated life tests under increased temperature and cell bias. At elevated temperatures it is observed that the longer the device is operated above its maximum power point voltage, the greater the efficiency loss will be. The mechanism can be explained by the built-in electric field of the solar cell opposing the thermal diffusion of ionic Cu, the applied bias effectively reducing the electric field strength, and, hence, enabling accelerated diffusion to the heterojunction [11]. A similar increase in efficiency loss because of an increased cell bias has been observed in accelerated life tests. When installed modules experience prolonged open-circuit conditions, cell bias is increased compared to the typical levels experienced when operating in normal, maximum power point conditions. This behaviour drives First Solar's recommendations that module open-circuit exposure time be minimized.

The magnitude of this initial efficiency loss is approximately 4–7% within the first one to three years, depending on climate and system interconnection factors, as shown in Fig. 5. High-temperature climates tend to accelerate this initial stabilization, while moderate climates tend to prolong this behaviour, so that it becomes difficult to distinguish from long-term device degradation.

To compensate for this initial efficiency loss, First Solar reduces the end-of-line measured module power to a lower nameplate power, which represents expected field-stabilized module power. To accomplish this, First Solar utilizes a proprietary module-rating process that applies an engineered performance margin (EPM). The EPM takes into account the expected initial stabilization derived from many megawatts of multi-year field exposure in hot climates. The EPM is applied at the end of the manufacturing line, after the simulator flash test and before module labelling.

"To compensate for this initial efficiency loss, First Solar reduces the end-of-line measured module power to a lower nameplate power, which represents expected field-stabilized module power."

On the basis of accelerated reliability and performance test data, combined with an historical evaluation of actual field performance, First Solar's energy prediction recommendation is to use nameplate module rating for the first year of energy prediction and to apply long-term degradation rates starting in the second year of operation. While the energy production in year one for a well-constructed system is likely to exceed nameplate-based energy prediction (because of the EPM), First Solar recommends maintaining nameplate-based energy prediction for a project's energy and financial pro forma in year one.

Long-term response – degradation

Starting in the second year of operation and for each year thereafter, First Solar recommends modelling system degradation rates of –0.5%/year in

temperate climates and –0.7%/year in high-temperature climates. First Solar has thoroughly studied the two primary drivers of long-term module degradation – device stability and package integrity. The combined evaluation of these two primary long-term behaviours is used to establish long-term modelled degradation rates.

"The copper diffusion mechanism, which drives the initial stabilization of the module, is also the primary contributor to the long-term degradation behaviour of the module."

Power Generation

The copper diffusion mechanism, which drives the initial stabilization of the module, is also the primary contributor to the long-term degradation behaviour of the module. On the basis of accelerated long-term light soaking and field data, it is observed that the rate of copper diffusion slows significantly as the device stabilizes in the first one to three years, and continues to drive a small sub-linear degradation of module efficiency year over year thereafter. The linear assumption is conservative, considering the underlying diffusion mechanisms, but in agreement with available field and accelerated life testing data.

A National Renewable Energy Laboratories (NREL) study captured in Fig. 6 provides some indication of observed degradation rates in multiple PV technologies' long-term operation. It also clearly shows that most technologies have demonstrated improvements in long-term observed degradation rates when comparing older vintage products built prior to the year 2000 ('Pre') with newer products built after the year 2000 ('Post'). Observed degradation rates for thin-film CdTe technology product built after 2000 are distinctly better than other thin-film technologies, and comparable to traditional crystalline silicon technologies.

"After almost two decades of monitoring, NREL confirms the excellent reliability of First Solar's module technology, with no module failures in system operation."

The long-term performance of First Solar thin-film CdTe modules can be more specifically observed by examining the 17-year study performed by NREL, which reports a long-term degradation-rate linear fit of –0.53%/year (Fig. 7), based on the performance of a system in Golden, Colorado, USA [13]. After almost two decades of monitoring, NREL confirms the excellent reliability of First Solar's module technology, with no module failures in system operation.

First Solar has one of the largest monitored PV solar installation databases in the world, with more than 270MW (AC) worldwide and expanding to well over 1GW (AC) in the next few years. Fig. 8 shows the performance data extracted from these systems for a variety of sites ranging from a few kW to tens of MW.

The predicted energy ratio (PER) is the lifetime ratio of actual energy produced to the energy predicted. The PER substantiates First Solar's field performance record and validates First Solar's accuracy in predicting field performance. Degradation guidance of –0.5%/year in temperate climates and –0.7%/year in high-temperature climates is modelled

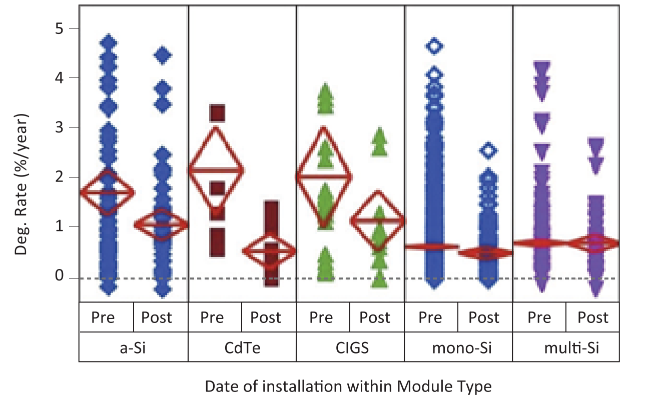

Figure 6. NREL study of degradation rates of various PV technologies [12].

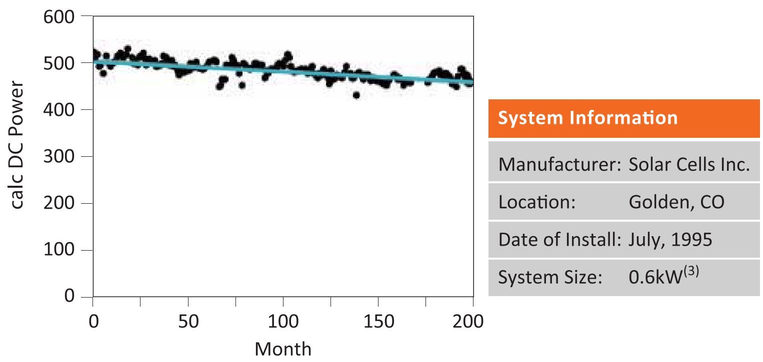

Figure 7. NREL January 2012 study of a First Solar system installed in 1995.

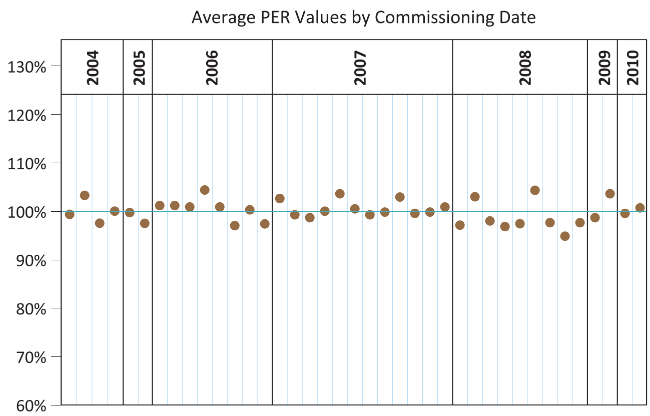

Figure 8. Predicted energy ratio for 270MW of installed systems using First Solar modules: >270MW monitored installations base, including >130MW of hot-climate deployments.

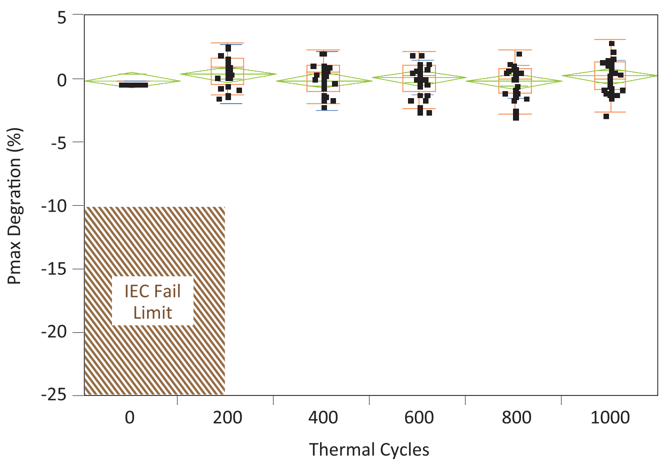

Figure 9. TC1000 testing results for First Solar modules (5X IEC TC200).

into predictions. As shown in Fig. 8, actual performance is close to 100% of the P50 prediction energy [14,15]. This indicates system performance consistent with First Solar's degradation model and supports the conclusion that First Solar can accurately predict system performance for power plants using its thin-film CdTe modules.

The reliability of module construction, which protects the active semiconductor device, is critical to maintaining reliable long-term product performance. First Solar conducts a variety of test sequences to ensure the longevity of the module material, encapsulation and connections. These tests consist of standardized certification protocols, extended versions of certification-based protocols, and proprietary accelerated life and stress tests. For example, one particularly applicable test for high-temperature climate performance is module thermal cycling (TC). This test cyclically exposes modules in a controlled environmental chamber to extreme temperatures from –40°C to +85°C. The intention is to stress connections in the module and compatibility of different materials' thermal expansion properties to ensure that the module maintains its power output and package integrity. The standard IEC-defined protocol for this test is 200 cycles (TC200) [16], and First Solar maintains successful IEC 61646 certification for the standard test protocol. To provide additional confidence in long-term reliability performance, First Solar modules are further evaluated in several tests which significantly extend these standard IEC protocols. As an example, a random population of 28 modules undergoes TC1000 testing consisting of five times more temperature cycles than the standard test protocol. Fig. 9 demonstrates that First Solar power output and electrical integrity remain effectively unchanged.

> "First Solar modules are further evaluated in several tests which significantly extend these standard IEC protocols."

Independent third parties, including NREL, have observed and validated First Solar's long-term performance. Reputable global independent engineering firms have validated First Solar's energy prediction model, and long-term performance and gigawatts of projects using First Solar technology have been successfully financed.

Warranty accruals in high-temperature conditions

High-temperature conditions directly affect warranty failures of PV modules and balance-of-system components. Elevated temperatures accelerate physical processes, resulting in increased stress on conductors, connectors and other electrical equipment. Heat also has a negative impact on stress corrosion cracking in glass [17], polymer creep [18] and impurity diffusion processes [19]. This is the case for all PV technologies.

As previously discussed, high-temperature conditions also influence the initial stabilization and degradation behaviour of First Solar CdTe modules. The EPM is applied to First Solar modules to account for this temperature-driven behaviour and provide appropriate rating with regard to First Solar performance modelling and warranty constructs. In consideration of all these factors, First Solar's comprehensive reliability and performance testing, combined with actual field performance in high-temperature conditions, predicts that warranty failure rates in high-temperature climates should be slightly higher than in temperate climates. In anticipation of increasing sales in high-temperature locations, First Solar proactively increased its warranty reserve by one percentage point to ensure sufficient reserves to cover slightly higher expected failure rates. As other PV companies gain experience in designing, building and operating utility-scale solar power plants in high-temperature climates, it is likely that higher warranty reserves in these conditions will become more common.

Conclusions

First Solar has characterized module performance in hot climates and has addressed many of the challenges related to deploying PV solar power plants in high-temperature conditions:

- Solar modules deployed in high-temperature climates operate most of the time at module temperatures above 25°C, where the better temperature coefficient of CdTe relative to crystalline silicon results in higher energy yield.
- First Solar accounts for initial stabilization in its module efficiency by applying an engineered performance margin in the nameplate module power rating so that it represents expected field-stabilized efficiency.
- First Solar's energy prediction recommendation is to use nameplate module rating for the first year of energy prediction and to apply long-term degradation rates starting in the second year of operation. First Solar's long-term degradation modelling recommendation is –0.5%/year for moderate climates and –0.7%/year for hot climates.
- Long-term degradation is substantiated by an understanding of physical mechanisms and is reinforced by a combination of third-party evaluation, field data comparisons to predictions, and accelerated lab testing.
- The detailed performance characteristics of First Solar's PV modules – including temperature coefficient, initial stabilization, EPM and long-term degradation – are critical inputs to an accurate energy prediction model for power plants in high-temperature conditions.
- First Solar has significant experience in building and operating solar plants in high-temperature conditions and proactively increased its warranty reserve to compensate for slightly increased expected warranty failure rates in high-temperature conditions.

References

[1] Yingli Solar 2011, YGE 285 Series Datasheet, 1.

[2] Solar World 2010, Sunmodule SW 130/140 poly R6A Datasheet, 2.

[3] First Solar 2012, First Solar FS Series 3 Datasheet, 2.

[4] First Solar Competitive Array 2006–2007, Perrysburg, Ohio, USA.

[5] Collins, F. 2010, "Field performance of thin-film", *PHOTON 2nd Thin-Film Conf.*

[6] King, D.L., Boyson, W.E. & Kratochvil, J.A. 2004, "Photovoltaic array performance model", Sandia National Laboratories, Albuquerque, New Mexico.

[7] First Solar US Desert Southwest Array Data.

[8] Munoz, M.A., Chenlo, F. & Alonso-Garcia, M.C. 2010, "Influence of initial power stabilization over crystalline-Si photovoltaic modules maximum power", *Progr. Photovolt.: Res. Appl.*

[9] Trina Solar 2011 (July), Trina Solar Limited Warranty, 2.

[10] Cahen, D., Hodes, G. & Gartsman, K. 2000 (August). "Overcoming degradation mechanisms in CdTe solar cells", Second Annual Report (prepared under Subcontract No. AAK-8-17619-15), Weizmann Institute of Science, Rehovol, Israel.

[11] Corwine, C.R. et al. 2004, "Copper inclusion and migration from the back contact in CdTe solar cells", Department of Physics, Colorado State University, USA [available online at www.physics.colostate.edu/groups/photovoltaic/PDFs/CuMigrAsPub.pdf].

[12] Jordan, D.C. & Kurtz, S.R. 2011 (August), "Photovoltaic degradation rates – An analytical review", National Renewable Energy Laboratory (NREL).

[13] NREL & SCI (Solar Cells Inc.) 2012 (April), "NREL module performance report", First Solar Application Note PD-5-615.

[14] First Solar. "Series 3 recommended parametric descriptions for PVSYST", First Solar Application Note PD-5-301-03 MS.

[15] First Solar. "System parameter specs for PVSYST simulations", First Solar Application Note PD-5-301-SS.

[16] IEC 61646 (May 2008), "Thin-film terrestrial photovoltaic (PV) modules – Design qualification and type approval", International Electrotechnical Commission, Edn 2.

[17] Wiederhorn, S.M. & Bolz, L.H. 1970, "Stress corrosion and static fatigue of glass", Institute for Materials Research, National Bureau of Standards, Washington, DC.

[18] Miller, D.C. et al. 2010, "Creep in photovoltaic modules: Examining the stability of polymeric materials and components", National Renewable Energy Laboratory (NREL).

[19] Baetzner, D.L. et al. 2003, "Study of spatially resolved impurity diffusion in CdTe solar cells using voltage dependent quantum efficiency", Thin Film Physics Group, Zurich.

About the Authors

Nicholas Strevel is a technical sales engineer at First Solar, specializing in PV module technology and performance. He has worked in the thin-film PV technology field for six years, in module manufacturing, application engineering and business development. Nicholas has a BSME in mechanical engineering from Michigan State University, and also studied at the Rheinisch-Westfälische Technische Hochschule Aachen.

Lou Trippel is module product line director at First Solar, where he leads module product management and technical sales and is responsible for First Solar's PV module product life cycle management program. He has a bachelor's degree in electrical engineering from the University of Dayton and a master's degree in technology management from Stevens Institute of Technology. Having previously held several positions on First Solar's product management and technical sales teams, Lou has over a decade of experience in new product development and product management.

Markus Gloeckler is vice president of advanced research at First Solar. He received a Ph.D. in solid-state physics from Colorado State University and a bachelor's degree from the University of Applied Sciences Regensburg, Germany. Markus collaborated at Colorado State with several members of the US thin-film partnership program and the National Renewable Energy Laboratory. Since joining First Solar, he has had responsibilities in the areas of product characterization, modelling, efficiency improvement and the physics of reliability.

Enquiries

First Solar
Tel: 1-877-850-FSLR (3757)
Email: info@firstsolar.com

Market Watch

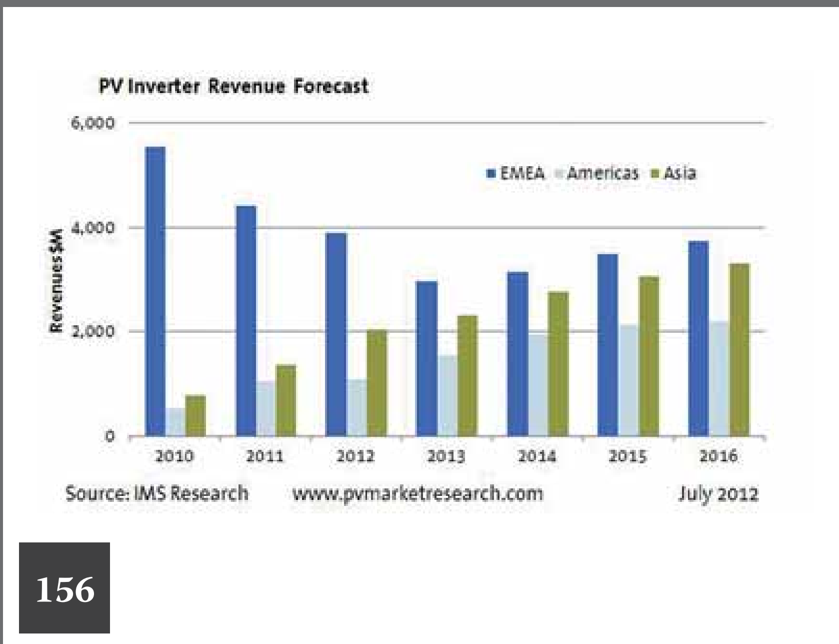

Photovoltaics market booming in USA; 1.7GW installed in first six months

IMS Research expects US PV installations to reach nearly 4.3GW in 2012.

According to the latest report from IMS Research, PV installations in the USA in the first half of the year have reached 1.7GW, a growth of over 120% compared to the same period a year ago. With utility-scale projects typically back-end loaded, the market research firm expects installations to reach nearly 4.3GW in 2012. As a result of the massive increase in US demand, the country is expected to become the third largest PV market in 2012, accounting for 40% of new capacity growth. In its 'Q3 PV Demand Report,' IMS Research predicted that the boom in the USA is expected to support the global PV market to grow by at least 3GW in 2012, despite the European market declining by 3GW in 2012, which is being driven by FiT cuts in key markets, namely Germany and Italy. Indeed, global demand is predicted to actually accelerate in the second half of 2012, driven by China, Japan and the Americas. IMS Research predicts installations will hit a new half-year record of almost 18GW in the second half of 2012. With installations expected to have exceeded 13GW in the first half of 2012, the global PV market is expected to exceed at least 31GW by the year end, up from approximately 27GW in 2011.

Financial and Business News Focus

CASM claims Chinese imports to USA down 60%

The Coalition for American Solar Manufacturing (CASM) has issued a release stating that Chinese solar imports were down by 60% since June 2011, totalling US$99.6 million from US$241.5 million. CASM cites the US Department of Commerce's US Imports of Merchandise database as its source, stating that this decline reflects the market's rising recognition of the costs, risks and uncertainties associated with importing Chinese solar cells and panels. While the year-on-year decrease is partly due to sharply falling module prices from 2011 to 2012, June 2012 imports of Chinese solar cells and panels were also down 20% from the previous month's total of US$124.1 million, which CASM attests was fully affected by both preliminary anti-subsidy duties. However, despite three months of declines, Chinese import levels for all of 2012 are still ahead of last year's record pace. For the first six months of this year, the total value of Chinese cell and panel imports reached US$1.32 billion, up from US$1.23 billion for the same period of 2011, an increase of 7.3%, according to the Commerce data. The increase is even more significant because dumped and subsidized Chinese pricing has lowered the per-watt average import values so dramatically in 2011 and 2012.

NPD Solarbuzz: Asia Pacific set to deliver 5.3GW of PV installations in fourth quarter

The expected geographical shift in PV demand away from Europe to the Asia Pacific region is turning into a surge, according to new research featured in the NPD Solarbuzz 'Asia Pacific Major PV Markets Quarterly.' Year-on-year growth is expected to be around 80% but 50% of that growth, which is equivalent to 5.3GW, is expected to occur in the fourth quarter of 2012. Key markets driving growth include China, India and Japan.

NPD Solarbuzz said that the APAC region had already experienced rapid growth, notably in the second quarter of this year, with 1.4GW installed, greater than 60% growth, year-on-year.

In particular, PV market demand in China grew by over 300% in Q2'12 to reach 0.6 GW, stimulated by deadline requirements for the completion of Golden Sun PV projects. The market research firm is already projecting demand in the Asia Pacific region is forecast to decline to just 2.1GW in the first quarter of next year as seasonal soften returns.

Although the European market is expected to tail off in the second half of the year, the European PV market grew 32% to 8.5GW installed, compared to the first half of 2011. However, incentive reductions in Germany, Italy and other major European PV markets continue

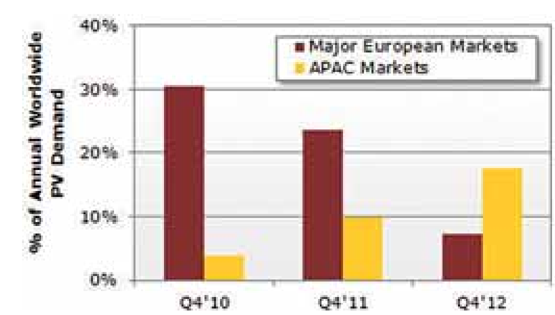

NPD Solarbuzz highlights demand shift from Europe to Asia in 2012.

to erode the demand-share previously commanded by these former PV market leaders. Growth within Europe is expected to shift to emerging markets during the next couple of years, including Austria, Denmark, Israel and various countries in the east and southeast of Europe.

Third-party-owned solar generated over US$1B in growth for CA since 2007 according to Sunrun report

Sunrun and PV Solar Report released a new study, which found that third-party-owned solar has delivered over US$1 billion to the California economy since 2007. The value was said to be determined by totalling the contract value for each third-party-owned solar installation in the state. Sunrun is lauded with starting the solar power service model for home solar in 2007 and is said to be the market leader with over US$1.5 million in solar equipment installed every day.

According to the report, the number of Californians who chose solar power service over cash purchase so far this year is 30 times greater than the total number in 2007. Sunrun and PV Solar Report state that the US$1 billion in funds went directly to the state's local businesses and communities.

France's cumulative PV capacity reaches 3.28GW

Cumulative installed PV capacity in France reached 3.28GW in the second quarter of 2012, up by 9.2% compared with the first quarter of this year, according to statistics from French grid operators ErDF and EDF SEI.

During the second quarter of this year, 254MW of PV capacity was connected in mainland France, down by 27.5%. The statistics indicate that installed PV capacity has been falling since September 2011. In the fourth quarter of 2011, 372.3MW of installed capacity was connected and in the first quarter of 2012, 350.7MW of PV capacity was installed.

In French territories outside of the mainland including Corsica, 362MW of installed PV capacity was connected during the second quarter of 2012, an increase of 6.8%.

Despite the declining figures in mainland France, France's new president, Francois Hollande, has been pushing its plans to increase renewable energy generation. At the end of July, Delphine Batho, the new minister for ecology, sustainable development and energy, announced the results of two tenders for solar plants which are expected to generate a cumulative investment of nearly €1 billion within the next two years.

IMS Research: Chinese government doubles installation target to rescue domestic PV manufacturers

China's PV manufacturing base saw a major setback in the first and second quarters of 2012, with a severe slump in exports, sparking the government to step in and further raise its PV installation target to 50GW, according to the latest quarterly report on China's PV market from IMS Research. Tough competition in the global market place, vast oversupply and falling prices has put Chinese manufacturers' balance sheets under huge pressure and China's government has responded by more than doubling its long-term installation target from 20 to 50 GW by 2020.

According to IMS Research, contrary to US and EU supplier accusations, Chinese PV suppliers have continued to suffer along with the entire global supplier base amid highly competitive market conditions. Challenging conditions in the first half of 2012 and a bleak outlook in many major markets following incentive revisions and an on-going trade war in the USA and Europe have resulted in production stalling. Although a small number of manufacturers have been able to maintain reasonable utilization levels, a large number of polysilicon fabs remain closed, meaning that average polysilicon production utilization in China fell below 50% in the second quarter of 2012.

At the beginning of July, Bloomberg New Energy Finance published figures demonstrating China securing hundreds of millions in dollars of financing. In the second quarter of 2012, China saw a surge in investment to US$18.3 billion, up 92% from the previous quarter. This in turn has diversified the range of products being sold into the market.

IMS Research forecasts that PV installations in China will be a key driver in the growth of the global PV market. Installations are expected to grow quickly in the second half of 2012, with over 10GW to be installed over the next two years.

Pike reports global installations of renewable distributed energy to reach 63.5GW per year by 2017

In its new research report, 'Renewable Distributed Energy Generation', Pike Research has estimated that annual worldwide installations of renewable distributed energy generation will almost triple between 2012 and 2017. Pike speculates that by 2017, 63.5GW per year will be reached, with almost 232GW of distributed renewable energy added over the five-year period.

Currently, distributed renewable installations represent less than 1% of total global electricity generating capacity. However, over the next five years, the tide is set to change and Pike notes that the majority of the new installations will be solar PV. Pike notes that worldwide PV module production capacity reached around 50GW by the end of 2011 and it expects that new solar additions will total 210GW between 2012 and 2017.

Global PV monitoring market will reach 23GW in 2012 and 50GW in 2016, report forecasts

The global PV monitoring market is predicted to reach 23GW in 2012, according to the Global PV Monitoring 2012 report published by GTM Research.

Moreover, the market — which includes inverter suppliers, independent monitoring vendors and project developers that integrate hardware and software to manage PV systems — is expected to further expand to reach a monitored PV capacity to almost 50GW by 2016, indicating robust opportunities for existing and new suppliers. At present, the report reveals, European independent monitoring vendors lead the market.

Monitoring technology is a key aspect of a PV plant's successful operation. However, according to GMT Research, the market has received a lack of attention because of its relatively low impact on the up-front cost of a PV system.

IMS Research: micro-inverter firms fastest growing as PV inverter market to surpass US$7 billion

The latest global PV inverter market report from IMS Research paints a mixed business environment for the sector that has more than 150 active suppliers. Although having defended reasonably well against price declines, compared to the rest of the supply chain, the market research firm is forecasting inverter sector revenues to only increase by 3% in 2012, while shipments increased nearly 25%.

The report noted that the global PV inverter market actually shrank marginally in terms of revenues in 2011, but shipments increased by more than 12%. This was a bonus for the inverter market due to an inventory overhang from the prior year.

On a regional basis, the PV inverter market in Europe is expected to continue to lose market dominance as key markets such as Germany and Italy experience PV system installation declines from 2013 onwards on the back of FiT reductions.

The market is still growing around the world but will become more fragmented, according to the market research firm. Global shipments of inverters are forecasted to increase at a double-digit rate over the next five years, with revenues exceeding US$9 billion by 2016.

With respect to suppliers and their market share rankings little has changed over the last few years, though market leader, SMA Solar Technology, continues to see its share erode. Slight gains and losses were experienced by the other major players such as Power-One, Kaco, Fronius and RefuSOL.

According to the report, the biggest market share gainers last year were those suppliers outside of the top 10 rankings, showing that the industry may not be consolidating just yet, according to IMS Research. Start-ups Enphase Energy and SolarEdge were two of the biggest market share gainers in 2011, whilst considerable gains were achieved by Advanced Energy and Emerson.

IMS Research: PV inverter revenue forecast.

World PV Inverter Supplier Rankings

Company Name	2009 Rank	2010 Rank	2011 Rank
SMA Solar Technology	1	1	1
Power-One	4	2	2
Kaco	3	4	3
Fronius	2	3	4
REFUsol	9	5	5

(Full market shares & rankings shown by country and power class in report)

Source: IMS Research www.pvmarketresearch.com July 2012

IMS Research: PV inverter supplier rankings.

PV equipment supplier rankings in 2012 dictated by accounting rules

According to NPD Solarbuzz, when final numbers are counted for capital equipment suppliers to the PV industry for 2012, the data will reveal a somewhat misleading picture. And one that was certainly not on the radar of any PV equipment supplier just 12 months ago.

This rather confusing outcome, according to Finlay Colville, Vice President of NPD Solarbuzz, is not only a consequence of the displaced euphoria that arose from overambitious spending in 2010-2011, but is also providing the backdrop for hesitancy in guidance as order intake levels remain highly depressed.

The basis of this predicament faced by all PV equipment suppliers is simple: equipment suppliers revenues today are not based upon capex driven by end-market demand pull. Rather, they are dominated by an accumulation of deferred revenues being recognized from orders placed up to 18 months ago and shipments being effected under customers' contractual obligations.

Therefore, rankings for 2012 are likely to be more a consequence of revenue-recognition accounting rules, rather than serving any addressable market created by new capacity required by the industry during 2012.

According to the market research firm, customer bullishness and access to capital often misled equipment suppliers into believing that their products or technologies were one step away from volume mass deployment and repeat-order frenzy. For experienced suppliers that served various technology-segment markets, this PV blip was treated with guarded caution: for equipment suppliers whose ascendency was underpinned by PV industry expansion only, growing backlogs created a virtual benchmark for future operating performance and often accelerated tool manufacturing expansion plans.

By mid-2011, backlogs of PV equipment suppliers had reached pandemic levels. At first, the goal was year-end revenue-recognition. Then into 2012, the focus turned to delivery under contract and accounts receivables for tooling shipped by year-end, but not recognized then as revenues. The combination of shipment (upon tool completion) and deferred delivery schedules has now become the basis of the 2012 confusion.

New order intake remains at chronic levels and any notion of this changing before year end is rapidly becoming less likely with the news that even the industry leaders are running fabs at 50-60% utilization rates — based only upon lines being classified by them as operating (or ramped) capacity today. Upgrade or retrofit orders are few and far between and will remain this way for several quarters until cost reduction has been fully exhausted across the value chain and a revised PV technology roadmap emerges in 2013. Of course, it would not be the PV industry if new players were not entering the arena, but the entrants here can be counted in low single-digits through 2012 — some two orders of magnitude lower than during 2010.

NPD Solarbuzz said that the focus for now is purely on equipment suppliers backlog levels and how much can be recognized as revenue during 2012. Or how much is finally taken off the books because the risk of delivery within a 12-month period is too high to count as a 'real' purchase order for future tool delivery. And for many of these cases, customer deposits may be the only salvation to fall back upon.

Europe

Austria
Renewable energy sources are dominant in the Austrian electricity production structure. About 70% of the total generation (which covers more or less the total electricity demand of Austria) is produced with renewable sources, about 56% with large hydro power (>10MW, currently not financially supported), 8% with small hydro (<10MW, supported with feed-in tariffs) and 3% with wind power and biomass.

Since 2002, the Green Energy Act has been amended three times between 2006 and 2008, with some of the amendments taking effect or being further revised in 2009. The feed-in tariff period was extended to 15 years for biomass and biogas and to 13 years for other technologies.

Bulgaria
The Bulgarian government has announced a 50% cut to solar feed-in tariffs, having only approved a new FiT in April. Effective July 1, chair of the State Commission for Energy and Water Regulation (DKEVR), Angel Semerdzhiev, told Parliament on Friday that the renewable energy surcharge was solely responsible for an increase in electricity rates.

Poland
In 2010, the Polish Photovoltaics Association estimated PV plants in Poland amounted to 1.3MW – although mostly off-grid generation. There are only two PV installations online with the total capacity of 0.012MW. The government of Poland is proposing a draft policy for FiTs of rates amounting to USD$0.334/kWh for solar PV plants up to 100kW, setting a renewable energy target of 2MW of PV capacity by 2020. Contract terms are expected to be 15 years. The new law is not expected to take effect until early 2013.

Ukraine
Europe's second largest country is expecting to meet its goal of generating 19% of energy from renewables by 2030. Under the Green Law, approved in April 2009, the state will purchase energy from renewable sources under the tariff system until 2030 and also ensures connection to the grid. The tariffs in the Ukraine are determined by the National Commission for Regulation of Electroenergetics, individually for each company, depending on the type of alternative energy it uses. Currently, for a 100kW solar PV system, the feed-in tariff has been set at €0.45/kWh.

United Kingdom
The UK Department of Energy and Climate Change (DECC) has published the results of its latest feed-in tariff comprehensive review, effective August 1. Due to low deployment levels since April the government decided to push back the implementation of the tariffs by one month. The new rates for 4kW systems will be £0.16/kWh and the payback time reduced from 25 to 20 years. The tariffs have been designed to offer a rate of return of 4.5% to 8% for a typical installation. DECC also proposed a degression method which would involve three-monthly tariff changes, a baseline degression of between 3.5 and 28%, depending on the rate of deployment and skipping the degression altogether if deployment is low.

Asia and Oceania

Japan
On June 18, 2012, Japan's Ministry of Economy, Trade and Industry (METI) announced very attractive pricing for sales of renewable energy to Japan's regional utilities under a new FiT. Under the FiT, solar projects over 10kW in size can be paid ¥42 (US$0.53) per kWh under a 20-year Power Purchase Agreement. These terms are in effect for the period from July 1, 2012 to March 31, 2013. Going forward they will be subject to annual review by a METI-appointed committee. The additional cost of the tariff over conventional power generation is directly passed on to consumers by means of a surcharge on all power consumers and the utility does not incur the additional cost.

South Korea
South Korea has pledged a 30% reduction in emissions by 2020 and if legislation is passed, it will become the third Asia Pacific country to tax polluters after Australia and New Zealand.

South Korea's solar feed-in tariff was cut in October 2008, resulting in only 10MW between October 2008 and March 2009 being installed in the entire country with a 500MW cap.

From 2009, a decremental rate has been applied to solar PV of 4% per year. The standard price for each of these power sources will be applied for 15 years.

The Philippines
The Philippines' Energy Regulatory Commission has approved an initial FiT rate for renewable energy. The FiT for all solar installations will be 9.68 PHP (US$0.23) per kWh, regardless of the system's size or technology. The ERC will review and adjust the approved rates at the end of the programme's initial three-year period or once installation targets have been met.

Africa and Middle East

Morocco
The International Finance Corporation and the government of Morocco have signed an agreement to support the development of a solar power plant to promote renewable sources of energy to meet growing electricity demands. The government aims to create 2,000MW of solar-generated electricity per year by 2020. This would represent 14% of the total electricity generated in 2020, avoiding yearly emissions of 3.7 million tons of carbon dioxide.

Saudi Arabia
Saudi Arabia is seeking investors for a US$109 billion plan to create a solar industry that generates a third of the nation's electricity by 2032, according to officials at the agency developing the plan. The world's largest crude oil exporter aims to have 41,000MW of solar capacity within two decades, said Maher al-Odan, a consultant at the King Abdullah City for Atomic and Renewable Energy.

Americas

Peru
Demand for energy in Peru is growing at 9% per year, with total energy capacity estimated to increase to 6,140MW between 2010 and 2020. Peru's renewable energy target is 33% of renewable energy generation by 2021. The Peruvian government uses reverse auctions, as opposed to feed-in tariffs or other incentives, as a market-based mechanism to foster growth of renewable energy capacity. Price ceilings for the second round of 2012 are expected to be lower than last year's. Osinergmin, the agency that organizes the tenders, based the 2010 ceiling prices on those in the USA and European markets, which tend to be higher than regional rates due to the use of feed-in tariffs. Currently, solar power has a ceiling price of US$269/MWh, although project developers asked for between US$215/MWh and US$225/MWh.

Compiled by Nilima Choudhury
Web and Publications Editor,
Solar Media Ltd.

Do peer effects matter? Assessing the impact of causal social influence on solar PV adoption

Bryan Bollinger, NYU Stern School of Business, New York, & **Kenneth Gillingham**, Yale School of Forestry and Environmental Studies, New Haven, Connecticut, USA

ABSTRACT
In this paper an assessment is made of the impact of causal peer effects found in a recent paper by Bollinger and Gillingham, simulating solar adoption over many markets in the presence of a causal peer effect. Heterogeneity in both the peer effect and the baseline adoption rate is introduced and their interaction assessed. The nature of the heterogeneity and the size of the peer effect both have implications for the resulting diffusion process. Causal peer effects have implications for firms and policymakers, who have the ability to utilize social spillover effects in their marketing activities in order to increase and expedite solar adoption.

Introduction

If I install a solar panel, are my neighbours more likely to install one too? A household's decision on whether or not to adopt a solar panel is determined by its preferences, the costs and benefits of the technology, and the state of the household's information regarding the technology. But it turns out that social contagion could also play a role. In Bollinger and Gillingham's 2012 Marketing Science paper [1], hereafter referred to as 'BG', the authors found evidence of causal 'peer effects' in the diffusion of solar PV panels, indicating that if there are multiple adopters in the same localized geographic area, one household's choice to adopt is influenced by others' decisions. These effects may occur as a result of information sharing or of even 'image motivation' from the conspicuous consumption of environmentally friendly goods. The causal nature of peer effects influencing the diffusion of solar PV technology is of critical interest to policymakers concerned about reducing greenhouse gas emissions to mitigate the potential consequences of global climate change. Furthermore, firms may be able to leverage these peer effects to expedite or increase the overall level of solar adoption by utilizing the social spillovers.

> "If there are multiple adopters in the same localized geographic area, one household's choice to adopt is influenced by others' decisions."

This paper uses the results from BG to assess the magnitude of the estimated peer effects on the diffusion of solar PV panels in California, USA. Counterfactual simulations are performed to determine how the adoption rates and cumulative levels of adoption would change if firms or policymakers were able to increase the peer effect by 10%.

Background

There has been a long history of government support for solar energy, both in the United States in general and in California specifically. At the federal level, solar incentives date back to the Energy Tax Act (ETA) of 1978. More recently, the Energy Policy Act of 2005 created a 30% tax credit for residential and commercial solar PV installations, but with a $2000 limit. The Energy Improvement and Extension Act of 2008 removed the $2000 limit, and the American Recovery and Reinvestment Act of 2009 temporarily converted the 30% tax credit to a cash grant.

California's activity in promoting solar pre-dates the federal activity, with efforts beginning as early as the creation of the California Energy Commission (CEC) in 1974. For several decades much of the emphasis was on larger systems, and the interest in distributed-generation solar PV did not pick up until the late 1990s. In 1997, California Senate Bill 90 created the Emerging Renewables Program, which directed investor-owned utilities to add a surcharge to electricity bills to promote renewable energy. The proceeds of this surcharge supported a $3/W rebate for solar installations, a major step in California support for the solar industry [2]. This support was built upon in the following years with the addition, in 1998, of 'net metering' (allowing owners of solar PV systems to receive credit for electricity sold back to the grid), and a state tax credit of up to 15% for solar PV installations starting in 2001, as reported in the 2009 California Public Utilities Commission (CPUC) report [3]. The state tax credit remained in place to the end of 2005.

While the California incentive programme that was put in place in 1997 was substantial, it was renewed on a year-by-year basis, leading to much uncertainty in the solar market. The elements for a longer-term, more predictable policy were put in place in California in August 2004, when Governor Schwarzenegger announced the 'Million Solar Roofs Initiative', setting a goal of one million residential solar installations by 2015. In January 2006, the CPUC established the California Solar Initiative (CSI), a $3.3 billion, 10-year programme aiming "to install 3000MW of new solar over the next decade and to transform the market for solar energy by reducing the cost of solar" [3]. The solar PV industry in California has grown dramatically over the past decade, at least in part because of declining costs and government subsidy programmes, but also in part because of social contagion effects.

Analysis

Measurement of the peer effect

The methodology used in BG isolates the causal effect of nearby installations on the adoption rate of solar PV panels by using a first-differences approach. The model of household adoption is given by:

$$Y_{zt} = \alpha + \beta b_{zt} + \gamma' X_{zt} + \eta_{zq} + \xi_t + \varepsilon_{zt} \qquad (1)$$

where Y_{zt} is the fraction of owner-occupied households in zip code z that had not previously adopted solar and decide to adopt solar on day t; η_{zq} are zip code-quarter fixed effects (q denotes a quarter); ξ_t are time indicator variables,

including year-month, day of the month and day of the week indicators; and ε_{zt} is a mean-zero stochastic error. X_{zt} contains additional explanatory variables that may vary over time, such as indicator variables for different levels of subsidy available for adopting solar.

The equation used for estimation is:

$$(Y_{zt} - Y_{zt-1}) = \beta(b_{zt} - b_{zt-1}) + \gamma'(X_{zt} - X_{zt-1}) + (\xi_t - \xi_{t-1}) + (\varepsilon_{zt} - \varepsilon_{zt-1}) \quad (2)$$

where BG dropped the first adoption in each zip-quarter so that the zip-quarter effects drop out of the estimation equation. BG estimated how a *change* in the installed base leads to a *change* in the adoption rate. The identifying assumption is that new installations do not contribute to the peer effect until they are completed, whereas the decision to adopt occurs before that, when the installation is first requested. These assumptions ensure that there is no correlation of the first-differenced error term with the first-differenced installed base, so β can be consistently estimated. This contrasts with traditional mean-differenced fixed effects estimation, in which there is a correlation of the mean-differenced error with the installed base by construction [1,4], so ordinary least-squares estimation results in biased estimates of the peer effect.

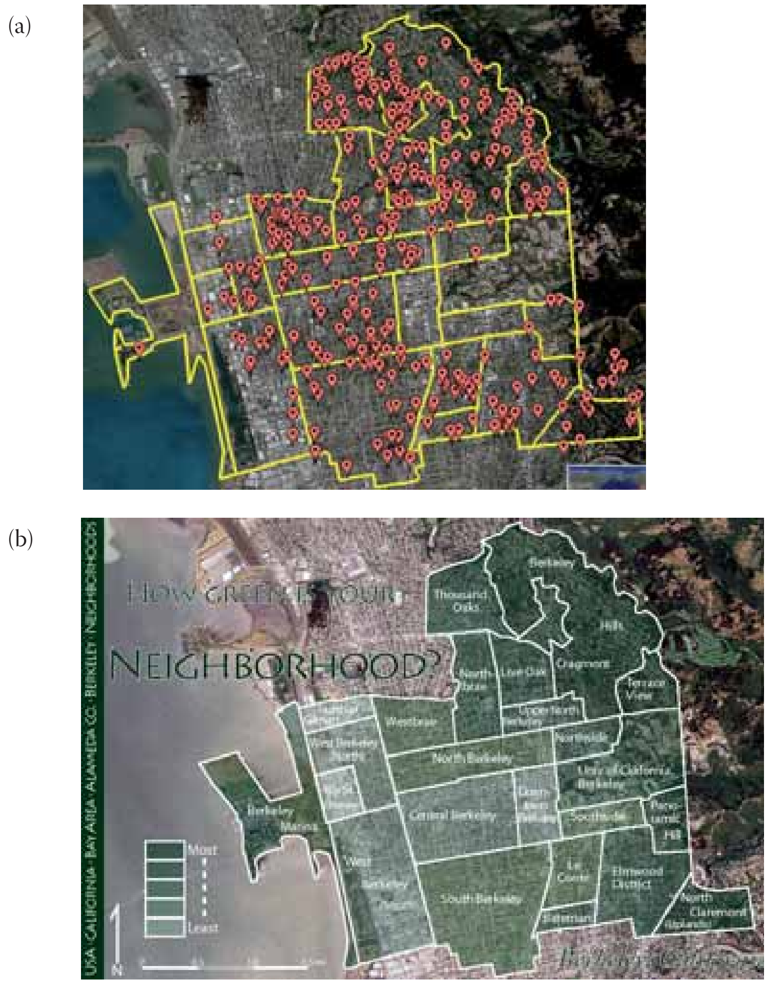

Figure 1. Google Earth view of Berkeley installations by neighbourhood 2001–2006: (a) Berkeley installations; (b) Berkeley neighbourhoods (created by Factle Maps [5]).

The size and nature of the peer effect

BG found that an extra installation in a particular zip code increases the daily household probability of an adoption by $\beta = 1.567 \times 10^{-6}$. This translates to an increase in the zip code adoption rate by 0.78 percentage points for those zip codes with the average number of owner-occupied homes. In addition, by assessing and finding a positive impact of previous installations on a street with the probability that more households on the same street adopt later, BG found that the peer effects operate at more localized levels.

> "Solar PV adoption rates are higher in zip codes where people have stronger preferences for environmentally friendly goods."

BG showed that solar PV adoption rates are higher in zip codes where people have stronger preferences for environmentally friendly goods, proxied for by the fraction of vehicle adoptions between 2001 and 2009 that were hybrids. Fig. 1(a) shows the exact locations of solar installations in neighbourhoods of Berkeley, California, between 1999 and 2006; Fig. 1(b) shows a map, created by Factle Maps [5], of how 'green' the neighbourhoods are. The greenest neighbourhoods are less populous yet have a high density of solar installations. Interestingly, while some clustering of installations appears to occur because of environmental preferences, BG found that there is clear evidence of clusters of solar panels, even after controlling for factors such as environmental preferences.

However, the magnitude of the clustering effect and how it influences the speed of adoption of solar panels depends on other demographic variables. BG found that zip codes with larger household sizes and the fraction of people with more than a 30-minute commute have larger peer effects, while zip codes with higher median household income and more people who carpool have smaller peer effects. Larger household sizes are associated with larger peer effects, perhaps indicating that the more the panels are seen, the greater the effect will be. If this is the case, more visible installations should have more of an effect as well. BG tested for this by measuring how the peer effect depends on the size of the installations. They found evidence that larger installations do have a larger impact on the peer effect. Since visibility appears to enhance the peer effect, increasing the visibility of adoptions would be expected to increase the rate of adoption. Indeed, this strategy can be seen with several installers putting up signs indicating that a solar PV panel has been installed.

> "The size of installations increases with the size of the zip code installed base."

While this evidence supports the notion that visibility of installations plays a role in the size of the peer effects, BG also found evidence that the peer effects may lead to reduced uncertainty in how consumers value the solar installations. It is hypothesized that if larger installed bases lead to less uncertainty in the per watt value of an installation, larger installed bases should also lead to larger installations, since the value of decreasing the risk is greater for larger installations. This is exactly what BG found – the size of installations increases with the size of the zip code installed base.

This result is consistent with the latest developments in the solar PV market. Companies such as SolarCity and Sungevity have recognized that reducing the consumer uncertainty about installing solar is critical to expanding the market. These companies lease solar panels to consumers; they perform the installation for free and take care of all the maintenance, and they then guarantee the system will perform as promised or they will pay the consumer the difference. By transferring the risk of installation to the installer, this may reduce moral hazard issues and lead to the installation of larger (and riskier) installations.

The finding that a larger installed base in a zip code leads to larger installations also suggests that other methods of information provision may also lead to increased adoption levels. The use of demonstration sites has been shown to have positive effects on the adoption of green technologies [6], although Kalish & Lilien [7] caution that such demonstrations for solar PV should only be used when the information to be learned is positive. Programmes such as PG&E's 'Neighborhood Solar Champions' training programme (Fig. 2) aim to leverage peer effects to provide such positive information to neighbours. "Solar can grow through trust and social dynamics like keeping up with the Joneses," says Sungevity's CMO Patrick Crane, formally of LinkedIn; indeed much of Sungevity's marketing strategy is now based on social interactions, beginning of course with the provision of an excellent customer experience in order to leverage such interactions [8].


Neighborhood Solar Champions

Seeking Solar Champions!

Would you like to become a Solar Champion in your SF neighborhood? The San Francisco Department of the Environment and PG&E are offering free solar training for SF citizens interested in helping spread the word about solar in their neighborhoods.

What: **Neighborhood Solar Champions Training Course**
When: **Check back in 2010 for future class offerings.** Classes are held several times per year on select Saturdays from 9:30-4:00. This includes the 10:00-12:00 Solar Power Basics for Residential Customers class.
Where: **PG&E's Pacific Energy Center, 851 Howard Street San Francisco, CA 94103**
Cost: **Free! Plus, lunch is provided for participating SF residents**

Requirements:

- Interest in promoting solar energy in your SF neighborhood
- Commit to giving at least two presentations in your neighborhood a year
- Comfortable with public speaking
- Ability to participate in one full day of training
- No prior solar technical experience necessary (though helpful)

For more information, please contact:

Jade Juhl
SF Department of the Environment
Email: jade.juhl@sfgov.org
Tel: (415) 355-3780

Lisa Shell
PG&E
Email: L1SB@pge.com
Tel: (415) 973-0305

We look forward to working with you as a Neighborhood Solar Champion!

SF Environment
Our home. Our city. Our planet.
Pacific Gas and Electric Company

Figure 2. Solar Champions Flyer.

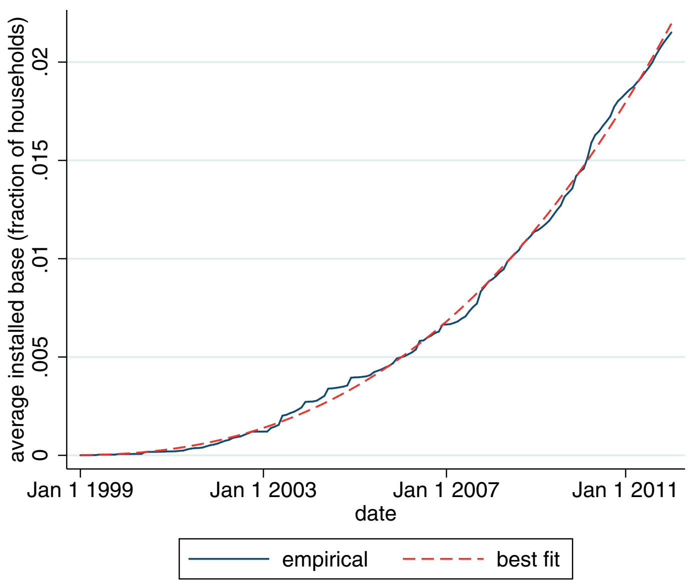

Figure 3. Zip code installed base.

Simulations

These findings have clear implications for marketers who are striving to reduce the high cost of consumer acquisition in the solar PV market. One of the findings in BG was that the peer effect may have increased slightly over time, which would support the notion that firms and policymakers in general are learning to utilize the peer effects in their marketing strategies. To assess the value of being able to leverage these peer effects, and to assess whether the magnitude of our statistically significant peer effect has any meaningful impact on the level of adoption, the diffusion of solar PV over twelve years is simulated using the estimated household-level peer effect of 1.567×10^{-6} and also using a peer effect 10% larger in size. Fig. 3 shows the actual average zip code installed base in the data, measured as the fraction of households in the zip code that have adopted.

For the simulations, 1000 identical zip codes with 1000 households apiece are considered, all of which have zero panels currently installed. The zip code sizes are normalized because it is desired to get an intuitive idea of the influence of an increased peer effect, as well as the presence of heterogeneity in the base adoption rate and the peer effect, without the further interactions with the zip code sizes. The normalization also makes the interpretation easier, since it does not matter whether the impact on adoption is measured in number of installations or in fraction of households who have installed. A baseline daily household adoption rate of 1×10^{-7} with an additive log exponential stochastic term multiplied by 1×10^{-8} is included. To allow for heterogeneity in both the peer effect and the baseline adoption rate, specifications are used in which the base rate and/or peer effect are heterogeneous, distributed normally with the means stated above, and standard deviations equal to half the means. Heterogeneity is important to include, since there may be large ramifications of heterogeneity for the overall levels of adoption. Moreover, if both the base adoption rate and the peer effect are heterogeneous, then whether they are positively or negatively correlated is crucial.

The simulations were performed 100 times and the mean results are reported here. Fig. 4(a) shows the average of the simulated installed bases (as a fraction of the owner-occupied homes) over twelve years, comparing what would happen with our estimated peer effect and with a peer effect 10% larger, with and without zip code heterogeneity in the base adoption rate. With homogeneous base rates, the 10% increase in the peer effect increases the average fraction (number) of households adopting (assuming homogeneous zip codes) from 0.0416 to 0.0579, an increase of 39%. With heterogeneous base rates, the increase is almost exactly the same, from 0.0416 to 0.0578. The addition of heterogeneity in the base rate has virtually no effect on the level of adoption, but the increase in the size of the peer effect has a large effect on overall adoption. These are our baselines for comparisons.

"The addition of heterogeneity in the base rate has virtually no effect on the level of adoption, but the increase in the size of the peer effect has a large effect on overall adoption."

Fig. 4(b) shows simulations with heterogeneity in the peer effect instead of the baseline adoption rate. Heterogeneity in the peer effect leads to an increase in the fraction of households adopting by 15.9%, from 0.0416 to 0.0482. The presence of heterogeneity leads to a smaller relative gain due to the 10% increase in the size of the peer effect, increasing adoption from 0.0482 to 0.0635, an increase of 31.7%. This level of adoption is, of course, higher since both the heterogeneity and increase in the peer effect lead to more adoption, and the absolute gain in the number of adoptions is (on average) 153, which is only slightly smaller than the increase of 163 for the homogeneous zip codes.

Fig. 4(c) includes perfectly positively correlated heterogeneity in both the peer effect and baseline adoption rate. The effect of the heterogeneity increases adoption from 0.0416 to 0.0545, an increase of 31.0%. Clearly, the correlation

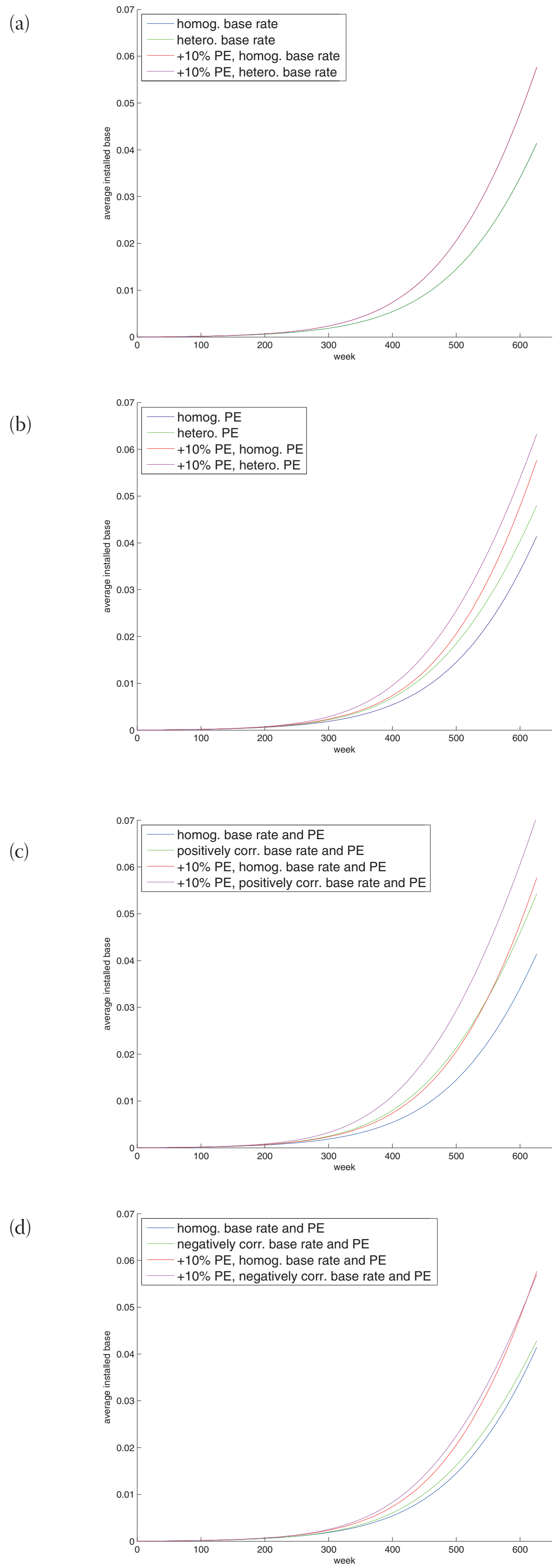

Figure 4. Simulation results: (a) heterogeneity in baseline adoption; (b) heterogeneity in peer effect (PE); (c) positively correlated heterogeneity in baseline adoption and PE; (d) negatively correlated heterogeneity in baseline adoption and PE.

in the heterogeneity helps to drive adoption. The 10% increase in the size of the peer effect leads to an increase in the installed base after twelve years from 0.0545 to 0.0710, an increase of 30.3%. The relative size of the increase in the peer effect is smaller than in the previous two simulations, but this is partly due to the fact that the correlated heterogeneity has already led to significantly more adoption.

In contrast, Fig. 4(d) includes perfectly negatively correlated heterogeneity in both the peer effect and the baseline adoption rate. When the peer effect heterogeneity is negatively correlated with the heterogeneity in the baseline adoption rate, the presence of heterogeneity increases adoption to only 0.0431, an increase of 3.6%. The increase in the peer effect further increases adoption to 0.0572, an increase of 32.7%. Adoption with perfectly negatively correlated heterogeneity leads to slightly less adoption than the scenario with heterogeneity on the base rate only (a decrease of 1.0%), and significantly less than when there is heterogeneity on the peer effect only (a decrease of 9.9%). Therefore, while heterogeneity leads to more adoption, negative correlation in the base rate and peer effect reduces adoption and can lead to a negative effect of heterogeneity on adoption. Since the relative gain from the increased peer effect is about the same, this also reduces the effectiveness of peer effect increases.

Discussion

The simulation results have some interesting implications for practitioners. The installation elasticity of the peer effect is approximately three, depending on the nature of the heterogeneity in baseline adoption rates and the peer effect. There is more value in increasing the peer effect in areas with high adoption rates (at least in this period where markets are far from saturated) but this may pose a challenge. Areas with high adoption rates may in fact be less likely to exhibit large peer effects if the mechanism behind the peer effects is the provision of information, and households in these areas are already informed regarding the benefits of solar.

It should be noted that the estimated peer effect in BG is not a structural estimate. While significant care was taken to establish the causality of the effect, one of the results is that the peer effect was estimated with limited structure imposed in the estimation. Thus, if market conditions change dramatically, it is entirely possible that the peer effect could change as well. While this can be a positive for marketers since there is scope for increasing the size of the peer effect, it also means that the peer effect may decrease as a result of other policies and marketing efforts used to increase solar adoption. This is an area worth further exploration.

Conclusion

BG established the existence of causal peer effects in the diffusion of solar panels, in addition to providing some suggestive evidence regarding some of the potential mechanisms underlying these social interaction effects. Visibility of installations seem to play a role in the size of the peer effect, which would be the case if there are image motivation effects, since the adoption of solar panels is an effective way of demonstrating 'greenness' through the conspicuous consumption of an environmentally friendly technology. In addition, transfer of information through word of mouth may also play an important role, supported by the fact that areas with larger installed bases have larger new installations, and larger installations are those that benefit the most from uncertainty reduction in the value of installing solar, made possible through information transfer via word of mouth. However, while BG found evidence that visibility and the transfer of information may both play a role in the mechanism behind the peer effects, more research is needed to establish their respective contributions.

> "The adoption of solar panels is an effective way of demonstrating 'greenness' through the conspicuous consumption of an environmentally friendly technology."

Finally, it would be useful to study how traditional marketing tools, as well as marketing intended to leverage peer effects, amplify and interact with social influence in the diffusion of solar panels and other green technologies. As this paper demonstrates, heterogeneity in the peer effect and baseline adoption rates also have significant effects on adoption, as would their interactions with such marketing tools. A better understanding of these interactions will help in determining how useful peer effects can be in expediting and increasing the overall adoption of solar.

References

[1] Bollinger, B. & Gillingham, K. [forthcoming], "Peer effects in the diffusion of solar photovoltaic panels", *Marketing Sci.*

[2] Taylor, M. 2008, "Beyond technology-push and demand-pull: Lessons from California's solar policy", *Energy Economics*, Vol. 30, No. 6, pp. 2829–2854.

[3] CPUC 2009, "California Solar Initiative annual program assessment", California Public Utilities Commission Go Solar California Report.

[4] Narayanan, S. & Nair, H. [forthcoming], "Estimating causal installed-base effects: A bias-correction approach", *J Marketing Res.*

[5] Factle Maps [available online at http://factle.com.s3-website-us-east-1.amazonaws.com/products.html].

[6] Bollinger, B. 2012, "Technology adoption in regulated markets: An empirical study of the Southern California dry cleaning industry" [working paper].

[7] Kalish, S. & Lilien, G.L. 1986, "A market entry timing model for new technologies", *Management Sci.* (Feb), Vol. 32, No. 2, pp. 194–205.

[8] Korosec, K. 2012, "Sun's up", *Marketing News* (May 31), pp. 20–23.

Market Watch

About the Authors

Bryan Bollinger is an Assistant Professor of Marketing at New York University Stern School of Business. His research interests lie at the intersection of marketing, empirical industrial organization and economic policy. Bryan's current research includes the diffusion of solar panels and supply-side learning by doing, green technology adoption by dry-cleaning firms, the effect of peak-pricing technologies on electricity consumption, and projects on advertising and pro-social marketing.

Kenneth Gillingham is an Assistant Professor of Environmental and Energy Economics at Yale University. His research concentrates on policies and measures for reducing greenhouse gases, with a particular focus on solar energy, energy efficiency and vehicle energy use. Kenneth has undertaken research in areas such as learning by doing and the cost of solar technology, landlord–tenant issues in residential energy use, and consumer response to gasoline prices.

Enquiries

Bryan Bollinger
NYU Stern School of Business
40 West 4th St, New York
NY 10012
USA
Email: bbolling@stern.nyu.edu

Kenneth Gillingham
Yale School of Forestry and Environmental Studies
195 Prospect Street
New Haven
CT 06511
Email: kenneth.gillingham@yale.edu

Self-consumption as the new Holy Grail of the PV industry: From theory to reality

Gaëtan Masson & **Marie Latour**, European Photovoltaic Industry Association (EPIA), Brussels, Belgium

ABSTRACT
There has been rapid development of renewables in Europe in the last decade thanks to various support schemes. These are now part of the electricity reality in Europe and will continue driving the energy revolution in the coming years. In the PV sector in particular, feed-in tariffs (FiTs) have proved quite successful: at the beginning of 2010 more than 51GW of PV systems were connected to the grid in the EU, compared to less than 5GW five years earlier. This translates to 2% of the electricity demand being fulfilled by PV systems in the EU27. But all coins are double-sided: FiTs have proved to be too successful in several countries, inducing uncontrolled market development. The time has come to identify how these mechanisms – and in particular support schemes based on pure electricity injection – should evolve in order to manage a sustainable transition to competitiveness.

Introduction

In a 2011 study [1], EPIA showed how PV competitiveness could be reached in the largest EU countries by 2020 given adequate political support. Since then, PV system prices have fallen more quickly than expected, resulting in competitiveness happening earlier, especially in countries that were close to a certain level of competitiveness. In addition, the current financial downturn, which has evolved into a real economic crisis, is putting any kind of policy under pressure, increasing the financial burden on taxpayers or electricity consumers.

All these elements together are driving towards new, renovated or complementary support schemes for renewables in general and PV in particular. PV especially is by nature decentralized, and a large portion of the market (70% in the EU in 2011) concentrates on rooftop installations, the electricity from which is consumed on site. This paves the way for a wide-scale development of support schemes based on compensation for local consumption of generated electricity, rather than focusing on electricity production only (as currently is the case of feed-in tariffs (FiTs) or green certificates).

This concept of compensation is fairly new in the PV sector. FiTs and similar support schemes were conceived for other types of renewable plant producing electricity for injection into the grid – wind turbines, biomass plants and geothermal plants. Since the schemes worked for these renewables, they were implemented in the same way for PV, with similar success. But the specifics of PV imposed a consideration of the main driver for investment in the rooftop segments: the compensation for local electricity consumption. With FiTs, the flow of electricity is measured in both directions and billed differently: consumers pay their electricity bill, while producers are paid for the electricity production.

This state of affairs has led to the rather strange situation where, despite real-time consumption, electricity is bought and sold at the same time. With the levelized cost of PV electricity (LCOE) now close to retail prices in certain countries and segments, this sounds rather strange and paves the way for compensation schemes: electricity brought to the consumer and electricity produced should naturally offset each other, either in real time or over a longer period of time.

> "Compensation mechanisms are based on the idea that PV electricity can be used in the first place for local consumption."

Self-consumption mechanisms

Compensation mechanisms are based on the idea that PV electricity can be used in the first place for local consumption, and that electricity should not be purchased from utility companies. There are several different options available for the part of the bill that can be compensated, depending on the country or region, as will be discussed next.

The mechanism of compensation in real time (or during a 15-minute time frame) will be called a 'self-consumption scheme.' A variant that allows compensating production and consumption during a larger time frame (up to one year) will be called a 'net-metering scheme.' In the latter, the network should be regarded as a long-term storage solution, with the PV electricity being occasionally injected without compensation and consumed later on.

Various intermediate schemes exist between these two. The debate has begun, however, to identify whether compensation can apply not only to the procurement price of electricity but also to grid costs and taxes.

Self-consumption ratios

It is widely accepted that a standard household running a PV system in central France or Germany can naturally achieve a level of self-consumption of around 30% (on a 15-minutes basis) without any specific measure being put in place. With regard to local consumption, the larger the system, the lower the self-consumption ratio. Optimization of the system size (annual production and consumption equalized) and the use of demand-side management tools, such as heat-pumps or a decentralized storage system, could increase that level to 70%. Reaching yet higher levels would require long-term local storage.

These relatively low levels can be explained by low consumption during weekdays in the summer, and high consumption in the winter at times when PV produces less electricity. On commercial or industrial rooftops, the self-consumption rate can be expected to reach 75% and above more easily because of the better correlation between consumption and production. Self-consumption rates of 100% are thus technically feasible, under conditions of size limitation for instance, and could therefore be considered equivalent to net-metering schemes.

Self-consumption incentivization schemes in Europe

In the last few years, several countries have implemented support schemes that aim to either replace or complete existing FiTs. The objective of all these schemes is to focus on the direct consumption of PV electricity in order to reduce or eliminate the associated FiTs.

The evolution in **Germany** towards incentivization of self-consumption started in 2011 with a premium tariff for self-consumed electricity. The remuneration was even higher if a rate of self-consumption over 30% was reached, encouraging prosumers to look for ways to increase their direct consumption ratio. Since then, the decreased generation cost of PV has prompted German authorities to consider self-consumption incentivization without a premium tariff: with the retail price of electricity in most cases now higher in the residential segment in this country than the generating cost for a PV system, self-consumption becomes obviously more profitable than an awarded FiT. The review of the German Renewable Energy Act (EEG) in 2012 has introduced a limiting factor for grid injection that can be interpreted as a way of favouring direct consumption. With a maximum injection of production of 90% for systems above 10kWp, the legislation sends the signal of a clear intention to favour self-consumption over pure production.

In **Italy**, the country's fifth energy bill – Quinto Conto Energia – introduced a specific self-consumption premium scheme which will be in place as from Q4 2012; the way it will work is very similar to the scheme introduced in Germany in 2011. The Scambio sul posto scheme will run in parallel: this was an initial (and complex) attempt to favour direct consumption, featuring a mix of net-metering aspects (especially for grid costs) and self-consumption (for electricity costs).

In **Belgium**, all regions have chosen a net-metering scheme for systems up to 10kW (10kVA). No remuneration is foreseen for the excess electricity generation that is then injected into the grid but uncompensated.

In the **Netherlands**, yearly-based net-metering is allowed for 'small users.' This applies to systems up to 15kWp with a grid connection limited to 80A in three phases, but compensation is received for only a maximum of 5000kWh. Consequently, this naturally limits the size of a system to meet this consumption in order to maximize the rate of return. Excess electricity generation can be sold at a price similar to wholesale prices (€0.05/kWh).

The case in **Denmark** is similar to that in the Netherlands, but limited to 6kW systems. The excess generation can be sold at €0.08/kWh (through a specific FiT).

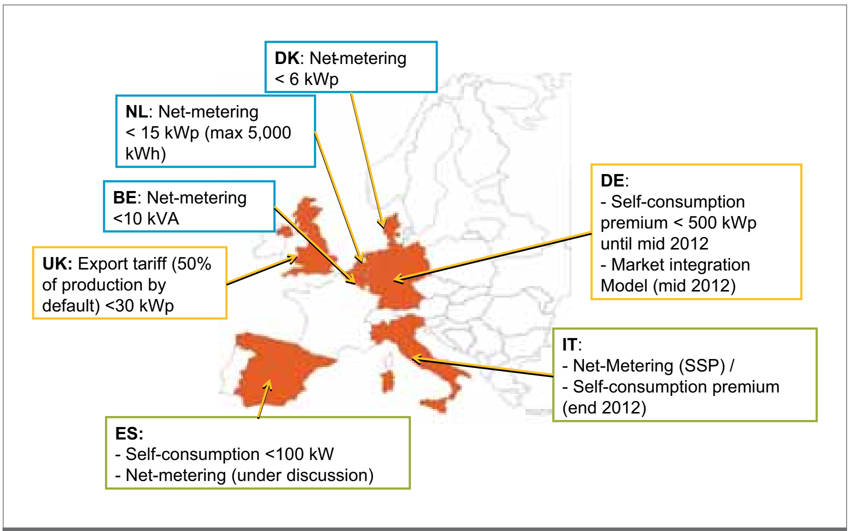

Figure 1. Overview of current net-metering and self-consumption schemes in the EU.

In **Spain**, self-consumption (without any specific premium) has been authorized since November 2011 for systems up to 100kW. The net-metering concept has not yet been finalized and discussions are still ongoing. A partial net-metering scheme could be introduced: the compensation of electricity would be granted on a yearly basis but some grid costs might have to be paid by the prosumer anyway. Moreover, the possibility of combining and net-metering the production from several users could be part of the discussion as well.

Finally, in the **UK**, the existence of an 'export tariff' for electricity injection into the grid (deemed by default to be 50% of PV production) could be regarded as an indirect self-consumption scheme. This system valorizes self-consumption, since the consumption invoice will decrease as the self-consumption electricity ratio increases.

Fig. 1 illustrates the situation in various countries in Europe: real net-metering systems exist in Denmark, Belgium and the Netherlands, and the scheme is being discussed in Spain. Self-consumption is favoured in Germany and soon will be in Italy too. Italy's Scambio sul posto is a hybrid scheme, with net-metering features combined with partial self-consumption aspects. The non-classical situation in the UK could be considered to be an indirect self-consumption scheme.

Comparison of existing schemes in Europe

Fig. 2 summarizes the different schemes in Europe that allow compensation. Italy, the UK and Germany favour self-consumption schemes, whereas net-metering is being considered in Denmark, Belgium and the Netherlands, and possibly in Spain in the future. The figure should be interpreted as follows:

- In order to compare all schemes, a residential household is assumed, with a yearly consumption of 3,500kWh and installed PV production of 3,300kWh per year.
- Of the electricity produced, 30% is instantaneously self-consumed and the remaining 70% is injected into the grid.
- The yellow bars represent FiTs for grid-injected electricity.
- In the case of net-metering on a yearly basis, part of the additional electricity needed for consumption is net-metered (i.e. withdrawn from the grid and debited against electricity previously injected) and the remaining part is purchased from the electricity retailer.
- The electricity consumed must be purchased from the grid operator; this is larger in the case of self-consumption, since with net-metering the total production compensates for electricity requirements (red bars).
- The net financial balance (green bars) is given by the total PV production minus the total grid withdrawal.
- The savings (purple bars) represents the money saved compared to a standard customer without a PV system.

Different points of view regarding self-consumption schemes

Direct consumption schemes have a major psychological advantage over FiTs: they consider only the difference between consumption and production, and therefore promote the very nature of decentralized PV. While FiTs show all electricity flows, compensation schemes focus on the net balance and look more closely at the physical reality of electricity exchanges between the prosumer and the grid. This is reflected in the exchanged cash flows as well in the reduced amounts being considered, which is an element of major importance in supporting PV

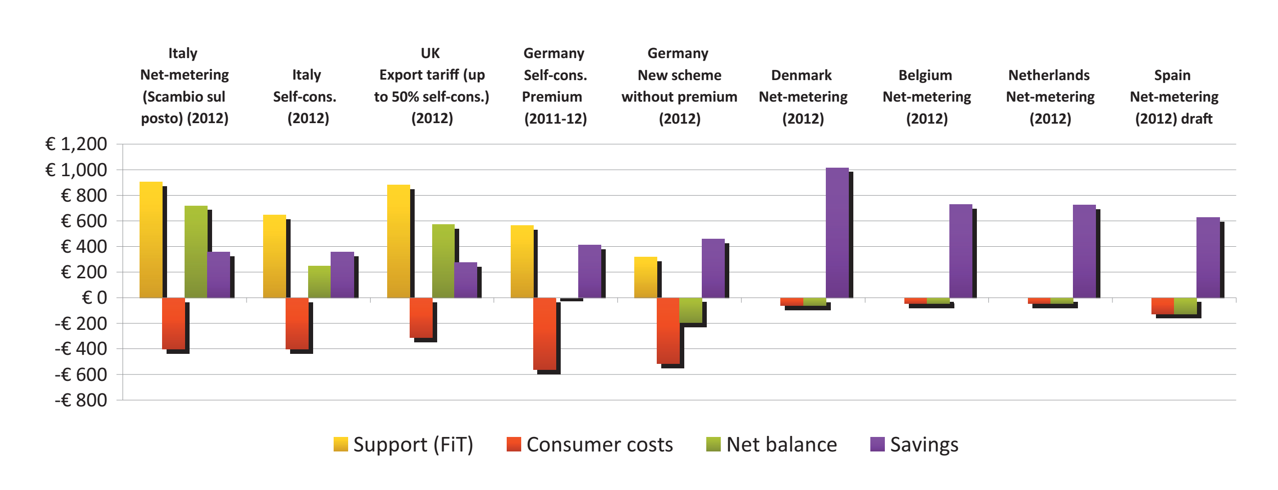

Figure 2. Yearly cash flow balance with self-consumption/net-metering incentives.

development during the transition to competitiveness, in a time of economic sensitivity for all players.

Depending on the scheme, the impacts on players in the electricity market could be quite different. First of all, electricity suppliers may have to support the cost of net-metering: this scheme obligates them to provide electricity for no charge during a part of the year, while PV produces excess electricity that is injected into the electricity network and therefore reduces the need for production. But whereas the reduction in revenues for the supplier is clear, the savings on the consumer side are less obvious. This imbalance could lead to severe opposition from suppliers with regard to accepting such net-metering schemes in the long term, while self-consumption does not trigger such opposition.

Grid operators may be the ones suffering the most from the situation: since grid costs are paid according to electricity consumption, prosumers will not pay part of the totality of their grid costs, in reality reducing the financing ability of grid operators. This situation is not specific to net-metering and affects self-consumption schemes as well.

Governments will see tax income decreasing as well. Although this is easily conceivable in a self-consumption scheme (if you grow tomato plants on your terrace, you do not pay taxes on these), net-metering schemes could force governments to find alternative ways to finance themselves through energy taxes.

Finally, from the consumer point of view, compensation schemes can be easily understood; in the case of self-consumption, the schemes encourage a positive behaviour by displacing part of the consumption during the production time. In the case of both net-metering and self-consumption, the evidence is that net-metering electricity flows can be a positive factor for enhancing PV acceptance. From a financial perspective, net-metering schemes maximize savings and eliminate the need for direct support to prosumers as soon as the LCOE of PV moves into the range of retail electricity prices: the cost of the support is transferred to the electricity suppliers, who absorb the long-term compensation costs. Self-consumption schemes, however, maintain cash flows towards electricity retailers.

> "Self-consumption schemes maintain cash flows towards electricity retailers."

Self-consumption and its impact on the competitiveness of PV

Either current compensation schemes are associated with financial support schemes such as FiTs or green certificates (Belgium), or they are considered as the sole support system, as in the Netherlands. All existing schemes at the beginning of 2012 considered the possibility of compensating taxes and grid costs at least for the portion of electricity that was consumed. But as we have seen, this does not happen automatically, and future compensation schemes may have to deal with partial compensation of either taxes or grid costs (or possibly both). In this case, the impact for prosumers on the competitiveness of PV can be quite important and should be taken into account.

Under the assumption that currently the retail price of electricity in Germany can basically be split into three equivalent parts, namely electricity, grid costs and taxes, the competitiveness of those PV systems with such a compensation scheme will vary. Fig. 3 highlights, for five different countries, the impact of non-compensation of taxes and grid costs on the incoming competitiveness of PV in the residential segment. Details for other segments have been published by EPIA in the second part of their study on competing in the energy sector [2].

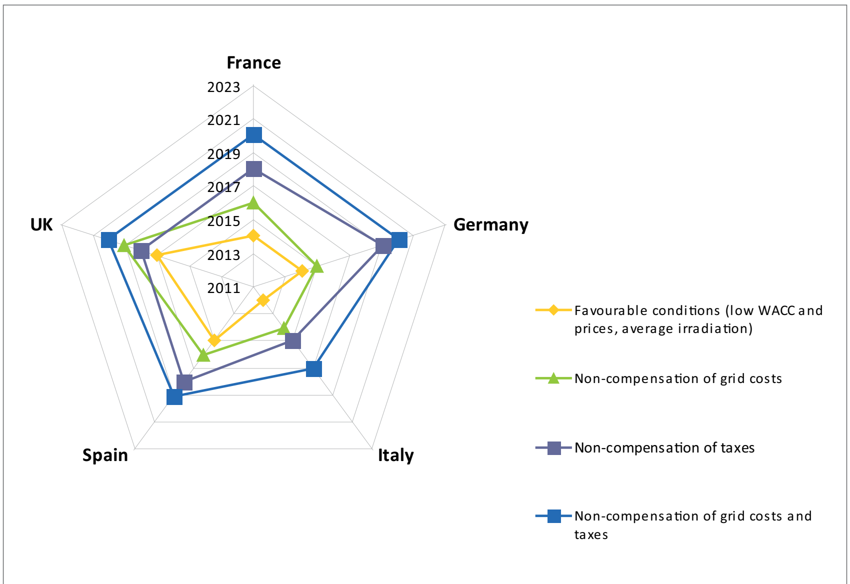

Figure 3. Impact of the non-compensation of grid costs or taxes on PV competitiveness in the residential segment.

Conclusion

The transition to competitiveness for PV is accomplished through adequate, intelligent support schemes that will progressively help to reduce and finally phase out existing FiTs. While the largest installations will require different support, prosumers in all market segments will finally have to compete with retail electricity prices. This transition could be smoothed by using compensation schemes such as the ones describe in this paper. Depending on local conditions, different versions of self-consumption schemes could be implemented and fine-tuned to accommodate country-specific needs.

> "Compensation could represent a smart and efficient means of paving the way for sustainable market development."

Net-metering schemes, despite their drawbacks, have already been successful in certain countries in kick-starting the development of some market segments. Discussions in Spain in 2011 and 2012 have indicated that this idea is not obsolete. While the Spanish market has evolved thanks to large systems, specific schemes (including net-metering) may need to be considered in the prosumer market, especially in the residential segment. In other countries with a large PV presence, compensation schemes certainly represent the future of PV development and require attention. Compensation could represent a smart and efficient means of paving the way for sustainable market development, on the basis of the natural competitiveness that PV is progressively achieving.

References

[1] EPIA 2011, "Solar photovoltaics competing in the energy sector – Part 1".

[2] EPIA 2012, study on grid integration to be presented in September at the *27th EU PVSEC*, Frankfurt, Germany.

About the Authors

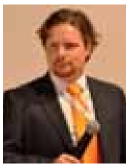

Gaëtan Masson manages EPIA's Business Intelligence Unit, which is dedicated to studying market, PV competitiveness and industry development, as well as grid integration, technology and sustainability impacts of PV. He contributes to IEA-PVPS, where he co-represents EPIA in its Executive Committee. Gaëtan is an electromechanical engineer (Université Libre de Bruxelles in Belgium), and also holds master's degrees in political sciences, in management (from the Solvay Business School) and in environmental studies.

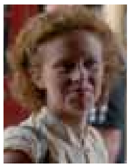

Marie Latour is a senior national policy advisor at EPIA. Within the Business Intelligence Unit at EPIA, she analyzes and advises on national policies in support of the development of PV markets. Marie also coordinates activities with national PV associations both in Europe and worldwide, as well as EPIA's participation in the European PV GRID and PV Parity projects. Co-author of several EPIA publications, she holds a French-Spanish master's degree in business management, and a master's in European affairs.

Enquiries

Marie Latour
Tel: +32 (0) 2 400 10 13
Email: m.latour@epia.org

Photovoltaics International

Advertisers & Web Index

To advertise within Photovoltaics International, please contact the sales department: Tel +44 (0) 20 7871 0123

Photovoltaics International

DON'T MISS: **Steps in large-scale project bankability** | **Reducing balance of system costs** | **Overview of n-type cell developments**

I would like to purchase a subscription.

Price: ☐ 1 x Issue **$59.00 USD** (includes international delivery)
☐ 4 x Issue **$199.00 USD** (includes international delivery) Please start my subscription with edition ....

Method of payment: ☐ Credit Card ☐ Bank Transfer

Name: ....
Job Title: .... Job Function: ....
Company: .... Div/Dept: ....
Street Address: ....
City: .... Post Code/Zip: ....
Country: ....
Telephone Number: .... Web URL: ....
E-mail: ....
For the purposes of our circulation audit, please indicate the last digit of your birth year (YYYY): ....

Company Activity (tick where appropriate):

☐ PV Manufacturer (inc. Thin Film & Module) ☐ Materials Supplier ☐ Equipment Supplier

If you ticked any of the above three options, please indicate the company technology type by ticking one or more of the boxes below:

☐ Si Cell ☐ Thin Film ☐ Module ☐ Concentrator ☐ Emerging ☐ Polysilicon ☐ Ingot/Wafer

☐ University ☐ Energy Utility Supplier ☐ Government Agency
☐ R&D Facility ☐ Financial Community ☐ Other (please specify ....)

In order to continually improve Photovoltaics International we require your feedback. We would be very grateful if you would answer the following questions:

(Q) Which section(s) of the publication are of interest to you? (please tick)

☐ Fab + Facilities ☐ Materials ☐ Cell Processing ☐ Thin Film
☐ PV Modules ☐ Power Generation ☐ Market Watch

(Q) What technical subjects do you wish to see in future editions?..

....

Signature:.. Date ....

Payment Details:

Fax on +44 (0) 20 7871 0101 or email info@pv-tech.org:

Type of credit card: ☐ VISA ☐ MasterCard ☐ American Express

Card Number: ....
Expiry Date: ....
3 Digit CVV Code (back of card): ....
Cardholder's name: ....

Post: Make cheques payable to **"Solar Media Ltd."**
Photovoltaics International, Trans-World House,
100 City Road, London EC1Y 2BP, UK
Online: PayPal - visit **www.photovoltaicsinternational.com/subscriptions**

To request an invoice please call on 020 7871 0148
or **email:** subscriptions@pv-tech.org

Bank Transfer Details:

Account Name:	Solar Media Ltd.
Account Number:	80686832
Sort Code:	20-39-53
Swift Code:	BARC GB 22
IBAN Number:	GB 42 BARC 203953 80 68 68 32
Bank:	Barclays Bank Plc, 10 Hart Street, Henley-on-Thames, Oxon, RG9 2AX.

All invoices are calculated in Pounds Sterling.

Any payments made in US$ must be made according to the appropriate exchange rate at the time of payment.

Two PIDs, but not from the same pod!

Competition in the PV module bragging rights contest doesn't stop at conversion efficiencies.

Over the last few years there has been a race to provide better performance and improved manufacturer warranties. This has also led to a range of tougher and extended module testing that exceeds conventional testing and certification standards.

Now it would seem the quality and performance bragging rights have also migrated to cover the phenomenon known as potential-induced degradation (PID).

PID is regarded as a key problem for monocrystalline cells and modules as it reduces the high-level performance of the module.

Canadian Solar has just claimed that it was 'among the first providers' to have passed two high-voltage endurance tests. The Photovoltaic Institute (PI) Berlin has tested the CS6-poly-series module, while the PV Evolution Labs has tested the CS5-mono-series and the CS6-poly-series modules for PID characteristics.

According to Canadian Solar, the standard set by the PI Berlin, TÜV Rhineland and the VDE (Association for Electrical, Electronic & Information Technologies) for PID testing meant that its modules were exposed to a negative socket voltage of 1,000 volts.

While in this state, the grounded module front was covered in either aluminium foil or a layer of water. The-before-and-after performance rate was measured with a flasher under standard test conditions (STC), providing the company the top rating, PID Class A, at PI Berlin.

To provide added assurance, Canadian Solar asked PI Berlin to double the standard stress time for what it said was 'the ultimate quality assurance.'

The standard test actually runs for a week; therefore, PI Berlin undertook the test for two weeks.

Now enter Q-Cells, which has also run PID tests on its modules, though it didn't state which ones were tested.

Q-Cells used TÜV Rheinland testing institute but according to the company went through a 'fourfold' PID test. Therefore the test lasted four weeks instead of the usual one week.

Even under this test, Q-Cells said that none of the solar modules displayed a decline in performance by accuracy of measurement (5% degradation or less), which proved the modules were PID resistant.

However, part of the problem in 'proving' quality, especially in respect of PID testing, is that there is not an industry-wide acknowledged testing standard. In the case of Canadian Solar PID tests, these were said to have been developed in collaboration with PV Evolution.

Q-Cells' series of module tests were conducted by TÜV Rheinland and Fraunhofer CSP to those organizations' methodologies.

Both press releases from the module manufacturers were obviously designed to provide customers with the assurances that their products performed excellently and provided confidence in their long-life capabilities.

However, once again we don't have a situation where such tests provide an apple-to-apple comparison. They're certainly not two peas from the same pod.

Shortly following the posting of this blog, Q-Cells kindly confirmed in the blog comments section that the modules in the PID testing were its Q.PRO-G2 and Q.BASE-G2 (polycrystalline, 60 cells). The company also kindly provided background to why VDE established the VDE Quality Tested programme in 2011.

According to the company, since IEC certification is only done once on a module series, continued production tweaks and developments, which could significantly alter the modules behaviour to PID and other factors such as damp heat, meant that a quality assurance programme was needed that was more comprehensive than IEC, especially as it required repeated testing of modules from the production lines on a quarterly basis. There seems no reason not to support such testing, which could and should become a standard within the industry.

However, the story does quite end there, as there have been several other companies reporting successful PID test results.

Yingli Green said its 'multicrystalline PV modules' had undergone, and successfully passed, PID testing at Intertek Group. The PID test was carried out under 85°C conditions, with 85% relative humidity and 1,000V of system voltage bias for a duration of 48 hours.

PV Evolution Labs (PVEL) also confirmed that Suniva passed its PID Certification programme (85˚C at 85% relative humidity) for 600 hours.

Finally, Sharp Corporation said that the Fraunhofer Center for Silicon Photovoltaics (CSP) had conducted PID tests on its ND-R250A5 module at 50°C and a relative humidity of 50%. Sharp noted that the test complied with National Renewable Energy Laboratory (NREL) testing standards (96 hours plus at 60°C, 85% humidity).

Despite the continued commoditization of PV modules it is clear that PID testing can show that not all modules are the same. The move by some manufacturers to closely control processing steps and material selection to mitigate PID is a sign of the industry tackling such issues. One day all modules should pass PID testing with flying colours and do so on a quarterly basis.

This column is a revised version of a blog that originally appeared on PV-Tech.org.

Mark Osborne is currently the Senior News Editor for *Photovoltaics International* and *PV-Tech* website. He has launched multiple technology titles in print and online, covering manufacturing in the automotive, shipping, semiconductor and solar sectors, in a publishing career spanning three decades.

INDIAN SOLAR

INVESTMENT & TECHNOLOGY

SUMMIT & EXHIBITION 2013

INDIAN SOLAR 2013 INVESTMENT & TECHNOLOGY

MAKING INDIA'S NATIONAL SOLAR MISSION A REALITY

2ND ANNUAL INDIAN SOLAR SUMMIT AND EXHIBITION
18–19 APRIL 2013, GUJARAT

ORGANISED BY

SOLAR MEDIA

CO-HOSTED BY

Government of Gujarat

THE 2013 INDIAN SOLAR SUMMIT, WITH THE INSTITUTIONAL SUPPORT OF THE GOVERNMENT OF GUJARAT.

INVESTMENT OPPORTUNITIES

- National Solar Mission Targets – 20GW installed by 2022 - Meet the project developers and EPCs responsible for delivering these targets

POWER PROJECT DEVELOPMENT

- Meet with state policy makers and become part of the US$110bn Indian solar value chain
- Gain access to Gujarat, Rajasthan & Karnataka bid committee members

MANUFACTURING INCENTIVES

- Understand the latest 'Special Incentive Package Schemes' for international manufacturers
- View the latest R&D and technology roadmap for India

WITH 2012'S EVENT ATTRACTING OVER 50 EXHIBITORS AND 1 000 VISITORS, DON'T MISS YOUR OPPORTUNITY TO SECURE YOUR PLACE AT THE 2013 INDIAN SOLAR SUMMIT, SET IN THE GATEWAY TO SOLAR.

2013 WILL BRING TOGETHER STATE POLICY MAKERS, SOLAR PROJECT DEVELOPERS, INVESTORS AND SOLAR EQUIPMENT SUPPLIERS TO SHARE THEIR KNOWLEDGE ON THE LATEST TECHNOLOGY AND DEVELOPMENT OPPORTUNITIES CURRENTLY SHAPING THE INDIAN SOLAR MARKET.

WWW.SOLARSUMMITINDIA.COM

For exhibiting and sponsorship options please contact
gnair@solarmedia.co.uk or +44 (0) 207 871 0122